ISSN 1881-7831 Online ISSN 1881-784X

DD&T

Drug Discoveries & Therapeutics

Volume 9, Number 1
February, 2015

www.ddtjournal.com

DD&T
Drug Discoveries & Therapeutics

ISSN: 1881-7831
Online ISSN: 1881-784X
CODEN: DDTRBX
Issues/Year: 6
Language: English
Publisher: IACMHR Co., Ltd.

Drug Discoveries & Therapeutics is one of a series of peer-reviewed journals of the International Research and Cooperation Association for Bio & Socio-Sciences Advancement (IRCA-BSSA) Group and is published bimonthly by the International Advancement Center for Medicine & Health Research Co., Ltd. (IACMHR Co., Ltd.) and supported by the IRCA-BSSA and Shandong University China-Japan Cooperation Center for Drug Discovery & Screening (SDU-DDSC).

Drug Discoveries & Therapeutics publishes contributions in all fields of pharmaceutical and therapeutic research such as medicinal chemistry, pharmacology, pharmaceutical analysis, pharmaceutics, pharmaceutical administration, and experimental and clinical studies of effects, mechanisms, or uses of various treatments. Studies in drug-related fields such as biology, biochemistry, physiology, microbiology, and immunology are also within the scope of this journal.

Drug Discoveries & Therapeutics publishes Original Articles, Brief Reports, Reviews, Policy Forum articles, Case Reports, News, and Letters on all aspects of the field of pharmaceutical research. All contributions should seek to promote international collaboration in pharmaceutical science.

Editorial Board

Editor-in-Chief:

Kazuhisa SEKIMIZU
The University of Tokyo, Tokyo, Japan

Co-Editors-in-Chief:

Xishan HAO
Tianjin Medical University, Tianjin, China
Munehiro NAKATA
Tokai University, Hiratsuka, Japan

Chief Director & Executive Editor:

Wei TANG
The University of Tokyo, Tokyo, Japan

Senior Editors:

Guanhua DU
Chinese Academy of Medical Science and Peking Union Medical College, Beijing, China
Xiao-Kang LI
National Research Institute for Child Health and Development, Tokyo, Japan
Masahiro MURAKAMI
Osaka Ohtani University, Osaka, Japan
Yutaka ORIHARA
The University of Tokyo, Tokyo, Japan
Tomofumi SANTA
The University of Tokyo, Tokyo, Japan
Hongbin SUN
China Pharmaceutical University, Nanjing, China
Fengshan WANG
Shandong University, Ji'nan, China
Wenfang XU
Shandong University, Ji'nan, China

Managing Editor:

Hiroshi HAMAMOTO
The University of Tokyo, Tokyo, Japan

Web Editor:

Yu CHEN
The University of Tokyo, Tokyo, Japan

Proofreaders:

Curtis BENTLEY
Roswell, GA, USA
Thomas R. LEBON
Los Angeles, CA, USA

Editorial and Head Office:

Pearl City Koishikawa 603,
2-4-5 Kasuga, Bunkyo-ku,
Tokyo 112-0003, Japan
Tel.: +81-3-5840-9697
Fax: +81-3-5840-9698
E-mail: office@ddtjournal.com

Drug Discoveries & Therapeutics

Editorial and Head Office

Pearl City Koishikawa 603, 2-4-5 Kasuga, Bunkyo-ku,
Tokyo 112-0003, Japan

Tel: +81-3-5840-9697, Fax: +81-3-5840-9698
E-mail: office@ddtjournal.com
URL: www.ddtjournal.com

Editorial Board Members

Alex ALMASAN
(Cleveland, OH)
John K. BUOLAMWINI
(Memphis, TN)
Jianping CAO
(Shanghai)
Shousong CAO
(Buffalo, NY)
Jang-Yang CHANG
(Tainan)
Fen-Er CHEN
(Shanghai)
Zhe-Sheng CHEN
(Queens, NY)
Zilin CHEN
(Wuhan, Hubei)
Shaofeng DUAN
(Lawrence, KS)
Chandradhar DWIVEDI
(Brookings, SD)
Mohamed F. EL-MILIGI
(6th of October City)
Hao FANG
(Ji'nan, Shandong)
Marcus L. FORREST
(Lawrence, KS)
Takeshi FUKUSHIMA
(Funabashi, Chiba)
Harald HAMACHER
(Tübingen, Baden-Württemberg)
Kenji HAMASE
(Fukuoka, Fukuoka)
Junqing HAN
(Ji'nan, Shandong)
Xiaojiang HAO
(Kunming, Yunnan)
Kiyoshi HASEGAWA
(Tokyo)
Waseem HASSAN
(Rio de Janeiro)
Langchong HE
(Xi'an, Shaanxi)
Rodney J. Y. HO
(Seattle, WA)
Hsing-Pang HSIEH
(Zhunan, Miaoli)
Yongzhou HU
(Hangzhou, Zhejiang)
Yu HUANG
(Hong Kong)
Hans E. JUNGINGER
(Marburg, Hesse)
Amrit B. KARMARKAR
(Karad, Maharashra)
Toshiaki KATADA
(Tokyo)
Gagan KAUSHAL
(Philadelphia, PA)
Ibrahim S. KHATTAB
(Kuwait)
Shiroh KISHIOKA
(Wakayama, Wakayama)
Robert Kam-Ming KO
(Hong Kong)
Nobuyuki KOBAYASHI
(Nagasaki, Nagasaki)
Norihiro KOKUDO
(Tokyo, Japan)
Toshiro KONISHI
(Tokyo)
Chun-Guang LI
(Melbourne)
Minyong LI
(Ji'nan, Shandong)
Xun LI
(Ji'nan, Shandong)
Jikai LIU
(Kunming, Yunnan)
Xinyong LIU
(Ji'nan, Shandong)
Yuxiu LIU
(Nanjing, Jiangsu)
Hongxiang LOU
(Jinan, Shandong)
Xingyuan MA
(Shanghai)
Ken-ichi MAFUNE
(Tokyo)
Sridhar MANI
(Bronx, NY)
Tohru MIZUSHIMA
(Tokyo)
Abdulla M. MOLOKHIA
(Alexandria)
Yoshinobu NAKANISHI
(Kanazawa, Ishikawa)
Weisan PAN
(Shenyang, Liaoning)
Rakesh P. PATEL
(Mehsana, Gujarat)
Shivanand P. PUTHLI
(Mumbai, Maharashtra)
Shafi qur RAHMAN
(Brookings, SD)
Adel SAKR
(Cairo)
Gary K. SCHWARTZ
(New York, NY)
Yuemao SHEN
(Ji'nan, Shandong)
Brahma N. SINGH
(New York, NY)
Tianqiang SONG
(Tianjin)
Sanjay K. SRIVASTAVA
(Amarillo, TX)
Chandan M. THOMAS
(Bradenton, FL)
Murat TURKOGLU
(Istanbul)
Hui WANG
(Shanghai)
Quanxing WANG
(Shanghai)
Stephen G. WARD
(Bath)
Yuhong XU
(Shanghai)
Bing YAN
(Ji'nan, Shandong)
Yun YEN
(Duarte, CA)
Yasuko YOKOTA
(Tokyo)
Takako YOKOZAWA
(Toyama, Toyama)
Rongmin YU
(Guangzhou, Guangdong)
Guangxi ZHAI
(Ji'nan, Shandong)
Liangren ZHANG
(Beijing)
Lining ZHANG
(Ji'nan, Shandong)
Na ZHANG
(Ji'nan, Shandong)
Ruiwen ZHANG
(Amarillo, TX)
Xiu-Mei ZHANG
(Ji'nan, Shandong)
Yongxiang ZHANG
(Beijing)

(*As of February 2015*)

CONTENTS

Volume 9, Number 1, 2015

Reviews

1 - 12 **Anti-tumor effects and cellular mechanisms of resveratrol.**
Guohua Han, Jufeng Xia, Jianjun Gao, Yoshinori Inagaki, Wei Tang, Norihiro Kokudo

13 - 22 **Oligonol, a low-molecular-weight polyphenol derived from lychee fruit, attenuates gluco-lipotoxicity-mediated renal disorder in type 2 diabetic *db/db* mice.**
Chan Hum Park, Jeong Sook Noh, Hajime Fujii, Seong-Soo Roh, Yeong-Ok Song, Jae Sue Choi, Hae Young Chung, Takako Yokozawa

23 - 32 **Chemical constituents and bioactivities of *Panax ginseng* (C. A. Mey.).**
Wenwen Ru, Dongliang Wang, Yunpeng Xu, Xianxian He, Yang-En Sun, Liyan Qian, Xiangshan Zhou, Yufeng Qin

Original Articles

33 - 37 **Antibiotic-producing bacteria from stag beetle mycangia.**
Atsushi Miyashita, Yuuki Hirai, Kazuhisa Sekimizu, Chikara Kaito

38 - 44 **Tauroursodeoxycholic acid attenuates inorganic phosphateinduced osteoblastic differentiation and mineralization in NIH3T3 fibroblasts by inhibiting the ER stress response PERK-eIF2α-ATF4 pathway.**
Fang Liu, Yazhou Cui, Pinglan Ge, Jing Luan, Xiaoyan Zhou, Jinxiang Han

45 - 52 **Enhanced anticancer activity of 5-FU in combination with Bestatin: Evidence in human tumor-derived cell lines and an H22 tumor-bearing mouse.**
Jin Li, Xuejian Wang, Jinning Hou, Yongxue Huang, Yingjie Zhang, Wenfang Xu

53 - 65 **Anti-metastatic action of anacardic acid targets VEGF-induced signalling pathways in epithelial to mesenchymal transition.**
Puttananjaiah Shilpa, Keshavaiah Kaveri, Bharathi P Salimath

Brief Reports

66 - 69 **Construction of recombinant adenoviral vector carrying *cyclinA2* gene**
Yu Han, Liu Hong, Cuiping Zhong, Jianhua Qiu

CONTENTS (*Continued*)

70 - 74 **Circadian rhythm of serum 25 (OH) vitamin D, calcium and phosphorus levels in the treatment and management of type-2 diabetic patients.**
Tariq Masood, Rajeev S Kushwaha, Ranjana Singh, Shivani Sailwal, Himanshu Pandey, Amit Varma, Raj K Singh, Germaine Cornelissen

Case Report

75 - 77 **Combination chemotherapy with S-1 and docetaxel for cutaneous angiosarcoma resistant to paclitaxel.**
Ikko Kajihara, Hisashi Kanemaru, Taiga Miyake, Jun Aoi, Shinichi Masuguchi, Satoshi Fukushima, Masatoshi Jinnin, Hironobu Ihn

Guide for Authors

Copyright

Review

DOI: 10.5582/ddt.2015.01007

Anti-tumor effects and cellular mechanisms of resveratrol

Guohua Han[1], Jufeng Xia[1], Jianjun Gao[1,2], Yoshinori Inagaki[1], Wei Tang[1,*], Norihiro Kokudo[1]

[1] *Hepato-Biliary-Pancreatic Surgery Division, Department of Surgery, Graduate School of Medicine, The University of Tokyo, Tokyo, Japan;*
[2] *Department of Pharmacology, School of Pharmaceutical Sciences, Qingdao University, Qingdao, Shandong, China.*

Summary **Resveratrol (3, 5, 4'-trihydroxystilbene) is a phytoalexin contained in a variety of plants, such as grapes, berries and especially in the dried roots of *Polygonum cuspidatum* Sieb. et Zucc. It has been shown to exhibit anti-oxidative and anti-inflammation activity, and to reverse the effects of aging. Its ability to suppress cell proliferation, induce apoptosis and suppress the metastasis and invasion in a number of cell lines has prompted a large interest from people for its use as an anti-tumor component. In this review, evidence of resveratrol's anti-tumor effects and molecular mechanisms are recapitulated. First, we present the anti-apoptosis, anti-invasion/metastasis and anti-inflammation effect of resveratrol; second, the main signaling pathways involved in these activities are described and summarized with the studies of different tumors involved. Resveratrol not only induces apoptosis of tumor cells through intrinsic/extrinsic pathways and cell cycle arrest, but also inhibits the invasion and metastasis abilities of tumors *via* modulating collagen degradation-related molecular targets. Altogether, the present findings suggest the anti-tumor potential of resveratrol against various types of cancers.**

Keywords: Resveratrol, anti-tumor, apoptosis, invasion, metastasis, molecular mechanism

1. Introduction

Resveratrol (3, 5, 4' -trihydroxystilbene) is a phytoalexin contained in a variety of plants, such as grapes, peanuts, berries and especially in the dried roots of a traditional Chinese medicine *Polygonum cuspidatum* Sieb. et Zucc (*1,2*). It exists as two geometric isomers: *cis*-(Z) and *trans*-(E) (*3*), and the *trans*-form can undergo isomerization to the *cis*- form when exposed to ultraviolet irradiation (*4*).

Resveratrol has a protective effect in response to stress, injury, ultraviolet irradiation and fungal infection (*1,2*). Previous studies have demonstrated that resveratrol has a number of biological activities and medicinal uses. It has been shown to exhibit anti-oxidative and anti-inflammation activity, and to reverse the effects of aging in rats (*5*). It also has a cardio-protective effect (*6*) that regular moderate consumption of red wine confers less risk of cardiovascular diseases due to its relatively high resveratrol concentration (0.1-14.3 mg/L), widely known as the "French Paradox" (*7*). There are also other effects, which include phytoestrogen activity (*8*), neuro-protective activity (*9*), and antidepressant activity (*10*).

Importantly, as a natural compound, resveratrol has been highly studied for not only the preventive effect for the diseases mentioned above, but also the anti-tumor effect against various cancers. Its ability to suppress cell proliferation, induce apoptosis and suppress metastasis and invasion in a number of cell lines makes resveratrol a natural weapon in the war against cancer (*11*). Cancer is a multistep disease characterized by uncontrolled cell growth and acquisition of metastatic properties (*12*). In this process, the activation of oncogenes and/or the inactivation of tumor suppressor genes lead to cell cycle arrest and apoptotic pathway suppression. Besides, malignant tumors gain metastasis and invasion ability due to the up-regulation of the pro-metastasis genes and pathways, such as Metalloproteinases (MMPs), and down-regulation of anti-metastasis genes, such as phosphatase and tensin homolog deleted on chromosome ten (PTEN). Cancer cells are known to

**Address correspondence to:*
Dr. Wei Tang, Hepato-Biliary-Pancreatic Surgery Division, Department of Surgery, Graduate School of Medicine, The University of Tokyo, 7-3-1 Hongo, Bunkyo-ku, Tokyo 113-8655, Japan.
E-mail: TANG-SUR@h.u-tokyo.ac.jp

have alterations in multiple cellular signaling pathways, and because of the complex communications between these signaling networks, cure of most human cancers remains a great challenge (*11*). The multiple-target regulating effect of resveratrol mentioned above is the molecular basis for its anti-tumor potential.

The health threat brought by cancer is becoming more severe. Cancer is the second leading cause of death after cardiovascular disorders (*11*), and according to World Health Organization (WHO), cancers figure among the leading causes of morbidity and mortality worldwide, with approximately 14 million new cases and 8.2 million cancer related deaths in 2012. Among various kinds of tumor types, the most common causes of cancer death are cancers of: lung, liver, stomach, colorectal, breast and esophageal cancer, and the number of new cancer cases is expected to rise by about 70% over the next two decades.

In this situation, the use of natural compounds of plants in preventing, suppressing or even curing the initiation and progression of malignancy is gaining attention rapidly. Not only because they can influence the processes underlying all three stages of carcinogenesis involving tumor initiation, promotion and progression and suppress angiogenesis and metastasis through regulating different molecular targets (*13*), but also due to their relatively low toxicity (*14*) that are frequently found in the therapy of surgery and chemotherapy. Resveratrol, as one of the most studied dietary compounds, has been demonstrated to interact with molecular targets affecting (anti-) apoptosis (P53, Bax/Bcl-2, Survivin; Caspase-9, 8, 7, 3, PARP), cell cycle (P21, Cyclins, cdks), protein kinases (MAPK, PI3K/AKT, JAK, Wnt), transcription factors (NF-κB, AP-1, Nrf-2), metastasis and invasion (MMP-2, 7, 9, VEGF), and so on (*13*). We discuss the anti-tumor effect and molecular mechanisms (Figure 1) of resveratrol against several cancers mentioned above with the most cancer deaths and both *in vitro* and *in vivo* studies (Table 1), advocating that resveratrol holds enormous potential as an anti-tumor component.

2. Effects of resveratrol on cell proliferation and apoptosis

Apoptosis is a cell death mechanism that may be prompted by several molecular pathways, among which the intrinsic and extrinsic (also known as "death receptor pathway") pathways are the best known (*17*). As it is recognized that a genetically controlled program governed commitment to and execution of apoptosis in a wide range of multicellular organisms, research in understanding the genes and biochemical events responsible for the process of apoptosis have been greatly enhanced (*16*). The discovery of the apoptotic program and the molecular pathways of it have led to development of specific cell-death-targeting therapies, which would allow the development of specific approaches to influence cells by small molecular or protein-based agents to target the apoptotic signaling pathway (*15*) to cure various related diseases including tumors. Resveratrol, as previous studies revealed, is generally a pro-apoptotic agent that could promote the apoptosis process in series of cancers. Here, we separate this part according to several different pathways involved in resveratrol's pro-apoptotic effect.

2.1. *Intrinsic pathway of apoptosis*

The intrinsic pathway is also known as mitochondrial pathway in which pro-apoptotic stimulus affects molecular targets and finally results in an increase of the release of free cytosolic cytochrome *c*, which subsequently leads to apoptosome formation, caspase sequence activation, cleavage of targeting proteins and DNA fragmentation initiating and executing the process of apoptosis (*16*).

In the intrinsic pathway, Bcl-2 and Bax are of great importance. Apoptosis regulator Bax promotes apoptosis by binding to and antagonizing the Bcl-2 protein. The ratio of Bcl-2/Bax protein regulates the sensitivity of cells to apoptosis: the higher this ratio is, the less sensitive the cells are to apoptosis, and the opposite statement is also correct. When stimulated by the pro-apoptotic stimulus, the Bax protein could directly or indirectly interact with and induce the opening of the mitochondrial voltage-dependent anion channel resulting in the release of cytochrome c and other pro-apoptotic factors to promote apoptosis (*25*).

In the MCF-7 breast cancer cell line treated with 10-5 M resveratrol, the reduction of the Bcl-2/Bax ratio through enhancement of p53-dependent transcriptional activity at least partially contributes to resveratrol's pro-apoptotic activity in this research (*19*). A similar effect and mechanism could also be found in MCF-7 and MDA-MB231 breast cancer cells treated with resveratrol where the up-regulation of Bax and p21 resulted from the up- regulation of ASPP1 (apoptosis stimulation protein of p53 1) (*20*). In the prostate cancer cell line LNCaP, resveratrol (5, 10, and 25 μM) induced apoptosis more strongly than other wine polyphenols such as gallic acid, tannic acid and quercetin through significant enhancement of caspase 3 and 7 activity (*21*). It can be seen that the apoptosis of Caco-2 and HCT116 colon cancer cell lines was promoted after treatment with resveratrol (*23*), accompanied with a dose-dependent elevation of the expression of pro-apoptotic proteins cleaved caspase 7, cleaved caspase 9 and cleaved poly (ADP- ribose) polymerase (PARP). The activation of caspase 9 and 7 are crucial steps in apoptosis to induce the cleavage of PARP, a marker of cell apoptosis, to be an early DNA damage response. In other research also studied on these two cell lines, increased Bax/Bcl-2 ratio was found (*24*), suggesting the pro-apoptotic effect of resveratrol

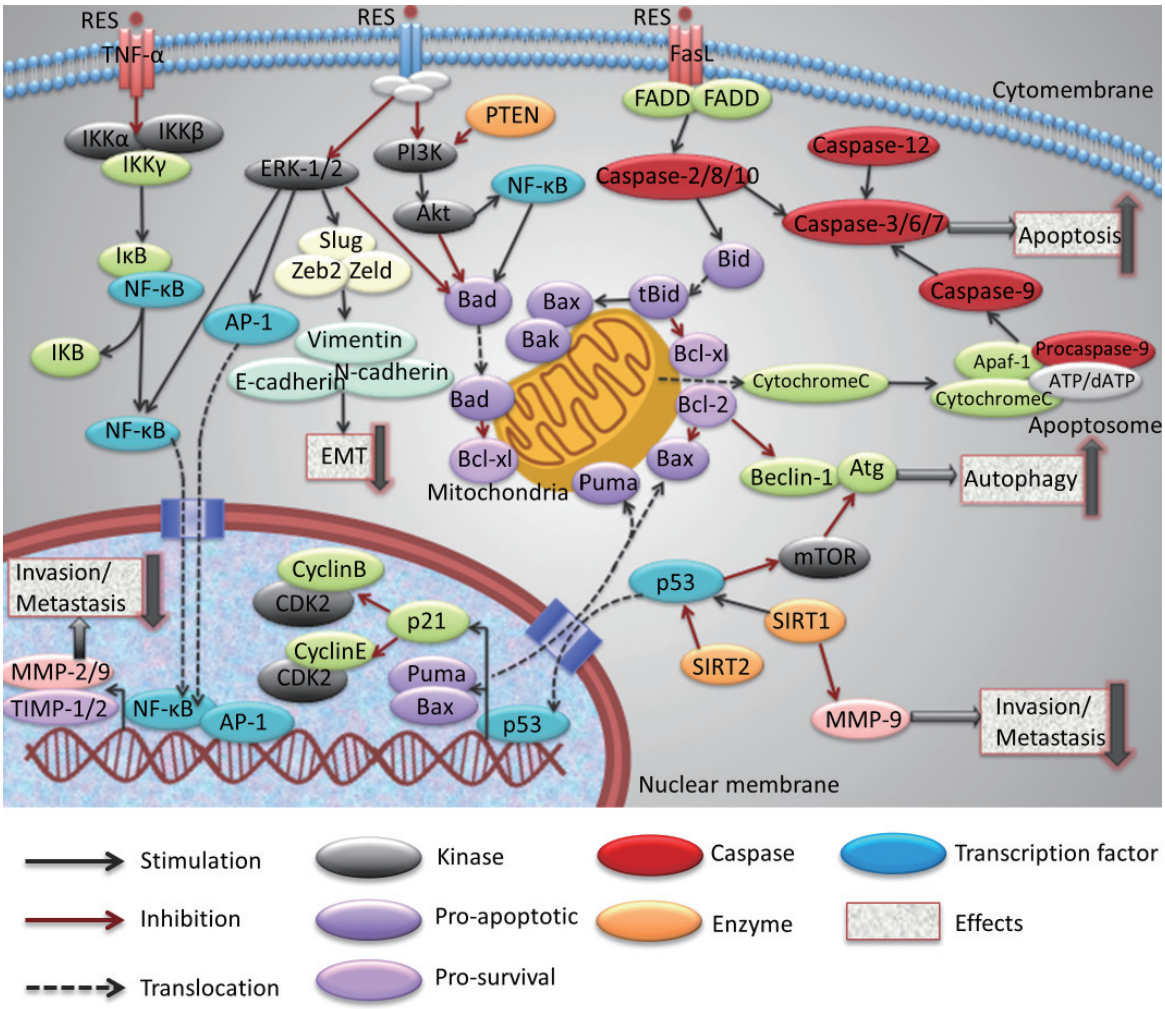

Figure 1. Anti-tumor effects and molecular mechanisms of resveratrol.

through influencing the intrinsic pathway. Treating ASTC-a-1 cells of human lung adenocarcinoma with 100 μM resveratrol (*25*) induced cell apoptosis specifically by intrinsic pathway as proved by the activation of caspase 3 and caspase 9 but not caspase 8 detected by fluorometric assay. A time-dependent loss of mitochondrial membrane potential was detected in combination with changes described above. Apoptosis-inducing factor (AIF) translocation into the nucleus was time-dependently elevated, and the knock down of AIF diminished resveratrol induced apoptosis, showing that in this research caspase 3 and 9 managed to induce apoptosis *via* the activation of AIF.

In vivo studies are consistent with the results derived from the *in vitro* studies. In an N-nitrosodiethylamine (DEN) induced hepatocellular carcinoma (HCC) of male Wistar rats (*26*), treatment with resveratrol either before or after the formation of HCC (20 mg/kg body weight for 15 days, from day 1 of DEN injection or the last two weeks after DEN injection) resulted in a decrease of α-fetoprotein and other known serum markers for HCC, such as aminotransferases, phosphatases, gamma-GT, and LDH. On the tissue level, H&E staining showed a remarkable difference in the tissue architecture compared to the untreated HCC model. Immunoblots showed that resveratrol prompted PARP cleavage, cytochrome *c* release, p53 expressioin and the conversion of procaspase 3 into active caspase 3 in HCC rat models. There was also elevation of Bax expression and drop of Bcl-2 expression at both transcriptional and translational levels. This research not only proved the equal effectiveness of the administration of resveratrol at the early or advanced stages of HCC, but also showed the relatively multilevel effects of this treatment. In another study of resveratrol's anti-cancer effect against HCC, the model was Sprague-Dawley rats with a single injection of diethylnitrosamine (DENA, 200 mg/kg) and subsequent promotion by phenobarbital (0.05%), the pre-administration of resveratrol (50, 100, 300 mg/kg body weight/day) dose-dependently reduced the incidence, total number and multiplicity of visible hepatocyte nodules (*27*). Mean nodule volume and its percentage of liver volume were also inhibited. Histopathological features were ameliorated and immunohistochemical detection revealed an increase of cell apoptosis. Bax expression was up-regulated while Bcl-2 was down-regulated, and

Table 1. Resveratrol against various types of cancer

Tumor types	Cell lines Animal models	Effects	Related mechanisms	*Ref.*
Breast cancer	MCF-7; MDA-MB231; BT474;	Apoptosis↑; Cell cycle arrest↑;	P53↑; P21↑; Bax/Bcl-2↑;	*19,20,38-40*
	4T1(BALB/C mouse model)	Cell proliferation↓; Cell invasion↓; Cell metastasis↓; EMT↓	Mitochondrial membrane potential↓; NF-κB↓; ERα↓; MMP-9↓	*57,66,67,71*
Hepatocellular carcinoma	HepG2; Hep3B; H4IIE;	Apoptosis↑; Cell cycle arrest↑;	Intrinsic/extrinsic apoptosis pathway↑; TIMP-1/2↑;	*18,26,27,*
	DENA-HCC model in SD rats	Cell proliferation↓; Cell invasion↓; Cell metastasis↓; Inflammation ↓	MAPK↓; NF-κB↓; FOXO3A↓; MMP-2/9↓; Hsp70↓; COX-2↓	*34-37,54,55, 59,64,80,81*
Colon cancer	HCT116; Caco-2; HT-29; DLD-1;	Apoptosis↑; Autophagy↑; Cell cycle arrest↑;	Intrinsic/extrinsic apoptosis pathway↑; P53↑;	*22-24,37,58,68, 79*
	SW480; COLO201; Lovo	Cell proliferation↓; Invasion↓; Metastasis↓; Glucose consumption↓	PI3K/AKT↓; ERK1/2↓; Wnt/β-catenin↓; MMP-7↓ NO↓; iNOS↓	
Prostate cancer	LNCaP; C42B; PC3; DU145	Apoptosis↑; Autophagy↑;	Intrinsic apoptosis pathway↑; PTEN↑; SIRT1↑;	*21,56,60,61,72*
		Cell proliferation↓; Invasion↓; Metastasis↓; EMT↓	p-AKT↓; E-cadherin↑ Androgen receptor (AR) ↓	
Lung adenocarcinoma/ NSCLC	ASTC-a-1; A549; H460	Apoptosis↑; Cell cycle arrest↑;	TRAIL receptor1/2↑; P53↑; P21↑; Intrinsic apoptosis pathway↑;	*25,41,42,69,73*
		Cell proliferation↓; Invasion↓; Metastasis↓; EMT↓	NF-κB↓; AP-1↓; MMP-9↓	
Gastric cancer	AGS; BGC-823; SGC-7901	Cell cycle arrest↑; Apoptosis↑; Senescence↑;	P21, P16↑; SIRT1↑;	*43,46*
		Cell proliferation↓; Invasion↓; Metastasis↓	Survivin↓; CyclinD1, CDK4,CDK6↓	
Esophageal cancer	EC109; EC9706; K562	Apoptosis↑; Autophagy↑;	Intrinsic apoptosis pathway↑; P53↑; Bax/Bcl-2↑	*47*
		Cell proliferation↓; Invasion↓; Metastasis↓		

they were demonstrated to be the mechanism of the anti-tumor effect of resveratrol in this HCC model.

As a whole, resveratrol could induce apoptosis in a variety of cancer types including HCC, breast cancer, lung cancer, colon cancer and prostate cancer through the intrinsic pathway of cell apoptosis, that is, some sort of stimulus disrupts the mitochondria membrane potential. This leads to the release of cytochrome *c* activating the caspases, which result in a cleavage of PARP and eventually, DNA fragmentation. Thus the whole process of the intrinsic apoptosis pathway finally causes cell apoptosis.

In order to improve the potency of resveratrol against tumor proliferation, several analogs of resveratrol have been synthesized. HS-1793, one of the analogs, showed stronger antitumor activity than resveratrol (*28*). It acted as a polyploidy inducer in prostate cancer LNCaP cells at a dose at which resveratrol couldn't induce multi-nucleation. During this process, caspase-3 degradation was detected, indicating that HS-1793 reduced the viability of LNCaP cells *via* the caspase-mediated pathway. An increase of p53 expression level was also detected in the polyploidy LNCaP cells. In a study about the higher hydroxylated resveratrol analogs (HHRA) on T cell leukemia Jurkat cells (*29*), the cytotoxic activity of 3, 30, 4, 40-tetrahydroxy-trans-stilbene (M6), 3, 4,

40, 5-tetrahydroxytrans-stilbene (M8) and 3, 30, 4, 40, 5, 50-hexahydroxy-trans-stilbene (M12) were compared with that of resveratrol, with IC_{50} values of 58.4 μM, 48.1 μM, 33.4 μM and 13.8 μM for Res, M6, M8, M12, respectively. Analogs possessing ortho-hydroxyl groups are stronger cytotoxic agents than compounds without this structure. The cytotoxicity was associated with the induction of oxidative stress in cancer cells. In research about the synthetic *cis*-polymethoxystilbenes (methylated analogs of *cis*-resveratrol) (*30*), they inhibited the proliferation and motility of melanoma cells with low micromolar specificity (IC_{50} < 10 μM) in contrast with the fact that both *trans*- and *cis*-resveratrol were ineffective at 10 μM. This effect was accompanied by a decrease of β-tubulin, a marker of metastatic melanoma cells. The increased anti-androgenic activity brought by a methoxy group on the C-4' of resveratrol and its analogs provided a more potent inhibition against prostate cancer cell LNCaP proliferation (*31*). In earlier studies about anti-androgen transcription, resveratrol was used at a concentration of 50 μM or higher, whereas in this study, the analogs were used at a concentration of 10 μM or less. Among them, 49-O-methylresveratrol (3, 5-dihydroxy-49-methoxystilbene) was the most effective one. Its stronger inhibition on Akt phosphorylation, which was related to androgen signaling was the underlying mechanism.

As for the structure-activity relationship, some studies were performed, demonstrating that the positions and numbers of hydroxy and methoxy groups were crucial for the inhibition effect of these components on SW480 and HepG2 tumor cells (*32*). The presence of a hydroxy group in a specific position and the presence of an increased inhibitory effect brought by a methoxy group were found in the analogs with an active tumor inhibition effect. In addition, at least one phenolic group was essential for the antitumor activity. These discoveries provided clues for further synthesis and research about resveratrol analogs against tumor cell proliferation.

2.2. *Extrinsic pathway of apoptosis*

The extrinsic pathway of apoptosis involves transmembrane receptor-mediated interactions, which are also called the TNF-induced (tumor necrosis factor) model and the Fas-Fas ligand-mediated model, both involving receptors of the TNF receptor (TNFR) family coupled to extrinsic signals (*33*). Upon ligand binding, cytoplasmic adapter proteins were recruited and associated with procaspase-8 *via* dimerization of the death effector domain, forming a death-inducing signaling complex (DISC) and resulting in the auto-catalytic activation of procaspase-8 (*34*). Downstream of the extrinsic pathway are the caspase sequence, separated as the initiator caspases, *e.g.* caspase 8, which was mentioned above, and the effector caspases, such as, caspase 3, 6, and 7. Effector caspases are activated by the initiator caspases activated to conduct the cell death program.

When H4IIE rat hepatoma cells are treated with 100 μM resveratrol for up to 24 h, activation of caspase 2 and 8/10 and consequently activation of caspase 3 were seen. No alteration of caspase 9 was detected. DNA fragmentation and formation of apoptotic nuclei were detected which demonstrated the induction of apoptosis by resveratrol in H4IIE cell line through the extrinsic pathway (*18*). In resveratrol treated colon cancer cell line HT-29, a concentration of 150 μM induced apoptosis in a time- dependent manner, and the activity of caspase 8/caspase 3 was increased without alteration of Bax or Bcl-2, which indicated that resveratrol induced apoptosis may be mediated through the death receptor pathway. The underlying mechanism is the enhancement of autophagy induced by resveratrol *via* increasing reactive oxygen species (ROS) production in HT-29, which was proved by the reduction of caspase 8/caspase 3 levels when the blocking of autophagy *via* 3-MA is conducted (*22*). In research on the colon cancer cell line of HCT116 and Caco2, resveratrol (100 μM) significantly activated the extrinsic apoptotic markers, caspase 3 and 8, with down-regulation of c-Myc and leptin (*24*).

In summary, the extrinsic pathway of resveratrol conducted on some cells express Fas or TNF receptors and can lead to apoptosis *via* ligand binding and protein cross-linking Finally, apoptosis is a coordinated and often energy-dependent process that involves the activation of a group of cysteine proteases called "caspases" and a complex cascade of events that link the initiating stimuli to the final demise of the cell (*34*).

2.3. *Apoptosis led by cell cycle arrest: importance of p53 and p21*

Tumor protein p53, also known as p53, is crucial in multicellular organisms, where it regulates the cell cycle and, thus, functions as a tumor suppressor, preventing cancer. P53 has been described as "the guardian of the genome" because of its role in conserving stability by preventing genome mutation. It can activate DNA repair proteins when DNA has sustained damage, or initiate apoptosis – programmed cell death – if DNA damage proves to be irreparable. Activated p53 binds DNA and activates expression of several genes including microRNA miR-34a (*35*), WAF1/CIP1 encoding for p21, a member of cyclin-dependent kinase inhibitor playing a crucial role in cell growth arrest (*36*), and hundreds of other down-stream genes. P21 (WAF1) binds to the G1-S/CDK (CDK1, CDK2 and CDK4/6) complexes (responsible for the G1/S transition in the cell cycle) inhibiting their activity. Many studies demonstrated that the activation of p21 might be due to a p53-dependent pathway (*37*) and p21 has been shown to be essential for p53-mediated G1/S boundary cell-

cycle arrest and cellular senescence triggered by DNA damage (*38*).

In HCC cell line HepG2 treated with 10^{-7} M resveratrol, an up-regulation of endothelial nitric oxide synthase (eNOS) transcription leads to the subsequent activation of p53, causing a G1 and G2/M cell cycle arrest that finally promoted the HepG2 cell apoptosis (*39*). In this research, though not mentioned directly, we can assume that the G1 phase arrest of cell cycle was *via* the p21 activation induced by the activation and elevation of p53 as the mechanisms described previously. As for the cyclins that take control of cell cycle progression, p53 is not the only factor to affect them. For the HepG2 cells that were treated with 200 μM of resveratrol, a decrease in S phase associated with a concomitant increase in G1 phase of cell cycle distribution was found by flow cytometry (*40*). Apoptosis was elevated and the survival pathways, such as p38 MAPK, Akt and Pak1, were down-regulated both in their expression and activity. This was found to be the reason for the decrease of cyclin D1 either by up-regulating p53 or directly influencing cyclin D1 expression and eventually inducing cell cycle arrest and apoptosis, being the upstream regulators of p53 and cyclins. A similar result was also found in HepG2 cells treated with 10 or 20 μg/mL resveratrol for 24h accompanied with an elevation of p21 expression detected by ELISA (*41*), supporting our previous suppositon. In HepG2 and HCT116 (colon cancer) cells, resveratrol also caused p53 elevation and thus increased apoptosis (*42*).

Some of the up and down-stream regulators of this process have been revealed. In breast cancer cell line MCF-7 and MDA-MB231, the elevation of ASPP1, which was induced as the target gene of increased E2F-1, might contribute to the up-regulation of p53 target genes Bax and p21, thereby sensitizing breast cancer cells to resveratrol-induced apoptosis (*20*). In an experiment treating MDA-MB231 cells with resveratrol, the downstream p53-dependent pro-apoptotic genes including *p53*, *c-fos*, *c-jun*, *p21*, *PIG3*, and *BAD* induced by resveratrol were also confirmed (*43*). Upstream of this molecular pathway was also suggested to be resveratrol's binding to integrin αvβ3, which caused subsequent activation of the ERK and/or p38 kinase pathway to finally activate p53 (*45*). In gastric cancer cells like SGC7901, resveratrol induced survivin decrease could also lead to cell cycle arrest, such as G0/G1 phase up-regulation and S, G2/M phase distribution down-regulation (*51*).

As for the role of p53 as a transcription factor, resveratrol could reduce the Bcl-2/Bax ratio through regulating the Bcl-2 and Bax promoters by affecting transcription factors p53 and NF-κB differently: enhancing p53-dependent transcriptional activity and reducing the NF-κB-dependent transcriptional activity (*19*). In A549 non-small cell lung cancer (NSCLC) cells treated with benzopyrene and/or resveratrol, resveratrol down-regulated IKK and NF-κB, causing decrease in the expression of cyclinD1, in which process the up-regulation of p53 and p21 also contributed to it. This finally resulted in G2/M cell cycle arrest and increase of cell apoptosis (*46*).

Some experiments performed on tumor cells revealed two new approaches for p53 and p21 in inducing apoptosis: senescence and autophagy. Resveratrol induced premature senescence was found to be associated with increased expression of p53 and p21 in NSCLC cells (*47*), suggesting that the activation of the p53-p21 pathway may play an important role in resveratrol induced senescence. The senescence was also found to be related to the increase of NAPDH oxidase-5 (NOX-5)-mediated ROS up-regulation, from which we could suppose that it is the increase of ROS induced p53 and p21 overexpression and resulted in the latter effect: senescence. The inducement of senescence by p21 was detected in the gastric cancer cell AGS, too (*48*). Resveratrol inhibited cell viability and clonogenic potential, as well as arrested cell cycle in the G1 phase and led to senescence instead of apoptosis. The underlying mechanisms of this effect is the deregulation of the cell cycle and senescence pathway molecularly, including cyclin D1, CDK4 and 6, p21 and p16, since p21 and p16 signaling pathways could participate in senescence progression mediated by various kinds of stress as demonstrated by previous studies (*49,50*). Treatment with resveratrol on the esophageal squamous cell carcinoma cell line (*52*) resulted in increase of autophagic response, marked by significant elevation of LC3-II in autophagosomes, up-regulation of multiple key autophagosome-regulatory proteins, such as Beclin-1 and ATG5, and the formation of acidic vesicular organelles (AVO), which was consistent with the cell death effect of resveratrol. This was induced through p53 regulation: p53 target-damage-regulated autophagy modulator (DRAM) may regulate autophagy by affecting the fusion of autophagosomes and lysosomes as previously described. This suggested another way of p53 to control the cell apoptosis process.

There also exists some discussion about the dosage of resveratrol leading to cell cycle arrest-related apoptosis. In an experiment treating MDA-MB231 cells with resveratrol, it was found that 10 μM of resveratrol could reduce the percentage of proliferating cells to 33%, and even at a concentration as low as 0.1 μM, resveratrol could also induce more than a 50% decrease in cancer cell numbers compared to control group, which was in contrast to a previous study stating that the IC_{50} values for inhibiting cell growth by resveratrol would be in the range of 5 to 10 μM (*43*). In other research with IC_{50} of 60.5 μM to inhibit cell proliferation of MCF-7 cells (*44*), when treated with 30 μM of resveratrol, cell cycle showed a decrease of G0/G1 phase and G2/M phase

accompanied with an increase in the S phase. When elevating the dose up to 90 μM, there was a decrease of S phase and an increase in G0/G1 phase distribution compared with that of 30 μM, suggesting a biphasic effect of resveratrol on this cell.

Some resveratrol analogs were found to have a stronger growth inhibition effect than resveratrol by inducing cell cycle arrest. Phoyunbene (PYB) (*trans*-3, 4'-dihydroxy-2', 3', 5-trimethoxystilbene) strongly inhibited the growth of HepG2 cells with an IC_{50} of 37.1 μM compared with resveratrol (IC_{50}: 80.3μM) (*48*). The inhibition effect was due to PYB's induction of G2/M cell cycle arrest and apoptosis, which were associated with its up-regulation of cyclinB1 and Bax, as well as the down-regulation of Bcl-2. By the way, in a transwell experiment, it was found that PYB inhibits the invasion of HepG2 cells more strongly than resveratrol. These results support the notion that structure modification of resveratrol can increase its antitumor effects, though the underlying mechanism was not elucidated.

2.4. *Role of SIRT1 in apoptosis*

Mammalian ortholog of the yeast silent information regulator 2 (SIRT1) is a NAD-dependent histone deacetylase belonging to a multigene family of sirtuins that contains 7 members with distinct and diverse functions. SIRT1 can mediate cellular metabolism and energy production through regulation of forkhead box protein O1 (FOXO1) activity and insulin sensitivity and modulate inflammatory responses through NF-κB or cell growth through inhibition of mTOR activity. Besides, SIRT1 can also protect cells from apoptosis in response to genotoxic stress (*54-58*). In contrast, there are some data which indicate that SIRT1 possesses significant tumor suppressor activity. Increased SIRT1 could delay some kinds of tumor progression and protect the body or tissue from various diseases including cancer, cardiovascular abnormalities and metabolic syndrome-associated diseases as previous studies indicated (*59*).

In glucose (2.8, 5.5, and 25 mM)-exposed HepG2 cells, resveratrol treatment (100 μM) suppressed cell proliferation that could be induced by a high glucose concentration of 25 mM (*60*). On the molecular level, resveratrol induced the expression of SIRT1 that further involved the effects of resveratrol on the suppression of p-STAT3 and p-AKT as well as in the cell proliferation of HepG2 under high glucose conditions. The down-regulation of p-STAT3 and p-AKT caused decrease of cyclinD1, VEGF and MMP-9 in this process. In Hep3B cells stably expressing hepatitis B virus (HBV) treated with resveratrol (100 μM), ectopic expression and enhanced activity of SIRT1 were seen, which attenuated JNK phosphorylation, a prerequisite for resistance to oxidative stress-induced apoptosis (*61*). On the other hand, some research indicated that resveratrol might not activate but inhibit SIRT1 signal in HepG2 cells. The inhibition of SIRT1 increased p53 acetylation and enhanced expression of p53 downstream target p21 and activation of caspase-3, finally resulting in the increased S phase arrest of cell cycle and apoptosis. The inhibitory effect of resveratrol on sirtuin 1, which comes from the class III histone deacetylases (HDACs), raised a question of how resveratrol affects other HDAC classes. Research showed that resveratrol functioned as a pan-HDAC inhibitor in HepG2 cells and induced apoptosis.

In prostate cancer cell lines treated with resveratrol, SIRT1 expression enhanced more in androgen-independent prostate cancer cell lines (C42B, PC3, and DU145) than in androgen-responsive (LNCaP) or nontumorigenic prostate cells (RWPE-1), without any significant effect on SIRT1 enzymatic activity (*62*). Inhibition of SIRT1 using a shRNA promoted cell proliferation and inhibited autophagy by down-regulation of p-S6K and 4E-BP1. Resveratrol reversed these effects suggesting that targeting the SIRT1/S6K-mediated inhibition of autophagy represented an effective strategy of prostate cancer prevention. In the breast cancer cell line MCF-7, resveratrol, through P38 MAPK phosphorylation, caused induction of p53 that recruited at the estrogen receptor α proximal promoter to inhibit its expression both in mRNA level and protein level (*63*). The detailed mechanisms were as follows: a specific interaction of p53 and HDAC was found and the latter one was phosphorylated. The tripartite complex p53/Sin3A/HDAC1 together with NF-Y was phosphorylated and enhanced and was correlated with SP-1 and RNA polymerase II release, resulting in the inhibition of cell transcriptional activity including that of estrogen receptor α in breast cancer. In this process, HDAC1 phosphorylation could be critical for the formation of p53 and Sin3A-HDAC1 complexes at the promoter site that involve p53 binding. Also in colon cancer cell lines DLD-1, SW480 and COLO201 treated with resveratrol, SIRT1 was decreased *via* the elevated-miR-34a-induced decrease of its downstream target gene E2F3, accompanied by an inhibition of PI3K/Akt as the upstream modulator of miR-34a (*64*). These resulted in an induction of apoptosis in colon cancer cells. In prostate cancer cell line DU145 and PC3M, resveratrol inhibited the metastasis associated protein1 (MTA1)/HDAC unit that was indicated to be a negative regulator of PTEN (*67*). Thus acetylated PTEN was able to accumulate in the nucleus and rehabilitate resulting in diminished p-Akt levels, which facilitated inhibition of prostate cancer. The bilateral effect of SIRT1, as a tumor promoter or a tumor suppressor, need to be studied more to figure out the exact mechanisms or prerequisites to determine which effect SIRT1 performs, further supporting the anti-tumor potential application in the future.

2.5. *Other molecular events inducing apoptosis*

In the DENA-initiated hepatocarcinogenesis model of SD rats, the decease of myosin light chain kinase (MLCK) was found to be associated with the induction of apoptosis by resveratrol (*65*), saying that MLCK might be implicated in the formation of integrin-positive adhesive structures. However, further studies are needed to demonstrate how these kinases mediate integrin-dependent functions. In prostate cancer cells PC3, resveratrol-evoked cytosolic free Ca^{2+} concentration increases concentration-dependently by evoking phospholipase C-independent Ca^{2+} release from the endoplasmic reticulum and Ca^{2+} entry *via* protein kinase C-regulated mechanisms (*66*). A low dose of resveratrol (1-10 μM) caused Ca^{2+} dependent cell proliferation, while at higher concentration it caused cell death, suggesting that in PC3 cells, resveratrol had a dual effect on cell viability.

3. Effects of resveratrol on tumor metastasis and invasion

3.1. *Resveratrol affects the expression and activity of MMPs*

The invasion and metastasis of cancer cells involve degradation of the environmental extracellular matrix (ECM) and basement membrane. This process is conducted through vatious proteolytic enzymes, such as Matrix metallopeptidase (MMPs). Among these enzymes, MMP-2 and MMP-9 are overexpressed in various malignant tumors to modulate cell invasion and metastasis (*68*). Both MMP-2 and MMP-9 enzymes are activated and capable of degrading type IV collagen, which is a major constituent of the basement membrane to ease cell mobility. On the other hand, tissue inhibitor metalloproteinase proteins (TIMPs) are a group of proteins consisting of TIMP-1, -2, -3 and -4 acting as natural MMP inhibitors (*69*). The effects of resveratrol on these molecular targets are summarized.

When treated with resveratrol (0-50 μM), the migration and invasion ability of phorbo-12-myristate 13-acetate (PMA)-treated HepG2 and Hep3B cell lines of HCC were both reduced in a dose-dependent manner. In HepG2 cells, the down-regulation of MMP-9 activity and up-regulation of TIMP-1 protein expression were found and in Hep3B cells, both the MMP-2 and MMP-9 activities were decreased accompanied with an increase in the protein expression level of TIMP-2 (*70*). These results suggested that resveratrol might exert anti-invasive and anti-migratory ability against hepatoma cells through regulation of MM-2, MMP-9, TIMP-1 and TIMP-2 activity and expression. In the process of regulating MMP-9, NF-κB was found to play an important role. The TNF-treated HepG2 cells expressed a high level of MMP-9, which was significantly suppressed by resveratrol through down-regulation of NF-κB expression resulting in downstream MMP-9 protein expression decrease and inhibition of invasion ability of HepG2 cells (*71*).

In breast cancer cell line MDA-MB231, resveratrol treatment (5 μM) inhibited the epidermal growth factor (EGF)-induced elevation of cell migration as well as expression of MMP-9. A subunit of the mammalian mediator complex for transcription called MED28, the overexpression of which could increase migration, was also reduced by resveratrol through the EGFR/PI3K signaling pathway (*72*). The *in vivo* research of breast cancer also confirmed the effect of inhibition of MMP-9 in the anti-metastasis process. BALB/c mice were injected with 4T1 cells with orally administered various concentrations of resveratrol (0, 100, 200 mg/kg body weight) (*73*). The numbers of pulmonary nodules were significantly decreased with a decreased plasma MMP-9 activity in response to the resveratrol treatment. A similar result was found in colorectal cancer cells LoVo and metastatic lung cancer cells A549 treated with resveratrol, resulting in invasion and metastasis inhibition (*74,75*). All together, resveratrol could inhibit invasion and metastasis both *in vitro* and *in vivo* through down-regulating the expression and activity of MMP-9.

3.2. *Resveratrol affects EMT*

Epithelial-to-mesenchymal transition (EMT) is thought to be a pivotal event in the initial step of the metastatic cascade allowing cells to acquire migratory, invasive and stem cell-like properties (*76*). Resveratrol has a significant effect on the process of EMT.

Resveratrol inhibits EGF induced EMT in breast cancer cell line MCF-7 through repressing EGF induced ERK activation (*77*), which resulted in the failure of EGF altering cell morphology, motility and EMT markers (Vimentin and N-cadherin) up-regulation. Transcription factors (Slug, Zeb1 and Zeb2) increased in EMT were also inhibited. Prostate cancer cells PC3 and LNCaP also experienced an EMT inhibition induced by resveratrol with a down-regulation of glioma-associated oncogene homolog 1 (Glil1), suggesting that the inhibition effect was realized through the Hedgehog signaling pathway (*78*). These provided a novel perspective on the role of resveratrol in preventing cancer progression as an EMT inhibitor. Experiments on the lung cancer cell line A549 also supported this conclusion (*79*).

Some studies suggested that we might not view the MMPs expression and the EMT process as separated parts. Over-expression of MMP-9 in A431-III cells might directly induce (or stimulate) EMT and the transcriptional factor, Snail, could cooperatively engage in this phenomenon as proved by using small interference RNA and MMP inhibitors (*70*). The up-regulation of MMP-2 and MMP-9 might initiate and

maintain long-term EMT (*80,81*). Considering their interactions and relationship, resveratrol's inhibition effect of them could be placed as a more important priority as an anti-cancer component.

4. Effects of resveratrol on inflammation

As previously mentioned, resveratrol has anti-oxidation, and anti-inflammation effects. An expending body of evidence suggests that inflammation-mediated processes, including the production of cytokines, chemokines, and reactive oxygen and nitrogen species may contribute to malignant cell transformation (*82,83*). A variety of studies have accumulated insights into the role of inflammation and oxidation in initiation, promotion and progression of cancers. In the process of tumor promotion activity by inflammation, components of the tumor microenvironment, such as tumor cells, stromal cells and infiltrated inflammatory/ immune cells generate an inflammatory state through proinflammatory expression and activation at an abnormal level. Many proinflammatory mediators, especially cytokines, and chemokines turn on the angiogenic switches mainly controlled by vascular endothelial growth factor, thus initiating inflammatory angiogenesis. This ends up with tumor angiogenesis, metastasis and invasion, upregulating the malignancy level of tumors (*82*).

Resveratrol can inhibit the inflammation response of colon cancer cell lines Caco-2 and SW480 induced by lipopolysaccharide (LPS) *via* inhibition of the NF-κB signaling pathway. Though the detailed mechanisms still need to be studied, it can be supposed that resveratrol inhibits NF-κB through a direct action on the nuclear transcription factor *via* phosphorylation inhibition, or by TLR-4 down-regulation (*84*).

The anti-inflammation effect of resveratrol was supported by research *in vivo* as well. In the DENA induced HCC model in SD rats, a 20-week administration of resveratrol (50, 100, 300 mg/kg) was shown to inhibit hepatocyte nodules in a dose-dependent manner (*85*) through the down-regulation of HSP70 and COX-2 expression by attenuating the translocation of NF-κB from the cytoplasm to the nucleus. In another study with the same administered dose of resveratrol, it was also found that the level and expression of hepatic TNF-α, IL-1β and IL-6 induced by DENA was reversed (*86,87*). Thus resveratrol mediated an anti-tumor effect of rat liver tumor *via* alteration of proinflammatory cytokines.

There was also research concerning resveratrol analogs that showed more activity in inhibiting inflammation. Polyhydroxy and polymethoxy substituted analogs of resveratrol were synthesized and some of them exhibited more potent anti-tumor and anti-inflammatory effects, such as hexahydroxystilbene (M8)'s down-regulating COX-2 and inducing apoptosis with a much lower concentration than resveratrol (*88*). A structure-activity study showed that increasing the number of OH groups and their position on the phenol ring could increase the ability of free radical scavenging, and the orthosemiquinones formed during metabolism or autoxidation enabled the analogs to have a stronger cytotoxic effect.

5. Conclusions

The current evidence for anti-tumor effects of resveratrol in certain types of cancers, including lung, liver, stomach, colorectal, breast and esophageal cancer, assessed with *in vitro* and *in vivo* research is reported. Resveratrol exhibits the anti-tumor effect through modulation of the apoptotic pathways, such as intrinsic pathway, extrinsic pathway, cell cycle arrest pathway and the pathways affecting SIRT, and also the pathways regulating cell invasion and metastasis abilities. In addition, the resveratrol anti-inflammatory effect is of great significance in the inhibition of tumor initiation and progression. The results obtained in the present research, in which resveratrol was evaluated as an anti-cancer natural component, are encouraging. However, further study is needed to define the effectiveness of resveratrol in the prevention and treatment of these cancers. Pharmacokinetic studies of resveratrol have revealed its poor bioavailability, which urge research on resveratrol analogs that could improve the beneficial effects. Research showed that proper structural change of chemical groups, such as the OH group, might increase the antitumor effect. These analogs have shown enhanced ability of anti-proliferation, anti-invasion and anti-inflammation. The anti-tumor effects of resveratrol analogs and the studies about the structure-activity relationship of them have brightened the future of resveratrol's application in cancer therapeutics and their transfer into clinical applications. Even if there are still unknown facts and unsolved problems to be faced, we can conclude that resveratrol holds promising anti-tumor potential against various cancers and it deserves further research and evaluation in the future.

References

1. Soleas GJ, Diamandis EP, Goldberg DM. Wine as a biological fluid: history, production, and role in disease prevention. J Clin Lab Anal. 1997; 11:287-313.
2. Hu Y, Wang S, Wu X, Zhang J, Chen R, Chen M, Wang Y. Chinese herbal medicine-derived compounds for cancer therapy: a focus on hepatocellular carcinoma. J Ethnopharmacol. 2013; 149:601-612.
3. Camont L, Cottart CH, Rhayem Y, Nivet-Antoine V, Djelidi R, Collin F, Beaudeux JL, Bonnefont-Rousselot D. Simple spectrophotometric assessment of the *trans-/cis*-resveratrol ratio in aqueous solutions. Anal Chim Acta. 2009; 634:121-128.
4. Lamuela-Raventos RM, Romero-Perez RI, Waterhouse AL, de la Torre-Boronat MC. Direct HPLC analysis of *cis*- and *trans*-resveratrol and piceid isomers in Spanish red

Vitis vinifera wines. J Agric Food Chem. 1995; 43:281-283.
5. Sato D, Shimizu N, Shimizu Y, Akagi M, Eshita Y, Ozaki S, Nakajima N, Ishihara K, Masuoka N, Hamada H, Shimoda K, Kubota N. Synthesis of glycosides of resveratrol, pterostilbene, and piceatannol, and their anti-oxidant, anti-allergic, and neuroprotective activities. Biosci Biotechnol Biochem. 2014; 78:1123-1128.
6. Lamont KT, Somers S, Lacerda L, Opie LH, Lecour S. Is red wine a SAFE sip away from cardioprotection? Mechanisms involved in resveratrol- and melatonin-induced cardioprotection. J Pineal Res. 2011; 50:374-380.
7. Carter LG, D'Orazio JA, Pearson KJ. Resveratrol and cancer: focus on *in vivo* evidence. Endocr Relat Cancer. 2014; 21:R209-225.
8. Gehm BD, McAndrews JM, Chien PY, Jameson JL. Resveratrol, a polyphenolic compound found in grapes and wine, is an agonist for the estrogen receptor. Proc Natl Acad Sci U S A. 1997; 94:14138-14143.
9. Villaflores OB, Chen YJ, Chen CP, Yeh JM, Wu TY. Curcuminoids and resveratrol as anti-Alzheimer agents. Taiwan J Obstet Gynecol. 2012; 51:515-525.
10. Hurley LL, Akinfiresoye L, Kalejaiye O, Tizabi Y. Antidepressant effects of resveratrol in an animal model of depression. Behav Brain Res. 2014; 268:1-7.
11. Shukla Y, Singh R. Resveratrol and cellular mechanisms of cancer prevention. Ann N Y Acad Sci. 2011; 1215:1-8.
12. Sarkar S, Horn G, Moulton K, Oza A, Byler S, Kokolus S, Longacre M. Cancer development, progression, and therapy: an epigenetic overview. Int J Mol Sci. 2013; 14:21087-21113.
13. Liu BL, Zhang X, Zhang W, Zhen HN. New enlightenment of French Paradox: resveratrol's potential for cancer chemoprevention and anti-cancer therapy. Cancer Biol Ther. 2007; 6:1833-1836.
14. Williams LD, Burdock GA, Edwards JA, Beck M, Bausch J. Safety studies conducted on high-purity *trans*-resveratrol in experimental animals. Food Chem Toxicol. 2009; 47:2170-2182.
15. Degterev A, Yuan J. Expansion and evolution of cell death programmes. Nat Rev Mol Cell Biol. 2008; 9:378-390.
16. Letai AG. Diagnosing and exploiting cancer's addiction to blocks in apoptosis. Nat Rev Cancer. 2008; 8:121-132.
17. Juan ME, Alfaras I, Planas JM. Colorectal cancer chemoprevention by trans-resveratrol. Pharmacol Res. 2012; 65:584-591.
18. Michels G, Wätjen W, Weber N, Niering P, Chovolou Y, Kampkötter A, Proksch P, Kahl R. Resveratrol induces apoptotic cell death in rat H4IIE hepatoma cells but necrosis in C6 glioma cells. Toxicology. 2006; 225:173-182.
19. Sakamoto T, Horiguchi H, Oguma E, Kayama F. Effects of diverse dietary phytoestrogens on cell growth, cell cycle and apoptosis in estrogen-receptor-positive breast cancer cells. J Nutr Biochem. 2010; 21:856-864.
20. Shi Y, Yang S, Troup S, Lu X, Callaghan S, Park DS, Xing Y, Yang X. Resveratrol induces apoptosis in breast cancer cells by E2F1-mediated up-regulation of ASPP1. Oncol Rep. 2011; 25:1713-1719.
21. Ferruelo A, Romero I, Cabrera PM, Arance I, Andrés G, Angulo JC. Effects of resveratrol and other wine polyphenols on the proliferation, apoptosis and androgen receptor expression in LNCaP cells. Actas Urol Esp. 2014; 38:397-404.
22. Miki H, Uehara N, Kimura A, Sasaki T, Yuri T, Yoshizawa K, Tsubura A. Resveratrol induces apoptosis *via* ROS-triggered autophagy in human colon cancer cells. Int J Oncol. 2012; 40:1020-1028.
23. Liu B, Zhou Z, Zhou W, Liu J, Zhang Q, Xia J, Liu J, Chen N, Li M, Zhu R. Resveratrol inhibits proliferation in human colorectal carcinoma cells by inducing G1/S-phase cell cycle arrest and apoptosis through caspase/cyclin-CDK pathways. Mol Med Rep. 2014; 10:1697-1702.
24. Fouad MA, Agha AM, Merzabani MM, Shouman SA. Resveratrol inhibits proliferation, angiogenesis and induces apoptosis in colon cancer cells: calorie restriction is the force to the cytotoxicity. Hum Exp Toxicol. 2013; 32:1067-1080.
25. Zhang W, Wang X, Chen T. Resveratrol induces mitochondria-mediated AIF and to a lesser extent caspase-9-dependent apoptosis in human lung adenocarcinoma ASTC-a-1 cells. Mol Cell Biochem. 2011; 354:29-37.
26. Rajasekaran D, Elavarasan J, Sivalingam M, Ganapathy E, Kumar A, Kalpana K, Sakthisekaran D. Resveratrol interferes with N-nitrosodiethylamine-induced hepatocellular carcinoma at early and advanced stages in male Wistar rats. Mol Med Rep. 2011; 4:1211-1217.
27. Bishayee A, Dhir N. Resveratrol-mediated chemoprevention of diethylnitrosamine-initiated hepatocarcinogenesis: inhibition of cell proliferation and induction of apoptosis. Chem Biol Interact. 2009; 179:131-144.
28. Jeong NY, Yoon YG, Rho JH, Lee JS, Lee SY, Yoo KS, Song S, Suh H, Choi YH, Yoo YH. The novel resveratrol analog HS-1793-induced polyploid LNCaP prostate cancer cells are vulnerable to downregulation of Bcl-xL. Int J Oncol. 2011; 38:1597-1604.
29. Kucinska M, Piotrowska H, Luczak MW, Mikula-Pietrasik J, Ksiazek K, Wozniak M, Wierzchowski M, Dudka J, Jäger W, Murias M. Effects of hydroxylated resveratrol analogs on oxidative stress and cancer cells death in human acute T cell leukemia cell line: prooxidative potential of hydroxylated resveratrol analogs. Chem Biol Interact. 2014; 209:96-110.
30. Morris VL, Toseef T, Nazumudeen FB, Rivoira C, Spatafora C, Tringali C, Rotenberg SA. Anti-tumor properties of cis-resveratrol methylated analogs in metastatic mouse melanoma cells. Mol Cell Biochem. 2015; 402:83-91.
31. Iguchi K, Toyama T, Ito T, Shakui T, Usui S, Oyama M, Iinuma M, Hirano K. Antiandrogenic activity of resveratrol analogs in prostate cancer LNCaP cells. J Androl. 2012; 33:1208-1215.
32. Chalal M, Delmas D, Meunier P, Latruffe N, Vervandier-Fasseur D. Inhibition of cancer derived cell lines proliferation by synthesized hydroxylated stilbenes and new ferrocenyl-stilbene analogs. Comparison with resveratrol. Molecules. 2014; 19:7850-7868.
33. Wajant H. The Fas signaling pathway: more than a paradigm. Science. 2002; 296:1635-1636.
34. Elmore S. Apoptosis: a review of programmed cell death. Toxicol Pathol. 2007; 35:495-516.
35. Mraz M, Malinova K, Kotaskova J, Pavlova S, Tichy B, Malcikova J, Stano Kozubik K, Smardova J, Brychtova Y, Doubek M, Trbusek M, Mayer J, Pospisilova S. miR-34a, miR-29c and miR-17-5p are downregulated in CLL patients with TP53 abnormalities. Leukemia. 2009; 23:1159-1163.
36. Gartel AL, Tyner AL. The role of the cyclin-dependent kinase inhibitor p21 in apoptosis. Mol Cancer Ther. 2002; 1:639-649.

37. Tschaharganeh DF, Xue W, Calvisi DF, *et al*. p53-dependent Nestin regulation links tumor suppression to cellular plasticity in liver cancer. Cell. 2014; 158:579-592.
38. Valente LJ, Gray DH, Michalak EM, Pinon-Hofbauer J, Egle A, Scott CL, Janic A, Strasser A. p53 efficiently suppresses tumor development in the complete absence of its cell-cycle inhibitory and proapoptotic effectors p21, Puma, and Noxa. Cell Rep. 2013; 3:1339-1345.
39. Notas G, Nifli AP, Kampa M, Vercauteren J, Kouroumalis E, Castanas E. Resveratrol exerts its antiproliferative effect on HepG2 hepatocellular carcinoma cells, by inducing cell cycle arrest, and NOS activation. Biochim Biophys Acta. 2006; 1760:1657-1666.
40. Parekh P, Motiwale L, Naik N, Rao KV. Downregulation of cyclin D1 is associated with decreased levels of p38 MAP kinases, Akt/PKB and Pak1 during chemopreventive effects of resveratrol in liver cancer cells. Exp Toxicol Pathol. 2011; 63:167-173.
41. Kuo PL, Chiang LC, Lin CC. Resveratrol-induced apoptosis is mediated by p53-dependent pathway in Hep G2 cells. Life Sci. 2002; 72:23-34.
42. Amiri F, Zarnani AH, Zand H, Koohdani F, Jeddi-Tehrani M, Vafa M. Synergistic anti-proliferative effect of resveratrol and etoposide on human hepatocellular and colon cancer cell lines. Eur J Pharmacol. 2013; 718:34-40.
43. Chin YT, Hsieh MT, Yang SH, *et al*. Anti-proliferative and gene expression actions of resveratrol in breast cancer cells *in vitro*. Oncotarget. 2014; 5:12891-12907.
44. Fernández-Pérez F, Belchí-Navarro S, Almagro L, Bru R, Pedreño MA, Gómez-Ros LV. Cytotoxic effect of natural *trans*-resveratrol obtained from elicited *Vitis vinifera* cell cultures on three cancer cell lines. Plant Foods Hum Nutr. 2012; 67:422-429.
45. Hsieh TC, Wong C, John Bennett D, Wu JM. Regulation of p53 and cell proliferation by resveratrol and its derivatives in breast cancer cells: an *in silico* and biochemical approach targeting integrin αvβ3. Int J Cancer. 2011; 129:2732-2743.
46. Ulasli SS, Celik S, Gunay E, Ozdemir M, Hazman O, Ozyurek A, Koyuncu T, Unlu M. Anticancer effects of thymoquinone, caffeic acid phenethyl ester and resveratrol on A549 non-small cell lung cancer cells exposed to benzo(a)pyrene. Asian Pac J Cancer Prev. 2013; 14:6159-6164.
47. Luo H, Yang A, Schulte BA, Wargovich MJ, Wang GY. Resveratrol induces premature senescence in lung cancer cells *via* ROS-mediated DNA damage. PLoS One. 2013; 8: e60065.
48. Wang G, Guo X, Chen H, Lin T, Xu Y, Chen Q, Liu J, Zeng J, Zhang XK, Yao X. A resveratrol analog, phoyunbene B, induces G2/M cell cycle arrest and apoptosis in HepG2 liver cancer cells. Bioorg Med Chem Lett. 2012; 22:2114-2118.
49. Yang Q, Wang B, Zang W, Wang X, Liu Z, Li W, Jia J. Resveratrol inhibits the growth of gastric cancer by inducing G1 phase arrest and senescence in a Sirt1-dependent manner. PLoS One. 2013; 8:e70627.
50. Papazoglu C, Mills AA. p53: at the crossroad between cancer and ageing. J Pathol. 2007; 211:124-133.
51. Kim WY, Sharpless NE. The regulation of *INK4/ARF* in cancer and aging. Cell. 2006; 127:265-275.
52. Liu ML, Zhang SJ. Effects of resveratrol on the protein expression of survivin and cell apoptosis in human gastric cancer cells. J BUON. 2014; 19:713-717.
53. Tang Q, Li G, Wei X, Zhang J, Chiu JF, Hasenmayer D, Zhang D, Zhang H. Resveratrol-induced apoptosis is enhanced by inhibition of autophagy in esophageal squamous cell carcinoma. Cancer Lett. 2013; 336:325-337.
54. Rahman S, Islam R. Mammalian Sirt1: insights on its biological functions. Cell Commun Signal. 2011; 9:11.
55. Cantó C, Auwerx J. PGC-1alpha, SIRT1 and AMPK, an energy sensing network that controls energy expenditure. Curr Opin Lipidol. 2009; 20:98-105.
56. Sun C, Zhang F, Ge X, Yan T, Chen X, Shi X, Zhai Q. SIRT1 improves insulin sensitivity under insulin-resistant conditions by repressing PTP1B. Cell Metab. 2007; 6:307-319.
57. Hariharan N, Maejima Y, Nakae J, Paik J, Depinho RA, Sadoshima J. Deacetylation of FoxO by Sirt1 plays an essential role in mediating starvation-induced autophagy in cardiac myocytes. Circ Res. 2010; 107:1470-1482.
58. Ghosh HS, McBurney M, Robbins PD. SIRT1 negatively regulates the mammalian target of rapamycin. PLoS One. 2010; 5:e9199.
59. Chung S, Yao H, Caito S, Hwang JW, Arunachalam G, Rahman I. Regulation of SIRT1 in cellular functions: role of polyphenols. Arch Biochem Biophys. 2010; 501:79-90.
60. Li Y, Zhu W, Li J, Liu M, Wei M. Resveratrol suppresses the STAT3 signaling pathway and inhibits proliferation of high glucose-exposed HepG2 cells partly through SIRT1. Oncol Rep. 2013; 30:2820-2828.
61. Srisuttee R, Koh SS, Malilas W, Moon J, Cho IR, Jhun BH, Horio Y, Chung YH. SIRT1 sensitizes hepatocellular carcinoma cells expressing hepatitis B virus X protein to oxidative stress-induced apoptosis. Biochem Biophys Res Commun. 2012; 429:45-50.
62. Li G, Rivas P, Bedolla R, Thapa D, Reddick RL, Ghosh R, Kumar AP. Dietary resveratrol prevents development of high-grade prostatic intraepithelial neoplastic lesions: involvement of SIRT1/S6K axis. Cancer Prev Res (Phila). 2013; 6:27-39.
63. De Amicis F, Giordano F, Vivacqua A, Pellegrino M, Panno ML, Tramontano D, Fuqua SA, Andò S. Resveratrol, through NF-Y/p53/Sin3/HDAC1 complex phosphorylation, inhibits estrogen receptor alpha gene expression *via* p38MAPK/CK2 signaling in human breast cancer cells. FASEB J. 2011; 25:3695-3707.
64. Kumazaki M, Noguchi S, Yasui Y, Iwasaki J, Shinohara H, Yamada N, Akao Y. Anti-cancer effects of naturally occurring compounds through modulation of signal transduction and miRNA expression in human colon cancer cells. J Nutr Biochem. 2013; 24:1849-1858.
65. Zhang XL, Yu H, Xiong YY, Ma ST, Zhao L, She SF. Resveratrol down-regulates Myosin light chain kinase, induces apoptosis and inhibits diethylnitrosamine-induced liver tumorigenesis in rats. Int J Mol Sci. 2013; 14:1940-1951.
66. Chang HT, Chou CT, Chen IL, Liang WZ, Kuo DH, Huang JK, Shieh P, Jan CR. Mechanisms of resveratrol-induced changes in [Ca(2+)]i and cell viability in PC3 human prostate cancer cells. J Recept Signal Transduct Res. 2013; 33:298-303.
67. Dhar S, Kumar A, Li K, Tzivion G, Levenson AS. Resveratrol regulats PTEN/Akt pathway through inhibition of MTA1/HDAC unit of the NuRD complex in prostate cancer. Biochim Biophys Acta. 2015; 1853:265-275.
68. Nelson AR, Fingleton B, Rothenberg ML, Matrisian LM. Matrix metalloproteinases: biologic activity and clinical implications. J Clin Oncol. 2000; 18:1135-1149.

69. Jinga DC, Blidaru A, Condrea I, Ardeleanu C, Dragomir C, Szegli G, Stefanescu M, Matache C. MMP-9 and MMP-2 gelatinases and TIMP-1 and TIMP-2 inhibitors in breast cancer: correlations with prognostic factors. J Cell Mol Med. 2006; 10:499-510.
70. Lin CY, Tsai PH, Kandaswami CC, Lee PP, Huang CJ, Hwang JJ, Lee MT. Matrix metalloproteinase-9 cooperates with transcription factor Snail to induce epithelial-mesenchymal transition. Cancer Sci. 2011; 102:815-827.
71. Yu H, Pan C, Zhao S, Wang Z, Zhang H, Wu W. Resveratrol inhibits tumor necrosis factor-alpha-mediated matrix metalloproteinase-9 expression and invasion of human hepatocellular carcinoma cells. Biomed Pharmacother. 2008; 62:366-372.
72. Lee MF, Pan MH, Chiou YS, Cheng AC, Huang H. Resveratrol modulates MED28 (Magicin/EG-1) expression and inhibits epidermal growth factor (EGF)-induced migration in MDA-MB-231 human breast cancer cells. J Agric Food Chem. 2011; 59:11853-11861.
73. Lee HS, Ha AW, Kim WK. Effect of resveratrol on the metastasis of 4T1 mouse breast cancer cells *in vitro* and *in vivo*. Nutr Res Pract. 2012; 6:294-300.
74. Ji Q, Liu X, Fu X, Zhang L, Sui H, Zhou L, Sun J, Cai J, Qin J, Ren J, Li Q. Resveratrol inhibits invasion and metastasis of colorectal cancer cells *via* MALAT1 mediated Wnt/ β-catenin signal pathway. PLoS One. 2013; 8: e78700.
75. Kim YS, Sull JW, Sung HJ. Suppressing effect of resveratrol on the migration and invasion of human metastatic lung and cervical cancer cells. Mol Biol Rep. 2012; 39:8709-8716.
76. Thiery JP, Sleeman JP. Complex networks orchestrate epithelial-mesenchymal transitions. Nat Rev Mol Cell Biol. 2006; 7:131-142.
77. Vergara D, Valente CM, Tinelli A, Siciliano C, Lorusso V, Acierno R, Giovinazzo G, Santino A, Storelli C, Maffia M. Resveratrol inhibits the epidermal growth factor-induced epithelial mesenchymal transition in MCF-7 cells. Cancer Lett. 2011; 310:1-8.
78. Li J, Chong T, Wang Z, Chen H, Li H, Cao J, Zhang P, Li H. A novel anti-cancer effect of resveratrol: reversal of epithelial-mesenchymal transition in prostate cancer cells. Mol Med Rep. 2014; 10:1717-1724.
79. Wang H, Zhang H, Tang L, Chen H, Wu C, Zhao M, Yang Y, Chen X, Liu G. Resveratrol inhibits TGF-β1-induced epithelial-to-mesenchymal transition and suppresses lung cancer invasion and metastasis. Toxicology. 2013; 303:139-146.
80. Qiao B, Johnson NW, Gao J. Epithelial-mesenchymal transition in oral squamous cell carcinoma triggered by transforming growth factor-beta1 is Snail family-dependent and correlates with matrix metalloproteinase-2 and -9 expressions. Int J Oncol. 2010; 37:663-668.
81. Lamouille S, Xu J, Derynck R. Molecular mechanisms of epithelial-mesenchymal transition. Nat Rev Mol Cell Biol. 2014; 15:178-196.
82. Kundu JK, Surh YJ. Inflammation: gearing the journey to cancer. Mutat Res. 2008; 659:15-30.
83. Allavena P, Germano G, Marchesi F, Mantovani A. Chemokines in cancer related inflammation. Exp Cell Res. 2011; 317:664-673.
84. Panaro MA, Carofiglio V, Acquafredda A, Cavallo P, Cianciulli A. Anti-inflammatory effects of resveratrol occur *via* inhibition of lipopolysaccharide-induced NF-κB activation in Caco-2 and SW480 human colon cancer cells. Br J Nutr. 2012; 108:1623-1632.
85. Bishayee A, Waghray A, Barnes KF, Mbimba T, Bhatia D, Chatterjee M, Darvesh AS. Suppression of the inflammatory cascade is implicated in resveratrol chemoprevention of experimental hepatocarcinogenesis. Pharm Res. 2010; 27:1080-1091.
86. Mbimba T, Awale P, Bhatia D, Geldenhuys WJ, Darvesh AS, Carroll RT, Bishayee A. Alteration of hepatic proinflammatory cytokines is involved in the resveratrol-mediated chemoprevention of chemically-induced hepatocarcinogenesis. Curr Pharm Biotechnol. 2012; 13:229-234.
87. Luther DJ, Ohanyan V, Shamhart PE, Hodnichak CM, Sisakian H, Booth TD, Meszaros JG, Bishayee A. Chemopreventive doses of resveratrol do not produce cardiotoxicity in a rodent model of hepatocellular carcinoma. Invest New Drugs. 2011; 29:380-391.
88. Szekeres T, Saiko P, Fritzer-Szekeres M, Djavan B, Jäger W. Chemopreventive effects of resveratrol and resveratrol derivatives. Ann N Y Acad Sci. 2011; 1215:89-95.

(Received January 21, 2015; Revised February 20, 2015; Accepted February 23, 2015)

Review

DOI: 10.5582/ddt.2015.01003

Oligonol, a low-molecular-weight polyphenol derived from lychee fruit, attenuates gluco-lipotoxicity-mediated renal disorder in type 2 diabetic *db/db* mice

Chan Hum Park[1], Jeong Sook Noh[2], Hajime Fujii[3], Seong-Soo Roh[1], Yeong-Ok Song[4], Jae Sue Choi[5], Hae Young Chung[6], Takako Yokozawa[1,6,7,*]

[1] *College of Korean Medicine, Daegu Haany University, Daegu, Korea;*
[2] *Department of Food Science & Nutrition, Tongmyong University, Busan, Korea;*
[3] *Amino Up Chemical Company, Ltd., Sapporo, Japan;*
[4] *Department of Food Science Nutrition, Pusan National University, Busan, Korea;*
[5] *Division of Food Science & Biotechnology, Pukyong National University, Busan, Korea;*
[6] *Molecular Inflammation Research Center for Aging Intervention, Pusan National University, Busan, Korea;*
[7] *Graduate School of Science and Engineering for Research, University of Toyama, Toyama, Japan.*

Summary **Oligonol is a phenolic product derived from lychee fruit extract containing catechin-type monomers and oligomers of proanthocyanidins, produced by a manufacturing process which converts polyphenol polymers into oligomers. These proanthocyanidins have been reported to exhibit beneficial bioactivities in many studies, and so oligonol, a rich source of polyphenol, is expected to show favorable effects on various chronic diseases. This article summarizes recent work whether oligonol has an ameliorative effect on diabetic indices and renal disorders associated with gluco-lipotoxicity-mediated oxidative stress, inflammation, and apoptosis in *db/db* mice with diabetes. Oligonol was able to improve diabetic indices, prevent the development of diabetic renal disease, and preserve renal cells and the renal morphological structure via the attenuation of reduced nicotinamide adenine dinucleotide phosphate (NADPH) oxidase-induced oxidative stress, inhibition of advanced glycation endproduct (AGE) generation, and prevention of apoptosis-induced cell death in *db/db* mice, being independent of changes in the body weight or serum glucose levels. The present study provides important evidence that oligonol exhibits a pleiotropic effect, representing renoprotective effects against the development of diabetic complications in type 2 diabetic *db/db* mice.**

Keywords: Oligonol, type 2 diabetes, renoprotective effects

1. Introduction

The major biochemical alterations in diabetes are hyperglycemia and dyslipidemia, leading to gluco- and lipotoxicity, respectively, which directly or indirectly account for diabetic complications in various organs such as nonalcoholic fatty liver disease, chronic kidney disease, pancreatic β-cell apoptosis, and diabetic cardiomyopathy (*1-4*).

Hyperglycemia causes oxidative stress by two mechanisms: firstly, by decreasing the regeneration of the important cellular antioxidant, reduced glutathione (GSH) from oxidized glutathione (GSSG), and, secondly, by decreasing the availability of reduced nicotinamide adenine dinucleotide phosphate (NADPH) (*5*). Furthermore, hyperglycemia-induced reactive oxygen species (ROS) stimulate the activation of protein kinase C (PKC), formation of advanced glycation endproducts (AGEs), and sorbitol accumulation. Also, an increase in ROS leads to the activation of nuclear factor-kappa B (NF-κB), and activated NF-κB can enhance the expression of proinflammatory cytokines, chemokines,

**Address correspondence to:*
Dr. Takako Yokozawa, Graduate School of Science and Engineering for Research, University of Toyama, 3190 Gofuku, Toyama 930-8555, Japan.
E-mail: yokozawa@inm.u-toyama.ac.jp

adhesion molecules, inflammatory receptors, and inflammatory enzymes such as inducible nitric oxide synthase (iNOS) and cyclooxygenase-2 (COX-2) (*6-8*).

Long-term hyperlipidemia, which is associated with the abnormal expression of transcriptional factors such as peroxisome proliferator-activated receptor (PPAR) α or sterol regulatory element-binding protein (SREBP) in the nucleus, increases non-esterified fatty acid (NEFA) uptake and accumulations of triglycerides and cholesterol in tissues such as the liver and kidney. In addition, critical toxicity caused by dyslipidemia is due to oxidative and carbonyl stress as a result of impaired antioxidant defense systems and increased ROS generated by the mitochondrial respiratory chain reaction, nonenzymatic glycation, and glucose autoxidation (*9-12*).

There have been many studies to identify effective therapeutic agents from natural sources for metabolic disorders such as obesity, diabetes mellitus, and its complications due to their absence of toxic and/or side effects (*13*). Currently, functional food and/or dietary ingredients with health benefits are given much attention due to the absence of adverse effects, abundant production, and application to various commercial products (*14*). Polyphenol-rich foods, such as wine, tea, coffee, and chocolate, have been receiving considerable attention as dietary sources of antioxidants that are valuable for human health. Polyphenols, including catechins and their derivatives, resveratrol, and curcumin, have attracted attention as functional foods with various bioactivities, such as anticancer, antimutagenic, antimicrobial, and antiviral activities (*15-17*).

The lychee (*Litchi chinensis*, Sapindaceae) has been consumed since ancient times in China and the southern area of Southeast Asia. The lychee is rich in polyphenols; Brat *et al*. (*18*) reported that its polyphenol content per edible part is second only to strawberries. A particular feature of lychee polyphenols is a phenolic product containing catechin-type monomers and oligomers of proanthocyanidins. Proanthocyanidins are structurally characterized as polymers of catechin and have a high molecular weight. However, their absorption in the body is low when administered orally, and so their *in vivo* activity is not as high as expected. Moreover, proanthocyanidins with a high molecular weight are practically insoluble in water and have an astringent taste, binding to salivary proteins and mucous membranes in the mouth (*19*), and making them difficult to use in the food industry. Tanaka *et al*. (*20*) were successful in converting high-molecular-weight proanthocyanidin into low-molecular-weight proanthocyanidin, which is utilizable in the food industry. Therefore, in this review, we summarize recent work on the effects of oligonol on diabetic indices and renal disorders associated with gluco-lipotoxicity-mediated oxidative stress, inflammation, and apoptosis in *db/db* mice with diabetes.

2. Conversion to low-molecular-weight proanthocyanidin

For a prolonged period, a thiolysis method has been used for the structural analysis of proanthocyanidin. In this method, based on a nucleophilic reaction, a compound possessing a thiol group binds to the end unit of proanthocyanidin fragmented under acidic conditions, and, accordingly, low-molecular-weight proanthocyanidin is stably obtained. However, as most compounds with a thiol group are not suitable for consumption, their application to food products is limited. Tanaka *et al*. (*20*) developed a technique to convert high-molecular-weight proanthocyanidins to low-molecular-weight proanthocyanidins without using thiol compounds, and have been successful in making the technology practicable. This method involves binding a compound possessing a phloroglucinol ring structure (such as catechin) as a nucleophilic compound to proanthocyanidin fragmented under acidic conditions. As shown in Figure 1, catechin

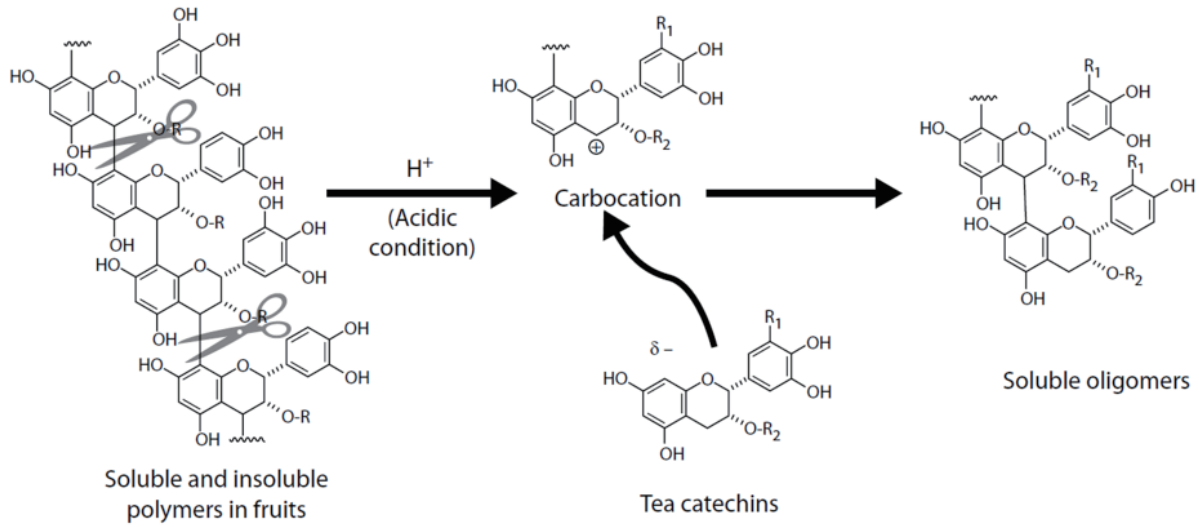

Figure 1. A conceptual diagram showing the conversion of proanthocyanidin to a low molecular weight. *Ref*. (*20*).

monomers are substituted at the C-4 position of fragmented proanthocyanidins with a high molecular weight and, as a consequence, low-molecular-weight proanthocyanidins are stably generated.

3. Oligonol

Oligonol is produced by oligomerizing polyphenol polymers derived from lychee fruit, as described previously (*21*). Briefly, dried lychee fruits, one of the richest sources of polyphenols, are extracted with 50% (v/v) ethanol. The filtrate is evaporated and passed through a DIAION HP-20 column, and eluted with ethanol. The eluate is evaporated to dryness, yielding a dark brown powder which contains a mixture of proanthocyanidins. The lychee extract is mixed with green tea extract, which provides an enriched source of monomeric procyanidins, and citric acid in water. The reaction mixture is heated at 60°C for 16 h, filtered through a DIAION HP-20 column, washed with water, and eluted with 40% (v/v) ethanol. Evaporation of the eluate yields a reddish brown powder containing the monomeric and oligomeric proanthocyanidin mixture. Oligonol comprises a polyphenol mixture of 15.3% monomers (including catechin) and 16.7% dimers (including procyanidin and catechin), whereas lychee fruit polyphenol comprises a mixture of 6.4% monomers and 9.8% dimers (Table 1). Oligonol is commercially available (Amino Up Chemical Co., Ltd., Sapporo, Japan). The safety of oligonol as a food or dietary supplement and as a pharmaceutical additive has already been confirmed (*21,22*).

4. Function of oligonol against diabetes-induced renal damage in *db/db* mice

There is accumulating evidence that oligonol can exert some biological effects *in vitro* and *in vivo*: anticancer (*23*) as well as antioxidant and anti-inflammatory effects (*24*), beneficial activity for nitric oxide bioavailability (*25*), and a regulatory effect on lipid metabolism (*26,27*). Indeed, dietary feeding with proanthocyanidins, which comprise oligonol, has been reported to induce a significant attenuation of tissue fat levels, without changing the total body mass of the animals compared with non-proanthocyanidin-fed animals (*28*). Thus, many beneficial physiological activities of oligonol have been reported, and this review was focused that oligonol has ameliorative effects on the kidney in type 2 diabetes.

Diabetic kidney damage is one of the most serious complications of diabetes mellitus and has been the most common cause of end-stage renal failure among patients undergoing chronic hemodialysis therapy since 1998 (*29*). Therefore, we proposed the effects of oligonol on diabetic indices and renal damage in type 2 diabetic *db/db* mice, as reported previously (*30,31*).

4.1. *Diabetic indices and renal histological examination*

To investigate the effect of oligonol, *db/db* mice were used. The spontaneous mutant strain C57BLKS/J *db/db* mice have a *db* gene mutation, a splicing mutation caused by a point mutation in the downstream intron of the leptin receptor gene, and so they are unresponsive to leptin. Leptin is a peptide hormone secreted by adipocytes, and it is involved in eating behavior and energy homeostasis. For this reason, after birth, homozygous type 2 diabetic (*db/db*) mice show unrepressed eating behavior, become obese, and develop severe insulin resistance associated with hyperinsulinemia and hyperglycemia (*32*). In this study, *db/db* mice showed diabetic characteristics, such as excessive body weight gain, increased food and water intakes, hyperglycemia, hyperinsulinemia, and hyperleptinemia, compared with homozygous control (*m/m*) mice. However, oligonol administration did not affect the body weight gain or serum glucose and leptin concentrations in spite of elevated serum insulin. In oligonol-administered *db/db* mice, the cause of increased insulin secretion is unclear and may be related to preservation of the pancreatic β-cell function by oligonol treatment. In addition, there were significant reductions in the serum lipid concentration (triglycerides, total cholesterol, and NEFA), ROS, and lipid peroxidation, as well as improvements in renal function parameters such as serum urea nitrogen and creatinine. Serum adiponectin concentrations were significantly higher in the oligonol-treated than in the vehicle *db/db* group, as shown in Table 2. Low adiponectin levels are associated with insulin resistance in type 2 diabetic patients and experimental animals (*33*). Unfortunately, we cannot measure the insulin sensitivity regarding the influence on target tissues such as muscle and fat. In addition to biofactors such

Table 1. Contents of oligonol and lychee fruit polyphenol

Items	Oligonol	Lychee fruit polyphenol
Monomers		
(+)-Catechin/(-)-Epicatechin	6.9%	6.4%
(-)-Epicatechin gallate	1.4%	n.d.
(-)-Epigallocatechin gallate	7.0%	n.d.
Dimers		
Procyanidin A1	6.2%	4.0%
Procyanidin A2	6.6%	3.3%
Procyanidin B1	0.4%	0.8%
Procyanidin B2	2.0%	1.7%
Catechin-epigallocatechin gallate	1.5%	n.d.

Oligonol comprises a polyphenol mixture of 15.3% monomers ((+)-catechin, (-)-epicatechin, (-)-epicatechin gallate, and (-)-epigallocatechin gallate) and 16.7% dimers (procyanidin A1, A2, B1, B2, and catechin-epigallocatechin gallate), while lychee fruit polyphenol comprises a mixture of 6.4% monomers and 9.8% dimers. *Ref.* (*31*).

Table 2. Hematological analyses

Items	*m/m*	*db/db*		
		Veh	O10	O20
Glucose (mg/dL)	153 ± 12***	594 ± 29	571 ± 61	668 ± 41
Insulin (ng/mL)	0.17 ± 0.08***	1.77 ± 0.18	1.71 ± 0.22	2.86 ± 0.32**
Leptin (ng/mL)	3.0 ± 0.4***	19.8 ± 0.3	19.5 ± 0.2	19.3 ± 0.4
Urea nitrogen (mg/dL)	31.5 ± 2.9**	44.4 ± 2.4	40.4 ± 2.4	28.6 ± 1.7***
Creatinine (mg/dL)	0.23 ± 0.02*	0.35 ± 0.04	0.37 ± 0.04	0.26 ± 0.02*
Triglyceride (mg/dL)	76 ± 6***	220 ± 18	197 ± 30	161 ± 20*
Total cholesterol (mg/dL)	76 ± 4***	157 ± 13	139 ± 8	124 ± 7*
NEFA (mEq/L)	0.74 ± 0.10***	1.41 ± 0.08	1.18 ± 0.13	1.10 ± 0.09*
Adiponectin (ng/mL)	6.12 ± 0.62***	2.42 ± 0.23	2.93 ± 0.20*	3.12 ± 0.12*
ROS (fluorescence/min/mL)	171 ± 27*	321 ± 42	214 ± 24*	145 ± 24**
TBARS (nmol/mL)	5.7 ± 0.2***	14.9 ± 1.3	13.4 ± 1.1	7.1 ± 0.3***

Values are mean ± S.E.M. Significance: * $p < 0.05$, ** $p < 0.01$, *** $p < 0.001$ *vs*. vehicle-treated *db/db* group. *m/m*, vehicle-treated *m/m* mice ($n = 6$); *db/db*-Veh, vehicle-treated *db/db* mice ($n = 10$); *db/db*-O10, oligonol 10 mg/kg body weight-treated *db/db* mice ($n = 10$); d*b/db*-O20, oligonol 20 mg/kg body weight-treated *db/db* mice ($n = 10$). *Ref*. (*30*).

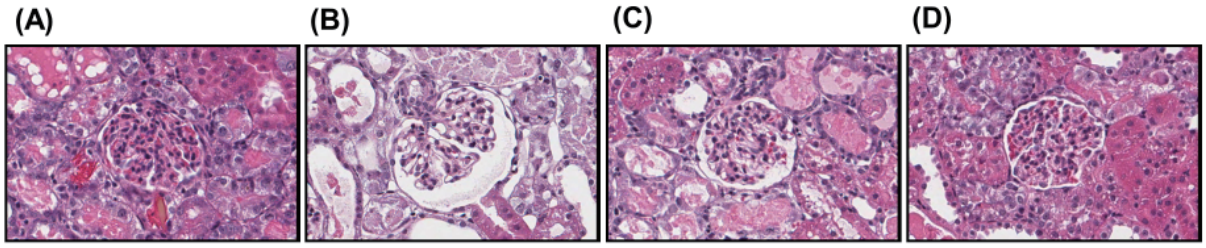

Figure 2. H/E staining of renal tissue. Vehicle-treated *m/m* mice **(A)**, vehicle-treated *db/db* mice **(B)**, oligonol 10 mg/kg body weight-treated *db/db* mice **(C)**, oligonol 20 mg/kg body weight-treated *db/db* mice **(D)**. Images are at 200x magnification. *Ref*. (*31*).

as the lipid profile and oxidative stress, kidney damage was controlled under type 2 diabetic conditions with oligonol administration. Figure 2 shows representative microphotographs of renal hematoxylin and eosin (H/E) staining. When compared with *m/m* mice (Figure 2A), the marked glomerular enlargement observed in *db/db* mice (Figure 2B) was clearly improved on oligonol treatment (Figures 2C and 2D). These results indicate that oligonol protects against renal injury induced in type 2 diabetic *db/db* mice.

To investigate the effects of oligonol on renal damage induced by hyperglycemia and abnormal lipid synthesis, the influence of hyperglycemia and hyperlipidemia in the kidneys of *db/db* mice was also examined. The renal contents of triglycerides and total cholesterol were significantly decreased by the administration of oligonol. These results indicate that the biological activities of oligonol in the serum of *db/db* mice are associated with lipid metabolism, such as synthesis or deposition for energy production.

Lipid homeostasis is regulated by a family of membrane-bound transcription factors called SREBPs. Up-regulations of SREBP-1 and SREBP-2 were reported in leptin-resistant mice such as *ob/ob* and $FVB^{db/db}$ mice (*34,35*). In our study, the increase in renal SREBP-1 and SREBP-2 in *db/db* mice was down-regulated by the administration of oligonol. This was probably related to the inhibition of renal triglyceride and total cholesterol accumulation. Furthermore, PPARs, with three isoforms (α, δ, and γ), are also involved in the long-term regulation of lipid metabolism, and their activity is modulated by endogenous lipid-derived ligands. When PPARα is activated, it promotes fatty acid oxidation, ketone body synthesis, and glucose-sparing (*36*) and ameliorates diabetes, insulin resistance, albuminuria, glomerular hypertrophy, and mesangial expansion in *db/db* mice (*37*). The decreased renal PPARα level in *db/db* mice was significantly increased on oligonol administration. These results clarify the effect of oligonol on regulations of both PPARα and SREBP protein expressions.

4.2. *Oligonol attenuates diabetes-induced renal damage triggered by ROS-related pathway*

Hyperglycemia and elevated NEFA levels result in the generation of ROS, and, consequently, increase oxidative stress. ROS not only directly damage cells by oxidizing DNA, proteins, and lipids, but also indirectly damage them by activating a variety of stress-sensitive intracellular signaling pathways such as NF-κB, p38 mitogen-activated protein kinase (MAPK), NH_2-terminal Jun kinase/stress-activated protein kinase, hexosamines, PKC, and AGE/receptor for AGE (RAGE). Activation of these pathways results in the increased expression of numerous gene products that cause cellular damage and play a major role in the etiology of later-stage complications of

Table 3. Biomarkers associated with oxidative stress in the kidney

Items	*m/m*	*db/db*		
		Veh	O10	O20
ROS (fluorescence/min/mg protein)	1057 ± 94**	3069 ± 327	1970 ± 282*	764 ± 112***
TBARS (nmol/mg protein)	1.11 ± 0.05**	1.51 ± 0.07	1.37 ± 0.05	1.18 ± 0.09*
GSH (μmol/mg protein)	3.02 ± 0.18	2.95 ± 0.09	3.23 ± 0.33	3.08 ± 0.17
GSSG (μmol/mg protein)	1.40 ± 0.03**	1.63 ± 0.04	1.47 ± 0.05*	1.52 ± 0.06
GSH/GSSG ratio	2.17 ± 0.13*	1.80 ± 0.04	2.19 ± 0.18	2.05 ± 0.15

Values are mean ± S.E.M. Significance: * $p < 0.05$, ** $p < 0.01$, *** $p < 0.001$ *vs*. vehicle-treated *db/db* group. *m/m*, vehicle-treated *m/m* mice ($n = 6$); *db/db*-Veh, vehicle-treated *db/db* mice ($n = 10$); *db/db*-O10, oligonol 10 mg/kg body weight-treated *db/db* mice ($n = 10$); d*b/db*-O20, oligonol 20 mg/kg body weight-treated *db/db* mice ($n = 10$). *Ref.* (*30*).

diabetes (*38*). Thus, the up-regulation of endogenous antioxidative systems and suppression of oxidative stress are important factors ameliorating diabetes and its complications.

We investigated ROS generation and lipid peroxidation, as biomarkers associated with oxidative stress, and also measured GSH and GSSG as indicators of an endogenous antioxidative system. Lipid peroxidation leads to oxidant production from many molecules, and, thus, amplifies oxidative damage (*39*). Our results showed that the level of ROS generation and that of lipid peroxidation in the serum and kidney were increased in *db/db* mice, which suggests that these mice show increased oxidative damage due to an elevation of ROS generation induced by hyperglycemia and hyperlipidemia. However, oligonol treatment exerted antioxidant activity, promoting decreased serum ROS and 2-thiobarbituric acid-reactive substance (TBARS) levels with corresponding effects on renal tissue in *db/db* mice (Tables 2 and 3). Regarding GSH/GSSG ratios, the *db/db* vehicle group showed a significant reduction compared with the *m/m* group, which resulted from the marked increase in the GSSG concentration in the kidney. However, oligonol treatment did not significantly alter the renal GSH level and GSH/GSSG ratio (Table 3). This suggests that the administration of oligonol would ameliorate oxidative stress under type 2 diabetes through the inhibition of ROS generation and lipid peroxidation, and, thus, it would result in the improvement of renal disorders caused by oxidative stress.

Many researchers have demonstrated that catechin and its derivatives exhibited a favorable antioxidative effect and attenuated oxidative stress under diverse, chronic, degenerative conditions (*40*). Furthermore, there is increasing evidence of the potential benefits of polyphenols containing catechin in the regulation of cellular processes such as redox control and the inflammatory response based on established animal models and clinical studies (*41,42*). Recently, our studies have shown that epigallocatechin gallate ameliorates glucose toxicity and renal injury, thereby alleviating renal damage caused by abnormal glucose metabolism-associated oxidative stress in diabetic nephropathy (*43*). Since oligonol contained catechin-based oligomers, we assumed that it could attenuate oxidative stress induced by chronic hyperglycemia and/or direct NADPH oxidase-dependent ROS generation in type 2 diabetes. In the kidney cortex of *db/db* mice, protein expressions of NADPH oxidase-4 (Nox-4) (NADPH oxidase homologs) and $p22^{phox}$/$p47^{phox}$ (subunit of NADPH oxidase) were increased, and Nox-4 was a major source of renal ROS through the p38 MAPK-dependent pathway (*44*). Our study demonstrated that oligonol decreased the renal ROS concentration as well as down-regulated the expression of NADPH oxidase, as shown in Table 3 and Figure 3. These results suggest that the attenuation of oxidative stress in renal tissue by oligonol is associated with the reduction of NADPH oxidase activity.

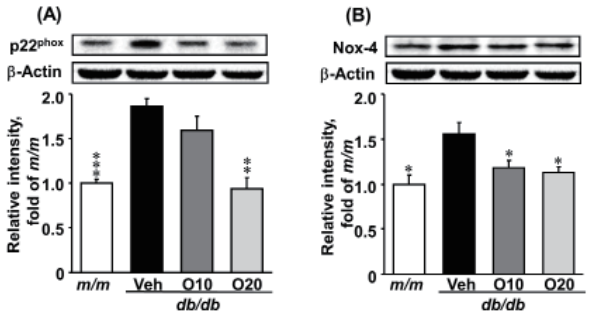

Figure 3. Renal $p22^{phox}$ (A) and Nox-4 (B) protein expressions. Values are mean ± S.E.M. Significance: * $p < 0.05$, ** $p < 0.01$, *** $p < 0.001$ *vs*. vehicle-treated *db/db* group. *m/m*, vehicle-treated *m/m* mice ($n = 6$); *db/db*-Veh, vehicle-treated *db/db* mice ($n = 10$); *db/db*-O10, oligonol 10 mg/kg body weight-treated *db/db* mice ($n = 10$); *db/db*-O20, oligonol 20 mg/kg body weight-treated *db/db* mice ($n = 10$). *Ref.* (*31*).

4.3. *Oligonol acts as a regulator of diabetes-induced renal damage through an AGE-related pathway*

AGEs are elevated under chronic hyperglycemia and excessive glucose uptake in tissues, and, furthermore, their formation can be accelerated by increased oxidative stress (*45*). Some polyphenols, including green tea catechins and epicatechins, chlorogenic acids, quercetin, and naringenin, could inhibit the absorption of glucose from the intestine *via* the inhibition of sodium-dependent glucose transporter (SGLT) 1 and SGLT2 (*46*). Glucose transporter isoform 2 (GLUT2)-

mediated glucose transport was inhibited by apigenin, quercetin, myricetin, and tea catechins (*47,48*). Polyphenol also shows a wide range of target tissue and is distributed in various organs, including the liver and kidney. Our study shows that the increased glucose concentration in the kidney of *db/db* mice is decreased by oligonol treatment. Thus, the decreased renal glucose concentration may be due to SGLT1, SGLT2, and GLUT2 inhibition.

AGEs are complex compounds formed *via* a nonenzymatic reaction between reducing sugars and amine residues on proteins, lipids, or nucleic acids (*49*). The intracellular production and accumulation of AGEs are closely linked to diabetic complications such as neuropathy, retinopathy, and nephropathy (*50,51*). Especially, there is a strong correlation between AGE accumulation and the duration and degree of severity of diabetic kidney disease (*52*). AGEs can interact with certain receptors, such as RAGE, to induce intracellular signaling, which leads to enhanced oxidative stress and the production of key proinflammatory and prosclerotic cytokines. Recently, attention has been focused on the essential roles of AGEs, that is, AGEs alter the structure and function of matrix tissue proteins, and AGE-modified proteins stimulate a variety of cellular responses *via* a specific cell surface receptor, resulting in the expression and activation of pathogenic mediators, *e.g.*, the extracellular matrix, oxidative stress, cytokines, and growth factors, implicated in the development and stimulation of diabetic renal diseases (*53*). We evaluated the protein expressions of AGEs and receptors, such as pentosidine, N^{ε}-(carboxymethyl)arginine (CMA), glycolaldehyde (GA)-pyridine, N^{ε}-(carboxymethyl)lysine (CML), N^{ε}-(carboxyethyl)lysine (CEL), and RAGE, in the kidney. These products are not only derived from intermediates of glucose metabolism and metabolites of glycolysis, but also serve as general bio-markers of oxidative stress resulting from carbohydrate and lipid oxidation reactions (*54*). Pentosidine, a cross-link between arginine and lysine, is a well-characterized AGE (*55*). Recently, serum pentosidine concentrations were shown to be closely associated with peripheral arterial disease in type 2 diabetes mellitus patients (*56*). Odani *et al*. (*57*) suggested that CMA was a new marker of diabetic complications, and that its serum concentration was increased in diabetic patients with non-renal failure compared with a healthy control group. CMA production increased in parallel with the incubation time, and its yield was greater than that of pentosidine (*58*). GA was formed either as a fragmentation product in the Maillard reaction or as a result of the myeloperoxidase-hydrogen peroxide-chloride reaction (*59,60*). GA-pyridine, a specific GA-derived AGE, has been described in foam cells and in the extracellular matrix of human atherosclerotic fibrotic lesions, and also reported to show mesangial accumulation in human renal disease (*61*). The hydroxy-amino acid L-serine is oxidized and converted to reactive carbonyl compounds, such as GA which is highly reactive with proteins, leading to the formation of CML (*60*). Taking the above-mentioned studies together, AGE formation, accumulation, and interaction with RAGE were increased and aggravated under the diabetic condition, consistent with our findings such as the up-regulated expression of these proteins in the kidney of type 2 diabetic mice. However, oligonol administration effectively down-regulated AGE-related protein expressions (RAGE, CMA, GA-pyridine, CML, and CEL) (Figure 4). These results suggest that the inhibitory activity of oligonol on AGE formation and its receptor expressions shows clinical potential, including its delay of AGE-related disorder development in diabetes. The reno-protective effects of oligonol against diabetes were not attributable to improved renal glycemic adjustment alone, but also likely reflected its antioxidant activity. The combined antioxidant and reduction of the glycation reaction by oligonol should be particularly advantageous and perhaps even synergistic in preventing renal injury and other diabetic complications.

4.4. *Oligonol attenuates diabetes-induced renal damage by ROS-sensitive pathway of inflammation and apoptosis*

A possible pathway of ROS-associated apoptosis was suggested by the observation that increased oxidative stress activates c-Jun N-terminal kinase (JNK) and p38 MAPK through apoptosis signal-regulating kinase 1 (*62*). JNK activation has been suggested to be involved in the regulation of tumor necrosis factor-α (TNF-α)-induced c-Jun kinase and apoptosis (*63*). Otherwise, the suppression of JNK and p38 MAPK mediated anti-apoptotic signaling (*64*). We evaluated the expression of pro-apoptotic cellular signal-related protein in diabetic renal tissues. The renal protein expressions of JNK, phosphor-JNK (p-JNK), c-Jun, and TNF-α were augmented in the diabetic *db/db* mice compared with normal *m/m* mice. These up-regulated proteins were markedly down-regulated by oligonol treatment, as reported previously (*31*). This indicates that the down-regulation of TNF-α or oxidative stress-mediated JNK signaling affected the renal apoptotic response.

Therefore, we subsequently examined renal apoptosis-related protein expression in the kidney of *db/db* mice with oligonol administration. Podocyte loss caused by detachment or apoptosis will lead to a decrease in the density of podocytes. Reduction of the podocyte density is an important determinant of progressive diabetic nephropathy and precedes the development of renal dysfunction and albuminuria in diabetic patients and animal models of diabetes mellitus (*65*). The marked increase in podocyte apoptosis observed during the early stage of diabetes

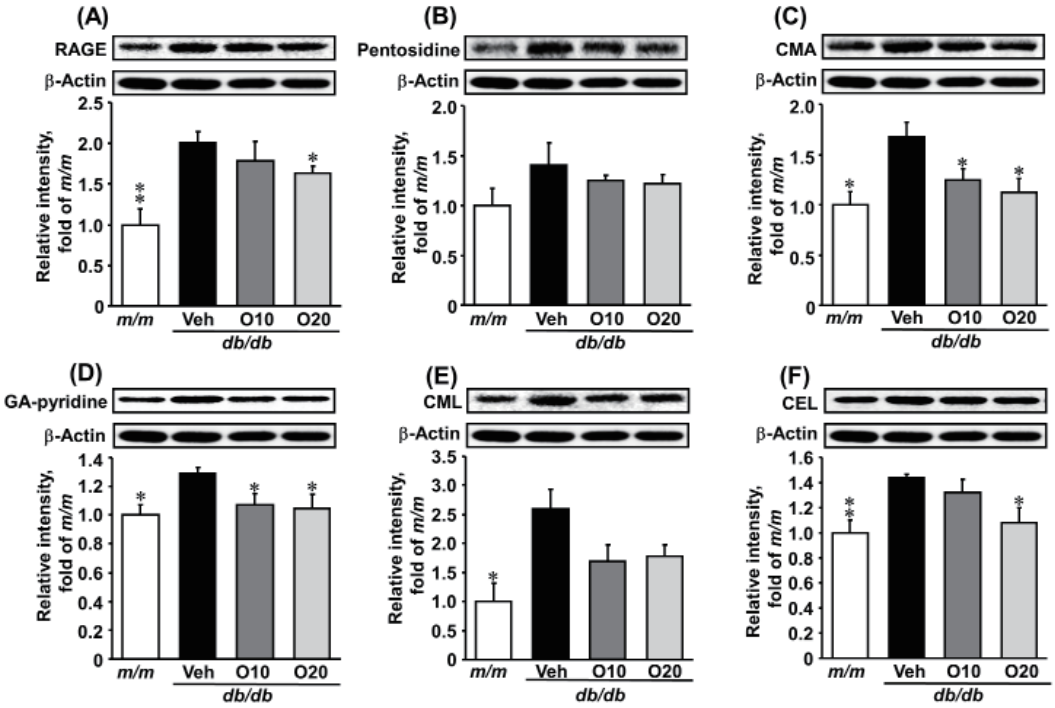

Figure 4. Renal RAGE (A), pentosidine (B), CMA (C), GA-pyridine (D), CML (E), and CEL (F) protein expressions. Values are mean ± S.E.M. Significance: * $p < 0.05$, ** $p < 0.01$ *vs*. vehicle-treated *db/db* group. *m/m*, vehicle-treated *m/m* mice ($n = 6$); *db/db*-Veh, vehicle-treated *db/db* mice ($n = 10$); *db/db*-O10, oligonol 10 mg/kg body weight-treated *db/db* mice ($n = 10$); *db/db*-O20, oligonol 20 mg/kg body weight-treated *db/db* mice ($n = 10$). *Ref*. (*31*).

in *db/db* mice is mediated to a large extent by the activation of NADPH oxidase and its contribution to the generation of ROS (*65*). Our results support the idea that the decrease in NADPH oxidase expression affected the proapoptotic protein expression. Oligonol administration led to a significant increase in Bcl-2 and survivin and reduction of Bax, cytochrome *c*, and caspase-3 protein in the renal tissue of *db/db* mice, as shown in a previously report (*31*). These data suggest that the attenuation of diabetic renal apoptosis is influenced by decreased NADPH oxidase-dependent oxidative stress and/or JNK-related signaling.

Under type 2 diabetes, the redox-sensitive intracellular signaling pathway is altered. In particular, one major intracellular target of hyperglycemia and oxidative stress is the transcription factor NF-κB. NF-κB can be activated by a wide array of exogenous and endogenous stimuli, including hyperglycemia, elevated NEFA, ROS, TNF-α, interleukin-1β, other proinflammatory cytokines, AGE-binding RAGE, and p38 MAPK. The activation of NF-κB induces the inflammation-related proteins COX-2 and iNOS, and the subsequent production of prostaglandin and nitric oxide (NO), respectively. NO reacts very rapidly with superoxide to form peroxynitrite and other NO-derived oxidants capable of damaging DNA and proteins (*66*). There is a vicious cycle involving NF-κB, oxidative stress, and inflammation under the diabetic condition. Therefore, the inhibition of NF-κB transcription plays a central role in regulating the pathophysiology of diabetic complications. Elevated protein expressions of NF-κBp65 and iNOS in the liver of *db/db* mice were markedly down-regulated by oligonol administration (*31*). Oligonol administration could adjust inflammation through the inhibition of the NF-κB pathway.

5. Conclusion

Oligonol, which is now available commercially as a new dietary ingredient, is an optimized phenolic product derived from lychee fruit polyphenols containing catechin-type monomers and low-molecular-weight oligomers (*21*). Based on recent studies, there is accumulating evidence that oligonol can induce some physiological and biochemical alterations *in vitro* and *in vivo*, such as the induction of apoptosis in cancer cells (*23*), antioxidant and anti-inflammatory effects in mice (*24*), and beneficial subjective effects on the feeling of fatigue in young athletes (*67*). Moreover, the oral administration of oligonol improves the regulation of genes for adipokines in white adipose tissue of mice on administering a high-fat diet (*26*). The dietary feeding of proanthocyanidins, which comprise oligonol, has been reported to induce the significant attenuation of tissue fat levels, without changing the total body mass of animals compared with non-proanthocyanidin-fed animals (*28*). In this review, we summarize our recent work: oligonol was able to improve diabetic indices, prevent the development of diabetic renal disease, and preserve renal cells and the renal morphological structure *via* the attenuation of NADPH oxidase-induced oxidative stress, inhibition of AGE generation, and prevention

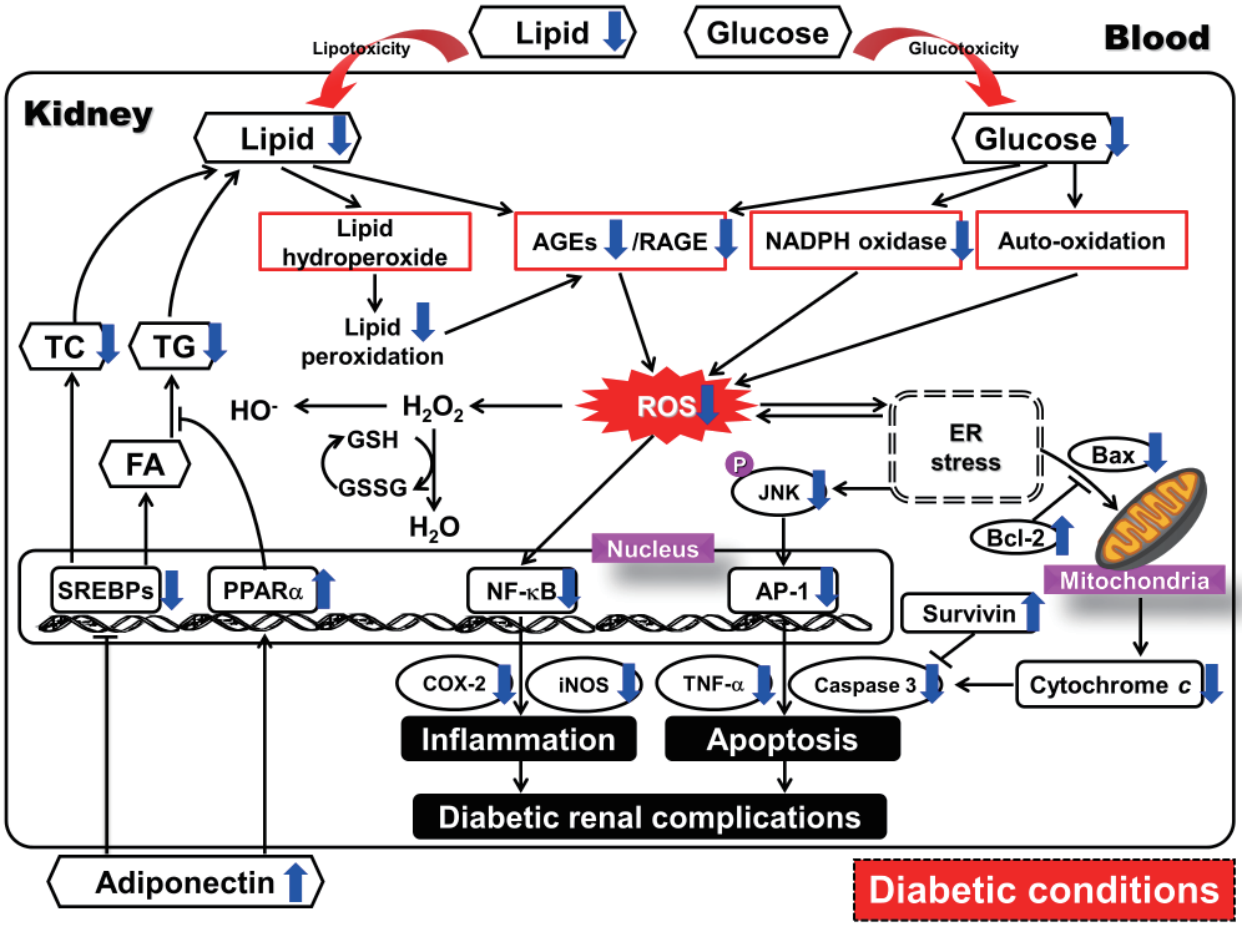

Figure 5. Predicted mechanism in renal tissues on administering oligonol against oxidative stress, AGE formation, and apoptosis. Oligonol attenuated glucose and lipid accumulation, the regulation of transcription factors for lipid metabolism, and subsequently decreased NADPH oxidase-derived ROS production in the kidney. Furthermore, oligonol ameliorated the values of AGE-related protein expressions (RAGE, CMA, GA-pyridinine, and CEL), anti-apoptotic protein expressions (Bcl-2 and survivin), and apoptotic protein expressions (JNK, p-JNK, AP-1, Bax, cytochrome *c*, and caspase-3 proteins).

of apoptosis-induced cell death in *db/db* mice, being independent of changes in the body weight or serum glucose levels (Figure 5). Accordingly, oligonol may be a promising dietary supplement for the prevention or delaying of diabetic renal complications. With respect to the current research, more clinical studies are needed on the management of hyperglycemia and inflammation in both healthy subjects and metabolic syndrome patients and its pharmaceutical kinetics in order to develop therapeutic agents.

References

1. Srikanthan P, Hsueh W. Preventing heart failure in patients with diabetes. Med Clin North Am. 2004; 88:1237-1256.
2. Younossi ZM, Gramlich T, Matteoni CA, Boparai N, McCullough AJ. Nonalcoholic fatty liver disease in patients with type 2 diabetes. Clin Gastroenterol Hepatol. 2004; 2:262-265.
3. Chang-Chen KJ, Mullur R, Bernal-Mizrachi E. β-Cell failure as a complication of diabetes. Rev Endocr Metab Disord. 2008; 9:329-343.
4. Kanwar YS, Wada J, Sun L, Xie P, Wallner EI, Chen S, Chugh S, Danesh FR. Diabetic nephropathy: Mechanisms of renal disease progression. Exp Biol Med (Maywood). 2008; 233:4-11.
5. Vander Jagt DL, Hassebrook RK, Hunsaker LA, Brown WM, Royer RE. Metabolism of the 2-oxoaldehyde methylglyoxal by aldose reductase and by glyoxalase-I: Roles for glutathione in both enzymes and implications for diabetic complications. Chem Biol Interact. 2001; 130-132:549-562.
6. Barnes PJ. Nuclear factor-κB. Int J Biochem Cell Biol. 1997; 29:867-870.
7. Yamamoto Y, Gaynor RB. Role of the NF-κB pathway in the pathogenesis of human disease states. Curr Mol Med. 2001; 1:287-296.
8. Zhang GL, Wang YH, Teng HL, Lin ZB. Effects of aminoguanidine on nitric oxide production induced by inflammatory cytokines and endotoxin in cultured rat hepatocytes. World J Gastroenterol. 2001; 7:331-334.
9. Maritim AC, Sanders RA, Watkins JB 3rd. Diabetes, oxidative stress, and antioxidants: A review. J Biochem Mol Toxicol. 2003; 17:24-38.
10. Rolo AP, Palmeira CM. Diabetes and mitochondrial function: Role of hyperglycemia and oxidative stress. Toxicol Appl Pharmacol. 2006; 212:167-178.
11. Nishikawa T, Araki E. Impact of mitochondrial ROS production in the pathogenesis of diabetes mellitus and

its complications. Antioxid Redox Signal. 2007; 9:343-353.
12. Gao L, Mann GE. Vascular NAD(P)H oxidase activation in diabetes: A double-edged sword in redox signaling. Cardiovasc Res. 2009; 82:9-20.
13. Winslow LC, Kroll DJ. Herbs as medicines. Arch Intern Med. 1998; 158:2192-2199.
14. Jones PJ, Varady KA. Are functional foods redefining nutritional requirements? Appl Physiol Nutr Metab. 2008; 33:118-123.
15. Nakayama M, Suzuki K, Toda M, Okubo S, Hara Y, Shimamura T. Inhibition of the infectivity of influenza virus by tea polyphenols. Antiviral Res. 1993; 21:289-299.
16. Hsieh TC, Wu JM. Differential effects on growth, cell cycle arrest, and induction of apoptosis by resveratrol in human prostate cancer cell lines. Exp Cell Res. 1999; 249:109-115.
17. Pal S, Choudhuri T, Chattopadhyay S, Bhattacharya A, Datta GK, Das T, Sa G. Mechanisms of curcumin-induced apoptosis of Ehrlich's ascites carcinoma cells. Biochem Biophys Res Commun. 2001; 288:658-665.
18. Brat P, Georgé S, Bellamy A, Chaffaut LD, Scalbert A, Mennen L, Arnault N, Amiot MJ. Daily polyphenol intake in France from fruit and vegetables. J Nutr. 2006; 136:2368-2373.
19. Haslam E. Natural polyphenols (vegetable tannins) as drugs: Possible modes of action. J Nat Prod. 1996; 59:205-215.
20. Tanaka T, Yoshitake N, Zhao P, Matsuo Y, Kouno I, Nonaka G. Production of oligomeric proanthocyanidins by fragmentation of polymers. Jpn J Food Chem. 2007; 14:134-139.
21. Kitadate K, Homma K, Roberts A, Maeda T. Thirteen-week oral dose toxicity study of Oligonol containing oligomerized polyphenols extracted from lychee and green tea. Regul Toxicol Pharmacol. 2014; 68:140-146.
22. Fujii H, Nishioka H, Wakame K, Magnuson BA, Roberts A. Acute, subchronic and genotoxicity studies conducted with Oligonol, an oligomerized polyphenol formulated from lychee and green tea extracts. Food Chem Toxicol. 2008; 46:3553-3562.
23. Jo EH, Lee SJ, Ahn NS, Park JS, Hwang JW, Kim SH, Aruoma OI, Lee YS, Kang KS. Induction of apoptosis in MCF-7 and MDA-MB-231 breast cancer cells by Oligonol is mediated by Bcl-2 family regulation and MEK/ERK signaling. Eur J Cancer Prev. 2007; 16:342-347.
24. Kundu JK, Chang EJ, Fujii H, Sun B, Surh YJ. Oligonol inhibits UVB-induced COX-2 expression in HR-1 hairless mouse skin – AP-1 and C/EBP as potential upstream targets. Photochem Photobiol. 2008; 84:399-406.
25. Zhang XH, Yokoo H, Nishioka H, Fujii H, Matsuda N, Hayashi T, Hattori Y. Beneficial effect of the oligomerized polyphenol oligonol on high glucose-induced changes in eNOS phosphorylation and dephosphorylation in endothelial cells. Br J Pharmacol. 2010; 159:928-938.
26. Sakurai T, Nishioka H, Fujii H, Nakano N, Kizaki T, Radak Z, Izawa T, Haga S, Ohno H. Antioxidative effects of a new lychee fruit-derived polyphenol mixture, oligonol, converted into a low-molecular form in adipocytes. Biosci Biotechnol Biochem. 2008; 72:463-476.
27. Ogasawara J, Kitadate K, Nishioka H, Fujii H, Sakurai T, Kizaki T, Izawa T, Ishida H, Ohno H. Oligonol, a new lychee fruit-derived low-molecular form of polyphenol, enhances lipolysis in primary rat adipocytes through activation of the ERK1/2 pathway. Phytother Res. 2009; 23:1626-1633.
28. Mittal A, Elmets CA, Katiyar SK. Dietary feeding of proanthocyanidins from grape seeds prevents photocarcinogenesis in SKH-1 hairless mice: Relationship to decreased fat and lipid peroxidation. Carcinogenesis. 2003; 24:1379-1388.
29. Iseki K, Nakai S, Shinzato T, Nagura Y, Akiba T. Increasing gender difference in the incidence of chronic dialysis therapy in Japan. Ther Apher Dial. 2005; 9:407-411.
30. Noh JS, Kim HY, Park CH, Fujii H, Yokozawa T. Hypolipidaemic and antioxidative effects of oligonol, a low-molecular-weight polyphenol derived from lychee fruit, on renal damage in type 2 diabetic mice. Br J Nutr. 2010; 104:1120-1128.
31. Park CH, Yokozawa T, Noh JS. Oligonol, a low-molecular-weight polyphenol derived from lychee fruit, attenuates diabetes-induced renal damage through the advanced glycation end product-related pathway in *db/db* mice. J Nutr. 2014; 144:1150-1157.
32. Sharma K, McCue P, Dunn SR. Diabetic kidney disease in the *db/db* mouse. Am J Physiol Renal Physiol. 2003; 284:F1138-F1144.
33. Rabe K, Lehrke M, Parhofer KG, Broedl UC. Adipokines and insulin resistance. Mol Med. 2008; 14:741-751.
34. Tobe K, Suzuki R, Aoyama M, Yamauchi T, Kamon J, Kubota N, Terauchi Y, Matsui J, Akanuma Y, Kimura S, Tanaka J, Abe M, Ohsumi J, Nagai R, Kadowaki T. Increased expression of the sterol regulatory element-binding protein-1 gene in insulin receptor substrate-$2^{-/-}$ mouse liver. J Biol Chem. 2001; 276:38337-38340.
35. Wang Z, Jiang T, Li J, Proctor G, McManaman JL, Lucia S, Chua S, Levi M. Regulation of renal lipid metabolism, lipid accumulation, and glomerulosclerosis in $FVB^{db/db}$ mice with type 2 diabetes. Diabetes. 2005; 54:2328-2335.
36. Ferré P. The biology of peroxisome proliferator-activated receptors: Relationship with lipid metabolism and insulin sensitivity. Diabetes. 2004; 53 (Suppl 1):S43-S50.
37. Park CW, Zhang Y, Zhang X, Wu J, Chen L, Cha DR, Su D, Hwang MT, Fan X, Davis L, Striker G, Zheng F, Breyer M, Guan Y. PPARα agonist fenofibrate improves diabetic nephropathy in *db/db* mice. Kidney Int. 2006; 69:1511-1517.
38. Evans JL, Goldfine ID, Maddux BA, Grodsky GM. Are oxidative stress-activated signaling pathways mediators of insulin resistance and β-cell dysfunction? Diabetes. 2003; 52:1-8.
39. Niki E, Yamamoto Y, Komuro E, Sato K. Membrane damage due to lipid oxidation. Am J Clin Nutr. 1991; 53 (1 Suppl):201S-205S.
40. Rietveld A, Wiseman S. Antioxidant effects of tea: Evidence from human clinical trials. J Nutr. 2003; 133:3285S-3292S.
41. Crespy V, Williamson G. A review of the health effects of green tea catechins in *in vivo* animal models. J Nutr. 2004; 134 (12 Suppl):3431S-3440S.
42. Leiherer A, Mündlein A, Drexel H. Phytochemicals and their impact on adipose tissue inflammation and diabetes. Vascul Pharmacol. 2013; 58:3-20.
43. Yamabe N, Yokozawa T, Oya T, Kim M. Therapeutic potential of (-)-epigallocatechin 3-*O*-gallate on renal

damage in diabetic nephropathy model rats. J Pharmacol Exp Ther. 2006; 319:228-236.
44. Sedeek M, Callera G, Montezano A, Gutsol A, Heitz F, Szyndralewiez C, Page P, Kennedy CR, Burns KD, Touyz RM, Hébert RL. Critical role of Nox4-based NADPH oxidase in glucose-induced oxidative stress in the kidney: Implications in type 2 diabetic nephropathy. Am J Physiol Renal Physiol. 2010; 299:F1348-F1358.
45. Yan SD, Schmidt AM, Anderson GM, Zhang J, Brett J, Zou YS, Pinsky D, Stern D. Enhanced cellular oxidant stress by the interaction of advanced glycation end products with their receptors/binding proteins. J Biol Chem. 1994; 269:9889-9897.
46. Bahadoran Z, Mirmiran P, Azizi F. Dietary polyphenols as potential nutraceuticals in management of diabetes: A review. J Diabetes Metab Disord. 2013; 12:43.
47. Song J, Kwon O, Chen S, Daruwala R, Eck P, Park JB, Levine M. Flavonoid inhibition of sodium-dependent vitamin C transporter 1 (SVCT1) and glucose transporter isoform 2 (GLUT2), intestinal transporters for vitamin C and glucose. J Biol Chem. 2002; 277:15252-15260.
48. Johnston K, Sharp P, Clifford M, Morgan L. Dietary polyphenols decrease glucose uptake by human intestinal Caco-2 cells. FEBS Lett. 2005; 579:1653-1657.
49. Goh SY, Cooper ME. The role of advanced glycation end products in progression and complications of diabetes. J Clin Endocrinol Metab. 2008; 93:1143-1152.
50. Baynes JW, Thorpe SR. Role of oxidative stress in diabetic complications: A new perspective on an old paradigm. Diabetes. 1999; 48:1-9.
51. Ahmed N. Advanced glycation endproducts – role in pathology of diabetic complications. Diabetes Res Clin Pract. 2005; 67:3-21.
52. Monnier VM, Bautista O, Kenny D, Sell DR, Fogarty J, Dahms W, Cleary PA, Lachin J, Genuth S. Skin collagen glycation, glycoxidation, and crosslinking are lower in subjects with long-term intensive versus conventional therapy of type 1 diabetes: Relevance of glycated collagen products versus HbA_{1c} as markers of diabetic complications. DCCT Skin Collagen Ancillary Study Group. Diabetes Control and Complications Trial. Diabetes. 1999; 48:870-880.
53. Yan SD, Schmidt AM, Anderson GM, Zhang J, Brett J, Zou YS, Pinsky D, Stern D. Enhanced cellular oxidant stress by the interaction of advanced glycation end products with their receptors/binding proteins. J Biol Chem. 1994; 269:9889-9897.
54. Koito W, Araki T, Horiuchi S, Nagai R. Conventional antibody against N^{ε}-(carboxymethyl)lysine (CML) shows cross-reaction to N^{ε}-(carboxyethyl)lysine (CEL): Immunochemical quantification of CML with a specific antibody. J Biochem. 2004; 136:831-837.
55. Sell DR, Nagaraj RH, Grandhee SK, Odetti P, Lapolla A, Fogarty J, Monnier VM. Pentosidine: A molecular marker for the cumulative damage to proteins in diabetes, aging, and uremia. Diabetes Metab Rev. 1991; 7:239-251.
56. Lapolla A, Piarulli F, Sartore G, Ceriello A, Ragazzi E, Reitano R, Baccarin L, Laverda B, Fedele D. Advanced glycation end products and antioxidant status in type 2 diabetic patients with and without peripheral artery disease. Diabetes Care. 2007; 30:670-676.
57. Odani H, Iijima K, Nakata M, Miyata S, Kusunoki H, Yasuda Y, Hiki Y, Irie S, Maeda K, Fujimoto D. Identification of N^{ε}-carboxymethylarginine, a new advanced glycation endproduct in serum proteins of diabetic patients: possibility of a new marker of aging and diabetes. Biochem Biophys Res Commun. 2001; 285:1232-1236.
58. Iijima K, Murata M, Takahara H, Irie S, Fujimoto D. Identification of N^{ε}-carboxymethylarginine as a novel acid-labile advanced glycation end product in collagen. Biochem J. 2000; 347:23-27.
59. Glomb MA, Monnier VM. Mechanism of protein modification by glyoxal and glycolaldehyde, reactive intermediates of the Maillard reaction. J Biol Chem. 1995; 270:10017-10026.
60. Anderson MM, Requena JR, Crowley JR, Thorpe SR, Heinecke JW. The myeloperoxidase system of human phagocytes generates N^{ε}-(carboxymethyl)lysine on proteins: a mechanism for producing advanced glycation end products at sites of inflammation. J Clin Invest. 1999; 104:103-113.
61. Nagai R, Hayashi CM, Xia L, Takeya M, Horiuchi S. Identification in human atherosclerotic lesions of GA-pyridine, a novel structure derived from glycolaldehyde-modified proteins. J Biol Chem. 2002; 277:48905-48912.
62. Wada T, Penninger JM. Mitogen-activated protein kinases in apoptosis regulation. Oncogene. 2004; 23:2838-2849.
63. Liu J, Minemoto Y, Lin A. c-Jun N-terminal protein kinase 1 (JNK1), but not JNK2, is essential for tumor necrosis factor alpha-induced c-Jun kinase activation and apoptosis. Mol Cell Biol. 2004; 24:10844-10856.
64. Widenmaier SB, Ao Z, Kim SJ, Warnock G, Mclntosh CH. Suppression of p38 MAPK and JNK via Akt-mediated inhibition of apoptosis signal-regulating kinase 1 constitutes a core component of the β-cell pro-survival effects of glucose-dependent insulinotropic polypeptide. J Biol Chem. 2009; 284:30372-30382.
65. Susztak K, Raff AC, Schiffer M, Böttinger EP. Glucose-induced reactive oxygen species cause apoptosis of podocytes and podocyte depletion at the onset of diabetic nephropathy. Diabetes. 2006; 55:225-233.
66. Surh YJ, Chun KS, Cha HH, Han SS, Keum YS, Park KK, Lee SS. Molecular mechanisms underlying chemopreventive activities of anti-inflammatory phytochemicals: down-regulation of COX-2 and iNOS through suppression of NF-κB activation. Mutat Res. 2001; 480-481:243-268.
67. Ohno H, Sakurai T, Hisajima T, Abe S, Kizaki T, Ogasawara J, Ishibashi Y, Imaizumi K, Takemasa T, Haga S, Kitadate K, Nishioka H, Fujii H. The supplementation of Oligonol, the new lychee fruit-derived polyphenol converting into a low-molecular form, has a positive effect on fatigue during regular track-and-field training in young athletes. Adv Exerc Sport Physiol. 2008; 13:93-99.

(Received January 22, 2015; Revised January 30, 2015; Accepted February 9, 2015)

Review

DOI: 10.5582/ddt.2015.01004

Chemical constituents and bioactivities of *Panax ginseng* (C. A. Mey.)

Wenwen Ru[1,2], Dongliang Wang[1,2,*], Yunpeng Xu[1,2], Xianxian He[1,2], Yang-En Sun[1,2], Liyan Qian[1,2], Xiangshan Zhou[1,2], Yufeng Qin[2]

[1] *National Engineering Technology Research Center of Glue of Traditional Medicine, Dong'e, Shandong, China;*
[2] *Shandong Dong-E-E-Jiao Co., Ltd., Dong'e, Shandong, China.*

Summary **Ginseng, *Panax ginseng* (C. A. Mey.), is a well-known Chinese traditional medicine in the Far East and has gained popularity in the West during the last decade. There is extensive literature on the chemical constituents and bioactivities of ginseng. In this paper we compiled the chemical constituents isolated and detected from ginseng including polysaccharides, ginsenosides, peptides, polyacetylenic alcohols, fatty acids, *etc*. Meanwhile we summarized the biological activities of ginseng, which have been reported over the past few decades, including: anti-aging activity, anti-diabetic activity, immunoregulatory activity, anti-cancer activity, neuroregulation activity, wound and ulcer healing activity, *etc*. Nevertheless, further studies to exploit other kinds of constituents and new biological activities of ginseng are still necessary to facilitate research and development in the future.**

Keywords: *Panax ginseng* (C. A. Mey.), chemical constituents, biological activities

1. Introduction

Ginseng, the roots and rhizomes of *Panax ginseng* C. A. Mey. (Araliaceae), is widely distributed in northeast China, the Korean peninsula, and Russia. According to different processing technology, it is divided into three categories, including fresh ginseng, white ginseng, and red ginseng. Ginseng has always been a valuable and important folk medicine for more than 2000 years in the East Asian countries, such as China, Korea, and Japan. Recently, along with the popularization of traditional Chinese herbs as dietary supplement in Western countries, *Panax ginseng* has been used more and more in North America and Europe as well as other parts of the world. Until now, a large amount of literature has been reported on the chemical constituents and bioactivities of ginseng. As listed in the literature, active constituents found in ginseng mainly include polysaccharides, ginsenosides, peptides, polyacetylenic alcohols, fatty acids and so on. In addition, pharmacological effects of ginseng have been demonstrated in cancer, diabetes mellitus, cardiovascular system, immune system, central nervous system, and so on (*1-3*).

In this review, we compile the major active components isolated from the three main kinds of ginseng over the past few decades. The biological activities of the crude extract and its constituents are also discussed.

2. Chemical constituents

Several classes of compounds have been isolated from Ginseng, including polysaccharides, ginsenoside, peptides, and ligans, *etc*. Some of their names, **1-85**, are collected in Table 1, and some of their structures, **1-85**, are shown in Figure 1. As can be seen, ginsenosides are the predominant active constituents of ginseng.

2.1. *Polysaccharides*

Polysaccharides are the most abundant components of ginseng. It has been reported that the polysaccharide content in ginseng is nearly 40% (by weight). This class of compounds was first isolated and documented in 1966 (*4*). The more biologically active carbohydrates in ginseng are acidic polysaccharides, known as ginsan,

**Address correspondence to:*
Dr. Dongliang Wang, National Engineering Technology Research Center of Glue of Traditional Medicine, Shandong Dong-E-E-Jiao Co. Ltd, Dong'e 252201, Shandong, China.
E-mail: wangdljp@126.com

which have the typical structure of pectin (*5,6*). In 2012, several water-soluble ginseng oligosaccharides with a degree of polymerization ranging from 2 to 10 were obtained from a warm-water extract of ginseng roots, among them, α-Glcp-(1-6)-α-Glcp, α-Glcp-(1-6)-α-Glcp-(1-4)-α-Glcp, α-Glcp-(1-6)-α-Glcp-(1-6)-α-Glcp-(1-4)-α-Glcp, and another six malto-oligosaccharides (*i.e.*, maltopentaose, maltohexaose, maltoheptaose, maltooctaose, maltononaose, maltodecaose) were detected (*7*).

2.2. *Ginsenosides*

Ginsenosides, known as saponins, are considered to be the major bioactive constituents of ginseng. The first saponin isolated from ginseng could be traced back to

Table 1. Chemical constituents of *Panax ginseng* C. A. Mey.

No.	Name	R_1	R_2	Reference
Protopanaxadiol ginsenosides				
1	20*S*-ginsengoside Ra_1	-glc(2-1)glc	-glc(6-1) ara(p) (4-1) xyl	*11,12*
2	20*S*-ginsengoside Ra_2	-glc(2-1)glc	-glc(6-1) ara(f) (2-1) xyl	*11,12*
3	20*S*-ginsengoside Ra_3	-glc(2-1)glc	-glc(6-1) glc(3-1) xyl	*13*
4	20*S*-ginsengoside Ra_4	-glc(2-1)glc(6) Bu	-glc(6-1) ara(p) (4-1) xyl	*14*
5	20*S*-ginsengoside Ra_5	-glc(2-1)glc(6) Ac	-glc(6-1) ara(p) (4-1) xyl	*14*
6	20*S*-ginsengoside Ra_6	-glc(2-1)glc(6) Bu	-glc(6-1) glc	*14*
7	20*S*-ginsengoside Ra_7	-glc(2-1)glc(6) Bu	-glc(6-1) ara(p)	*14*
8	20*S*-ginsengoside Ra_8	-glc(2-1)glc(4) Bu	-glc(6-1) ara(f)	*14*
9	20*S*-ginsengoside Ra_9	-glc(2-1)glc(6)Bu	-glc(6-1) ara(f)	*14*
10	20*S*-ginsengoside Rb_1	-glc(2-1)glc	-glc(6-1) glc	*12,15,16*
11	20*S*-ginsengoside Rb_2	-glc(2-1)glc	-glc(6-1) ara(p)	*12,15,16*
12	20*S*-ginsengoside Rb_3	-glc(2-1)glc	-glc(6-1) xyl	*12,17*
13	20*S*-ginsengoside Rc	-glc(2-1)glc	-glc(6-1) ara(f)	*12,15,16*
14	20*S*-ginsengoside Rd	-glc(2-1)glc	-glc	*12,15,16*
15	20*S*-ginsengoside Rg_3	-glc(2-1)glc	-H	*12,16,18*
16	20*R*-ginsengoside Rg_3	-glc(2-1)glc	-H	*16*
17	20*R*-ginsengoside Rh_2	-glc	-H	*19*
18	20*S*-ginsengoside Rh_2	-glc	-H	*16*
19	20*S*-ginsengoside Rs_1	-glc(2-1)glc(6) Ac	-glc(6-1) ara(p)	*12,14*
20	20*S*-ginsengoside Rs_2	-glc(2-1)glc(6) Ac	-glc(6-1) ara(f)	*12,14*
21	20*S*-ginsengoside Rs_3	-glc(2-1)glc(6) Ac	-glc(6-1) ara(f)	*20*
22	malonyl-20*S*-ginsengosideRa_3	-glc(2-1)glc(6) mal	-glc(6-1) ara(3-1)xyl	*21*
23	malonyl-20*S*-ginsengosideRb_1	-glc(2-1)glc(6) mal	-glc(6-1) glc	*14,22*
24	malonyl-20*S*-ginsengosideRb_2	-glc(2-1)glc(6) mal	-glc(6-1) ara(p)	*22*
25	malonyl-20*S*-ginsengosideRc	-glc(2-1)glc(6) mal	-glc(6-1) ara(f)	*22*
26	malonyl-20*S*-ginsengosideRd	-glc(2-1)glc(6) mal	-glc	*22*
27	malonyl-20*S*-notoginsengosideR_4	-glc(2-1)glc(6) mal	-glc(6-1) glc(6-1) xyl	*23*
28	20*S*-gypenosideXVII	-glc	-glc(6-1) glc	*14*
29	20*S*-notoginsenoside-Fe	-glc	-glc(6-1) ara(f)	*24*
30	20*S*-notoginsenoside R_4	-glc(2-1)glc	-glc(6-1) glc(6-1) xyl	*13,25*
31	20*S*-pseudo-ginsenoside R_{C1}	-glc(2-1)glc(6) Ac	-glc	*14*
32	20*S*-quinquenoside R_1	-glc(2-1)glc(6) Ac	-glc(6-1) glc	*12,14*
33	20*S*-vinaginsenoside R_{16}	-glc(2-1)xyl	-glc	*14*
Protopanaxatriol ginsenosides				
34	20*S*-ginsenoside Re	-glc(2-1) rha	-glc	*12,16,26*
35	20*S*-ginsenoside Re_1	-glc	-glc(3-1) glc	*27*
36	20*S*-ginsenoside Re_2	-glc(3-1) glc	-glc	*27*
37	20*S*-ginsenoside Re_3	-glc	-glc(4-1) glc	*27*
38	20*S*-ginsenoside Re_4	-glc	-glc(6-1) ara(f)	*27*
39	20*S*-ginsenoside Re_6	-glc	-glc(6) Bu	*27*
40	20*S*-ginsenoside Rf	-glc(2-1) glc	-H	*12,16,26*
41	20*S*-ginsenoside Rg_1	-glc	-glc	*12,16,18,28*
42	20*S*-ginsenoside Rg_2	-glc(2-1) rha	-H	*12,16,26*
43	20*R*-ginsenoside Rg_2	-glc(2-1) rha	-H	*12,16,25*
44	20-gluco-20*S*-ginsenoside Rf	-glc(2-1) glc	-glc	*12,17*
45	20*S*-ginsenoside Rh_1	-glc	-H	*16,18*
46	20*R*-ginsenoside Rh_1	-glc	-H	*16*
47	20*S*-koryoginsenoside R_1	-glc(6-1) Bu	-glc	*18,24,27*
48	20*S*-notoginsenoside N	-glc(4-1) glc	-glc	*27*
49	20*S*-notoginsenoside R_1	-glc(2-1) xyl	-glc	*12,18,27*
50	20*S*-notoginsenoside R_2	-glc(2-1) xyl	-H	*25,27*
51	20*S*-yesanchinoside D	-glc(6)Ac	-glc	*27*

(to continue)

Table 1 (continued). Chemical constituents of *Panax ginseng* C. A. Mey.

No.	Name	R_1	R_2		Reference
Protopanaxadiol and Protopanaxatriol ginsenosides with modified side chain					
52	Ginsenjilinol	I-2-1	-glc(2-1) glc	-H	*24*
53	ginsenoside F_4	I-2-2	-glc(2-1) rha	-	*29,30*
54	ginsenoside Re_5	I-2-3	-glc(2-1) glc	-H	*27*
55	ginsenoside Rf_2	I-2-4	-glc(2-1) rha	-	*31*
56	ginsenoside Rg_5	I-1-1	-glc(2-1) glc	-	*30,32,33*
57	ginsenoside Rg_6	I-2-5	-glc(2-1) rha	-	*30,34*
58	ginsenoside Rh_4	I-2-6	-glc	-	*30,35,36*
59	ginsenoside Rk_1	I-1-2	-glc(2-1) glc	-H	*30,36*
60	ginsenoside Rk_2	I-1-3	-glc	-H	*36*
61	ginsenoside Rk_3	I-2-7	-H	-Oglc	*30,36*
62	ginsenoside Rs_4	I-1-4	-glc(2-1) glc(6)Ac	-	*30,37*
63	ginsenoside Rs_5	I-1-5	-glc(2-1) glc(6)Ac	-H	*30,37*
64	ginsenoside Rs_6	I-2-8	-glc(6)Ac	-	*37*
65	ginsenoside Rs_7	I-2-9	-H	-glc(6)Ac	*38*
66	koryoginsenosideR_2	I-1-6	-glc(2-1) glc	-glc(6-1)glc	*18*
Oleanane ginsenosides					
67	ginsenoside Ro	II-1	-glcUA(2-1)glc	-glc	*12,15*
68	ginsenoside Ri	II-1	-H	-ara(f)	*38*
69	ginsenoside Romethyl ester	II-1	-(6'-Me)glcUA(2-1)glc	-glc	*39*
70	polyacetyleneginsenoside-Ro	II-1	-(6'-PAE)glcUA(2-1)glc	-glc	*39*
Alkaloids					
71	N_9-formylharman				*40,41*
72	ethyl β-carboline				*40,41*
73	perlolyrine				*40, 41*
74	1-carbobutoxy-β-carboline				*42, 43*
75	1-carbomethoxy-β-carboline				*42, 43*
Glucosides					
76	isomaltol-α-D-glucopyranoside				*44, 45*
77	ketopropyl-α-D-glucopyranoside				*44, 45*
78	adenosine				*44, 45*
Phenolic acids					
79	maltol (3-hydroxy-2-methyl-4-pyrone)				*46*
80	salicylic acid				*47*
81	vanillic acid				*47*
82	*p*-hydroxycinnamic acid				*47*
Others					
83	thiazole				*43*
84	gomisin N				*48*
85	gomisin A				*48*

1854 (*3*). Later, the chemical structures of several ginseng saponins were characterized in the 1960s (*8*). Saponin components are a type of triterpenoidal dammarane glycosides, named ginsengosides Rx according to their mobility on TLC plates, with polarity decreasing from "a" to "h" (*9*). According to the positioning of sugar moieties at carbon -3 and -6, ginsenosides can be divided into protopanaxadiol type (protopanaxadiol type, I-1 type) and protopanaxatriol type (protopanaxatriol type, I-2 type); since the I-1 and I-2-type chiral carbon C-20 position substituted poor isobutyl, and is further divided into 20 (S) and 20 (R). To date, more than 70 ginsenosides, **1-70**, have been isolated from the three main kinds of ginseng, among them, ginsenosides Rb_1, Rb_2, Rc, Rd, Rgl, Rg_2, and Re are major constituents of white and red ginsengs, while ginsenosides Rg_3, Rg_5, and Rg_6 are known to be unique constituents of red ginseng (*10*). Names of the compounds and their corresponding reference are compiled in Table 1, and structures of **1-70** are shown in Figure 1.

2.3. *Alkaloids*

In 1986, three β-carboline alkaloids were isolated from the root of ginseng by Han *et al*. for the first time (*40,41*). In the following year, two other β-carboline alkaloids were reported by Jong *et al*. (*42,43*). Their structures, **71-75**, are shown in Figure 1.

2.4. *Glucosides*

Based on spectral and chemical evidence, three

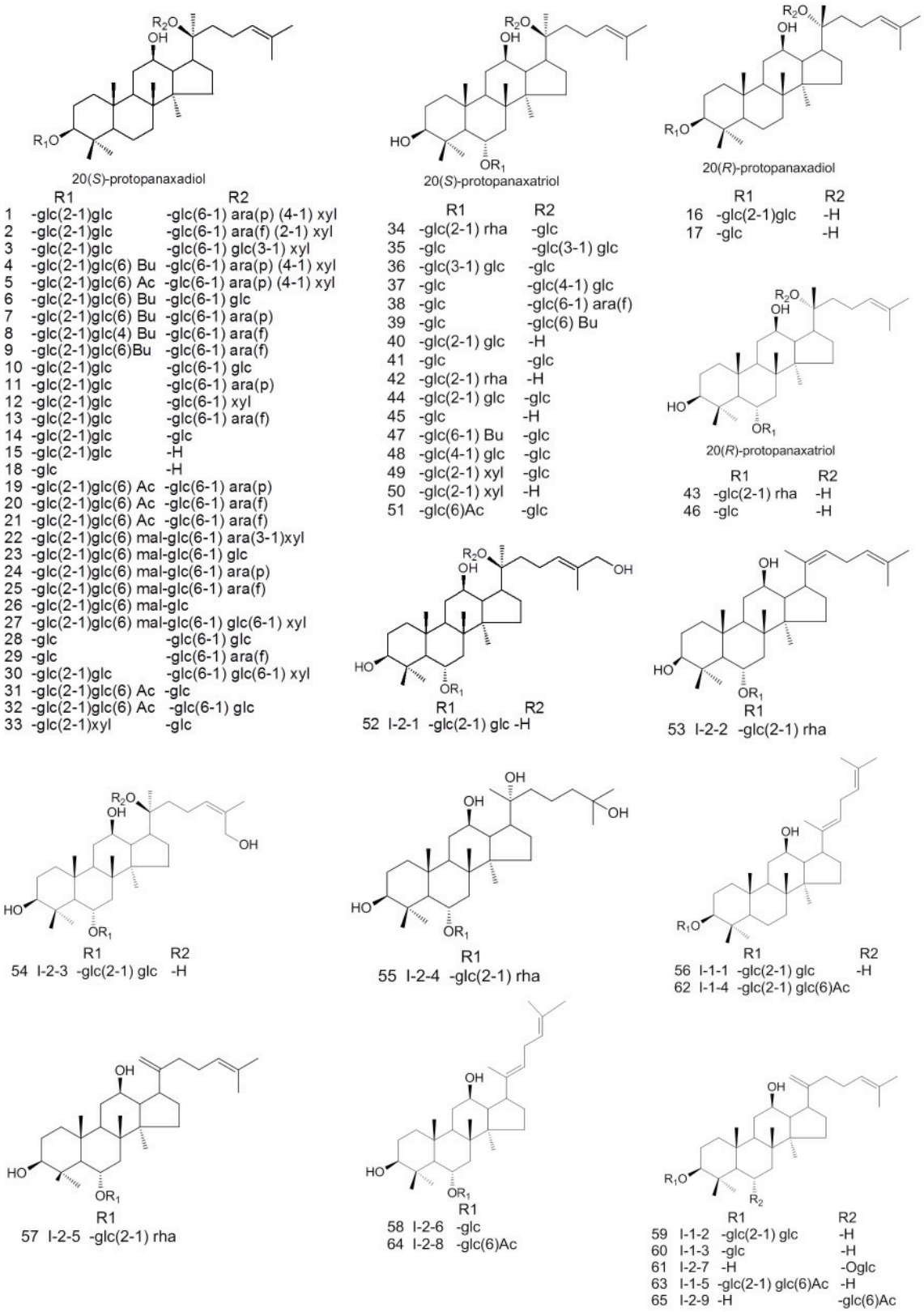

Figure 1. The structure of chemical constituents of Panax ginseng C. A. Mey. (to continue)

glycosides isolated from red ginseng were characterized as isomaltol-α-D-glucopyranoside (**76**), ketopropyl-α-D -glucopyranoside (**77**) and adenosine (**78**). However, these compounds are not found in white ginseng (*44,45*).

2.5. *Phenolic acid*

In 1979, maltol (3-hydroxy-2-methyl-4-pyrone) (**79**) was isolated from ginseng (*46*). In 1981, another three

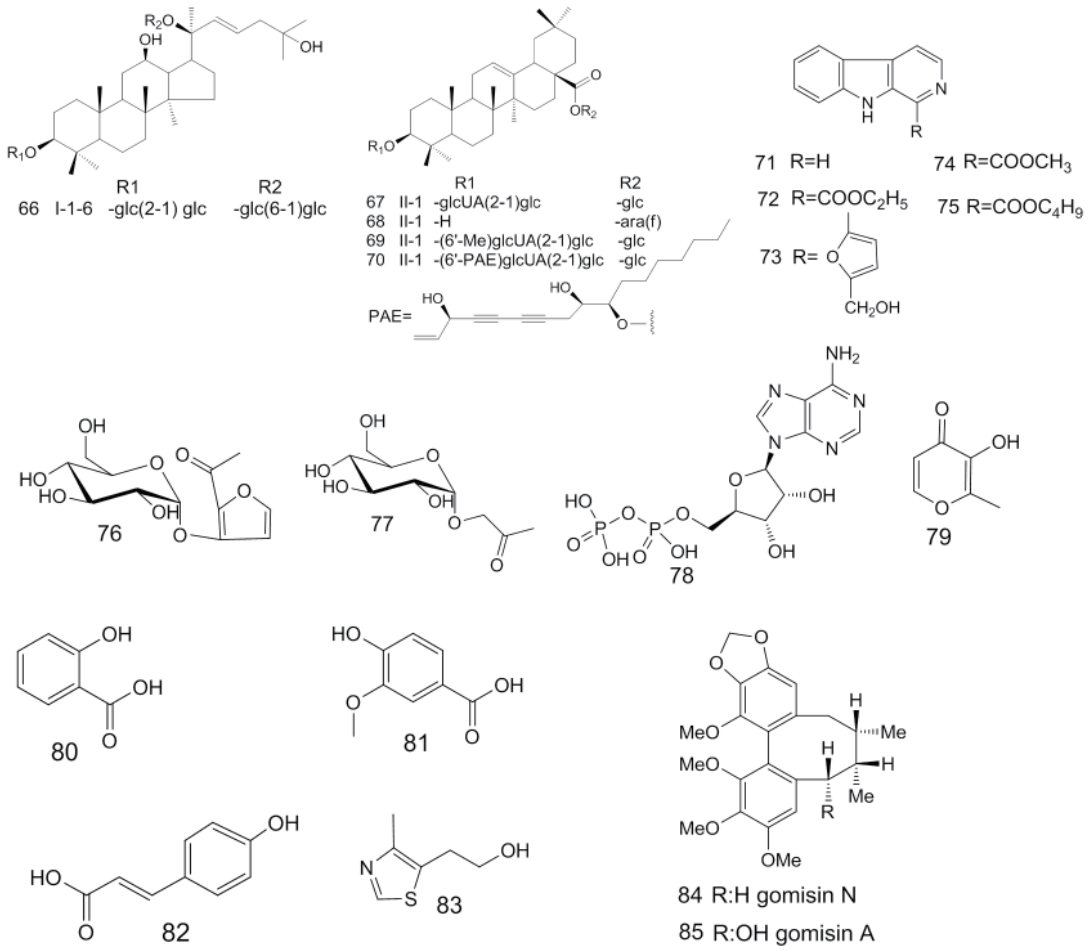

Figure 1 (continued). The structure of chemical constituents of Panax ginseng C. A. Mey.

phenolic acids were obtained from the ether-soluble acidic fraction of fresh ginseng, and they were identified by chemical and spectrometric methods to be salicylic acid (**80**), vanillic acid (**81**), and p-hydroxycinnamic acid (**82**) (*47*).

2.6. *Others*

Besides all the constituents listed above, in 1988, a thiazole (**83**) was isolated by Jong *et al*. (*43*). In 1990, two lingans were isolated from Korean red ginseng and their chemical structures were elucidated as gomisin N (**84**) and gomisin A (**85**) by spectrometric analysis (*48*).

3. Biological activities

3.1. *Anti-aging activity*

Ginseng, as a well-known traditional medicine and tonic, has been used for a panacea or promoting longevity. Abundant evidence suggested that oxidative stress plays a central role in the process of biological aging (*49*). Excessive oxidative stress leads to cell death and mitochondrial dysfunction (*50*). Some research indicated that ginseng extracts had been shown to improve learning and memory in normal, aged or brain-damaged animals (*51,52*). In 1981, Han *et al*. identified that salicylic acid (**80**) and vanillic acid (**81**) had potent antioxidant activity in the liver of ethanol-intoxicated mice, whereas p-hydroxycinnamic acid (**82**) did not have the effect (*47*). In 1991, Bernhard *et al*. reported that ginseng extract could enhance the age-dependency of learning ability in the passive avoidance test in female rats (*53*). In 1996, it was found that maltol (**79**) was an antioxidant with little prooxidant activity by comparing it with some antioxidant phenolic compounds (*54*). It has been reported that several ginsenosides have the function of ameliorating impaired memory function. For example, ginsenosides Rb_1 (**10**) and Rg_1 (**41**) have been shown to accelerate memory acquisition of rats on a Y-maze task and they also enhanced the cognitive function of mice in a Morris water maze (*55*). Yamaguchi *et al*. have also reported that Rg_1 (**41**) improved the scopolamine-induced impaired performance of rats in a radial-arm maze. Rb_1 (**10**) and its metabolite M_1 were reported to improve

memory disorders, axonal atrophy, and synaptic loss in a mouse model of Alzheimers disease (AD) that was induced by an *i.c.v*, injection of $A_{\beta(25-35)}$ (*56*). In 2005, Bao *et al*. indicated that ginsenosides Rg_3(S) (**15**) Rg_5 (**56**) and Rk_1 (**59**) significantly reversed the memory dysfunction induced by ethanol or scopolamine, and their neuroprotective actions against excitotoxicity may be attributed to their memory enhancing effects (*57*).

3.2. *Anti-diabetic activity*

In 1990, ginseng had been reported to improve glucose homeostasis and insulin sensitivity (*58*). In 2001, Chung *et al*. reported that oral administration of ginseng root to diabetic KKAy mice for 4 weeks reduced blood glucose levels similar to that of an insulin sensitizer (*59*). Rb_2 (**11**) was found to be the most effective component of ginsenosides for streptozatocin-diabetic rats (*60*). In 2004, it was reported that wild ginseng ethanol extract could prevent type 2 diabetes mellitus and possibly obesity in IRC mice through improving the insulin resistance index and decreasing white and brown adipocytes diameters (*61*). In 2011, Lee *et al*. reported that Rb_2 might inhibit palmitate-induced gluconeogenesis *via* AMP-activated protein kinase (AMPK)-induced small heterodimer partner (SHP) by relieving estrogen receptor (ER) stress (*62,63*).

3.3. *Immunoregulatory activity*

Ginseng has been used for more than 2000 years in oriental countries to enhance stamina and immune function. In 1994, the antigenicity of the aqueous extract of red ginseng (ARG) was evaluated in guinea pigs, the results suggested that ARG has no antigenicity but it was confirmed not to suppress immune reactions (*64*). Ginsan, a polysaccharide isolated from ginseng, had been shown to be a potent immunomodulator, producing several cytokines (tumor necrosis factor-α (TNF-α), interleukin-1β (IL-1β), interleukin-2 (IL-2), interleukin-6 (IL-6), interleukin-12 (IL-12), interferon-γ (IFN-γ), granulocyte-macrophage colony-stimulating factor (GM-CSF)) and stimulating lymphoid cells to proliferate (*65*). In 2004, the mechanism of the immunomodulator activity of ginsan was investigated, and the results showed that ginsan at a dose of 100 mg/kg could cause marked elevation (1.7-2 fold) of heme oxygenase (HO) activity, decrease total hepatic cytochrome P-450 (CYP450) levels (by 20-34%), and prolong zoxazolamine-induced paralysis time (by 65-70%), and did not seem to cause hepatic injury, since serum aspartate aminotransferase (AST), alanineaminotransferase (ALT), and alkaline phosphatase (ALP) activities and levels of total bilirubin and albumin were not changed (*66*). In 2005, ginsan was found to improve γ radiation-induced immunosuppression through inducing mRNA expression of Th1 and Th2 type cytokines, and restoring mRNA expression of INF-γ and Th1 cytokines (*67*). In 2008, it was reported that red ginseng acidic polysaccharide and pidotimod had synergistic immunostimulating activity against cyclophosphamide-induced immunosuppression through stimulating splenic T cell and B cell proliferation and increasing the nitric oxide from peritoneal macrophages and natural killer cell (NK cell) activity (*68*). In 2013, Wang *et al*. demonstrated that ginseng acidic polysaccharide had potential therapeutic effects for chronic fatigue syndrome by enhancing malondialdehyde and lactate dehydrogenase levels in serum and lowering superoxide dismutase and glutathione peroxidase in mice *in vivo* (*69*).

3.4. *Anti-cancer activity*

Ginseng has been shown to have powerful anticancer properties. Saponin and non-saponin compounds from ginseng roots were reported to show cytotoxic activities against various kinds of cancer cell lines in culture, such as L1210, L5187Y, Hela cells, Sarcoma 180 cells, A549, SK-OV-3, SK-Mel-2, P388, and K562 *et al*. (*70*). In 1991, Kikuchi *et al*. reported that ginsenoside Rh_2 (**17/18**) inhibited human ovarian cancer growth in a nude mice model (*71*). In 2002, Lee *et al*. reported that ginsenoside Rb_1 (**10**), Rc (**13**) and Re (**34**) could act as a weak phytoestrogen in MCF-7 human breast cancer cells by binding and activating the estrogen receptors at both the mRNA and protein levels (*72,73*). In 2004, it was found that ginsenoside Rg_3 (**15/16**) and Rh_2 (**17/18**)-induced cell detachment and inhibition of the proliferation of prostate cancer cells and might be associated with modulation of three modules of MAP kinases (extracellular signal-regulated kinase, *p38* mitogen-activated protein kinase, and c-Jun N-terminal kinase). Furthermore, the increase of LogP and decrease of C-6 steric hindrance, which were caused by deglycosylation by intestinal bacteria could increase anti-androgen-independent prostate cancer activity (*74,75*). In 2005, compound K, ginsenoside metabolite, was found to inhibit the growth of human monocytic leukemia cells U937 through up-regulating of *p21* and activating Jun N-terminal kinase in the G1 phase (*76*). Rg_3 (**15/16**) was discovered to inhibit tumor cell proliferation and induce cell apoptosis in mice with induced liver cancer (*77*). In 2009, Fishbein *et al*. suggested a potential for red ginseng as an adjuvant therapy in the treatment of colorectal cancer, *via* a synergistic action (*78*). In 2011, Rk_1 (**59**) was found to induce apoptosis in SK-MEL-2 human melanoma *in vitro* through up-regulation of Fas, FasL, and Bax protein expression and down-regulation of procaspase-8, procaspase-3, mutant *p53* and *bcl-2* protein expression (*79*).

3.5. *Neuroregulation activity*

In 1985, Kim *et al*. elucidated that supplement of the

saponin fraction of ginseng could increase the amount of norepinephrine and dopamine (DA) in mouse brain. In 1997, it was reported that ginseng total saponin (GTS) could modulate the methamphetamine-induced striatal dopaminergic neuronal systems by inhibiting methamphetamine-induced DA increase (*80*). In 1998, Kim *et al*. reported GTS can modulate dopaminergic activity at both presynaptic and postsynaptic dopamine receptors (*81*). Furthermore, it was found that GTS might be useful in the prevention and therapy of the behavioral side effects induced by psychotropic agents by attenuating the morphine-induced cAMP signaling pathway (*82*). In 2004, ginsenoside Rh_2 (**17**/**18**) and compound K were found to improve ischemic brain injury (*83*). In 2008, ginsenosides Rb_1 (**10**), Rb_2 (**11**), Rc (**13**), Rd (**14**), Re (**34**), Rf (**40**) and Rg_1 (**41**) were found to regulate nociceptive processing induced by pro-inflammatory cytokines (TNF-α, IL-1β, and IFN-γ) (*84*). In 2009, it was reported that red ginseng extract could modulate nerve growth factors (NGF) expression in the steroid-induced polycystic ovary (POC) rat model by decreasing ovarian concentrations of NGF protein and NGF mRNA (*85*).

3.6. *Lipid-regulating and antithrombotic activities*

It was found that ginseng saponin, one of major component of *Panax ginseng* had influence on lipid metabolism. Saponin stimulated the absorption, metabolism and transport of lipids (*86*). It had been also reported that ginseng saponin decreased plasma cholesterol and triglyceride levels and inhibited aortic atheroma formation in animals with hypercholesterolemia caused by long administration of high cholesterol or feeding on a diet containing high cholesterol (*86*). In 1984, it was reported that red ginseng saponin showed no significant change of high-density lipoproteincholesterol-cholesterol (HDL-cholesterol) level but it lowered plasma levels of total cholesterol and highly elevated those of triglyceride in Wistar male rats fed on a diet high in cholesterol and triglyceride (*86*). In 2006, it was identified that Rg_3 (**15**/**16**) might be effective in metabolic syndrome (MetSyn) by comparing the anti-MetSyn effect of vinegar-processed ginseng radix and non-processed ginseng radix in a high fat diet induced MetSyn ICR mouse model (*87*). In the same year, it was reported that red ginseng had a potent antithrombotic effect *in vivo*, which may be due to antiplatelet rather than anticoagulation activity, and its intake may be beneficial to individuals with high risk of thrombotic and cardiovascular diseases (*88*).

3.7. *Wound and ulcer healing activity*

In 2002, it was reported that ginsenoside Rb_2 (**11**) could enhance epidermal cell proliferation by upregulating the expression of proliferation- related factors (*89*). In 2006, Shin *et al*. reported that ginsenoside Rh_3 metabolized from ginsenoside R_5 (**56**) could improve chronic dermatitis or psoriasis by the regulation of IL-1β, TNF-α and IFN-γ produced by macrophage cells and Th cells (*90*). In 2003, Rb_1 (**10**) was found to exhibit an anti-ulcer effect through increasing mucus secretion (*91,92*).

3.8. *Other activities*

In 1986, Lee *et al*. reported that ginseng saponin could interact directly with Na^+-K^+-ATPase before disruption of membrane barriers of sarcolemmal vesicles, however, it decreased the number of phosphorylation sites (*93*). In 1996, it was reported that GTS could modulate various cellular activities by inhibiting gap junction channel reconstitution (*94*). In 2001, Ginseng saponin had been reported to induce IP_3-mediated Ca^{2+} release from ERs for the activation of Ca^{2+}-activated Cl- channel in *Xenopus* oocytes (*95,96*). Furthermore, it was found that CaM could modulate ginseng saponin-mediated Ca^{2+}-activated Cl^- channel activation (*97*). In 2003, Rc (**13**) was found to enhance I_{GABA} in oocytes expressing human $GABA_A$ receptor in *Xenopus* oocytes (*98*). In 2006, it was reported that tissue culture root of wild *Panax ginseng* had feasibility as a therapeutic agent for spermatogenic disorders (*99*).

4. Conclusions

Panax ginseng (C. A. Mey.) has been used as traditional Chinese medicine for more than two thousand years. More than a hundred compounds were isolated from the root of ginseng, and a majority of them were ginsenosides, which showed a broad range of biological activities. Nevertheless, further studies to exploit other kinds of constituents and new biological activities of ginseng are still necessary to facilitate research and development in the future.

Acknowledgements

The authors are grateful for financial support from National Engineering Technology Research Center of Glue of Traditional Medicine, Shandong Dong-E-E-Jiao Co. Ltd. and National "Major Drug Discovery" Science and Technology Major Project (Project No. 2011ZX09201-201-10).

References

1. Hu SY. The genus *Panax ginseng* in Chinese medicine. Economic Botany. 1976; 30:11-28.
2. Cao H, Bi PX, Hu XY. The ginseng plants: Commercial products and quality assessment. J Chin Integr Tradit Western Med. 1997; 4:25.
3. Park JD, Rhee DK, Lee YH. Biological activities and

chemistry of saponins from *Panax ginseng* CA Meyer. Phytochem Reviews. 2005; 4:159-175.
4. Ovodov YS, Solov'eva TF. Polysaccharides of *Panax ginseng*. Chem Natural Compounds. 1966; 2:243-245.
5. Tomoda M, Takeda K, Shimizu N, Gonda R, Ohara N, Takada K, Hirabayashi K. Characterization of two acidic polysaccharides having immunological activities from the root of *Panax ginseng*. Biol Pharm Bull. 1993; 16:22-25.
6. Baek SH, Lee JG, Park SY, Bae ON, Kim DH, Park JH. Pectic polysaccharides from *Panax ginseng* as the antirotavirus principals in ginseng. Biomacromolecules, 2010; 11:2044-2052.
7. Wan D, Jiao L, Yang H, Liu S. Structural characterization and immunological activities of the water-soluble oligosaccharides isolated from the *Panax ginseng* roots. Planta. 2012; 235:1289-1297.
8. Uvarova NI, Gorshkova RP, Strigina LI, Elyakov GB, Kochetkov NK. Glycosides from ginseng roots IV. Isolation of new glycosides from ginseng. Chem Natural Comp. 1965; 1:63-66.
9. Huang KC. The pharmacology of Chinese herbs. CRC press, 1998.
10. Ryu JH, Park JH, Eun JH, Jung JH, Sohn DH. A dammarane glycoside from Korean red ginseng. Phytochem. 1997; 44:931-933.
11. Besso H, Kasai R, Saruwatari Y, Ginsenoside-Ra1 and Ginsenoside-Ra2, new dammarane-saponins of ginseng roots. Chem Pharm Bull.1982; 30:2380-2385.
12. Kasai R, Besso H, Tanaka O, Fuwa T. Saponins of red ginseng. Chem Pharm Bull. 1983; 31:2120.
13. Matsuura H, Kasai R, Tanaka O, Saruwatari Y, Kunihiro K, Fuwa T. Further studies on dammarane-saponins of ginseng roots. Chem Pharm Bull. 1984; 32:1188-1192.
14. Zhu GY, Li YW, Hau DKP, Jiang ZH, Yu ZL, Fong WF. Protopanaxatriol-type ginsenosides from the root of *Panax ginseng*. J Agric Food Chem. 2010; 59:200-205.
15. Sanada S, Kondo N, Shoji J, Tanaka O, Shibata S. Studies on saponins of ginseng, strctures of ginsenoside-Re, ginsenoside-Rf and ginsenoside-Rg2. Chem Pharm Bull. 1974; 22:2407-2412.
16. Isao KM, Yoshiawa MY. Chemical studies on crude drug precession 1. On the constituents of ginseng radix rubra (1). Yakugaku Zasshi. 1983; 103:611-613.
17. Sanada S, Shoji J, Shibata S. Quantitative analysis of ginseng saponins. Chem Pharm Bull. 1978; 26:1694-1697.
18. Kim DS, Chang YJ, Zedk U, Zhao P, Liu Y Q, Yang CR. Dammarane saponins from *Panax ginseng*. Phytochemistry. 1995; 40:1493-1497.
19. Zhong FL, Liu JP, Lu D, Li YP. Studies on chemical consitituents of *Panax ginseng*. Chin Trad Med. 2008; 30:241-243.
20. Baek NI, Kim JM, Park JH, Ryu JH, Kim DS, Lee YH, Kim SI. Ginsenoside Rs3, a genuine dammarane-glycoside from Korean red ginseng. Arch Pharm Res. 1997; 20:280-282.
21. Ruan CC, Liu Z, Li X, Liu X, Wang LJ, Pan HY, Zhang LX. Isolation and characterization of a new ginsenoside from the fresh root of *Panax ginseng*. Molecules. 2010; 15:2319-2325.
22. Kitagawa I, Taniyama T, Hayashi T, Yoshikawa M. Malonyl-ginsenoside Rb1, Malonyl-ginsenoside Rb_2, Malonyl-ginsenoside Rc, and Malonyl-ginsenoside Rd 4 new malonylated dammarane-type triterpene oligoglycosides from ginseng radix. Chem Pharm Bull. 1983; 31:3353-3356.
23. Sun GZ, Li XG, Liu Z, Wang JY, Zheng YN, Yang XW. Isolation and structure characterization of malonyl-notoginsenoside-R4 from the root of *Panax ginseng*. Chem J Chin Univ. 2007; 28:1316.
24. Wang HP, Yang XB, Yang XW, Liu JX, Wang YP, Zhang LX. Chemical constituents from roots and rhizomes of *panax ginseng* cultivated in Jilin province. Chin J Chin Mater Med. 2013; 38:2807.
25. Dou DQ, Ren J, Chen Y, Pei YP, Chen YJ. Study on the chemical constituents of the roots of commercial ginseng. Chin J Chin Mater Med. 2003; 28:522-524.
26. Sanada S, Kondo N, Shoji J, Tanaka O, Shibata S. Studies on saponins of ginseng structures of ginsenoside-Re, ginsenoside-Rf and ginsenoside-Rg2. Chem Pharm Bull. 1974; 22:2407-2412.
27. Yu JL, Dou DQ, Chen XH, Yang HZ, Guo N, Cheng GF. Protopanaxatriol-type ginsenosides differentially modulate type 1 and type 2 cytokines production from murine splenocytes. Planta Medica, 2005; 71:202-207.
28. Nagai Y, Tanaka O, Shibata S. Chemical studies on the oriental plant drugs XXIV: Structure of ginsenoside-Rg_1, a neutral saponin of ginseng root. Tetrahedron. 1971; 27:881-892.
29. Ryu JH, Park JH, Kim TH, Sohn DH, Kim JM, Park JH. A genuine dammarane glycoside, (20E)-ginsenosideRf 4 from Korean red ginseng. Arch Pharm Res. 1996; 19:335-336.
30. Zhang YC, Pi ZF, Liu CM, Song FR, Liu ZQ, Liu SY. Analysis of low-polar ginsenosides in steamed *Panax ginseng* at high-temperature by HPLC-ESI-MS/MS. Chem Res Chin Univ. 2012; 8:31-36.
31. Park JD, Lee YH, Kim SI. Ginsenoside Rf2, a new dammarane glycoside from Korean red ginseng (*Panax ginseng*). Arch Pharm Res. 1998; 21:615-617.
32. Baek NI, Kim SI, Park JH. Ginsenoside Rg5, a genuine dammarane glycoside from Korean red ginseng. The Ginseng Review. 1996; 22:88-92.
33. Kim SI, Park JH, Ryu JH, Park JD, Lee YH, Park JH, Baek NI. Ginsenoside Rg5, a genuine dammarane glycoside from Korean red ginseng. Arch Pharm Res. 1996; 19:551-553.
34. Baek NI, Kim DS, Lee YH, Park JD, Lee CB, Kim SI. Ginsenoside Rh4, a genuine dammarane glycoside from Korean Red Ginseng. Planta medica. 1996; 62:86-87.
35. Baek NI, Kim DS, Lee YH, Park JD. Isolation of a novel dammarane-glycoside, ginsenoside Rh4, from Korean red ginseng. The Ginseng Review. 1995; 20:84-86.
36. Park IH, Kim NY, Han SB, Kim JM, Kwon SW, Kim HJ, Park JH. Three new dammarane glycosides from heat processed ginseng. Arch Pharm Res. 2002; 25:428-432.
37. Park IH, Han SB, Kim JM, Piao L, Kwon SW, Kim NY, Park JH. Four new acetylated ginsenosides from processed ginseng (sun ginseng). Arch Pharm Res. 2002; 25:837-841.
38. Fu L, Li XG, Yang SR. Isolated and identified of new gisenoside of oleanolic acid type from fresh *Panax ginseng* roots. J Jilin Agr Univ. 1998; 20:30-34.
39. Zhang H, Lu Z, Tan GT, Qiu S, Farnsworth NR, Pezzuto JM, Fong HH Polyacetyleneginsenoside-Ro, a novel triterpene saponin from *Panax ginseng*. Tetrahedron lett. 2002; 43:973-977.
40. Han BH, Park MH, Han YN, Woo LK. Alkaloidal components of *Panax ginseng*. Arch Pharm Res. 1986;

9:21-23.
41. Han YN, Ryu SY, Han BH, Woo LK. Spinacine from *Panax ginseng*. Arch Pharm Res. 1987; 10:258-259.
42. Park JD, Kim MW, Yoo SJ, Wee JJ. Chemical studies on the ether-soluble alkaloidal fraction of *Panax ginseng*. Isolation of 1-carbobutoxy-β-carboline and 1-carbomethoxy-β-carboline. Arch Pharm Res. 1987; 10:197-199.
43. Park JD, Kim MW, Yoo SJ, Wee JJ. A thiazole and two β-carboline constitutents from *Panax ginseng*. Arch Pharm Res. 1988; 11:52-55.
44. Matsuura H, Hirao Y, Yoshida S, Kunihiro K, Fuwa T, Kasai R, Tanaka O. Study of red ginseng: New glucosides and a note on the occurence of rnaltol. Chem Pharm Bull. 1984; 32:4674.
45. Han BH, Park MH, Han YN. Isolation of isomaltol-α-D-glucopyranoside and ketopropyl-α-D-glucopyranoside from Korean red ginseng. Arch Pharm Res. 1985; 8:257-260.
46. Han BH, Park MH, Woo LK, Woo WS, Han YN. Antioxidant components of Korean ginseng. Korean Biochem J. 1979; 12:33.
47. Han BH, Park MH, Han YN. Studies on the antioxidant components of Korean ginseng (III). Arch Pharm Res. 1981; 4:53-58.
48. Huh BH, Lee IR, Han BH. Lingans from Korean red ginseng. Arch Pharm Res. 1990; 13:278-281.
49. Muller FL, Lustgarten MS, Jang Y, Richardson A, Van Remmen H. Trends in oxidative aging theories. Free Radical Bio Med. 2007; 43:477-503.
50. Bolli R. Preconditioning: A paradigm shift in the biology of myocardial ischemia. Am J Physiol Heart Circ Physiol. 2007; 292:19-27.
51. Zhong YM, Nishijo H, Uwano T, Tamura R, Kawanishi K, Ono T. Red ginseng ameliorated place navigation deficits in young rats with hippocampal lesions and aged rats. Physiol Behav. 2000; 69:511-525.
52. Kennedy DO, Scholey AB. Ginseng: Potential for the enhancement of cognitive performance and mood. Pharmacol Biochem Behav. 2003; 75:687-700.
53. Jaenicke B, Kim EJ, Ahn JW, Lee HS. Effect of *Panax ginseng* extract on passive avoidance retention in old rats. Arch Pharm Res. 1991; 14:25-29.
54. Suh DY, Han YN, Han BH. Maltol, an antioxidant component of Korean red ginseng, shows little prooxidant activity. Arch Pharm Res. 1996; 19:112-115.
55. Mook JI, Hong HS, Boo JH, Lee KH, Yun SH, Cheong MY, Joo I, Huh K, Jung MW. Ginsenoside Rb1 and Rg_1 improve spatial learning and increase hippocampal synaptophysin level in mice. J Neurosci Res. 2001; 63:509-515.
56. Tohda C, Matsumoto N, Zou K, Meselhy MR, Komatsu K. β(25-35)-induced memory impairment, axonal atrophy, and synaptic loss are ameliorated by M1, A metabolite of protopanaxadiol-type saponins. Neuropsychopharmacology. 2004; 29:860-868.
57. Bao HY, Zhang J, Yeo SJ, Myung CS, Kim HM, Kim JM, Kang JS. Memory enhancing and neuroprotective effects of selected ginsenosides. Arch Pharm Res. 2005; 28:335-342.
58. Sonnenborn U, Proppert Y. Ginseng (*Panax ginseng* CA Meyer). Brit J Phytother. 1991; 2:3-14.
59. Chung SH, Choi CG, Park SH. Comparisons between white ginseng radix and rootlet for antidiabetic activity and mechanism in KKAy mice. Arch Pharm Res. 2001; 24:214-218.
60. Yokozawa T, Kobayashi T, Oura H, Kawashima Y. Hyperlipemia-improving effects of ginsenoside-Rb_2 in strepzotocin-diabetic rats. Chem Pharm Bull. 1985; 33:3893-3898.
61. Yun SN, Moon SJ, Ko SK, Im BO, Chung SH. Wild ginseng prevents the onset of high-fat diet induced hyperglycemia and obesity in ICR mice. Arch Pharm Res. 2004; 27:790-796.
62. Lee KT, Jung TW, Lee HJ, Kim SG, Shin YS, Whang WK. The antidiabetic effect of ginsenoside Rb_2 *via* activation of AMPK. Arch Pharm Res. 2011; 34:1201-1208.
63. Jung MS, Chung SH. AMP-activated protein kinase: A potential target for ginsenosides. Arch Pharm Res. 2011; 34:1037-1040.
64. Lee JW, Rhee MH, Park KH. Antigenicity studies of the aqueous extract of red ginseng in guinea pigs. Arch Pharm Res. 1994; 17:154-160.
65. Song JY, Han SK, Bae KG, Lim DS, Son SJ, Jung IS, Yi SY, Yun YS. Radioprotective effects of ginsan, an immunomodulator. Radiat Res. 2003; 159:768-774.
66. Song JY, Akhalaia M, Platonov A, Kim HD, Jung IS, Han YS, Yun YS. Effects of polysaccharide ginsan from *Panax ginseng* on liver function. Arch Pharm Res. 2004; 27:531-538.
67. Han SK, Song JY, Yun YS, Yi SY. Ginsan improved Th1 immune response inhibited by gamma radiation. Arch Pharm Res. 2005; 28:343-350.
68. Du XF, Jiang CZ, Wu CF, Won EK, Choung SY. Synergistic immunostimulating activity of pidotimod and red ginseng acidic polysaccharide against cyclophosphamide-induced immunosuppression. Arch Pharm Res. 2008; 31:1153-1159.
69. Wang J, Sun C, Zheng Y, Pan H, Zhou Y, Fan Y. The effective mechanism of the polysaccharides from *Panax ginseng* on chronic fatigue syndrome. Arch Pharm Res. 2014; 37:530-538.
70. Baek NI, Kim DS, Lee YH, Park JD, Lee CB, Kim SI. Cytotoxicities of ginseng saponins and their degradation products against some cancer cell lines. Arch Pharm Res. 1995; 18:164-168.
71. Kikuchi Y, Sasa H, Kita T, Hirata J, Tode T, Nagata I. Inhibition of human ovarian cancer cell proliferation *in vitro* by ginsenoside Rh_2 and adjuvant effects to cisplatin *in vivo*. Anti-cancer Drugs. 1991; 2:63-68.
72. Lee YJ, Jin YR, Lim WC, Park WK, Cho JY, Jang S, Lee SK. Ginsenoside-Rb1 acts as a weak phytoestrogen in MCF-7 human breast cancer cells. Arch Pharm Res.2003; 26:58-63.
73. Lee YJ, Jin YR, Lim WC, Ji SM, Cho JY, Ban JJ, Lee SK. Ginsenoside Rc and Re stimulate c-fos expression in MCF-7 human breast carcinoma cells. Arch Pharm Res. 2003; 26:53-57.
74. Kim HS, Lee EH, Ko SR, Choi KJ, Park JH, Im DS. Effects of ginsenosides Rg_3 and Rh_2 on the proliferation of prostate cancer cells. Arch Pharm Res. 2004; 27:429-435.
75. Li W, Liu Y, Zhang JW, Ai CZ, Xiang N, Liu HX, Yang L. Anti-androgen-independent prostate cancer effects of ginsenoside metabolites *in vitro*: Mechanism and possible structure-activity relationship investigation. Arch Pharm Res. 2009; 32:49-57.
76. Kang KA, Kim YW, Kim SU, Chae S, Koh YS, Kim HS, Hyun JW. G1 phase arrest of the cell cycle by a ginseng

metabolite, compound K, in U937 human monocytic leukemia cells. Arch Pharm Res. 2005; 28:685-690.
77. Li X, Guan YS, Zhou XP, Sun L, Liu Y, He Q, Mao YQ. Anticarcinogenic effect of 20 (R)-ginsenoside Rg3 on induced hepatocellular carcinoma in rats. J Sichuan Univ (Med Sci Edi). 2005; 36:217-220.
78. Fishbein AB, Wang CZ, Li XL, Mehendale SR, Sun S, Aung HH, Yuan CS. Asian ginseng enhances the anti-proliferative effect of 5-fluorouracil on human colorectal cancer: Comparison between white and red ginseng. Arch Pharm Res. 2009; 32:505-513.
79. Kim JS, Joo EJ, Chun J, Ha YW, Lee JH, Han Y, Kim YS. Induction of apoptosis by ginsenoside Rk1 in SK-MEL-2-human melanoma. Arch Pharm Res. 2012; 35:717-722.
80. Oh KW, Kim HS, Wagner GC. Inhibitory effects of ginseng total saponin on methamphetamine-induced striatal dopamine increase in mice. Arch Pharm Res. 1997; 20:516-518.
81. Kim HS, Zhang YH, Fang LH, Lee MK. Effect of ginseng total saponin on bovine adrenal tyrosine hydroxylase. Arch Pharm Res. 1998; 21:782-784.
82. Kim HC, Shin EJ, Jang CG, Lee MK, Eun JS, Hong JT, Oh KW. Pharmacological action of *Panax Ginseng* on the behavioral toxicities induced by psychotropic agents. Arch Pharm Res. 2005; 28:995-1001.
83. Bae EA, Hyun YJ, Choo MK, Oh JK, Ryu JH, Kim DH. Protective effect of fermented red ginseng on transient focal ischemic rats. Arch Pharm Res. 2004; 27:1136-1140.
84. Seo YJ, Kwon MS, Choi HW, Jang JE, Lee JK, Sun Y, Suh HW. Intracerebroventricular gisenosides are antinociceptive in proinflammatory cytokine-induced pain behaviors of mice. Arch Pharm Res. 2008; 31:364-369.
85. Pak SC, Kim SE, Oh DM, Shim KM, Jeong MJ, Lim SC, Bae CS. Effect of Korean red ginseng extract in a steroid-induced polycystic ovary murine model. Arch Pharm Res. 2009; 32:347-352.
86. Moon CK, Kang NY, Yun YP, Lee SH, Lee HA, Kang TL. Effects of red ginseng-crude saponin on plasma lipid levels in rats fed on a diet high in cholesterol and triglyceride. Arch Pharm Res. 1984; 7:41-45.
87. Yun SN, Ko SK, Lee KH, Chung SH. Vinegar-processed ginseng radix improves metabolic syndrome induced by a high fat diet in ICR mice. Arch Pharm Res. 2007; 30:587-595.
88. Yu JY, Jin YR, Lee JJ, Chung JH, Noh JY, You SH, Yun YP. Antiplatelet and antithrombotic activities of Korean Red Ginseng. Arch. Pharm. Res. 2006; 29:898-903.
89. Choi S. Epidermis proliferative effect of the *Panax ginseng* Ginsenoside Rb_2. Arch Pharm Res. 2002; 25:71-76.
90. Shin YW, Bae EA, Kim DH. Inhibitory effect of ginsenoside Rg5 and its metabolite ginsenoside Rh3 in an oxazolone-induced mouse chronic dermatitis model. Arch Pharm Res. 2006; 29:685-690.
91. Jeong CS. Effect of butanol fraction of *Panax ginseng* head on gastric lesion and ulcer. Arch Pharm Res. 2002; 25:61-66.
92. Jeong CS, Hyun JE, Kim YS, Lee ES. Ginsenoside Rb1 the anti-ulcer constituent from the head of *Panax ginseng*. Arch Pharm Res. 2003; 26:906-911.
93. Lee SW, Lee JS, Kim YH, Jin KD. Effect of ginseng saponin on the Na^+, K^+-ATPase of dog cardiac sarcolemma. Arch Pharm Res. 1986; 9:29-38.
94. Hong EJ, Huh K, Rhee SK. Effect of ginseng saponin on gap junction channel reconstituted with connexin 32. Arch Pharm Res. 1996; 19:264-268.
95. Choi S, Rho SH, Jung SY, Kim SC, Park CS, Nah SY. A novel activation of Ca^{2+}-activated Cl^- channel in Xenopus oocytes by ginseng saponins: Evidence for the involvement of phospholipase C and intracellular Ca^{2+} mobilization. Br J Pharmacol. 2001; 132:641-648.
96. Choi S, Kim HJ, Ko YS, Jeong SW, Kim YI, Simonds WF, Nah SY. Gαq/11 coupled to mammalian phospholipase C β3-like enzyme mediates the ginsenoside effect on Ca^{2+}-activated Cl^- current in the Xenopus oocyte. J Biol Chem. 2001; 276:48797-48802.
97. Lee JH, Jeong SM, Lee BH, Kim JH, Ko SR, Kim SH, Nah SY. Effect of calmodulin on ginseng saponin-induced Ca^{2+}-Activated CI-channel activation in Xenopus laevis oocytes. Arch Pharm Res. 2005; 28:413-420.
98. Choi SE, Choi S, Lee JH, Whiting PJ, Lee SM, Nah SY. Effects of ginsenosides on GABAA receptor channels expressed in Xenopus oocytes. Arch Pharm Res. 2003; 26:28-33.
99. Park JS, Hwang SY, Lee WS, Yu KW, Paek KY, Hwang BY, Han K. The therapeutic effect of tissue cultured root of wild *Panax ginseng* CA Mayer on spermatogenetic disorder. Arch Pharm Res. 2006; 29:800-807.

(Received January 23, 2015; Revised February 3, 2015; Accepted February 10, 2015)

Original Article

DOI: 10.5582/ddt.2015.01000

Antibiotic-producing bacteria from stag beetle mycangia

Atsushi Miyashita, Yuuki Hirai, Kazuhisa Sekimizu, Chikara Kaito*

Laboratory of Microbiology, Graduate School of Pharmaceutical Sciences, The University of Tokyo, Tokyo, Japan.

Summary **The search for new antibiotics or antifungal agents is crucial for the chemotherapies of infectious diseases. The limited resource of soil bacteria makes it difficult to discover such new drug candidate. We, therefore, focused on another bacterial resource than soil bacteria, the microbial flora of insect species. In the present study, we isolated 40 strains of bacteria and fungi from the mycangia of three species of stag beetle, *Dorcus hopei binodulosus*, *Dorcus rectus*, and *Dorcus titanus pilifer*. We identified those species with their ribosomal DNA sequences, and revealed that *Klebsiella* spp. are the most frequent symbiont in the stag beetle mycangia. We examined whether these microorganisms produce antibiotics against a Gram-negative bacterium, *Escherichia coli*, a Gram-positive bacterium, *Staphylococcus aureus*, or a fungus, *Cryptococcus neoformans*. Culture supernatants from 33, 29, or 18 strains showed antimicrobial activity against *E. coli*, *S. aureus*, or *C. neoformans*, respectively. These findings suggest that bacteria present in the mycangia of stag beetles are useful resources for screening novel antibiotics.**

Keywords: Antimicrobial agents, Indigenous microorganisms, *Dorcus* species

1. Introduction

The discovery of antibiotics has greatly contributed to the treatment of infectious diseases. Due to the emergence of methicillin-resistant *Staphylococcus aureus* and multi-drug resistant *Pseudomonas*, however, further discovery of antibiotics with novel structures or novel molecular actions is crucial (*1*). Furthermore, even fewer antifungal agents are available than antibacterial agents and only four lineages of polyenes, azoles, candins, and flucytosines are in clinical use. The search for new antifungal agents is therefore also needed. Soil bacteria are a source for producing antibiotics, but the discovery rate of antibiotics from soil bacteria has decreased over the years (*2*). Therefore, we continue to search for new microbial sources of novel antibiotics.

Various species of microorganisms are present in all living organisms. Insect species are various and comprise two-thirds of all animal species, but their indigenous microorganisms as a source of antibiotics have not been fully investigated. Thus, the indigenous microorganisms of insects are promising biologic resources. Raising various species of stag beetles is a popular hobby in Japan and techniques for their maintenance are well established (*3*), making stag-beetles a promising biological resource. Female stag beetles have a microbe-storage organ, named the mycangium, that contains xylose-fermenting yeasts closely related to *Pichia* spp. (*4*). Stag beetle larvae eat xylose-rich rotting wood, and the utilization of xylose by *Pichia* yeast is essential for the stag beetle larvae, because stag beetles cannot directly utilize xylose (*4*). The *Pichia* yeast in the mycangium are thought to be attached to the surface of the eggs, enabling vertical transmission from adult to larvae (*4*). In *Musca domestica*, bacteria on the surfaces of the fly eggs facilitate fly larvae growth by inhibiting the growth of pathogenic fungi (*5*). Based on these findings, we hypothesized that microorganisms other than *Pichia* yeast exist in the mycangia of stag beetles, where they produce antibiotics that inhibit the growth of pathogenic microorganisms. In the present study we have revealed the presence of bacteria in the mycangia of stag beetles, and that they produce antimicrobial substances.

Released online in J-STAGE as advance publication January 25, 2015.

**Address correspondence to:*
Dr. Chikara Kaito, Laboratory of Microbiology, Graduate School of Pharmaceutical Sciences, The University of Tokyo, Hongo 7-3-1, Bunkyo-ku, Tokyo 113-0033, Japan.
E-mail: kaito@mol.f.u-tokyo.ac.jp

2. Materials and Methods

2.1. *Animals*

Captive bred adults of *Dorcus hopei binodulosus* were purchased from a breeder and bred. The larvae were raised using a mycelium bottle (TSUKIYONO KINOKOEN Ltd., Gunnma, Japan, *http://www.tsukiyono.co.jp*) and the emerged females (n = 7) were used for the study. A wild female *Dorcus titanus pilifer* was collected from a dry riverbed at the Suzuka River in the Mie prefecture in Japan in 2009, and its offspring larvae were raised using mycelium bottles. Adult females (n = 5) in the second generation were used for the study. *Dorcus rectus* larvae were collected from decayed woods in a dry riverbed at the Suzuka River in the Mie prefecture in Japan in 2011. The larvae were raised to adults and the females (n = 5) were used for the study.

2.2. *Isolation of microorganisms from mycangia*

The stag beetle mycangia were excised according to the method described by Tanahashi *et al*. (*4*). The tissues were dissected in saline using sterile scissors and the samples were spread onto 1.5% agar plates of potato nutrient broth (PNB; 24 g potato dextrose broth, 8 g nutrient broth, 1 L water). The plates were incubated at 23°C for at least 1 d. The developing colonies were distinguished by their morphologies and then aerobically cultured in liquid PNB for 5 d at 23°C.

2.3. *Extraction of genomic DNA*

Microbial cells in 2 ml of liquid culture were collected by centrifugation at 204,00×g for 5 min. The cells were lysed by vigorous vortex in lysis buffer (5 mM Tris-HCl [pH8.0], 0.5 mM ethylenediaminetetraacetic acid (EDTA), 50 mM NaCl, 1% Triton-X 100, 0.5% sodium dodecyl sulfate, 100 mg/mL glass beads, 50% buffered phenol). The samples were centrifuged at 204,00×g for 5 min and each aqueous supernatant was mixed with 1 volume of 2-propanol and 0.1 volume of 3M sodium acetate. The samples were then centrifuged at 204,00×g for 10 min and the precipitates were washed with 70% EtOH. The precipitated DNA samples were dried and dissolved in Tris-EDTA buffer (10 mM Tris-HCl [pH 8.0], 1 mM EDTA).

2.4. *Identification of microbial species*

DNA fragments containing 16S rDNA were amplified by PCR using oligonucleotide primers (Table 1) and genomic DNAs was used as the template according to a previous method (*4*). The PCR reaction mixture was incubated at 94˚C for 2 min and then for 30 cycles (94˚C, 15 s; 55 ˚C, 30 s; 68˚C 2 min). When the DNA fragments were not amplified, another amplification for eukaryotic 18S rDNA was performed according to a previous method (*6*). Each amplified DNA fragment was sequenced and similar sequences were searched using NCBI BLAST (*http://blast.ncbi.nlm.nih.gov/Blast.cgi*). The rDNA sequences have been deposited in GenBank (accession numbers; AB862496 to AB862537).

2.5. *Measurement of antimicrobial activity*

S. aureus RN4220, *E. coli* JM109, and *C. neoformans* H99 were cultured in Luria-Bertani broth, tryptic soy broth, and potato dextrose broth, respectively. The overnight cultures were diluted 5000 times with PNB and poured into microplates. Two-fold serial dilutions of the culture supernatants of the microorganisms isolated from the mycangia were filtered using 0.22-µm polyvinylidene difluoride membranes and poured into the microplates. The plates were incubated overnight at 37˚C and the growth of *S. aureus*, *E. coli*, or *C. neoformans* was examined.

Table 1. Primers used in this study

Taget	Name of primer	Sequence
16S rDNA	U1	CCAGCAGCCGCGGTAATACG
	U2	ATCGGCTACCTTGTTACGACTTC
	9F	GAGTTTGATCCTGGCTCAG
	1541R	AAGGAGGTGATCCAGCC
	U515F	GTGCCAGCMGCCGCGGTAA
	E1541R	AAGGAGGTGATCCANCCRCA
	U1510R	GGTTACCTTGTTACGACTT
18S rDNA	ITS4	TCCTCCGCTTATTGATATGC
	ITS5	GGAAGTAAAAGTCGTAACAAGG
	LS1	AGTACCCGCTGAACTTAAG
	NL4	GGTCCGTGTTTCAAGACGG

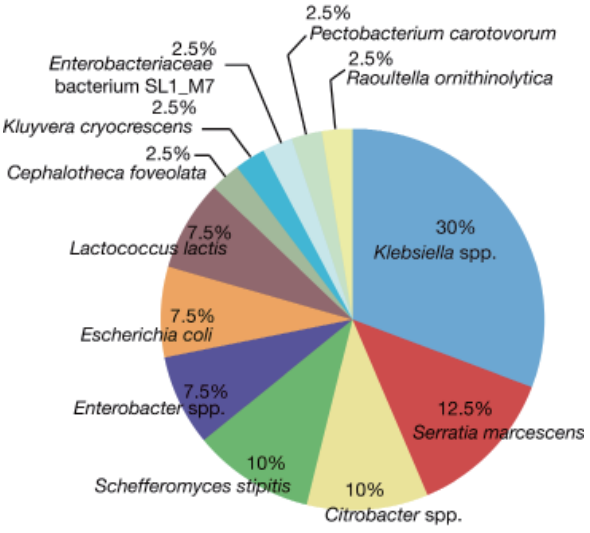

Figure 1. Microbial species isolated from stag beetle mycangia. Proportions of 40 microbial strains isolated from stag beetle mycangia are presented. Numbers in graph represent percentages against whole strains.

3. Results

3.1. *Identification of microbial species from the mycangia of Dorcus hopei binodulosus, Dorcus rectus, and Dorcus titanus pilifer*

Mycangia of female *Dorcus hopei binodulosus*, *Dorcus rectus*, and *Dorcus titanus* pilifer were excised and their suspensions were scattered in saline. The samples were spread on PNB agar plates and incubated at 23˚C. The appeared colonies were distinguished by their morphologies, cultured in liquid PNB, and then their genomic DNA was extracted. DNA fragments containing 16S rDNA or 18S rDNA were amplified by PCR and sequenced. The most frequent bacterial species was *Klebsiella* sp. and the second most frequent species was *Serratia marcescens* (Figure 1). Other species were in the genuses of *Enterobacter*, *Escherichia*, *Lactococcus*, *Citrobacter*, *Kluyvera*, *Raoultella*, *Pectobacterium*, or *Scheffersomyces* (Table 2). *Scheffersomyces* is a

Table 2. Antimicrobial activities in the culture supernatants of microbes isolated from stag beetle mycangia

Strain ID	Source[1]	Microbial species	Similarity[2] (%)	Growth inhibitory activity[3]		
				E. coli	*S. aureus*	*C. neoformans*
DCBM1	*Dorcus hopei binodulosus*	*Klebsiella oxytoca*	100	-	-	2
DCBM2	*Dorcus hopei binodulosus*	*Serratia marcescens*	99	-	4	4
DCBM3	*Dorcus hopei binodulosus*	*Scheffersomyces stipitis*	99	-	-	-
DCBM4	*Dorcus hopei binodulosus*	*Citrobacter koseri*	100	> 8	> 8	-
DCBM5	*Dorcus hopei binodulosus*	*Scheffersomyces stipitis*	100	-	-	-
DCBM6	*Dorcus hopei binodulosus*	*Serratia marcescens*	100	-	2	4
DCBM7	*Dorcus hopei binodulosus*	*Enterobacteriaceae bacterium SL1_M7*	99	4	2	-
DCBM8	*Dorcus hopei binodulosus*	*Serratia marcescens*	100	8	2	-
DCBM9	*Dorcus hopei binodulosus*	*Enterobacter aerogenes*	99	2	2	-
DCBM10	*Dorcus hopei binodulosus*	*Cephalotheca foveolata*	99	2	2	-
DCBM11	*Dorcus hopei binodulosus*	*Klebsiella oxytoca*	99	8	4	-
DCBM12	*Dorcus hopei binodulosus*	*Klebsiella oxytoca*	100	16	2	-
DCBM13	*Dorcus hopei binodulosus*	*Klebsiella oxytoca*	99	8	4	-
DCBM14	*Dorcus hopei binodulosus*	*Klebsiella oxytoca*	99	8	4	-
DCBM15	*Dorcus hopei binodulosus*	*Enterobacter asburiae*	100	4	2	-
DCBM16	*Dorcus hopei binodulosus*	*Escherichia coli*	99	2	2	-
DRM1	*Dorcus rectus*	*Lactococcus lactis*	100	ND	4	-
DRM2	*Dorcus rectus*	*Citrobacter sp.*	99	2	4	-
DRM3	*Dorcus rectus*	*Pectobacterium carotovorum*	99	8	-	-
DRM4	*Dorcus rectus*	*Scheffersomyces stiptis*	99	8	2	-
DRM5	*Dorcus rectus*	*Lactococcus lactis*	100	2	-	-
DRM6	*Dorcus rectus*	*Citrobacter sp. A9IG*	99	4	2	-
DRM7	*Dorcus rectus*	*Klebsiella oxytoca*	99	32	-	2
DRM8	*Dorcus rectus*	*Klebsiella sp.*	99	8	-	4
DRM9	*Dorcus rectus*	*Klebsiella oxytoca*	100	8	-	4
DRM10	*Dorcus rectus*	*Escherichia coli*	99	4	2	-
DRM11	*Dorcus rectus*	*Enterobacter gergoviae*	98	16	2	4
DRM12	*Dorcus rectus*	*Escherichia coli*	99	4	2	2
DRM13	*Dorcus rectus*	*Lactococcus lactis*	99	ND	2	2
DTPM1	*Dorcus titanus pilifer*	*Klebsiella oxytoca*	100	8	-	4
DTPM2	*Dorcus titanus pilifer*	*Citrobacter farmeri*	99	16	2	4
DTPM3	*Dorcus titanus pilifer*	*Serratia marcescens*	99	16	2	4
DTPM4	*Dorcus titanus pilifer*	*Kluyvera cryocrescens*	100	4	4	64
DTPM5	*Dorcus titanus pilifer*	*Klebsiella oxytoca*	100	4	2	4
DTPM6	*Dorcus titanus pilifer*	*Klebsiella oxytoca*	100	8	-	4
DTPM7	*Dorcus titanus pilifer*	*Klebsiella oxytoca*	99	8	4	-
DTPM8	*Dorcus titanus pilifer*	*Serratia marcescens*	99	8	2	4
DTPM9	*Dorcus titanus pilifer*	*Serratia marcescens*	99	16	2	4
DTPM10	*Dorcus titanus pilifer*	*Raoultella ornithinolytica*	99	2	4	2
DTPM11	*Dorcus titanus pilifer*	*Scheffersomyces stiptis*	99	2	-	-

[1] "Source" indicates the stag beetle species used for isolating microorganisms. [2] "%" indicates the percent similarity of the isolated microorganisms to the microbial species listed in "Microbial species". [3] Antimicrobial activities against *S. aureus*, *E. coli*, and *C. neoformans* were measured. Numbers in the right three columns are reciprocals of dilutions of the culture supernatants that inhibited microbial growth. "-" means not detected. ND means not determined.

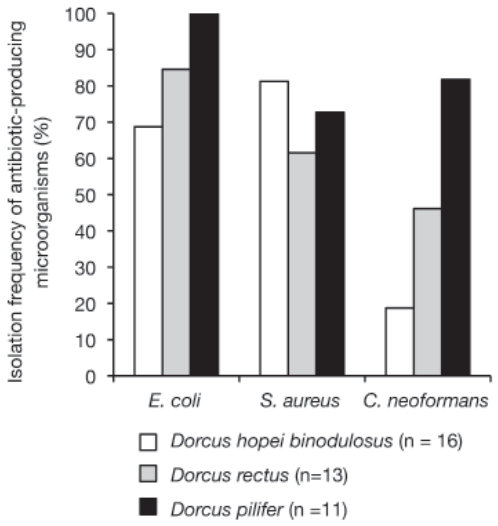

Figure 2. Isolation frequency of antibiotic-producing microorganisms from three different stag beetles. Isolation frequencies of microbial strains with growth inhibitory activity against *E. coli*, *S. aureus*, and *C. neoformans* are shown according to the stag beetle species.

Pichia yeast that is reported to be present in stag beetle mycangia (*4*).

3.2. *Antimicrobial activities in culture supernatants of the mycangial microbes*

We measured growth inhibitory activities of culture supernatants of microbes isolated from the stag beetle mycangia against *E. coli*, *S. aureus*, and *C. neoformans*. Of 40 strains isolated from mycangia, 33, 29, or 18 strains showed growth inhibitory activities against *E. coli*, *S. aureus*, or *C. neoformans*, respectively (Table 2). Microbes that inhibit the growth of *E. coli* or *S. aureus* were isolated at almost the same frequency from the three stag beetle species (Figure 2). Many microbes that inhibit the growth of *C. neoformans* were isolated from *Dorcus titanus pilifer*, whereas few were isolated from *Dorcus hopei binodulosus* (Figure 2).

4. Discussion

The present study demonstrated the existence of microbes in stag beetle mycangia that produce antibiotics against *E. coli*, *S. aureus*, and *C. neoformans*. This finding clearly indicates that the microbial flora of stag beetle mycangia comprise a promising source of novel antimicrobial agents.

Antimicrobial activities against *E. coli* or *S. aureus* were observed at almost the same frequency between indigenous microorganisms from *Dorcus hopei binodulosus*, *Dorcus rectus*, and *Dorcus titanus pilifer*. Antifungal activities against *C. neoformans* were frequently observed in microorganisms obtained from *Dorcus titanus pilifer*, but rarely in those from *Dorcus hopei binodulosus*. Larvae of *Dorcus hopei binodulosus* preferred woods decayed by white-rot fungus, which are often found in high positions of standing dead woods with low moisture (*7*). Larvae of *Dorcus titanus pilifer*, on the other hand, preferred woods decayed by brown-rot fungus, which are often located in underground positions of standing dead woods or in fallen trees with high moisture (*7*). Larvae of *Dorcus* rectus preferred both types of decayed woods (*7*). The humid environment inhabited by larvae of *Dorcus titanus pilifer* is assumed to contain more pathogenic fungi than a drier environment. Therefore, larvae of *Dorcus pilifer* may protect themselves against infection by antifungal agents produced by the indigenous microorganisms.

Antifungal activities were frequently observed in the culture supernatants of *Klebsiella oxytoca* and *Serratia marcescens* isolated from stag beetle mycangia (Table 2). *Klebsiella oxytoca* was present on housefly eggs and inhibited fungal growth to promote fly larvae growth (*5*). Thus, the role of *Klebsiella oxytoca*, inhibition of fungal growth may be conserved in insects, including houseflies and stag beetles. In addition, *Serratia marcescens* was pathogenic to various species of insects (*8,9,10,11*). The virulence properties of *Serratia marcescens* against insects differed from strain to strain, and some strains were non-pathogenic (*9*). Such non-pathogenic *Serratia marcescens* may have a role to protect the host animal from fungal infection by producing anti-fungal agents. The biological significance of the antibiotic-producing indigenous microorganisms in the stag beetle requires further investigation.

Acknowledgements

This work was supported by Grants-in-Aid for Scientific Research. This study was supported in part by the Naito Foundation, the Mochida Memorial Foundation, and the Genome Pharmaceuticals Institute.

References

1. Stein GE Antimicrobial resistance in the hospital setting: impact, trends, and infection control measures. Pharmacotherapy. 2005; 25:44S-54S.
2. Clardy J, Fischbach MA, Walsh CT New antibiotics from bacterial natural products. Nat Biotechnol. 2006; 24:1541-1550.
3. Kojima H. Breeding Technique of Lucanid Beetles. Tokyo, Mushi-sha, Japan, 1996.
4. Tanahashi M, Kubota K, Matsushita N, Togashi K Discovery of mycangia and the associated xylose-fermenting yeasts in stag beetles (Coleoptera: Lucanidae). Naturwissenschaften. 2010; 97:311-317.
5. Lam K, Thu K, Tsang M, Moore M, Gries G Bacteria on housefly eggs, Musca domestica, suppress fungal growth in chicken manure through nutrient depletion or antifungal metabolites. Naturwissenschaften. 2009; 96:1127-1132.
6. Suh SO, Blackwell M Three new beetle-associated yeast

species in the Pichia guilliermondii clade. FEMS Yeast Res. 2004; 5:87-95.
7. Kubota K, Kubota N Beetles of genus Dorcus (Coleoptera, Lucanidae) boring into dead wood of willow trees (Salix spp.). Jyumokuigakukenkyu. 2004; 8:17-22.
8. Flyg C, Kenne K, Boman HG Insect pathogenic properties of Serratia marcescens: phage-resistant mutants with a decreased resistance to Cecropia immunity and a decreased virulence to Drosophila. J Gen Microbiol. 1980; 120:173-181.
9. O'Callaghan M, Garnham ML, Nelson TL, Baird D, Jackson TA The Pathogenicity of Serratia Strains to Lucilia sericata (Diptera: Calliphoridae). J Invertebr Pathol. 1996; 68:22-27.
10. Inglis GD, Lawrence AM, Davis FM Pathogens associated with southwestern corn borers and southern corn stalk borers (Lepidoptera: Crambidae). J Econ Entomol. 2000; 93:1619-1626.
11. Tan B, Jackson TA, Hurst MR Virulence of Serratia strains against Costelytra zealandica. Appl Environ Microbiol. 2006; 72:6417-6418.

(Received January 9, 2015; Accepted January 13, 2015)

Original Article

DOI: 10.5582/ddt.2015.01008

Tauroursodeoxycholic acid attenuates inorganic phosphate-induced osteoblastic differentiation and mineralization in NIH3T3 fibroblasts by inhibiting the ER stress response PERK-eIF2α-ATF4 pathway

Fang Liu[1,2], Yazhou Cui[1], Pinglan Ge[1,2], Jing Luan[1], Xiaoyan Zhou[1], Jinxiang Han[1,*]

[1] *Key Laboratory for Biotech Drugs of the Ministry of Health, Shandong Medical Biotechnological Center, Shandong Academy of Medical Sciences, Ji'nan, Shandong, China;*
[2] *School of Medicine and Life Sciences, University of Jinan-Shandong Academy of Medical Science, Ji'nan, Shandong, China.*

Summary **Ectopic ossification occurs in a wide range of common and genetic diseases, but its molecular mechanisms and effective therapeutic targets remain to be clarified. The aim of the study is to investigate whether endoplasmic reticulum (ER) stress is involved in ectopic ossification and ER stress inhibitor tauroursodeoxycholic acid (TUDCA) has potential to treat the pathological conditions. In this study, inorganic phosphate (Pi)-induced NIH3T3 fibroblasts induced osteogenesis and mineralization was used as an *in vitro* model for ectopic ossification. Various concentrations of TUDCA (0.1, 1, 5, 10 μM) were added during osteogenic induction. Osteoblast differentiation and minerlization were determined by RT-qPCR, alkaline phosphatase (ALP) activity assay, Alizarin Red-S (AR-S) staining, and calcium deposition. ER stress signalling components were detected by Western-blot analysis. We found ER stress was activated by inorganic phosphate in NIH3T3 cells. During osteogenic induction, TUDCA inhibited NIH3T3 cells ALP activity and mineral nodule formation. In addition, TUDCA caused decreased expression of osteoblastic markers *Runx2*, *Col1a1*, *ALP*, *OCN*. Mechanistically, TUDCA inhibited the ER stress response PERK-eIF2α-ATF4 pathway during osteogenesis. In conclusion, TUDCA could inhibit fibroblasts mineralization *via* supressing the ER stress response PERK-eIF2α-ATF4 pathway, and has potential pharmacologic and therapeutic applications for treating ectopic ossification associated diseases.**

Keywords: Endoplasmic reticulum stress, ectopic ossification, tauroursodeoxycholic acid, eIF2α, AFT4

1. Introduction

Ectopic ossification is a complex process characterized by the formation of ectopic bone or the deposition of calcium phosphate complexes within muscles, connective tissue, or nerves in aberrant locations (*1-4*). The ossification processes may be caused by heredity, surgical intervention or trauma (*2,3*). Common diseases for ectopic ossification include diffuse idiopathic skeletal hyperostosis, ankylosing spondylitis, osteoarthritis, and other heritable disorders of vascular and skin mineralization (*2,4*). The molecular mechanism of ectopic ossification has always been a concern, but the exact pathogenic mechanism remains elusive. At present, in the surgical setting, the two most common preventative modalities are radiotherapy and indomethacin, a non-steroidal anti-inflammatory drug (NSAID), but both treatment modalities carry the risk of particular side effects (*2*), therefore, effective treatment is extremely urgent.

The endoplasmic reticulum (ER) is a cellular compartment that plays a critical role in protein synthesis, folding, and transportation including important proteins in osteoblast differentiation, such as osteocalcin and

**Address correspondence to:*
Dr. Jinxiang Han, Key Laboratory for Rare Disease Research of Shandong Province, Key Laboratory for Biotech Drugs of the Ministry of Health, Shandong Medical Biotechnological Center, Shandong Academy of Medical Sciences, Ji'nan, Shandong 250062, China.
E-mail: jxhan9888@aliyun.com

collagen (*5*). Efficient functioning of the ER is essential for cellular function and survival. Once ER homeostasis is disrupted in a number of cellular stress conditions, such as UV, viral infection, nutritional deprivation and others (*6*), unfolded and misfolded proteins will accumulate in the ER lumen, resulting in ER stress, and the unfolded protein response (UPR) occurs (*7-12*). The ER stress response PERK-eIF2α-ATF4 pathway can be activated. Zhang *et al*. (*13*) reported PERK was required for prenatal and postnatal bone development. PERK was responsible for highly phosphorylated eIF2α, in Perk-/- mice, and the secretory pathway in osteoblasts cannot efficiently process and secrete procollagen, which caused severe skeletal dysplasias. Wei *et al*. (*14*) also found PERK was essential for neonatal skeletal development to regulate osteoblast proliferation and differentiation. Perk-/- mice were severely osteopenic, which was caused by a deficiency in the number of mature osteoblasts, impaired osteoblast differentiation, and reduced type I collagen secretion. Atsushi Saito *et al*. (*15*) demonstrated that ATF4 expression and function were influenced by the loss of PERK *in vivo* and *in vitro* and confirmed that ER stress during osteoblast differentiation activated PERK-eIF2α-ATF4 signaling followed by the promotion of gene expression essential for osteogenesis such as osteocalcin (*OCN*) and bone sialoprotein (*BSP*). Numerous reports have suggested ER stress occurs and is involved in osteoblast differentiation, however whether ER stress is associated with ectopic ossification remains uninvestigated.

TUDCA is a bile acid present in human bile at a low concentration and has a very good safety profile, and the normal concentration range in human plasma is 0.4-4 μM. It has been proved that TUDCA can enhance ER folding ability to prevent protein aggregation and thus protect cells against ER stress (*16*). TUDCA has been widely used in treatment of disease, such as, cholelithiasis, cholestatic liver disease, diabetes mellitus, obesity, and atherosclerosis, it works *via* preventing ER stress, as a classical ER stress inhibitor (*17-22*). Studies have demonstrated that TUDCA could markedly prevent Aortic valve (AV) calcification, and attenuate AV osteoblastic differentiation in both rabbit and mouse models of AV calcification *via* inhibition of ER stress and could suppress oxidized low density lipoprotein (oxLDL)-induced osteoblastic differentiation in cultured valvular interstitial cells (VICs) (*23*) and could alleviate advanced glycation end product-induced apoptosis and osteoblastic differentiation of stromal cells *via* alleviating ER stress (*22,24*).

In this study, we induced NIH3T3 cells mineralization with 3 mM inorganic phosphate ($NaPO_4$, Pi), treated with different amounts of TUDCA (0.1, 1, 5, 10 μM), examined the important indicators of osteoblastic differentiation and mineralization and ER stress response to investigate if ER stress is associated with ectopic ossification and can TUDCA inhibit fibroblasts ectopic ossification *via* supressing the ER stress response PERK-eIF2α-ATF4 pathway.

2. Materials and Methods

2.1. *Cell culture and treatment*

NIH3T3 cell line was acquired from the Cell Bank of Type Culture Collection of the Chinese Academy of Sciences (Shanghai, China), and cultured in Dulbecco's modified Eagle's medium (DMEM) (Gibco, Carlsbad, CA, USA) supplemented with 10% (v/v) fetal bovine serum (Gibco, Carlsbad, CA, USA), 100 U/mL penicillin, and 100 μg/mL streptomycin in a humidified 5% CO_2 atmosphere at 37°C. The cells were cultured either in basic or osteogenic medium (OM) supplemented with 3 mM inorganic phosphate ($NaPO_4$, Pi) (Sangon Biotech, Shanghai, China) as described previously (*25*). Different concentrations (0.1, 1, 5, 10 μM) of TUDCA (Santa Cruz, USA) were added as indicated.

2.2. *Quantitative real-time polymerase chain reaction (RT-qPCR) analysis*

Total RNA was isolated from the cultures using the TRIzol reagent (Invitrogen, USA) according to the manufacturer's protocol. First-strand cDNA was synthesized with ReverTra Ace qPCR RT kit (Toyobo, Osaka, Japan). RT-PCR was performed with THUNDERBIRD SYBR qPCR Mix (Toyobo, Osaka, Japan) using LightCycler 480 thermocycler (Roche Applied Science, Mannheim, Germany). Relative mRNA levels of all genes were first normalized to the levels of 36B4 and then normalized to the average of negative control group levels. The primer sequences for the transcripts quantified by this method are shown (Table 1).

2.3. *ALP avtivity assay*

NIH3T3 cells were cultured with osteogenic medium (OM) for 9 days and then treated with TUDCA at given concentrations as described above in basic

Table 1. Quantitative real-time PCR was performed using each specific primer set

Target genes	Primer sequences
Runx2-fwd	AGTAGCCAGGTTCAACGATCTGA
Runx2-rev	GACTGTTATGGTCAAGGTGAAACTCTT
Col1a1-fwd	CACCCCAGCCGCAAAGAGT
Col1a1-rev	CGGGCAGAAAGCACAGCACT
ALP-fwd	TGGCTCTGCCTTTATTCCCTAGT
ALP-rev	AAATAAGGTGCTTTGGGAATCTGT
OCN-fwd	TGCTTGTGACGAGCTATCAG
OCN-rev	GAGGACAGGGAGGATCAAGT
36B4-fwd	AAGCGCGTCCTGGCATTGTCT
36B4-rev	CCGCAGGGGCAGCAGTGGT

fwd, forward; rev, reverse.

medium for 24 hours, ALP activity was performed by the standard protocols. Briefly, NIH3T3 cells were washed with phosphate-buffered saline (PBS) (pH 7.4) and lysed with non-denatured tissue/cell lysate, RIPA (Solarbio, China). ALP activity was assayed using the commercial kit (LabAssay ALP kit, Wako, Japan), and protein content was determined with BCA protein assay (Beyotime, Shanghai, China). ALP activity was normalized by the protein content.

2.4. *Mineralization analysis*

For mineralization analysis, NIH3T3 cells were cultured with osteogenic medium (OM) treated with TUDCA at given concentrations as described above for 14 days. Mineralization was determined using Alizarin Red-S (AR-S) staining kit (GENMED, USA) by the standard protocols. For quantitation of mineralization analysis, the stained cultures were incubated with 10% (w/v) cetylpyridium chloride at 37°C for 1 h, optical density of the supernatant was measured at 562 nm.

2.5. *Quantification of calcium deposition*

NIH3T3 cells were cultured with osteogenic medium (OM) treated with TUDCA at given concentrations as described above for 9 days. Calcium deposition in the plates was quantified by the o-cresolphthalein complexone method using a calcium colorimetric assay kit (Sigma, USA) in accordance with the manufacturer's instructions. Briefly, cells were washed with tris-buffered saline and decalcified using 0.6 N HCl for 24 hours at room temperature, and the calcium content of HCl supernatants was subsequently subjected to calcium colorimetric assay. After decalcification, each cell layer was washed with PBS and solubilized with 0.1 N NaOH containing 0.1% SDS. The protein concentration was measured with BCA protein assay (Beyotime, Shanghai, China). The calcium content of the cell layer was normalized to protein content.

2.6. *Western blot analysis*

Proteins were extracted from NIH3T3 cells under the designated conditions using Western Blot-IP lysis buffer (Beyotime, Shanghai, China). The lysates were incubated on ice for 45 min. After centrifugation at 14,000 × g for 15 min, the soluble proteins in the extracts were quantified. Protein-equivalent samples were subjected to SDS-PAGE for Western blotting. The following antibodies were used: anti-P-eIF2α (1:1,000, CST, USA), anti-T-eIF2α (1:1,000, CST, USA), anti-ATF4 (1:1,000, PTG, China), anti-Runx2 (1:1,000, Stan Cruz, USA), anti-β-actin (1:1,000, PTG, China). Immunoreactivity was determined using enhanced chemiluminescence (ECL) (Millipore Corporation, Billerica, MA, USA) chemiluminescence reaction.

2.7. *Statistics*

Measurements in each experiment were run in triplicate. For quantitative data, results are reported as the mean ± S.D. To determine the differences between groups, one-way analysis of variance (ANOVA) was carried out using SPSS software (version 17.0), with significance accepted at $p < 0.05$.

3. Results

3.1. *Effects of TUDCA on the expression of osteoblast-specific markers in Pi-induced NIH3T3 cells*

RT-qPCR was performed to measure the expression of osteoblast-specific markers including *Runx2*, *Col1a1*, *ALP* and *OCN*. As shown in Figure 1, compared with the osteogenic group, the mRNA expression of *Runx2*, *Col1a1*, *ALP* and *OCN* significantly decreased at 24 hours or 9 days with treatment of various concentrations of TUDCA (0.1, 1, 5, 10 μM) in a dose-dependent manner. However, the osteogenic group mRNA expression of *ALP* also decreased compared with the negative control group at 9 days.

3.2. *TUDCA inhibited ALP activity of NIH3T3 cells induced by inorganic phosphate*

ALP activity was assessed as an important indicator of osteoblastic lineage to study the effect of TUDCA on osteogenic differentiation. ALP activity was

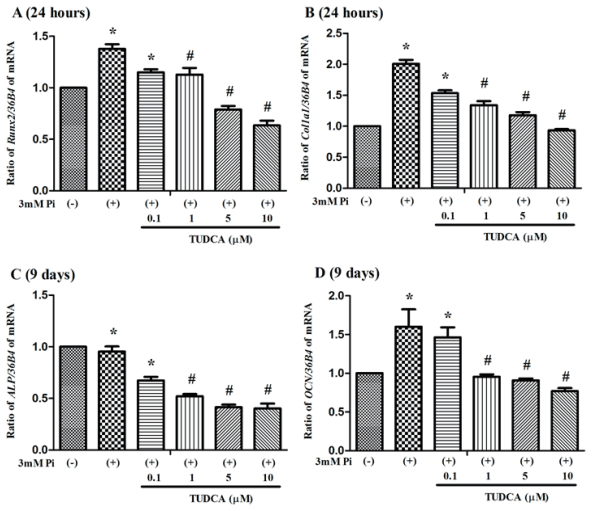

Figure 1. Effects of TUDCA on the expression of osteoblast-specific markers in Pi-induced NIH3T3 cells. Cells were cultured in osteogenic medium (OM) for 6 hours and then treated with TUDCA in basic medium for 24 hours or in osteogenic medium (OM) supplemented with TUDCA for 9 days. Total RNA was extracted and measured by RT-qPCR for *Runx2* **(A)**, *Col1a1* **(B)**, *ALP* **(C)** and *OCN* **(D)**. All mRNA expression levels were normalized to 36B4. (mean ± S.D., $n = 3$). * $p < 0.05$, *vs*. negative control group; # $p < 0.05$, *vs.* osteogenic induction group.

determined at 10 days (osteogenic induction for 9 days and treatment with TUDCA in basic medium for 24 hours). As shown in Figure 2, with osteoblast induction, ALP activity increased, when treated with various concentrations of TUDCA, ALP activity significantly decreased in a dose-dependent manner (21%, 34.8%, 35%, and 37.2% decreases with 0.1, 1, 5 and 10 μM of TUDCA, respectively). These data suggest that TUDCA can significantly inhibit ALP activity during osteogenic differentiation in NIH3T3 cells in a dose-dependent manner.

3.3. *TUDCA inhibited mineralization of NIH3T3 cells induced by inorganic phosphate*

To evaluate the effect of TUDCA on mineralization in the NIH3T3 cells matrix, alizarin red staining was performed at 14 days with osteogenic induction in the presence or absence of TUDCA at given concentrations. As is shown in Figure 3A, obvious matrix mineralization can be observed, but mineralization decreases with

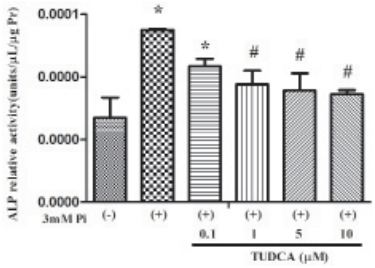

Figure 2. TUDCA inhibited ALP activity of NIH3T3 cells induced by inorganic phosphate. NIH3T3 cells were cultured in osteogenic medium for 9 days and then in basic medium with TUDCA (0.1, 1, 5, 10 μM) for 24 hours. ALP activity was assessed on day 10. (mean ± S.D., $n = 3$). * $p < 0.05$, *vs*. negative control group; # $p < 0.05$, *vs*. osteogenic induction group.

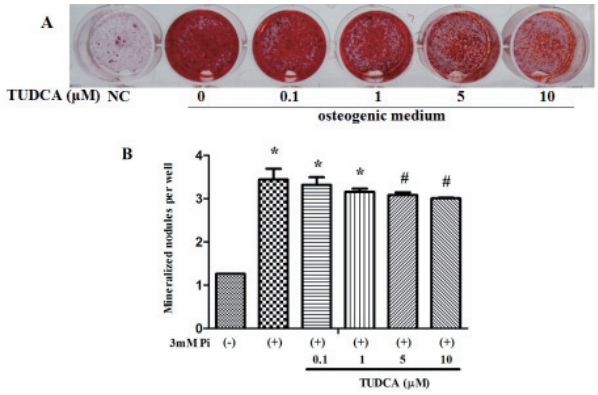

Figure 3. TUDCA inhibited mineralization of NIH3T3 cells induced by inorganic phosphate. Observations for mineralization **(A)** and quantitation of mineralization **(B)**. NIH3T3 cells were cultured in osteogenic medium (OM) with TUDCA (0.1, 1, 5, 10 μM) for 14 days and incubated with 10% (w/v) cetylpyridium chloride at 37°C for 1 h, optical density of the supernatant was measured at 562 nm. (mean ± S.D., $n = 3$). * $p < 0.05$, *vs*. negative control group; * $p < 0.05$, *vs*. negative control group; # $p < 0.05$, *vs*. osteogenic induction group. NC: negative control.

TUDCA treatment, the higher the concentration of TUDCA the more obvious inhibition. The quantitation of mineralization data (Figure 3B) suggests that TUDCA can significantly inhibit mineralization of NIH3T3 cells during osteogenic differentiation in a dose-dependent manner (3.5%, 8.3%, 10.4%, and 12.6% decreases with 0.1, 1, 5 and 10 μM of TUDCA, respectively).

3.4. *Effects of TUDCA on calcium deposition of NIH3T3 cells induced by inorganic phosphate*

To further evaluate the effect of TUDCA on calcification in NIH3T3 cells, quantification of calcium deposition was examined at 9 days under different conditions. In basic medium, NIH3T3 cells accumulated very little calcium mineral, in contrast, in the presence of 3 mM Pi, calcium deposition dramatically increased as shown in Figure 4 (calcified group versus uncalcified control: 41.5), but calcium deposition in NIH3T3 cells decresaed with TUDCA treatment (4.7%, 14%, 14.6%, and 32.6% decreases with 0.1, 1, 5 and 10 μM of TUDCA, respectively).

3.5. *ER stress is activated by inorganic phosphate in NIH3T3 cells*

To determine whether ER stress is activated by inorganic phosphate in NIH3T3 cells compared to other conditions, such as thapsigargin and tunicamycin (*6*), the expression of total and phosphorylated eIF2α in ER

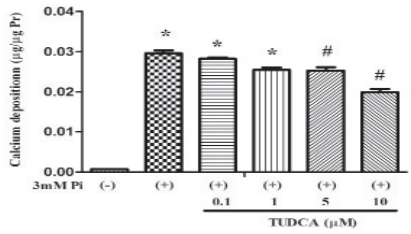

Figure 4. Effects of TUDCA on calcium deposition of NIH3T3 cells induced by inorganic phosphate. NIH3T3 cells were cultured in osteogenic medium (OM) with TUDCA (0.1, 1, 5, 10 μM) for 9 days. Cells were decalcified with 0.6 N HCl for 24 hours. The calcium content was determined by the o-cresolphthalein complexone method. After decalcification, the protein of the cell layer was extracted. The calcium content of the each cell layer was normalized to protein content. Data were mean ± S.D., $n = 3$. * $p < 0.05$, *vs*. negative control group; # $p < 0.05$, *vs*. osteogenic induction group.

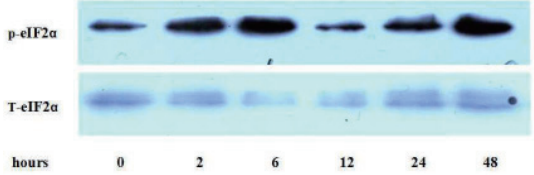

Figure 5. ER stress is activated by inorganic phosphate in NIH3T3 cells. NIH3T3 cells were cultured in osteogenic medium for 0, 2, 6, 12, 24 hours. The proteins were extracted for Western blot analysis of the expression of total and phosphorylated eIF2α (P-eIF2α and T-eIF2α).

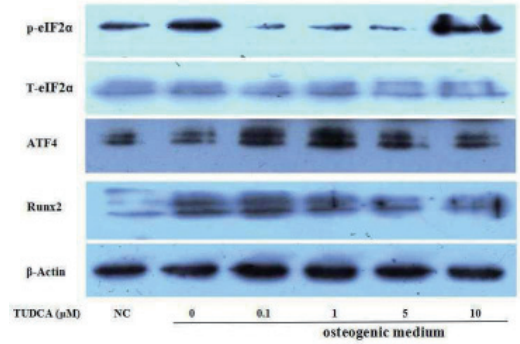

Figure 6. TUDCA inhibits the ER stress response PERK-eIF2α-ATF4 pathway in NIH3T3 cells induced by inorganic phosphate. Cells were cultured in osteogenic medium (OM) for 6 hours and then treated with TUDCA in basic medium for 24 hours. Proteins were extracted for Western blot analysis.

stress response mediated PERK-eIF2α-ATF4 signaling was evaluated by Western blot analysis. In Figure 5, inorganic phosphate ($NaPO_4$, Pi) was shown to induce phosphorylated eIF2α, especially at 6 hours and 48 hours, while no significant change occurred in the level of total eIF2α. Western blot analysis revealed Pi could stimulate ER Stress, like thapsigargin and tunicamycin.

3.6. *TUDCA inhibits the ER stress response PERK-eIF2α-ATF4 pathway in NIH3T3 cells induced by inorganic phosphate*

To further address the mechanism by which TUDCA inhibits Pi-induced NIH3T3 osteoblastic differentiation and mineralization, we examined the levels of total and phosphorylated eIF2α and ATF4 in the ER stress response PERK-eIF2α-ATF4 pathway in NIH3T3 cells induced by inorganic phosphate. As depicted in Figure 6, Western blot analysis demonstrated TUDCA significantly attenuated phosphorylation of eIF2α and ATF4, while no significant changes in the level of total eIF2α. Runx2 occurred, as a master regulator of osteoblast differentiation and bone formation, was examined, as depicted, TUDCA also attenuated the expression of Runx2. Together with other results, these results indicate that TUDCA can inhibit NIH3T3 fibroblast mineralization *via* suppressing the ER stress response PERK-eIF2α-ATF4 pathway.

4. Discussion

NIH3T3 is a fibroblastic cell line with osteoblastic potential similar to C3H10T1/2 cells and MC3T3 cells, and can be induced into osteoblastic differentiation and mineralization *in vitro* (*26*), although it does not retain an ability to differentiate into osteoblast-like cells and is often used as a negative control during the study of osteoblastogenesis. As a mineralization inducer, inorganic phosphate ($NaPO_4$, Pi) has been widely used to induce osteoblast differentiation and mineralization (*25,27*), and Beck GR Jr *et al*. (*25*) has reported inorganic phosphate (Pi), as an inducer, can induce osteopontin expression in NIH3T3 cells in response to increased phosphate levels similar to the effect seen in MC3T3-E1 cells, namely, inorganic phosphate ($NaPO_4$, Pi) can induce osteoblastic differentiation and mineralization in NIH3T3 cells. Therefore, in this study, inorganic phosphate (Pi)-induced NIH3T3 fibroblasts induced osteogenesis and mineralization was used as an *in vitro* model for ectopic ossification.

Ectopic ossification occurs in a wide range of common and genetic diseases, but its molecular mechanisms and effective therapeutic targets remain to be clarified. In this study, we first explored the effect of TUDCA on the NIH3T3 fibroblast mineralization *in vitro* model for ectopic ossification. *Runx2* is a crucial transcription factor, is expressed in the earliest stage of osteogenic differentiation, and can trigger osteoblast differentiation as well as bone ECM proteins collagen type I (Col1a1) and osteocalcin (OCN) (*28,29*). ALP is an early marker of osteogenic differentiation. Col1a1 is the key for extracellular matrix (*30*). OCN is an osteoblast-specific marker for the late stage of osteoblast differentiation (*15*). Therefore, the expression of important osteoblast-specific genes, *Runx2*, *Col1a1*, *ALP* and *OCN* were assayed at 24 hours or 9 days. RT-qPCR results demonstrated that TUDCA significantly inhibited osteoblast-specific gene expression, and in addition, ALP activity, as an important indicator of osteoblastic differentiation also was assessed. Together with Alizarin Red-S (AR-S) staining and quantitation of mineralization and calcium deposition assays, all of these results indicated TUDCA could play an inhibition role in a dose-dependent manner in NIH3T3 cells during osteogenic differentiation. Therefore, we can conclude that TUDCA can inhibit ectopic ossification as a chemical chaperone.

A number of cellular stress conditions, UV, viral infection, and nutritional deprivation can trigger ER stress, and ER stress can also be induced by thapsigargin and tunicamycin (*6*). In this study, we also further demonstrated that ER stress could be activited by inorganic phosphate (Pi) in NIH3T3 fibroblasts, like thapsigargin and tunicamycin. Reports have suggested ER stress was induced during osteoblast differentiation and could activate ER stress response PERK-eIF2α-ATF4 pathways (*13-15*). In the PERK-eIF2α-ATF4 pathway, active PERK phosphorylates eIF2α, specifically promoting the translation of the activating transcription factor 4 (ATF4). ATF4 has been proven to be a critical transcription factor downstream of PERK signaling branches of ER stress, ATF4 can not regulate osteocalcin and bone sialoprotein transcription but also preserves mature osteoblast function including the synthesis of collagen, the most abundant extracellular protein found in bones (*15*). As a classical ER stress inhibitor, TUDCA has been proven to decrease the expression of phosphorylated eIF2α and ATF4 (*16-22*). In a recent study, Zhejun Cai *et al*. (*23*), found that TUDCA

protected against oxLDL-induced ER stress in VICs, significantly suppressed osteoblastic differentiation and protected against hypercholesterolemia-induced AV calcification in animal models. Therefore, in our study, we also investigated the effect of TUDCA on ER stress response mediated PERK-eIF2α-ATF4 pathway in an *in vitro* model for ectopic ossification, found TUDCA significantly suppressed the expression of phosphorylated eIF2α and ATF4, and the result is consistent with previous reports. Runx2, as a master regulator of osteoblast differentiation and bone formation, was examined, and TUDCA also attenuated the expression of Runx2. Taken together, we conclude ER stress is involved in ectopic ossification and TUDCA can inhibit mineralization *via* alleviating ER stress.

In addition, the chemical chaperone TUDCA has been proven to be protective in various diseases, such as, diabetes mellitus, obesity, and atherosclerosis, *via* prevention of ER stress. Previous reports show TUDCA enhances the adaptive capacity of ER, increases insulin sensitivity and reverses type 2 diabetes in obese mice by decreasing ER stress in the hypothalamus (*16*) and can alleviate advanced glycation end product-induced apoptosis and osteoblastic differentiation of stromal cells *via* alleviating ER stress (*22,24*). It was also discovered that TUDCA could decrease the lipid content of adipocytes and reduce body mass in obese humans by attenuation of ER stress (*31,32*) and prevent both the maturation of adipocytes from preadipocytes and weight gain in ob/ob mice by decreasing ER stress (*33,34*). Therefore, based on these facts, TUDCA might lead to a novel therapeutic approach in ectopic ossification associated diseases.

In conclusion, our results indicate that TUDCA can inhibit fibroblast's mineralization *via* suppressing the ER stress response PERK-eIF2α-ATF4 pathway. These findings provide novel insights into the mechanisms of ectopic ossification and TUDCA has potential pharmacologic and therapeutic applications for treating ectopic ossification associated diseases.

Acknowledgements

This study was supported by National Natural Science Foundation of China (81371909) and Key Projects in the National Science & Technology Pillar Program during the Twelfth Five-year Plan Period (2013BAI07B01).

References

1. Li Q, Jiang Q, Uitto J. Ectopic mineralization disorders of the extracellular matrix of connective tissue: Molecular genetics and pathomechanisms of aberrant calcification. Matrix Biol. 2014; 33:23-28.
2. Popovic M, Agarwal A, Zhang L, Yip C, Kreder HJ, Nousiainen MT, Jenkinson R, Tsao M, Lam H, Milakovic M, Wong E, Chow E. Radiotherapy for the prophylaxis of heterotopic ossification: A systematic review and meta-analysis of published data. Radiother Oncol. 2014; 113:10-17.
3. Edwards DS, Clasper JC. Heterotopic ossification: A systematic review. J R Army Med Corps. 2014. pii: jramc-2014-000277.
4. Li Q, Uitto J. Mineralization/anti-mineralization networks in the skin and vascular connective tissues. Am J Pathol. 2013; 183:10-18.
5. Kousteni S. Osterix finds its master. EMBO Rep. 2011; 12:382-383.
6. Hamamura K, Yokota H. Stress to endoplasmic reticulum of mouse osteoblasts induces apoptosis and transcriptional activation for bone remodeling. FEBS Lett. 2007; 581:1769-1774.
7. Kaufman RJ. Stress signaling from the lumen of the endoplasmic reticulum: Coordination of gene transcriptional and translational controls. Genes Dev. 1999; 13:1211-1233.
8. Ron D. Translational control in the endoplasmic reticulum stress response. J Clin Invest. 2002; 110:1383-1388.
9. Rutkowski DT, Kaufman RJ. A trip to the ER: Coping with stress. Trends Cell Biol. 2004; 14:20-28.
10. Boot-Handford RP, Briggs MD. The unfolded protein response and its relevance to connective tissue diseases. Cell Tissue Res. 2010; 339:197-211.
11. Marciniak SJ, Ron D. Endoplasmic reticulum stress signaling in disease. Physiol Rev. 2006; 86:1133-1149.
12. Minamino T, Komuro I, Kitakaze M. Endoplasmic reticulum stress as a therapeutic target in cardiovascular disease. Circ Res. 2010; 107:1071-1082.
13. Zhang P, McGrath B, Li S, Frank A, Zambito F, Reinert J, Gannon M, Ma K, McNaughton K, Cavener DR. The PERK eukaryotic initiation factor 2 alpha kinase is required for the development of the skeletal system, postnatal growth, and the function and viability of the pancreas. Mol Cell Biol. 2002; 22:3864-3874.
14. Wei J, Sheng X, Feng D, McGrath B, Cavener DR. PERK is essential for neonatal skeletal development to regulate osteoblast proliferation and differentiation. J Cell Physiol. 2008; 217:693-707.
15. Saito A, Ochiai K, Kondo S, Tsumagari K, Murakami T, Cavener DR, Imaizumi K. Endoplasmic reticulum stress response mediated by the PERK-eIF2(alpha)-ATF4 pathway is involved in osteoblast differentiation induced by BMP2. J Biol Chem. 2011; 286:4809-4818.
16. Ozcan U, Yilmaz E, Ozcan L, Furuhashi M, Vaillancourt E, Smith RO, Görgün CZ, Hotamisligil GS. Chemical chaperones reduce ER stress and restore glucose homeostasis in a mouse model of type 2 diabetes. Science. 2006; 313:1137-1140.
17. Ceylan-Isik AF, Sreejayan N, Ren J. Endoplasmic reticulum chaperone tauroursodeoxycholic acid alleviates obesity-induced myocardial contractile dysfunction. J Mol Cell Cardiol. 2011; 50:107-116.
18. Galán M, Kassan M, Choi SK, Partyka M, Trebak M, Henrion D, Matrougui K. A novel role for epidermal growth factor receptor tyrosine kinase and its downstream endoplasmic reticulum stress in cardiac damage and microvascular dysfunction in type 1 diabetes mellitus. Hypertension. 2012; 60:71-80.
19. Galán M, Kassan M, Kadowitz PJ, Trebak M, Belmadani S, Matrougui K. Mechanism of endoplasmic reticulum stress-induced vascular endothelial dysfunction. Biochim Biophys Acta. 2014; 1843:1063-1075.

20. Lee YY, Hong SH, Lee YJ, Chung SS, Jung HS, Park SG, Park KS. Tauroursodeoxycholate (TUDCA), chemical chaperone, enhances function of islets by reducing ER stress. Biochem Biophys Res Commun. 2010; 397:735-739.
21. de Almeida SF, Picarote G, Fleming JV, Carmo-Fonseca M, Azevedo JE, de Sousa M. Chemical chaperones reduce endoplasmic reticulum stress and prevent mutant HFE aggregate formation. J Biol Chem. 2007; 282:7905-7912.
22. Chen Y, Liu CP, Xu KF, Mao XD, Lu YB, Fang L, Yang JW, Liu C. Effect of taurine-conjugated ursodeoxycholic acid on endoplasmic reticulum stress and apoptosis induced by advanced glycation end products in cultured mouse podocytes. Am J Nephrol. 2008; 28:1014-1022.
23. Cai Z, Li F, Gong W, Liu W, Duan Q, Chen C, Ni L, Xia Y, Cianflone K, Dong N, Wang DW. Endoplasmic reticulum stress participates in aortic valve calcification in hypercholesterolemic animals. Arterioscler Thromb Vasc Biol. 2013; 33:2345-2354.
24. Tanaka K, Yamaguchi T, Kaji H, Kanazawa I, Sugimoto T. Advanced glycation end products suppress osteoblastic differentiation of stromal cells by activating endoplasmic reticulum stress. Biochem Biophys Res Commun. 2013; 438:463-467.
25. Beck GR Jr, Zerler B, Moran E. Phosphate is a specific signal for induction of osteopontin gene expression. Proc Natl Acad Sci U S A. 2000; 97:8352-8357.
26. Shui C, Scutt AM. Mouse embryo-derived NIH3T3 fibroblasts adopt an osteoblast-like phenotype when treated with 1alpha, 25-dihydroxyvitamin D(3) and dexamethasone *in vitro*. J Cell Physiol. 2002; 193:164-72.
27. Beck GR Jr, Knecht N. Osteopontin regulation by inorganic phosphate is ERK1/2-, protein kinase C-, and proteasome-dependent. J Biol Chem. 2003; 278:41921-41929.
28. Ducy P, Zhang R, Geoffroy V, Ridall AL, Karsenty G. Osf2/Cbfa1: A transcriptional activator of osteoblast differentiation. Cell. 1997; 89: 747-754.
29. Komori T. Regulation of bone development and maintenance by Runx2. Front Biosci. 2008; 13:898-903.
30. Couchourel D, Aubry I, Delalandre A, Lavigne M, Martel-Pelletier J, Pelletier JP, Lajeunesse D. Altered mineralization of human osteoarthritic osteoblasts is attributable to abnormal type I collagen production. Arthritis Rheum. 2009; 60:1438-1450.
31. Gregor MF, Yang L, Fabbrini E, Mohammed BS, Eagon JC, Hotamisligil GS, Klein S. Endoplasmic reticulum stress is reduced in tissues of obese subjects after weight loss. Diabetes. 2009; 58:693-700.
32. Gregor MF, Hotamisligil GS. Thematic review series: Adipocyte Biology. Adipocyte stress: The endoplasmic reticulum and metabolic disease. J Lipid Res. 2007; 48:1905-1914.
33. Basseri S, Lhoták S, Sharma AM, Austin RC. The chemical chaperone 4-phenylbutyrate inhibits adipogenesis by modulating the unfolded protein response. J Lipid Res. 2009; 50:2486-2501.
34. Ozcan L, Ergin AS, Lu A, Chung J, Sarkar S, Nie D, Myers MG Jr, Ozcan U. Endoplasmic reticulum stress plays a central role in development of leptin resistance. Cell Metab. 2009; 9:35-51.

(Received January 16, 2015; Revised February 11, 2015; Accepted February 22, 2015)

Original Article

DOI: 10.5582/ddt.2015.01006

Enhanced anticancer activity of 5-FU in combination with Bestatin: Evidence in human tumor-derived cell lines and an H22 tumor-bearing mouse

Jin Li[1], Xuejian Wang[2], Jinning Hou[1], Yongxue Huang[3], Yingjie Zhang[1,*], Wenfang Xu[1,*]

[1] *Department of Medicinal Chemistry, School of Pharmaceutical Sciences, Shandong University, Ji'nan, Shandong, China;*
[2] *Key Laboratory of Applied Pharmacology in Shandong Province, Department of Pharmacology, School of Pharmacy, Weifang Medical College, Weifang, Shandong, China;*
[3] *Bochuang International Medical Institute, Weifang, Shandong, China.*

Summary **The clinical use of 5-fluorouracil (5-FU) is increasingly limited by low response rates, adverse reactions, and toxicity. A drug combination offers a new strategy for appropriate use of 5-FU. Bestatin, an aminopeptidase N (APN) inhibitor, has been used as an adjuvant chemotherapy drug because of its actions to suppress tumorigenesis and invasion. The current study evaluated the anticancer efficacy of 5-FU plus Bestatin at the cellular and animal level. The combination killed more colonic cancer, hepatic carcinoma, and ovarian cancer cells and fewer nonmalignant human embryonic kidney (HEK293) and Chinese hamster ovary (CHO) cells than 5-FU or Bestatin alone. Moreover, 41.58% of ES-2 and 20.86% of PLC/PRF/5 cell apoptosis was caused by the combination of the two, while 5-FU caused apoptosis of 20.86% of ES-2 cells and 8.85% of PLC/PRF/5 cells. The cell cycle was arrested in the S and G0/G1 phases when a combination of the two was used. In an experiment involving mice bearing tumors, a combination of the two had a rate of tumor inhibition of 61.98%, while 5-FU alone had a rate of tumor inhibition of just 49.17%. In addition, the combination of the two was safer than either drug alone and did not cause weight loss or death. In conclusion, combining 5-FU and Bestatin could enhance the anticancer activity of 5-FU and decrease its cytotoxicity. These results suggest that 5-FU plus Bestatin has greater efficacy as a tumor therapy.**

Keywords: Drug combination, APN/CD13 inhibitor, Bestatin, 5-FU, anticancer or antitumor action

1. Introduction

Chemotherapy is an important form of cancer treatment that is widely used to treat malignant tumors in clinical practice. Cytotoxic drugs such as ADM, 5-fluorouracil (5-FU), cisplatin, and mitomycin are "star" drugs among chemotherapeutics. 5-FU is commonly used in clinical practice to treat oophoroma, breast cancer, neck and head cancer, and gastrointestinal malignancies (*1*). 5-FU inhibits cell proliferation and growth by pretending to be uracil, suppressing the activity of thymidylate synthase (TS) (*2*). Cancer cells are damaged when the synthesis of deoxyadenosine triphosphate (dTMP) is disturbed. However, 5-FU alone results in a low response rate, and adverse reactions to it and its toxicity have gradually forced it out of the limelight. 5-FU has been found to result in serious adverse reactions and toxicity to the healthy body by causing conditions such as myelo-suppression, nausea, emesis, and hand-foot syndrome (*3,4*). In addition, its clinical use is highly limited due to drug resistance. To overcome these shortcomings, a novel strategy in the form of a drug combination has been used to treat cancer using 5-FU. A combination of 5-FU with other cytotoxic drugs, such as oxaliplatin, or novel biological agents, such as monoclonal antibodies, are less toxic because of the reduced dose of each drug and can prolong survival

**Address correspondence to:*
Dr. Wenfang Xu and Dr. Yingjie Zhang, Department of Medicinal Chemistry, School of Pharmaceutical Sciences, Shandong University, Ji'nan, Shandong 250012, China.
E-mail: wenfxu@163.com (Xu WF)
E-mail: zhangyingjie@sdu.edu.cn (Zhang YJ)

(*2,5-7*). Murad *et al*. reported that a combination of paclitaxel and 5-FU provided an effective and safe regimen for the treatment of advanced gastric cancer (*8*). Identifying more appropriate agents for use in combination with 5-FU would improve the treatment of cancer.

Bestatin, a commercially available APN/CD13 inhibitor, has been used as an adjuvant chemotherapy drug because of its anticancer activity to suppress tumor invasion and induce cell apoptosis. Bestatin also works as an immunoenhancer in oncotherapy. It prolonged the survival of patients with acute adult non lymphocytic leukemia (*9*). Aminopeptidase N (EC 3.4.11.2, APN), also known as CD13, is a zinc-dependent transmembrane metallo-peptidase belonging to the M1 family; APN degrades preferentially proteins with an N-terminal neutral amino acid, such as Phe, Leu, and Gly (*10-12*). Widely expressed in various tissues (*13,14*), APN/CD13 plays important roles in various biological processes, such as antigen presentation, signal transduction, and angiogenesis (*15*). APN/CD13 is overexpressed in many tumor cells, including melanoma, thyroid cancer, prostate cancer, pancreas cancer, and myeloid leukemia (*16,17*), and APN/CD13 has been implicated in angiogenesis and cancer progression (*18*). It assists the degradation of type IV collagen, possibly contributing to tumor invasion and metastasis (*19,20*). APN/CD13 has been identified as promoting the generation of tumor vasculature and other types of new blood vessels (*21-24*). Therefore, APN/CD13 has been regarded as a significant target for anticancer agent development (*3*).

5-FU is a well-known cytotoxic drug used in chemotherapy, but its use is limited due to its low response rates, adverse reactions, and considerable toxicity. The APN inhibitor Bestatin could enhance immunity and possesses antitumor activity to some extent. Recently, Haraguchi *et al*. found that 5-FU plus Bestatin strongly inhibited liver tumor growth in a NOD/SCID mouse model (*25*). Haraguchi *et al*. noted that APN/CD13 was a therapeutic target in human liver cancer stem cells (CSC). The treatment of liver cancer may be improved by combining Bestatin and 5-FU to disrupt APN/CD13^{+} cells (CSC) by respectively up-regulating the ROS level and inhibiting the proliferation of general cancer cells. In additional, treatment with 5-FU or doxorubicin could up-regulate APN/CD13 expression on the surface of PLC/PRF/5 cells. Therefore, combining the APN/CD13 inhibitor with a cytotoxic anticancer drug may prolong patient survival and greatly reduce the suffering of patients. A combination of 5-FU and Bestatin could serve as an effective therapy to treat cancer with a low level cytotoxicity. The current study evaluated the pharmaceutical activity of 5-FU plus Bestatin in colonic cancer, hepatic carcinoma, and ovarian cancer cell lines and nonmalignant human embryonic kidney and Chinese hamster ovary cell lines. The anticancer activity of the two drugs was also assessed in animals. Results should indicate whether this drug combination has potential as a chemotherapy regimen.

2. Materials and Methods

2.1. *Materials*

5-FU was purchased from Hisun Pharmaceutical (Zhejiang, China). Bestatin and 5-FU were dissolved in DMSO and diluted with saline solution or cell culture medium before use.

MTT [(3-[4, 5-dimethyl-2-thiazolyl]-2, 5-diphenyl-2H-tetrazolium bromide)] and L-leucine-p-nitro-anilide were from Solarbio (Beijing, China). PE anti-human CD13 was from BD (New York, the USA). Hoechst 33342 and an Annexin-V/FITC and PI apoptosis detection kit were purchased from Beyotime (Jiangsu, China). Microsomal aminopeptidase from porcine kidney microsomes was from Sigma-Aldrich (Shanghai, China). Male Kunming mice were supplied by the Experimental Animal Center of Shandong University. The ratio of combination of the two drugs means the molar concentration ratio.

2.2. *Cell lines and culture*

Cancer cells (HCT-116, HepG2, ES-2, and PLC/PRF/5 cells) were maintained in RPMI-1640 medium. In addition, human embryonic kidney (HEK293) cells were cultured in DMEM medium, and Chinese hamster ovary (CHO) cells were cultured in DMEM:F-12 (1:1) medium. All media were supplemented with 10% (v/v) heat-inactivated fetal bovine serum, 100 IU/mL penicillin, and 100 IU/mL streptomycin in a 5% CO2 humidified atmosphere at 37°C. Cells were harvested with 0.25% EDTA-Trypsin.

2.3. *Assay of enzyme activity*

The enzyme activity of the drugs were determined using L-leu-p-nitro-anilide as a substrate and microsomal aminopeptidase from porcine kidney microsomes in 50 mM PBS buffer, pH 7.2, at 37°C. The mixture of the APN/CD13 enzyme and drug compounds was incubated at 37°C for 5 min. The substrate was then added and the resulting mixture was incubated for another 30 min at 37°C. The hydrolysis of the substrate was measured by following the change in absorbance monitored at 405 nm with a Micro-plate Reader (ThermoFisher, Shanghai, China). The experiment was repeated more than three times.

APN/CD13 activity on the surface of ES-2 cells was estimated by measuring the hydrolysis of L-leucine-p-nitro-anilide. A cell suspension (2.86×10^6/mL) in 1× PBS buffer was added to a 96-well plate (70 μL) containing 1~256 μM of 5-FU or 3.125~400 μM of the combined drugs. Subsequently, L-leucine-p-nitro-anilide

was added to a final concentration of 1.6 mM and the mixture was incubated for 1 h in a thermostatic shaker at 37°C, 100 rpm. APN/CD13 activity was then estimated by measuring the absorbance at 405 nm as described before. The experiment was repeated more than three times.

2.4. *MTT assay*

The cell viability of four cancer cell lines exposed to drugs was evaluated using an MTT assay and 96-well plates. HEK293 and CHO cells were chosen to evaluate the toxicity of compounds with the MTT assay. In brief, cells were seeded on 96-well plates at 4000/well. After incubation for 24 h, cells were treated with Bestatin, 5-FU, or a combination of the two (the ratio of the concentration of 5-FU to Bestatin was 1:1, 2.5:1, 5:1, and 10:1). After incubation for another 48h, 0.5% MTT was added to each well. Four hours later, 200 μL DMSO was added and mixed for 10 min. The absorbance values at 490 nm were then recorded using the Micro-plate Reader (ThermoFisher). The experiment was repeated more than three times.

2.5. *Clonogenic assay*

A clonogenic assay was performed to evaluate the effect of the compounds on cancer cell growth over a relatively long duration of exposure. PLC/PRF/5 and ES-2 cells, seeded on six-well plates (250 cells per well), were exposed to 5-FU, Bestatin, and a combination of the two (5-FU:Bestatin, 5:1) for two consecutive weeks at 37°C. Cells were fixed with fresh 4% paraformaldehyde at room temperature for 15 min and stained with Giemsa. Cell images were captured using an inverted microscope (magnification ×4, Olympus, Beijing, China). The colonies (more than 50 cells) in each experimental group were counted and were then compared to the control. The experiment was repeated more than three times.

2.6. *Assay of Hoechst 33342 staining*

PLC/PRF/5 and ES-2 cells seeded on 6-well plates (1×10^5 per well) were exposed to 5-FU (10 μM for PLC/PRF/5, 4 μM for ES-2) and 5-FU plus Bestatin (5:1, 10 μM for PLC/PRF/5, 4 μM for ES-2) for 24 h. Cells were then stained with Hoechst 33342 at 37°C for 15 min in the dark. The apoptotic cells were stained blue and were observed using the Olympus inverted microscope (magnification ×20).

2.7. *Flow cytometry*

Flow cytometry was used to evaluate the expression of APN/CD13 on cells. Cells were harvested and washed with cold 1× PBS buffer. PE anti-human CD13 was added to 1×10^6 cells in 100 μL 1× PBS. After incubation for 15 min in 4°C, cells were washed and analyzed using flow cytometry.

Cell apoptosis and cell cycles were determined using flow cytometry. PLC/PRF/5 and ES-2 cells seeded on 6-well plates (1×10^5 per well) were treated with 5-FU (2 μM) and Bestatin (2 μM) and 5-FU plus Bestatin (5:1, 2 μM) for 48 h. Cells were harvested and washed with cold binding buffer. Phosphatidylserine on the surface of apoptotic cells was quantitatively detected using an Annexin-V/FITC and PI apoptosis detection kit in accordance with the manufacturer's instruction. Cell cycles were detected using PI staining. Cell apoptosis and cell cycles were analyzed using flow cytometry.

2.8. *Animal experiment*

All experiments concerning living laboratory animals were performed the approval of the local ethics committee. Mice were inoculated subcutaneously with injections of 1×10^7/mL H22 cells. When the tumor was approximately 0.2 cm^3 in size, mice were divided randomly into five groups. A: Control group; B: Combination group 1 treated with 5-FU (15 mg/kg/day) plus Bestatin (7.5 mg/kg/day); C: Combination group 2 treated with 5-FU (7.5 mg/kg/day) plus Bestatin (3.65 mg/kg/day); D: Bestatin group (50 mg/kg/day); and E: 5-FU group (15 mg/kg/day). 5-FU and Bestatin were dissolved in DMSO and diluted with 1× PBS to the appropriate concentration. Each mouse was administered 100 μL of the drug solution in the abdominal cavity every time. All groups were treated with drugs for 2 weeks. Inhibition of tumor growth was calculated at the end of the treatment to determine antitumor action.

3. Results

3.1. *Expression of APN/ CD13 and inhibition of APN/ CD13 enzyme activity*

The extent to which compounds inhibited APN/CD13 enzyme activity was estimated by quantifying the APN/ CD13 enzymatic cleavage of the substrate L-leucine-p-nitro-anilide. As shown in Table 1, APN/ CD13 activity

Table 1. SAPN/CD13 enzymatic activity of 5-FU, Bestatin, and a combination of the two

Compounds	IC_{50} (μM, mean ± S.D.)[a]	IC_{50} of Bestatin[b]
5-FU	> 256	
Bestatin	3.50 ± 0.39	3.50
5FU:Bestatin (1:1)	9.35 ± 2.98	4.68
5FU:Bestatin (2.5:1)	19.3 ± 3.94	5.51
5FU:Bestatin (5:1)	21.9 ± 6.88	3.65
5FU:Bestatin (10:1)	37.5 ± 6.99	3.41

[a] Data are expressed as mean values from three independent experiments. [b] IC_{50} values for Bestatin were calculated from the corresponding IC_{50} for Bestatin and 5-FU.

was significantly inhibited in all groups treated with Bestatin, as indicated by IC_{50} values at the micromole level. 5-FU did not suppress APN/CD13 activity because of its large IC_{50} with respect to APN/CD13. The four groups treated with a combination of Bestatin and 5-FU had an IC_{50} like that for Bestatin alone, indicating that 5-FU did not affect interaction between Bestatin and APN/CD13.

Moreover, the influence of 5-FU on the binding of Bestatin to APN/CD13 was investigated at the cellular level. First, flow cytometry was used to detect the level of APN/CD13 expression in a panel of cells, including PLC/PRF/5, HepG2, HCT-116, and ES-2 cells (Figure 1). Over-expressing APN/CD13, ES-2 cells were selected to evaluate the APN/CD13 activity on the cell surface in groups treated with drugs. The results are shown in Table 2 and lead to a similar conclusion as before, *i.e.* that 5-FU did not inhibit APN/CD13 activity and that it did not influence the binding of Bestatin to APN/CD13.

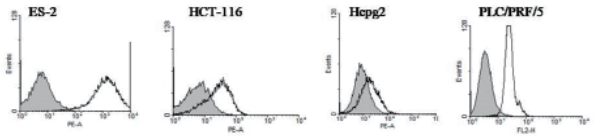

Figure 1. Level of APN/CD13 expression in various cells. The expression of APN/CD13 on the cell surface was evaluated using flow cytometry with PE anti-human CD13. The left peak in each histogram represents negative cells and the right represents APN/CD13-positive cells.

Table 2. APN/CD13 enzymatic activity on the cell surface of cells treated with 5-FU, Bestatin, and a combination of the two

Compounds	IC_{50} (μM, mean ± S.D.)[a]	IC_{50} of Bestatin[b]
5-FU	> 256	
Bestatin	57.2 ± 5.8	57.2
5-FU:Bestatin (1:1)	98.9 ± 16.5	49.4
5-FU:Bestatin (2.5:1)	112 ± 19.8	32.0
5-FU:Bestatin (5:1)	164 ± 49.8	27.3
5-FU:Bestatin (10:1)	1051 ± 41.1	95.5

[a] Data are expressed as the mean values from three independent experiments. [b] IC_{50} values for Bestatin were calculated from the corresponding IC_{50} for Bestatin and 5-FU.

3.2. *In vitro assay of inhibition of proliferation and cytotoxicity*

To explore the effects of compounds on human cancer cell lines and non-malignant cells *in vitro*, the IC_{50} was assessed with an MTT assay using a panel of human cancer cell lines, namely HCT-116 (colonic cancer), HepG2 (hepatic carcinoma), ES-2 (ovarian cancer), and PLC/PRF/5 (hepatic carcinoma). The IC_{50} was also assessed with an MTT assay using a panel of non-malignant cells, namely CHO and HEK293 cells. As shown in Table 3, combining Bestatin with 5-FU inhibited the growth of cancer cells at a lower concentration than Bestatin or 5-FU alone. With high IC_{50} values, Bestatin displayed little cytotoxicity to a panel of cancer cells and non-malignant cells. 5-FU strongly inhibited non-malignant CHO and HEK293 cells, but 5-FU plus Bestatin had relatively lower cytotoxicity (Table 4). When the ratio of the concentration of 5-FU to Bestatin was 5:1, the combination had a relatively higher efficacy and lower toxicity. At a ratio of 10:1, the combined drugs did not have a marked increase in

Table 3. The anti-proliferative action (IC_{50}) of Bestatin plus 5-FU in 4 strains of cancer cells and 2 strains of non-malignant cells

Cells	Compds/IC_{50}(μM, mean ± S.D.)[a]					
	1:1[b]	2.5:1[b]	5:1[b]	10:1[b]	5-FU	Bestatin
HCT-116	20.9 ± 4.81	16.7 ± 2.02	8.59 ± 0.90	6.03 ± 2.5	22.3 ± 2.58	43.5 ± 2.14
HepG2	17.3 ± 1.65	16.5 ± 0.99	8.08 ± 0.32	10.0 ± 1.95	15.2 ± 4.47	64.4 ± 2.43
ES-2	24.5 ± 0.85	18.2 ± 2.83	9.76 ± 4.63	5.79 ± 1.76	23.1 ± 0.42	49.3 ± 2.37
PLC/PRF/5	61.4 ± 7.73	31.7 ± 2.46	22.8 ± 1.33	24.5 ± 3.36	87.9 ± 14.2	769 ± 38.8
HEK293	ND[c]	ND[c]	33.45 ± 9.50	18.8 ± 6.79	7.70 ± 0.93	> 200
CHO	ND[c]	ND[c]	38.17 ± 9.22	20.0 ± 2.62	7.70 ± 0.70	> 200

[a] Data from an MTT assay and the mean from 3 repetitions and the standard deviation. [b] Ratio refers to the molar ratio of 5-FU and Besatin. [c] Not detected.

Table 4. The rate of tumor inhibition for 5-FU, Bestatin, and a combination of the two in a Kunming mouse model with subcutaneous H22 tumor cells

Compounds	Dose	Survived/total mice	Tumor weight (mean ± S.D.)	Inhibition rate[a] (%)
control	PBS	7/7	2.42 ± 0.94 g	
5-FU	15 mg/kg/day	5/7	1.23 ± 0.54 g	49.2
Bestatin	50 mg/kg/day	7/7	1.68 ± 0.89 g	30.6
5-FU:Bestatin (5:1)	7.5 mg/kg/day+3.65 mg/kg/day	7/7	1.20 ± 0.66 g	50.4
5-FU:Bestatin (5:1)	15.0 mg/kg/day+7.5 mg/kg/day	7/7	0.92 ± 0.47 g	62.0

[a] The tumors were weighed after mice were sacrificed, and the inhibitory effect in each group was defined as a percentage of the control tumor weight.

anticancer but they did have greater cytotoxicity to non-malignant cells. Therefore, the appropriate molar ratio of 5-FU to Bestatin was determined to be 5:1.

A colony assay revealed similar results, as shown in Figure 2A. PLC/PRF/5 and ES-2 cells were chosen for the colony-forming assay. The colony-forming ability of cancer cells was effectively inhibited by a combination of the two drugs. Bestatin plus 5-FU inhibited cancer cells by 54.1% in PLC/PRF/5 cells and 92.8% in ES-2 cells, while 5-FU alone inhibited cancer cells by 39.2% in PLC/PRF/5 cells and 95.2% in ES-2 cells. In contrast, Bestatin alone had no effect on colony formation in the two cell lines, which may have been due to its low concentration.

3.3. *Induction of apoptosis and prevention of cell cycle progression*

Hoechst 3342 staining was performed to determine whether 5-FU plus Bestatin induced cell apoptosis. Significant morphological changes in PLC/PRF/5 and ES-2 cells were observed after treatment with combined drugs for 24 h. Cells with a bright blue nucleus after Hoechst staining are known to have cellular shrinkage and nuclear fragmentation, which are typical features of apoptotic cells. Figure 3 indicates that the combination of Bestatin plus 5-FU resulted in more apoptotic cells than 5-FU or Bestatin alone. To further measure the percentage of apoptotic and necrotic cancer cells, Annexin-V/PI staining was analyzed using flow cytometry. Figure 4 shows the specific percentage of PLC/PRF/5 and ES-2 cells. The combination of the two drugs significantly induced cell apoptosis at a rate of 20.86% in PLC/PRF/5 cells and 41.58% in ES-2 cells, while 5-FU or Bestatin alone resulted in relatively low rates of apoptosis in both PLC/PRF/5 cells (< 10%) and ES-2 cells (< 30%). These results indicate that the drug combination inhibited cell growth by greatly inducing apoptosis.

The cell cycles of PLC/PRF/5 cells treated with 5-FU or Bestatin alone or in combination were also examined. Flow cytometry (Figure 5) revealed that 5-FU exposure induced cells to remain in the S phase while Bestatin increased the number of cells in the G0/G1 phase. The results of the combination of the two drugs indicated that the cell cycle was arrested in the G0/G1and S phase.

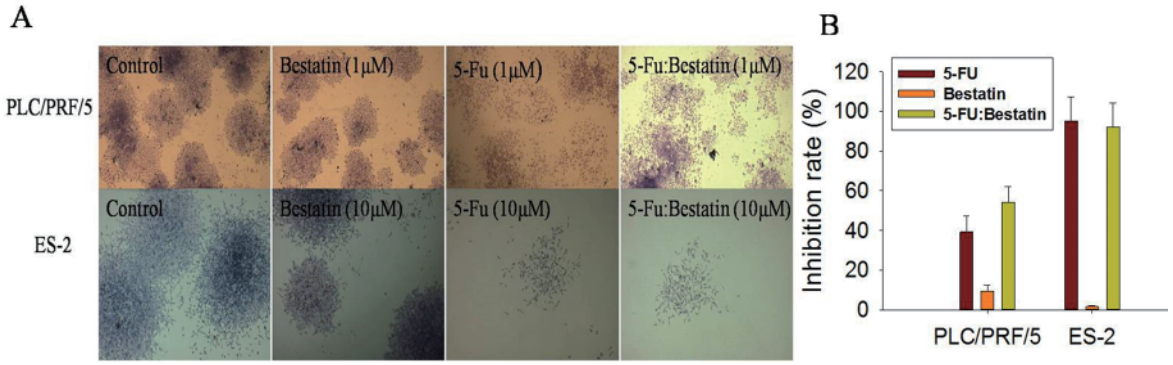

Figure 2. Colony formation by PLC/PRF/5 and ES-2 cells observed under an inverted microscope. A: PLC /PRF/5 and ES-2 cells were stained with Giemsa after treatment with drugs for two consecutive weeks, and images were captured using an inverted microscope (magnification×4). **B**: The inhibition rate was estimated by counting the number of colonies containing more than 50 cells. The ratio of the concentration of 5-FU to Bestatin was 5:1 in the colony-forming test.

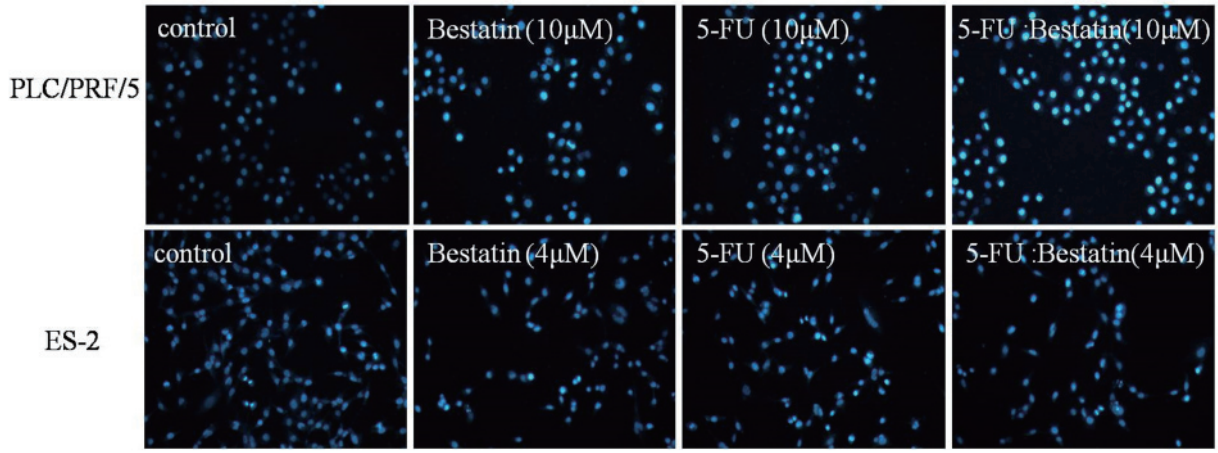

Figure 3. Hoechst staining of PLC/PRF/5 and ES-2 cells observed using fluorescence microscopy. Photos were taken after PLC/PRF/5 and ES-2 cells were exposed to 5-FU (10 μM for PLC/PRF/5, 4 μM for ES-2) and Bestatin plus 5-FU (1:5; 10 μM for PLC/PRF/5, 4 μM for ES-2) for 24 h (magnification ×20). The brighter blue cells are apoptotic cells.

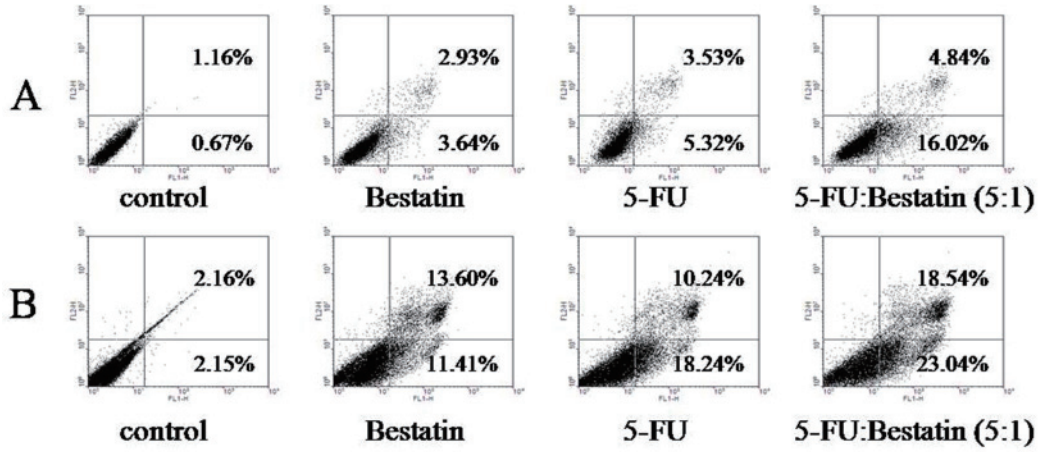

Figure 4. Cell apoptosis after PLC/PRF/5 and ES-2 cells were treated with drugs for 48h. Cells stained with annexin-V/FITC and propidium iodide (PI) were analyzed using flow cytometry. **(A)** PLC/PRF/5 cells: control, Bestatin (2 μM), 5-FU (2 μM), 5-FU:Bestatin 5:1 (2 μM); **(B)** ES-2 cells: control, Bestatin (2 μM), 5-FU (2μM), 5-FU:Bestatin 5:1 (2 μM).

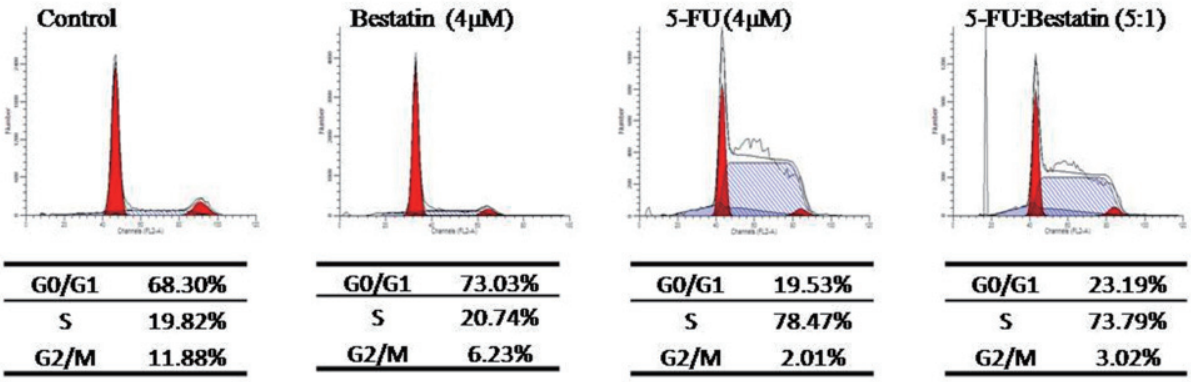

Figure 5. PLC/PRF/5 cells in different cells cycles in response to treatment with Bestatin and 5-FU alone or in combination. Tables under the graphics indicate the percentage of cells in different phases of the cell cycle when treated with Bestatin and 5-FU alone or in combination.

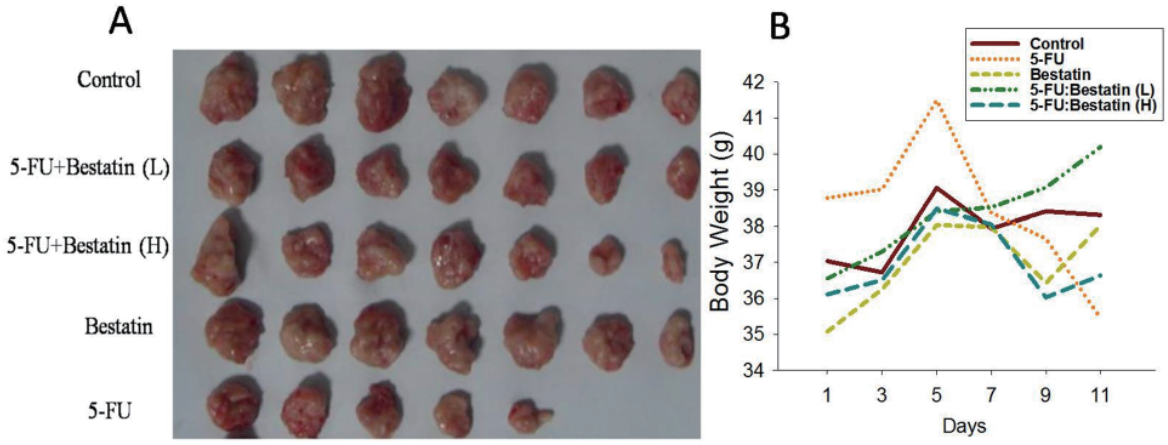

Figure 6. Data from an experiment with mice bearing H22 tumors. A: Picture of dissected H22 tumor tissues from Kunming mice. The photo was taken with a camera once mice were sacrificed. **B**: The body weight of mice in each group was recorded for two weeks.

3.4. *Assay of antitumor activity in vivo*

To evaluate the antitumor action of 5-FU plus Bestatin *in vivo*, a Kunming mouse model was established with subcutaneous H22 tumor cells using 5-FU and Bestatin as the positive control. Figure 6A and Table 4 show that a combination of the two significantly inhibited tumor growth in contrast to the control drugs. In comparison

to 5-FU (15 mg/kg/day) alone, the combination of 5-FU and Bestatin used half the dose of 5-FU (7.5 mg/kg/day), but the two had similar rates of inhibition (about 50%). Bestatin inhibited the tumor by only ~30% at a large dose (50 mg/kg/day). In contrast to 5-FU alone, a combination of 5-FU and a low dose of Bestatin (7.5mg/kg/day) increased the rate of inhibition from 49.2% to 62.0%. In addition, two mice in the 5-FU group died while no mice in the other groups died, indicating the substantial toxicity of 5-FU and its reduced toxicity when used with Bestatin. The mean weight of mice in each group is shown in Figure 6B. 5-FU resulted in weight loss after three days of drug delivery while the Bestatin group and the combination groups tolerated the treatment well.

4. Discussion

Although 5-FU is commonly used as an anticancer drug, its clinical use is increasingly limited due to drug resistance, adverse reactions, and toxicity. A drug combination provides a novel strategy to enhance its efficacy and reduce its toxicity when treating cancer. APN, also known as CD13, is a zinc-dependent M_1-class metalloprotease that is over-expressed in cancer cells; APN plays important roles in various biological processes, such as antigen presentation, signal transduction, and angiogenesis (*22,26*). APN/CD13 is considered to be an important target for developing anticancer agents. Moreover, APN/CD13 has been found to be a biomarker of liver cancer stem cells (*27,28*). Bestatin is widely used as an APN/CD13 inhibitor in adjuvant chemotherapy and it prolongs patient survival.

The current study investigated the anticancer activity of 5-FU plus Bestatin *in vitro* and *in vivo*. An assay of enzyme activity at the protein and cell level revealed that 5-FU did not disturb APN/CD13 activity and that it did not influence the binding of Bestatin to APN/CD13. This signals the possibility that 5-FU and Bestatin could work along both lines. An assay of inhibition of proliferation and cytotoxicity *in vitro* revealed that a combination of 5-FU and Bestatin had greater anti-proliferative action on human cancer cells with a lower level of cytotoxicity in normal cells than 5-FU or Bestatin alone. Moreover, Hoechst 3342 staining of PLC/PRF/5 and ES-2 cells revealed that the combined drugs had greater activity in triggering apoptosis. Flow cytometry revealed that the drug combination resulted in 10% more apoptotic cells than 5-FU or Bestatin alone. In an analysis of cell cycles, exposure to 5-FU and Bestatin induced cells to remain in the S and G0/G1 phases. All of these results in vitro indicate that the combined drugs had greater efficacy than either drug alone. In an experiment involving H22 tumor-bearing mice, 5-FU in combination with a small quantity of Bestatin significantly inhibited tumor growth. 5-FU killed two mice and resulted in weight loss while the combination of the two resulted in no deaths and no loss of weight. 5-FU plus Bestatin shines because of its lower level of toxicity and superior therapeutic action. A study *in vivo* revealed that combining 5-FU and Bestatin ensured the survival rate for mice and also significantly inhibited tumor growth.

In conclusion, this study has described the broad-spectrum anticancer activity of 5-FU in combination with the APN/CD13 inhibitor Bestatin. A combination of 5-FU and Bestatin has superior anticancer action and a lower cytotoxicity in normal cells than 5-FU or Bestatin alone *in vitro* and *in vivo*. The preliminary mechanisms for cell apoptosis and cell cycles induced by this combination have been discussed as well. The current results provide important information for clinical cancer therapy. Combining Bestatin with 5-FU therapy may improve the treatment of cancer.

Acknowledgements

This work was supported by the National High-tech R&D Program of China (Program 863) (Grant No.2014AA020523), Major National Scientific and Technological Projects of the Ministry of Science and Technology of China (Grant no. 2011ZX09401-015), the National Natural Science Foundation of China (Grant nos. 21302111, 81373282 and 21172134), and the China Postdoctoral Science Foundation (Grant no. 2014T70654).

References

1. Zhang DQ, Guo Q, Zhu JH, Chen WC. Increase of cyclooxygenase-2 inhibition with celecoxib combined with 5-FU enhances tumor cell apoptosis and antitumor efficacy in a subcutaneous implantation tumor model of human colon cancer. World J Surg Oncol. 2013; 11:16.
2. de la Cueva A, de Molina AR, Álvarez-Ayerza N, Ramos MA, Cebrián A, del Pulgar TG, Lacal JC. Combined 5-FU and ChoKα inhibitors as a new alternative therapy of colorectal cancer: Evidence in human tumor-derived cell lines and mouse xenografts. PloS one. 2013; 8:e64961.
3. Cui SX, Zhang HL, Xu WF, Qu XJ. 13F-1, a novel 5-fluorouracil prodrug containing an Asn-Gly-Arg (NO2) COOCH3 tripeptide, inhibits human colonic carcinoma growth by targeting aminopeptidase N (APN/CD13). Eur J Pharmacol. 2014; 734:50-59.
4. Giorgio E, Caroti C, Mattioli F, Uliana V, Parodi MI, D'Amico M, Fucile C, Marini V, Forzano F, Cassola G, Martelli A, Faravelli F, Di Maria E. Severe fluoropyrimidine-related toxicity: Clinical implications of DPYD analysis and UH2/U ratio evaluation. Cancer Chemoth Pharmacol. 2011; 68:1355-1361.
5. Shang W, Qiao J, Gu C, Yin W, Du J, Wang W, Zhu M, Han M, Lu W. Anticancer activity of an extract from needles and twigs of Taxus cuspidata and its synergistic effect as a cocktail with 5-fluorouracil. BMC Complem Altern M. 2011; 11:123.
6. Giacchetti S, Perpoint B, Zidani R, Le Bail N, Faggiuolo R, Focan C, Chollet P, Llory J, Letourneau Y, Coudert

B. Phase III multicenter randomized trial of oxaliplatin added to chronomodulated fluorouracil-leucovorin as first-line treatment of metastatic colorectal cancer. J Clin Oncol. 2000; 18:136-147.
7. Douillard J, Sobrero A, Carnaghi C, Comella P, Diaz-Rubio E, Santoro A, Van Cutsem E. Metastatic colorectal cancer: Integrating irinotecan into combination and sequential chemotherapy. Annals of Oncology. 2003; 14:7-12.
8. Murad AM, Petroianu A, Guimaraes RC, Aragao BC, Cabral LO, Scalabrini-Neto AO. Phase II trial of the combination of paclitaxel and 5-fluorouracil in the treatment of advanced gastric cancer: A novel, safe, and effective regimen. Am J Clin Oncol. 1999; 22:580-586.
9. Ichinose Y, Genka K, Koike T, Kato H, Watanabe Y, Mori T, Iioka S, Sakuma A, Ohta M. Randomized double-blind placebo-controlled trial of bestatin in patients with resected stage I squamous-cell lung carcinoma. J Natl Cancer Inst. 2003; 95:605-610.
10. Luan Y, Xu W. The structure and main functions of aminopeptidase N. Curr Med Chem. 2007; 14:639-647.
11. Ito K, Nakajima Y, Onohara Y, Takeo M, Nakashima K, Matsubara F, Ito T, Yoshimoto T. Crystal structure of aminopeptidase N (proteobacteria alanyl aminopeptidase) from Escherichia coli and conformational change of methionine 260 involved in substrate recognition. J Biol Chem. 2006; 281:33664-33676.
12. Addlagatta A, Gay L, Matthews BW. Structure of aminopeptidase N from Escherichia coli suggests a compartmentalized, gated active site. Proc Natl Acad Sci U S A. 2006; 103:13339-13344.
13. Breljak D, Gabrilovac J, Boranic M. Aminopeptidase N/CD13 and haematopoietic cells. Haema. 2003; 6:453-461.
14. Firla B, Arndt M, Frank K, Thiel U, Ansorge S, Täger M, Lendeckel U. Extracellular cysteines define ectopeptidase (APN, CD13) expression and function. Free Radic Biol Med. 2002; 32:584-595.
15. Jardinaud F, Banisadr G, Noble F, Melik-Parsadaniantz S, Chen H, Dugave C, Laplace H, Rostene W, Fournie-Zaluski MC, Roques BP, Popovici T. Ontogenic and adult whole body distribution of aminopeptidase N in rat investigated by in vitro autoradiography. Biochimie. 2004; 86:105-113.
16. Kehlen A, Lendeckel U, Dralle H, Langner J, Hoang-Vu C. Biological significance of aminopeptidase N/CD13 in thyroid carcinomas. Cancer Res. 2003; 63:8500-8506.
17. Ikeda N, Nakajima Y, Tokuhara T, Hattori N, Sho M, Kanehiro H, Miyake M. Clinical significance of aminopeptidase N/CD13 expression in human pancreatic carcinoma. Clin Cancer Res. 2003; 9:1503-1508.
18. Guzman-Rojas L, Rangel R, Salameh A, Edwards JK, Dondossola E, Kim YG, Saghatelian A, Giordano RJ, Kolonin MG, Staquicini FI, Koivunen E, Sidman RL, Arap W, Pasqualini R. Cooperative effects of aminopeptidase N (CD13) expressed by nonmalignant and cancer cells within the tumor microenvironment. Proc Natl Acad Sci U S A. 2012; 109:1637-1642.
19. Benoist J-M, Keime F, Montagne J, Noble F, Fournié-Zaluski M-C, Roques BP, Willer J-C, Le Bars D. Depressant effect on a C-fibre reflex in the rat, of RB101, a dual inhibitor of enkephalin-degrading enzymes. Eur J Pharmacol. 2002; 445:201-210.
20. Papapetropoulos A, Ryan JW, Antonov A, Virmani R, Kolodgie FD, Gerrity RG, Catravas JD. Human aortic endothelial cell aminopeptidase N. Immunopharmacology. 1996; 32:153-156.
21. Bauvois B, Dauzonne D. Aminopeptidase-N/CD13 (EC 3.4.11.2) inhibitors: Chemistry, biological evaluations, and therapeutic prospects. Med Res Rev. 2006; 26:88-130.
22. Mina-Osorio P. The moonlighting enzyme CD13: Old and new functions to target. Trends Mol Med. 2008; 14:361-371.
23. Fukasawa K, Fujii H, Saitoh Y, Koizumi K, Aozuka Y, Sekine K, Yamada M, Saiki I, Nishikawa K. Aminopeptidase N (APN/CD13) is selectively expressed in vascular endothelial cells and plays multiple roles in angiogenesis. Cancer Lett. 2006; 243:135-143.
24. Aozuka Y, Koizumi K, Saitoh Y, Ueda Y, Sakurai H, Saiki I. Anti-tumor angiogenesis effect of aminopeptidase inhibitor bestatin against B16-BL6 melanoma cells orthotopically implanted into syngeneic mice. Cancer Lett. 2004; 216:35-42.
25. Haraguchi N, Ishii H, Mimori K, Tanaka F, Ohkuma M, Kim HM, Akita H, Takiuchi D, Hatano H, Nagano H, Barnard GF, Doki Y, Mori M. CD13 is a therapeutic target in human liver cancer stem cells. J Clin Invest. 2010; 120:3326-3339.
26. Riemann D, Kehlen A, Langner J. CD13-not just a marker in leukemia typing. Immunology today. 1999; 20:83-88.
27. Christ B, Stock P, Dollinger MM. CD13: Waving the flag for a novel cancer stem cell target. Hepatology. 2011; 53:1388-1390.
28. Nagano H, Ishii H, Marubashi S, Haraguchi N, Eguchi H, Doki Y, Mori M. Novel therapeutic target for cancer stem cells in hepatocellular carcinoma. J Hepatobiliary Pancreat Sci. 2012; 19:600-605.

(Received February 1, 2015; Revised February 9, 2015; Accepted February 10, 2015)

Original Article

DOI: 10.5582/ddt.2014.01042

Anti-metastatic action of anacardic acid targets VEGF-induced signalling pathways in epithelial to mesenchymal transition

Puttananjaiah Shilpa[1,*], Keshavaiah Kaveri[1,2,*], Bharathi P Salimath[1,3,]**

[1] *Department of Studies in Biotechnology, University of Mysore, Manasagangotri, Mysore, India;*
[2] *Maharani's PU College, Narayanasastri road, Mysore, India;*
[3] *Petit Institute for Bioengineering and Bioscience, Georgia Institute of Technology, Atlanta, GA, USA.*

Summary **Anacardic acid is a major constituent of nutshell of cashew. In this study, we have isolated it from the leaves of *Anacardium Occidentale* L. using polarity-based fractionation and confirmed the structure using GC-MS, NMR and FT-IR. The main focus of this study is to harness the molecular mechanism of anti-metastatic action of anacardic acid (A1). We have used MCF-7, a weak metastatic and U-87, a highly metastatic, breast and glioma cell lines respectively, for our study. We have shown that VEGF increases migration and invasion activities of MCF-7 cells, upon overexpression of Twist and Snail genes. It is observed from the current study that exposure of MCF-7 cells to A1 resulted in upregulation of epithelial marker E-cadherin with a concomitant decrease in the expression of mesenchymal markers Twist and Snail gene expression besides exhibiting a strong anti-migratory and anti-invasive activity. In metastatic U-87 glioma cells, treatment with A1 decreased the phosphorylation of MAP kinases, inhibited the translocation of Sp1 and down regulated VEGF and Flt-1 gene expression. Overall, the current findings demonstrate for the first time that anacardic acid functions as a potent EMT inhibitor by targeting VEGF signaling pathway, providing a novel template for drug discovery.**

Keywords: *Anacardium occidentale* L., anacardic acid, epithelial to mesenchymal transition, anti-metastatic, vascular endothelial growth factor

1. Introduction

Anacardium occidentale L., a member belonging to Anacardiaceae family, has a great economic and medicinal value (*1*). *A. occidentale* L. has been found to have antibacterial, antiulcer, antitumor activity through suppression of hypoxia and angiogenic factors (*2*). Anacardium nut oil has been shown to have an apoptotic effect on tumor cell lines like acute myeloblastic leukemia, breast carcinoma, and cervical epithelial carcinoma (*3*). Sheela *et al*. has shown that an ethanolic extract of *A. occidentale* L. leaves suppresses vascular endothelial growth factor (VEGF) induced angiogenesis of both *in vivo* and *in vitro* (*4*). Nevertheless, studies either directly comparing non angiogenic role of VEGF to *A. occidentale* L. or its antimetastatic activity has not been well studied. In the present paper, an attempt to understand the anti-metastatic efficacy of anacardic acid (A1) in tumeriogenic but weakly metastatic breast cancer cells (MCF-7) and highly metastatic brain tumor cells, glioblastoma multiforme (U-87) is made.

Greater than 90% of deaths in breast cancer are attributed to metastatic disease where the primary tumor has invaded distant sites. To infiltrate host tissues, carcinoma cells of primary tumor separate from the tumor mass by breaking their basement membrane and cell-cell contacts, known as adherens junctions (*5-7*). Functional loss of E-cadherin has been reported to induce epithelial-mesenchymal transition (EMT) in several cancers (*8,9*). The resulting cells lose their flexible structure and enhance migration through the extracellular matrix (*10,11*). Until now, many growth factors including HGF, TGF-β, and EGF have been found to induce EMT (*12*). Recent research suggests that VEGF signalling is not limited to angiogenesis, but plays an important role in breast cancer cell migration

*These authors contributed equally to this works.
***Address correspondence to:*
Dr. Bharathi P Salimath, Department of Biotechnology, University of Mysore, Manasagangotri, Mysore 560006, India.
E-mail: salimathuom@gmail.com

and invasion (*13*). Most of the growth factors which induce EMT activation and modulation of transcription factors repress epithelial genes, such as those encoding E-cadherin and cytokeratins, and activate transcription programmes which specify fibroblast-like motility and an invasive phenotype (*14,15*). Transcription factors like Twist, Snail basic Helix Loop Helix (bHLH) families, two double zinc finger and homeodomain (ZEB) factors trigger EMT (*16*). Previously it has been shown that Twist and Snail transcription factors play key role during EMT by repressing the E-cadherin, the major epithelial cell adhesion molecule. However, it has recently been shown that over-expression of Twist in breast cancer animal model regulates EMT by promoting tumor cell invasion. The ectopic expression of Twist resulted in EMT and induced metastasis in cells.

Many studies have revealed that natural compounds act as antiangiogenic and apoptotic agents against human cancers. However, there is a continued search for novel nontoxic components for treating metastatic tumors. In the present study, an effort has been made to elucidate the molecular mechanisms involved in the anti-angiogenic and anti-metastatic effect of the compound A1 against breast cancer (MCF-7 cells) and highly metastatic glioma, (U-87 cells). Moreover, in the present study, MCF-7 cells are stimulated with VEGF, to demonstrate that MCF-7 cells exhibit epithelial phenotype with high expression of E-cadherin and less expression of detectable mesenchymal markers. It is also shown from the current studies that A1 inhibits proliferation, migration and invasion of MCF-7 breast cancer cells. In addition, it is also shown from the current research that the interplay of A1 with EMT regulators such as E-cadherin, Twist and Snail in order to inhibit metastasis of MCF-7 cells. Further the cellular and molecular mechanisms underlying the regulation of EMT by VEGF, Twist, and Snail and signaling pathway governing the same have been elucidated.

2. Materials and Methods

2.1. *Cell culture*

MCF-7 (non-metastatic breast cancer cell line), U-87 (most aggressive malignant primary brain cancer cell line) and HEK293 cells (Normal human embryonic kidney cells) are obtained from National Centre for Cell Science (NCCS); Pune, INDIA. Cells are cultured in Dulbecco's modified Eagle's medium (DMEM; Gibco, USA). Culture medium is supplemented with 10% Fetal Bovine Serum (FBS) and 100 units/ml Streptomycin and Penicillin from GIBCO laboratories, Grand Island, NY, USA). [^{3}H] thymidine is procured from the Baba Atomic Research Centre, Mumbai, India. Mammalian transfection assay kits, luciferase, CAT and β-galactosidase assay kits are from Promega, USA. All other reagents used are of the highest analytical grade.

2.2. *Processing of A. occidentale leaves and purification of the active compound*

The shade-dried leaves (1 kg) are powdered and extracted using 5 L of methanol at room temperature for 24 h. Polarity-based partial fractionation of the methanol extract is carried out using solvents such as hexane, ethyl acetate, and triple distilled water. The solvents are evaporated by rotary evaporator and all the fractions are verified for anti-angiogenic activity using human umbilical vein endothelial cells (HUVECs) tube formation assay. The ethyl acetate extract which exhibited positive activity, is further subjected to silica gel column chromatography (Merck 60-200 mesh size) and eluted with differential ratios of ethyl acetate: methanol (100:0, 95:5, 90:10, 50:50, and 0:100). The sub-fractions collected are subjected to TLC using ethyl acetate: methanol as a solvent system. The fraction EA 1 (ethyl acetate: methanol (100:0) that showed the maximum inhibitory effect on tube formation by HUVEC's is further subjected for purification (silica gel column chromatography, Merck 60-200 mesh size) and eluted with ethyl acetate: methanol (50:50 to 0:100) to obtain seven sub fractions (EA 1.1 to EA 1.7); with EA 1.1 being the most active component. EA 1.1 is further subjected to column chromatography using neutral alumina (Grade 3) to remove unwanted pigments (Scheme 1). The active compound thus obtained is validated and structurally characterized.

2.3. *High-performance liquid chromatography (HPLC) and spectral studies*

HPLC purification is carried out using a modular HPLC instrument (Ultrasep ES 10 RP 18 6.0 µm, reverse phase C18 column) (Tokyo, Japan). The mobile phase is chloroform/ethyl acetate (80:20) at 1.80 mL/min; absorbance is monitored at 280 nm. Each analysis is carried out by dissolving 25 mg of sample in 5 mL of ethyl acetate. The flow rate of the sample is 1 mL/min and ran for 30 min.

GC-MS of the isolated compound is done in Thermo LCQ Deca XP MAX (Bremen, Germany) (Range: m/z = 1 – 900). GC-MS recorded the retention time and mass to charge ratio (m/z). These experiments are carried out at Department of Chemistry, Indian Institute of Science, Bangalore, Karnataka, India.

^{1}H NMR spectrum is recorded on a Varian T-60 spectrometer and ^{13}C NMR spectrum is obtained on a Bruker WH-270 (Chicago, USA) machine at a probe temperature of 25°C. Spectra (^{1}H NMR, ^{13}C NMR) are recorded using 10 mg of the sample dissolved in 1 mL of chloroform and chemical shifts are reported relative to tetramethylsilane (TMS) in ppm and coupling constants in hertz. These experiments are performed at NMR research centre, Indian Institute of Science, Bangalore, Karnataka, India. All solvents used are

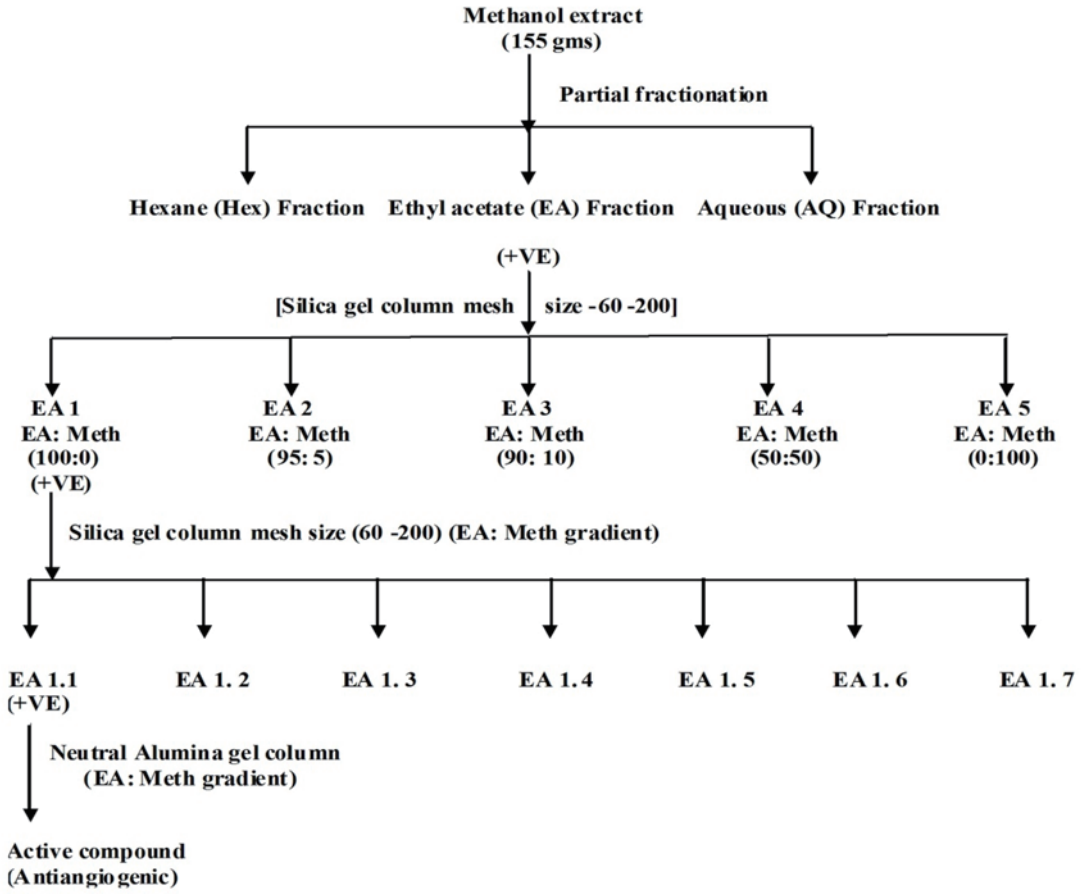

Scheme 1. General scheme followed for the extraction and purification of active substance from *A. occidentale*.

distilled prior to use.

The UV-visible absorption spectrum of the active compound is measured using a Hitachi U3400 spectrophotometer (El Cajon, CA, USA). The compound is dissolved in chloroform to a final concentration of approximately 1 mg/mL and then filtered. The filtrate is used for recording the spectrum. The spectrum is recorded for two different portions for consistency.

The FT-IR spectrum of the active compound is recorded using Bruker FT-IR Multiscan 15 Sf II (Ettlingen, Germany) instrument employing the KBr pellet technique. Approximately 0.2 mg of isolated compound is thoroughly mixed with 300 mg of KBr to prepare the sample pellet.

2.4. *Endothelial cell tube formation assay*

Tube formation of HUVECs is performed as per manufacturer's instructions (*17*). Briefly, a 96 well plate is coated with 50 µL of matrigel which is allowed to solidify at 37°C for 1 h. HUVECs (4×10^4 cells/ well) are seeded on the solidified matrigel and cultured in EGM containing various concentrations of active compound A1 (0.01 g, 0.1 µg, 0.5 µg, 1 µg and 2 µg) for 24 h. VEGF (10 ng) is added to induce tube formation to each well except for the control without VEGF. After incubation at 37°C and 5% CO_2 the enclosed networks of complete tubes from five randomly chosen fields are photographed using an inverted microscope with an attached CCD camera (Carl Zeiss, Germany).

2.5. *Transient transfection and ectopic expression of genes*

To determine the effect of VEGF and/ or A1 on proliferation, migration and invasion activities of MCF-7 cells, cells are seeded in six well plates and cultured to 60-70% confluency prior to transient transfection. On the subsequent day, cells (MCF-7) are transfected with pGL3 plasmid containing human gene construct of E-cad -624bp or Twist -824 bp or Snail -900 bp using calcium phosphate transfection kit (Promega, USA) as per the manufacturers instruction. A similar protocol is used to transfect U-87 or HEK293 cells. These cells are transfected with pLUC plasmid containing human gene construct of VEGF promoter site (-2,068 bp to +50 bp) with a luciferase reporter gene. The transfected cells are used for the following assays.

2.6. *Cell proliferation assay*

In vitro cell proliferation assay is carried out using [^{3}H] thymidine incorporation into DNA in rapidly multiplying cells as described earlier (*18*). The Twist

or Snail gene transfected cells (1×10^4 cells/well) are seeded on 12-well plates in DMEM media and grown in 5% CO_2 at 37°C for 48 h. On the third day, [^{3}H] thymidine (1 µCi /mL medium) is added and the effect of VEGF (10 ng) or A1 (50 µM) is tested on proliferation of transfected cells. After 48 h, the cells are trypsinized and washed with phosphate-buffered saline (PBS) and high molecular weight DNA is precipitated using ice-cold trichloroacetic acid (10%). Scintillation fluid (5 mL) is added to all the samples and radioactivity is measured in a liquid scintillation counter (Perkin Elmer Tri-Carb 2900 TR, Downer's groove, IL, USA).

2.7. *Transwell invasion assay*

Invasion assay is performed as described earlier (*19*). Twist or Snail gene transfected or untransfected MCF-7 (2×10^4 cells per well) cells are treated with mitomycin C (10 ng/mL) for 2 h and seeded onto the top chamber of transwell which is precoated with 0.1% gelatin. The bottom chamber of transwell is filled with basal media containing VEGF (10 ng/mL) or A1 (50 µM) or VEGF and A1, followed by overnight incubation. The non-migrated cells are swabbed using cotton bud and gelatine coated transwells are fixed with 4% ice cold paraformaldehyde and cells are stained using haematoxylin. The cells are photographed under an inverted microscope. The cells are measured using ImageJ (version1.47).

2.8. *Cell migration assay (scratch assay)*

MCF-7 cells (1×10^5) ectopically expressing either Twist or Snail gene inserts are cultured to a confluent monolayer. The assay is performed as described earlier (*20*). The cells are serum starved overnight prior to treatment with mitomycin-C (10 ng/mL) for 2 h. The monolayer is wounded using 200 µL pipette tip. Fresh basal media is added followed by treatment with or without VEGF (10 ng) or A1 (50 µM) and incubated at 37°C and 5% CO_2. The movement of cells in the scratched area are photographically monitored at 0 and 24 h after the treatment using an inverted microscope. The cells are measured using Image J (version1.47).

2.9. *Gene (VEGF/E-cadherin/Twist/Snail) promoter and luciferase reporter gene analysis*

In order to determine the effect of A1 on regulation of E-cadherin, Twist or Snail gene expression in MCF-7 cells and VEGF gene expression in U-87 and HEK293 cells; respective gene promoter-luciferase reporter assays are performed. Cells are transiently transfected as mentioned above. The transfected cells are incubated for different time intervals either with or without VEGF (10 ng) or A1 (50 µM) or VEGF and A1. Cell extracts were prepared and assayed for luciferase activity using the luciferase assay kit.

2.10. *Flt-1 gene promoter CAT enzyme reporter assay*

U-87 and HEK293 cells are transiently transfected with 2 µg of Flt-1 CAT reporter plasmid. After 24 h of transfection, the cells are serum starved overnight and treated with or without VEGF or A1 or VEGF+ A1 for 48 h. pRSV-β gal is co-transfected to serve as an internal control for transfection efficiency. After 48 h of transfection, cell extract are prepared and assayed for CAT activity using CAT assay kit (Promega, USA).

2.11. *Immunoblot analysis of JNK and ERK activity*

The activity of ERK or JNK is measured by western blotting. Briefly, U-87 cells are grown to confluency, and serum starved for 24 h. Cells are incubated with or without VEGF (10 ng/mL) or A1 (50 µM) for different time intervals (0, 2, 5, 10, 15, 30, and 60 min). Cells are washed with PBS, collected in modified cold radio immune precipitation buffer (RIPA) and homogenized on ice. Extracts are clarified at 10,000 g/30 min/4°C. The proteins were separated on SDS PAGE and transferred to a PVDF membrane. The membranes are incubated with antibodies against anti-pJNK and anti-pERK respectively.The membranes were then developed using the Luminol reagent and analyzed using phosphor image analyzer (Fujifilm, FLA5000, Tokyo, Japan).

2.12. *Electrophoretic mobility shift assay (EMSA)*

Extraction of nuclear proteins and electrophoretic mobility shift assay (EMSA) are performed. Briefly, U-87 cells are grown to 80-90% confluency in petri plates and are serum deprived for 12 h before treatment. Cells are then treated with 50 µM of A1 with different time intervals (4, 8, 16, 32, and 48 h). Nuclear extract prepared from U-87 is used to examine the effect of A1 on Sp1–DNA binding activity using specific oligonucleotide probe for Sp1 binding element in the VEGF gene.

2.13. *Statistical analyses*

Unless stated otherwise, all experiments were performed in triplicates. Wherever appropriate, the data are expressed as mean and compared using one-way analysis of variance. Statistical significance of differences between control, A1, VEGF, VEGF and A1 treated cells are determined by Duncan's multiple range test (DMRT). For all tests, $p < 0.05$ is considered statistically significant. All of the analyses are performed using the SPSS for Windows, version 13.0 (SPSS Inc.).

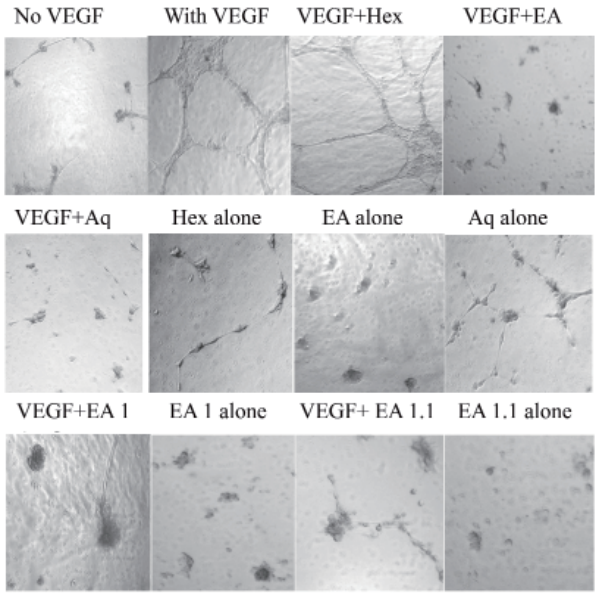

Figure 1. Effect of different fraction of *A. occidentale* extract on VEGF- induced tube formation. HUVECs (1 × 10^4 cells) cultured in EGM with 5 µg of different fractions and sub-fractions were added to the matrigel coated 96 well plate. After incubation for 8 hours at 37°C, capillary networks were photographed and quantified (Magnification: 40×). All data are presented as mean from different experiments with triplicates and means of ± SEM (n = 3).

3. Results

3.1. *Isolation and characterization of the anti-angiogenic compound from A. occidentale*

The effect of hexane, ethyl acetate and water extracted compounds on *in vitro* tube formation assay is shown in Figure 1. In, VEGF induced formation of tube like structures and the extracts per se did not have any effect on the growth of endothelial cell-tubes. However, ethyl acetate fraction (EA 1.1) showed positive antiangiogenic activity against HUVECs ability to form tube like structures; and ethyl acetate fraction is selected for further purification (Figure 1). The active fraction obtained after passing through alumina gel column, when subjected to TLC, showed a single band (Supplementary Figure 1a, *http://www.ddtjournal.com/docindex.php?year=2015&kanno=1*) which is scraped and used for further analysis.

3.2. *HPLC and GC-MS profile of the active compound*

In the HPLC analysis (Supplementary Figure 1b, *http://www.ddtjournal.com/docindex.php?year=2015&kanno=1*), the extracted compound gave three peaks which are observed at retention times of 5.45, 6.71, and 9.12 min with a ratio of the integrated peak area of 3:1:2 respectively. Anacardic acid isolated from natural cashew nut shell liquid (CNSL) using supercritical carbon dioxide ($scCO_2$) has revealed a similar HPLC profile which showed three peaks observed at retention times of 5.47, 6.69 and 9.23 min with a ratio of the integrated peak area 3:1:2 respectively (*21*).

In GC-MS analysis (Supplementary Figure 2, *http://www.ddtjournal.com/docindex.php?year=2015&kanno=1*), the extracted compound showed three major peaks with molecular ions of *m/z (mass/charge)* = 343.104, 345.411, and 347.231, matching the three peaks observed in HPLC analysis. These three HPLC peaks correspond to anacardic acid components with tri-, di- and monoene in their alkenyl side chains with abundances of 51%, 18%, and 31% respectively. In addition, a relatively weak peak with a molecular ion of *m/z* = 351.436 is observed which corresponds to the anacardic acid component with a saturated side chain. Similar LC-MS analysis results are reported for $scCO_2$ extracted anacardic acid which showed three major peaks with molecular ions of m/e = 343.284, 345.304, and 347.327 respectively (*22*).

Fraction EA 1.1, extracted from the leaves of *A. occidentale* is eluted in mobile phase ethyl acetate/methanol (9:1), detected by UV 254 nm.

HPLC purification carried out using a modular HPLC instrument Ultrasep ES 10 RP 18 6.0 µm reverse phase C18 column. Mobile phase is chloroform/ethyl acetate (80:20) at 1.80 mL/min; absorbance is monitored at 280 nm. Each analysis is carried out by dissolving 25 mg of sample in 5 mL of ethyl acetate. The flow rate of the sample is 1 mL/min and ran for 30 min.

3.3. *Spectral analysis of the active compound*

The UV-visible spectrum of the active compound showed two major peaks (λ_{max}) at 260 and 361 nm that are contributed by the 2-hydroxybenzoic acid substructure (Supplementary Figure 3a, *http://www.ddtjournal.com/docindex.php?year=2015&kanno=1*). This result is analogous with the results obtained from the UV-visible spectrum of the $scCO_2$ extracted anacardic acid which showed two peaks at 246 and 314 nm (*22*).

The FT-IR spectrum of the extracted compound (Supplementary Figure 3b, *http://www.ddtjournal.com/docindex.php?year=2015&kanno=1*) showed peaks: 3,377.1 (Ar-OH), 2925.8 and 2854.5 (aliphatic C-H), 1463.9 (aromatic CdC), 1375.2 (-COOH). (Aliphatic CdC) nearly comparable result was reported for the FT-IR spectrum of the $scCO_2$ extracted anacardic acid (*22*).

The ^{1}H NMR results [$CDCl_3$, δ (ppm)] clearly showed the substitution pattern of the aromatic ring (Supplementary Figure 4, *http://www.ddtjournal.com/docindex.php?year=2015&kanno=1*). The presence of three aromatic protons observed at δ 6.791 (d), 6.833 (d), and 7.258 (t) indicates that the extracted material contained only the trisubstituted benzene ring. The presence of the alkyl side chain (one of the substitutes) was indicated by alkenyl protons at δ 0.862 (m, 3H,

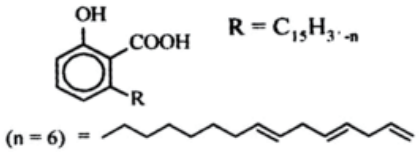

Figure 2. Chemical structure of A1.

-CH_3), δ 1.310, 1.586, 2.026, 2.776, and 2.983 (m, 28H, -CH_{2-}), δ 4.998 (m, mixed, 1H, -CHdCH-), and δ 5.354 and 5.819 (m, 4H, -CHdCH-). The phenolic and carboxyl (the other two substitutes) protons are assigned at δ 5.026 (m, mixed, 1H) and 11.026.

^{13}C NMR showed the similar pattern for ($CDCL_3$, 300MHz) 12.921 q, 14.101 q, 22.691 q, 23.916 q, 29.7 t, 35.121 t, 35.0 t, 36.135, 36.521, 37.107, 42.827, 43.181, 46.082, 70.023 t, 73.561 s, 76.0413 d, 81.321 d, 108.351 t, 132.253 d, 136.731 d, 150.081s. The ^{1}H NMR spectrum and ^{13}C NMR spectrum of the compound is shown in (Supplementary Figure 5, *http://www.ddtjournal.com/docindex.php?year=2015&kanno=1*) Similar ^{1}H and ^{13}C NMR spectra are obtained for the $scCO_2$ extracted anacardic acid (22).

All these analytical and spectral data appear to confirm the compound to be $C_{15}H_3$' 6-[8(Z), 11(Z), 14-pentadecatrienyl] salicylic acid (anacardic acid) (Figure 2). The molecular formula of the compound obtained from the elemental analysis and the molecular mass (343.248) by mass spectrometry is found to be $C_{22}H_{31}O_3$.

3.4. *A1 inhibits VEGF-induced proliferation of Twist or Snail expressing MCF-7 cells*

The effect of A1 on the proliferation of Twist or Snail transfected or untransfected MCF-7 cells is investigated. Cells are treated for 24 h with or without VEGF (10 ng) or A1 (50 µM) or VEGF plus A1 and cell proliferation rate is measured by ^{3}[H] thymidine incorporation assay. The resulting data demonstrated that VEGF increased proliferation of MCF-7 cells in which either Twist or Snail genes were overexpressed by transient transfection. Cell proliferation rate is increased by 84% and 72% in comparison with untransfected cells. Addition of A1 along with VEGF significantly decreased the proliferation rate of twist (62%) and snail (27%) compared to transfected control cells. These results suggest that A1 exhibits potent anti-proliferative activity (Figure 3).

3.5. *A1 inhibits VEGF-induced cell migration in Twist or Snail expressing cells*

The migration of cells to heal the wound made on a lawn of cells is measured at time zero and 24 hours. Effect of A1 is also studied on its ability to inhibit cell

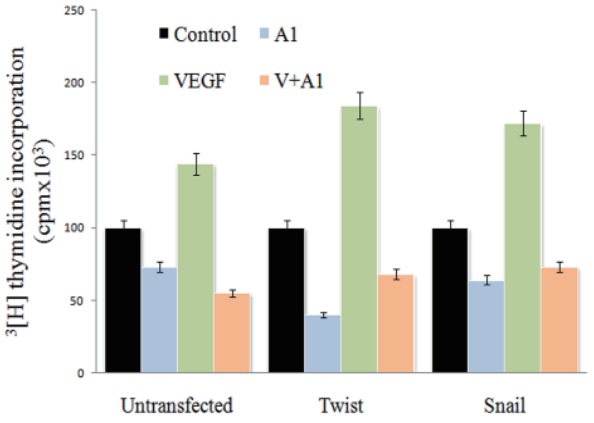

Figure 3. A1 inhibits VEGF-induced proliferation of MCF-7 cells. Effect of A1 treatment on proliferation of Untransfected and Twist or Snail transfected cells was evaluated using thymidine incorporation assay. Cell proliferation data shown is mean ± SEM of three samples. These results were similar in 3 independent experiments.

migration induced by Twist or Snail transfected cells in the mechanically wounded area. Results clearly showed that transfected cells when treated with VEGF filled the scratch area more rapidly than the cells which are treated with A1 or VEGF plus A1. Quantitative analysis of migration assay showed that VEGF treated cells ectopically expressing Twist or Snail effectively migrated faster in closing of wound when compared to that of cells treated with A1 alone or A1with VEGF. These results suggested that Twist or Snail increases the migration of MCF-7 cells and these transcription factors are down-stream in VEGF signalling pathway in migrating MCF-7 cells (Figure 4)

3.6. *A1 inhibits VEGF-induced invasion in Twist or Snail overexpressing cells*

Epithelial to mesenchymal phenotype is an essential component which confers invasion of cancer cells. To obtain more conclusive evidence on the role of VEGF and its target transcription factors Twist and Snail in EMT, verification is done to understand if forced expression of Twist or Snail enhances VEGF triggered invasion of MCF-7 cells when compared to the untransfected cells. A 46% and 38% increase is seen in VEGF induced invasion, in Twist or Snail over expressing cells respectively. As shown in Figure 5, the result indicated that in the presence of VEGF the invasion of Twist or Snail transfected cells into the gelatin coated transwell membrane is more efficient as compared to cells without the ectopic expression of Twist and Snail. Whereas in A1 treated cells, significant inhibition of invasiveness (63% and 52%) was evident.

3.7. *Regulation of Twist, Snail and E-cadherin genes by VEGF and A1*

The results in Figure 6a indicate that in MCF-7 cells,

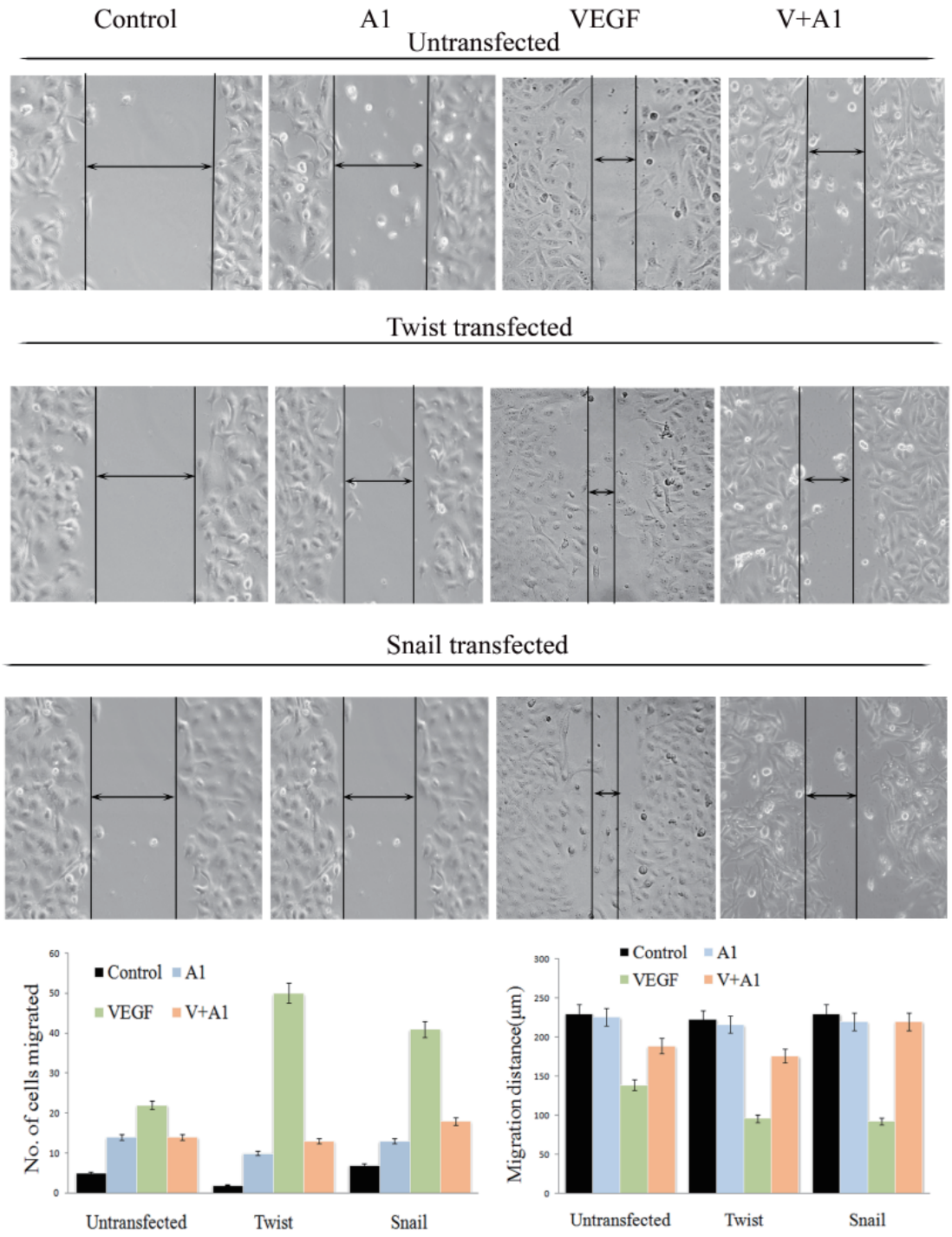

Figure 4. A1 inhibits VEGF-induced cell migration in Twist or Snail expressing cells. Effect of A1 treatment on migratory potential of Untransfected and Twist or Snail transfected cells was analyzed through wound healing assay. Representative photographs of initial and final wounds are shown at 40× magnification. The number of cells migrated and the distance of migration are shown as mean ± SEM of three samples.

VEGF increases the expression of *Twist* and *Snail* genes. When compared to the expression of *Snail* gene, the expression of *Twist* gene is increased by two folds by VEGF. However, VEGF at the concentration used decreased E-cadherin expression. The data also indicated that A1 inhibits VEGF induced expression of both *Twist* and *Snail* genes and enhances the expression of *E-cadherin* gene in control untransfected MCF-7 cells but not in either Twist or Snail-transfected cells.

3.8. *A1 increases expression of E-cadherin gene in cells overexpressing Twist or Snail genes*

In order to verify if A1 up-regulates *E-cadherin* gene expression in MCF-7 cells in which *Twist* and *Snail* genes are overexpressed, E-cadherin promoter-luciferase reporter genes are co-expressed. The data on increased reporter gene activity (Figure 6b) indicates that A1 induces the expression of E-cadherin in MCF-7 cells in

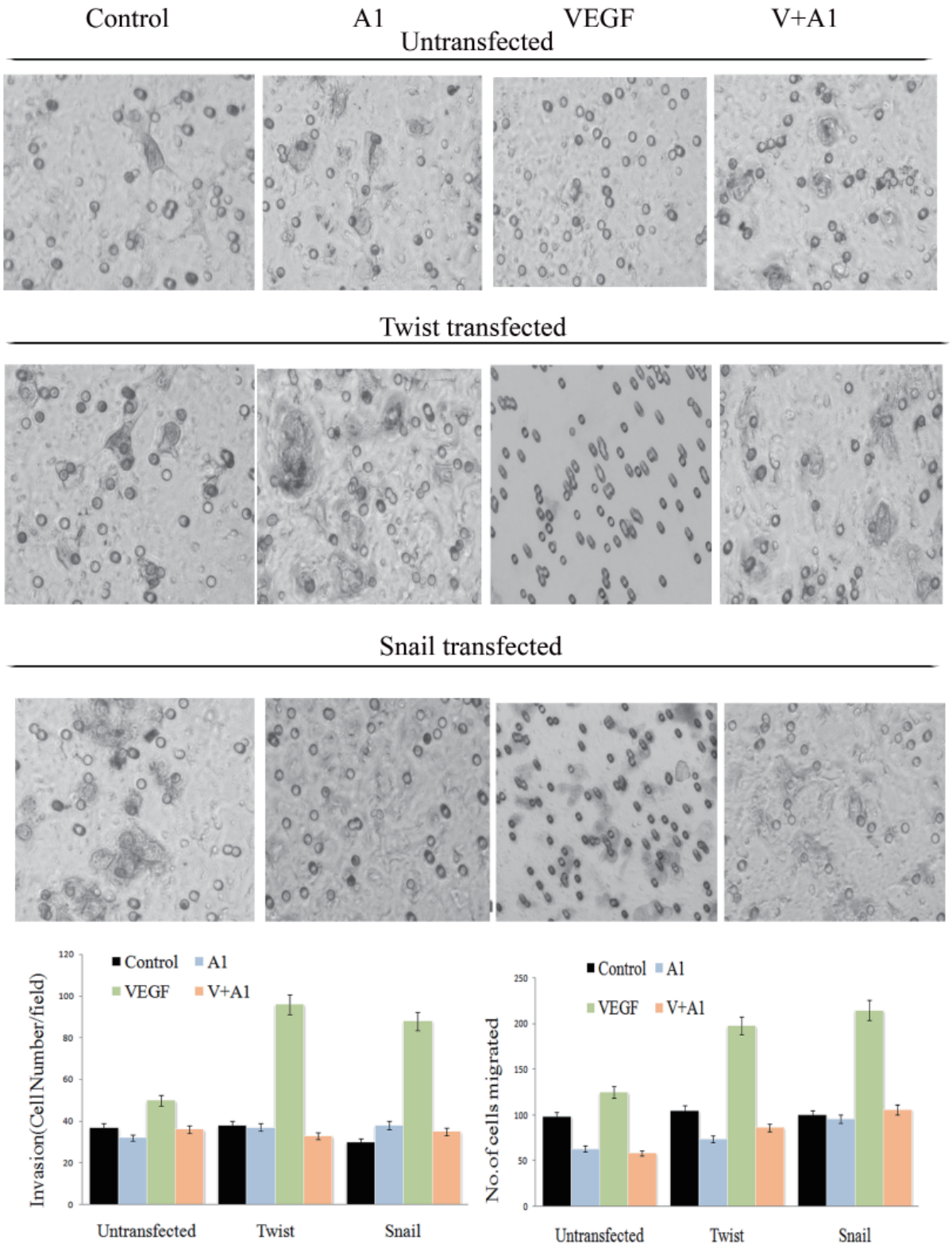

Figure 5. A1 inhibits VEGF induced invasion activity of MCF-7 cells. Effect of A1 treatment on the invasion potential of untransfected and Twist or Snail transfected cells was evaluated using transwell migration chambers. Cell invasion data shown is mean ± SEM of three samples. These results were similar in 3 independent experiments.

context to overexpression of *Twist* or *Snail* genes. When compared to the activity of luciferase reporter (100 relative light units), in control *Twist* or *Snail* transfected cells, the activity is found in A1 treated cells either in presence or absence of VEGF which was 60 to 80% higher.

3.9. *A1 down regulates VEGF gene expression*

The effect of A1 on the transcriptional regulation of the VEGF promoter in HEK293 (normal) and U-87 (highly proliferating) cells is investigated further. Cells are transiently transfected with a VEGF promoter

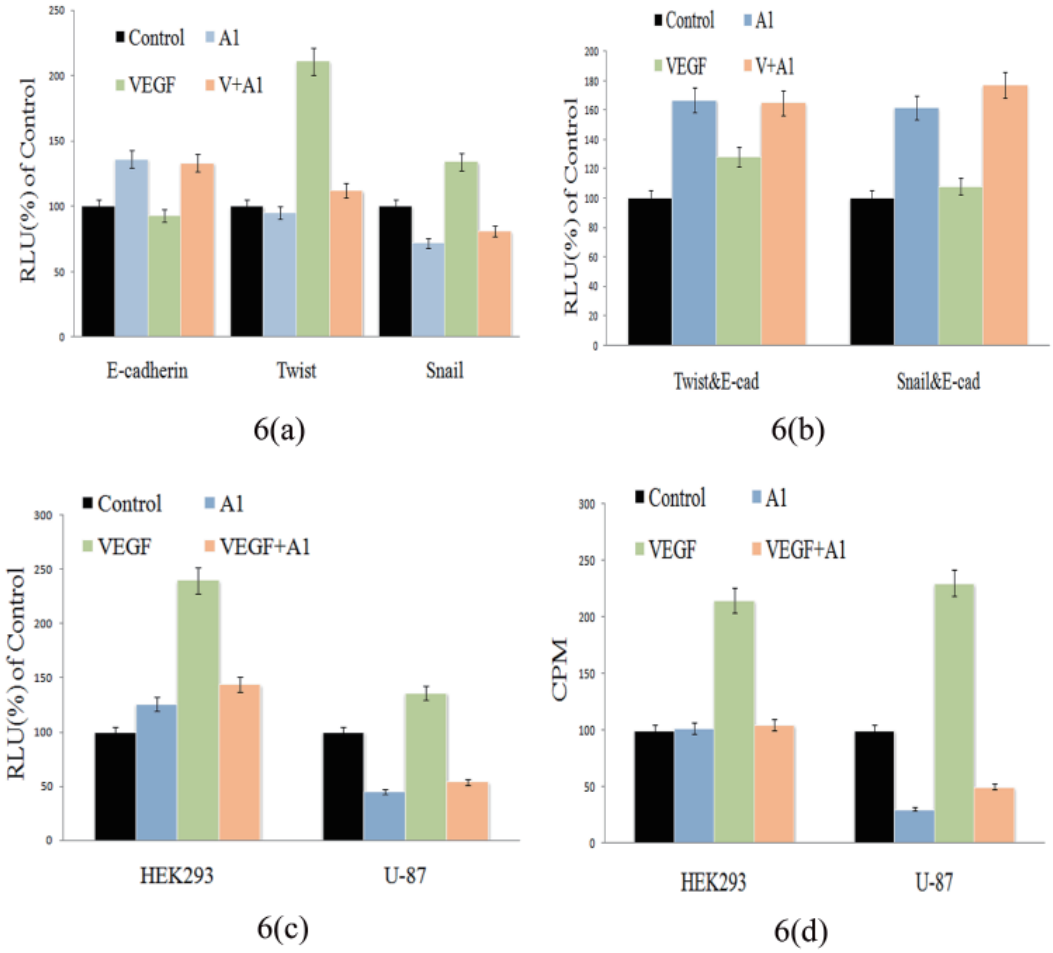

Figure 6. A1 inhibits, VEGF upregulates *Twist*, *Snail*, and *E-cadherin* genes in MCF-7 cells. Promoter reporter analysis **(a-c)**; CAT assay **(d)**. **(a)** Regulation of *Twist*, *Snail*, and *E-cadherin* genes by VEGF and A1. MCF-7 cells were transiently transfected with E-cadherin or Twist or Snail promoter luciferase reporter genes. The cells were treated with A1 alone, with and without VEGF. After 48 hours of transfection cells were lysed and assayed for luciferase activity. 1-Control cells, 2-A1 alone, 3-VEGF, 4-VEGF + A1. Values are mean of triplicate ± SEM. **(b)** A1 increases expression of *E-cadherin* gene in cells over expressing *Twist* or *Snail* genes. MCF-7 cells were transiently co transfected with *E-cadherin/Twist* or *E-cadherin/Snail* genes. The cells were treated with A1 alone, with and without VEGF. Forty-eight hours after transfection cells were lysed and assayed for luciferase activity. 1-Control cells, 2-A1 alone, 3-VEGF, 4-VEGF + A1. Values are mean of triplicate ± SEM. **(c)** A1 down regulates *VEGF* gene expression. HEK293 and U-87 cells were transiently co-transfected with 2 µg of reporter plasmid pLuc 2068 and 2 µg of the β-galactosidase expression plasmid RSV-β gal using calcium phosphate precipitation method. The cells were treated with A1 alone, with and without 10 ng of VEGF. After 48 hours transfection, cells were assayed for luciferase activity. 1-Control cells, 2-A1 alone, 3-VEGF, 4-VEGF + A1. Values are mean of triplicates ± SEM. **(d)** A1 promotes upregulation of *Flt-1* gene. HEK293 and U-87 cells were transiently co-transfected with 2 µg of plasmid Flt-1 CAT and 2 µg of the β galactosidase expression plasmid RSV β gal. The cells were treated with A1 alone and with or without 10 ng of VEGF. Forty-eight hours after transfection, cells were assayed for CAT enzyme activity. 1-Control cells, 2-A1 alone, 3-VEGF, 4-VEGF + A1. Values are mean of triplicates ± SEM.

luciferase-reporter (-2,018 to +50) plasmid pLUC -2,068bp. The results (Figure 6c) indicated that VEGF upregulated its gene nearly 5 folds in the untransformed HEK293 cells. However, highly metastatic glioblastoma (U87) cell showed less intense upregulation of *VEGF* gene by VEGF per se. The data also indicated that A1 inhibits *VEGF* gene expression both in HEK293 and U87 cell lines.

3.10. *A1 promotes upregulation of Flt-1 gene*

As VEGF regulates its own gene expression in both U-87 and HEK293 cell lines, a further investigation of the regulation of VEGF receptor *Flt-1* gene expression by transiently transfecting with Flt-1 promoter-CAT reporter constructs is performed. The results in Figure 6d indicate that when compared to the expression of VEGF receptor gene (*Flt-1*) in HEK 293 cells, the expression is significantly higher in U-87 cells. Upon verification of the effect of A1 on VEGF receptor *Flt-1* gene expression in these cell lines, the data revealed that A1 is a potent inhibitor of *Flt-1* gene.

3.11. *A1 inhibits phosphorylation of JNK and ERK MAP kinases*

To delineate the molecular mechanism by which A1 inhibits VEGF induced metastasis, the potential involvement of MAP Kinases in transducing the molecular metastatic signals by VEGF and amelioration

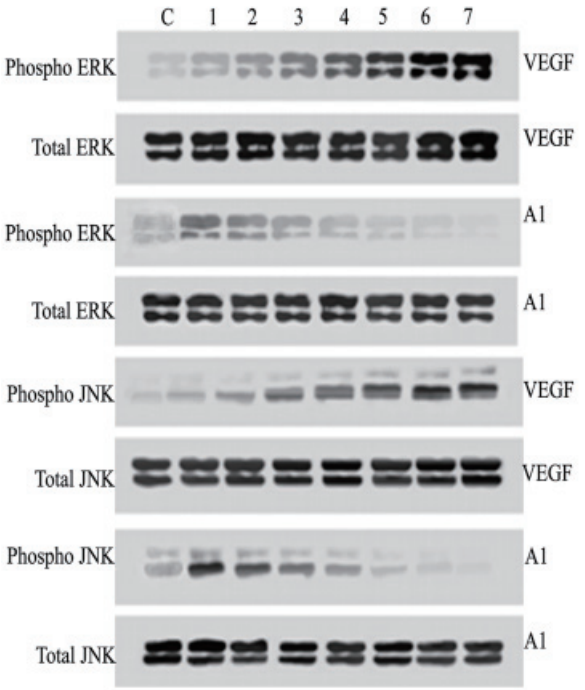

Figure 7. A1 inhibits VEGF-induced phosphorylation of ERK and JNK in glioma cells. Whole cell extracts were prepared from control and A1 treated U-87 cells. About 150 μg of protein was resolved on SDS-PAGE (12.5%). Western blot analysis was performed using antibodies against phospho JNK, total JNK, phospho ERK and total ERK. C: control cells with 0 min incubation with VEGF, 1: 2 min, 2: 5 min, 3: 10 min, 4: 15 min, 5: 30 min, 6: 60 min, and 7: 120 min incubation with VEGF.

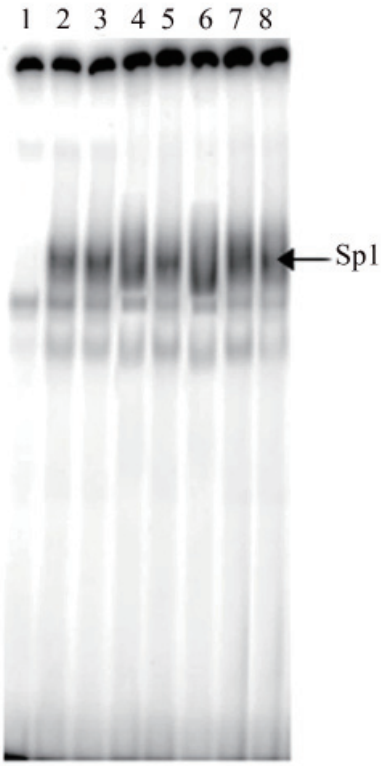

Figure 8. A1 inhibits binding of Sp1 to VEGF promoter site. Nuclear extracts were prepared from U-87 cells treated with or without A1. Sp1 DNA binding activity was assayed by EMSA using Sp1 oligonucleotides (Lane 1: Labelled probe, Lane 2: Labelled probe + control nuclear extract; Lanes 3-7: nuclear extract of 4 h, 8 h, 16 h, 32 h, and 48 h time kinetics with 10 μg of A1 + labelled oligos; Lane 8: Supershift of Sp1).

of the same by A1 is investigated by validating the enzyme activity using immunoblotting. The results in Figure 7 clearly indicate that VEGF activates both extra cellular signal regulated kinase (ERK)1/2 and phosphor-Jun NH2-terminal kinase (JNK) in a time-dependent manner. Both the kinases are inhibited by A1. However the control cells showed an initial increase in kinase activity and whenever treated with A1 showed an inhibition. Interestingly, the total levels of both the kinases are not affected by A1. These results support a critical role of MAPK pathway in activating VEGF induced metastasis.

3.12. *A1 inhibits translocation of Sp1*

In highly metastatic U-87 cells, the transcription factor Sp1 is detected in the nucleus. Since they rapidly proliferate and multiply, Sp1 translocates from cytosol to nucleus. When treated with A1, the translocation of Sp1 is inhibited and is found in the cytosolic region of the cells and this is confirmed by electrophoretic mobility shift assay (EMSA) using nuclear extracts prepared from control as well as A1 treated U-87 cells and oligonucleotides for Sp1. The results indicated that there is strong inhibition of binding of Sp1 transcription factor to its cognate promoter sequence on *VEGF* gene in A1 treated U-87 cells. In contrast, in the nuclear extract of control U-87 cells, there is strong binding of Sp1 to its promoter sequence (Figure 8).

4. Discussion

The data presented in the present study clearly establishes the role of E-cadherin in tumor invasion and metastasis. In this study two cell lines, MCF-7, which is tumorigenic but weakly metastatic and U-87 glioma cells which are highly metastatic are used. It is shown that exogenous expression of either Twist or Snail in MCF-7 cells, confer on them better ability to migrate and invade *in vitro*. Furthermore, the mechanisms that might be responsible for this effect have been elucidated.

Epithelial to mesenchymal transition is a crucial process in embryogenesis (*23*) and tumor progression, by which epithelial cells show loss of cell-cell adhesion, reduced basal cell polarity and acquired fibroblastic phenotype with increased cell motility, migration and metastasis (*24*). The process is triggered by autocrine and paracrine signals. Natural compounds with an anti-cancer potential have to be endowed with benefits such as, being non-toxic, cost-effective, physiologically bio-available and have multiple molecular targets their use in treating human cancers. Identification of mechanism-

based naturally occurring inhibitors of tumour invasion and metastasis holds promise for treatment of metastatic tumors. Studies have identified diet derived natural products such as garlic-derived chemicals (*25*), soy constituent genistein (*26,27*), green tea polyphenols (*28*) and vegetable constituent benzyl isothiocyanate as natural product derived inhibitors of EMT in cancer cells (*29*). It has been reported that herbal medicines including *A. occidentale* L. indicates a lack of clinical efficacy for supporting their use in patients (*30*). Although there are lot of importance of *A. occidentale* and its major constituents in human health, little is known about its anti-angiogenic and anti-metastatic ability and the mechanism for its pharmacological activities. We have reported that *A. occidentale* crude extract inhibits *in vivo* angiogenesis by repression of the cytokine VEGF gene expression (*4*).

Activity-guided (formation of tube like structures by HUVEC's) fractionation of the leaves of *A. occidentale* L. using different solvents resulted in ethyl acetate extract exhibiting maximum anti-angiogenic efficacy by inhibiting tube formation by HUVEC's. Isolation, purification, and characterization of the active substance from ethyl acetate extract yielded us the active compound which was further characterised using LC-MS, UV-visible spectrum, FT-IR spectrum, ^{1}H NMR spectrum and ^{13}C NMR spectrum. Anacardic acid isolated from natural CNSL using supercritical carbon dioxide ($scCO_2$) has revealed a similar HPLC profile, LC-MS analysis results, UV-visible spectrum, FT-IR spectrum, ^{1}H NMR spectrum and ^{13}C NMR spectrum (*21*). Analogous spectral results have been reported during the isolation and identification of anacardic acid derivatives from Brazilian propolis. Anacardic acid obtained by CNSL has shown comparable spectroscopic results. The combination of these spectroscopic and chromatography results, with reference to the findings reported in the literature, confirmed that the plant extract (EA1.1) obtained and structurally characterized was Anacardic acid (A1).

The data presented in the present study clearly establishes the role of E-cadherin in tumor invasion and metastasis. It is shown that exogenous expression of either Twist or Snail in MCF-7 cells, confer on them better ability to migrate and invade *in vitro*. Furthermore, examination of the mechanisms that might be responsible for this effect revealed that evidence from previous reports indicate that pancreatic cancers with the deregulated VEGFR-1 pathway possess a high likelihood for local invasion, molecular alterations and subsequent metastasis (*31*). Previous evidences suggest that ectopic expression of Twist resulted in breast cancer cells metastasis to lung in animal model (*17*). This model also fits with the reported involvement of Snail in local invasion and lymph node metastases of breast tumor (*18,32*). In this study, it is shown that Twist or Snail transfected MCF-7 cells undergo representative EMT, characterized by the acquisition of mesenchymal phenotype upon treating the transfected cells with VEGF. Current results clearly indicate that VEGF treatment of Twist or Snail transfected cells increased proliferation, migration and invasion when compared with untransfected cells. A1 significantly inhibited cell proliferation, migration and invasion. These results are consistent with the mechanistic role of Twist and Snail signaling in the processes of EMT and that the suppression of Twist and Snail signaling leads to the reversal of EMT. Collectively, the current result suggests that the suppression of VEGF induced *Twist* or *Snail* gene by A1 treatment strategies could be useful for the reversal of EMT phenotype.

Over-expression of Twist and Snail in breast cancer cells induces EMT *via* upregulation of *VEGF* gene expression thus facilitating metastasis in high grade tumor, but not in non-metastatic tumor (*33, 34*). Accordingly, the results presented have shown that VEGF significantly increases *Twist* and *Snail* gene expression and down-regulates *E-cadherin* gene expression when compared to the expression of the afore said genes in cells treated with A1. Because of A1 suppresses expression of *Twist* and *Snail* gene and increases transcription of E-cadherin, it is reasonable to conclude that transcriptional repression of VEGF induced *Twist* and *Snail* genes represent the mechanism by which A1 inhibits EMT.

The present study determines that A1 has a role in the prevention and /or treatment of metastatic tumors where epithelial to mesenchymal transition is an underlying mechanism. To the best of our knowledge this is the first study that reveals the molecular mechanism of anti EMT activity of A1. It is further shown that inhibition of VEGF secretion could be due to inhibition of Sp1 translocation to nucleus. Sp1 transcription factor regulates many genes involved in tumor promotion, angiogenesis and metastasis (*35*). Thus, it is becoming increasingly clear that compounds that block Sp1 activation could be highly useful for the treatment of cancer. This is confirmed by electrophoretic mobility shift assay (EMSA) where A1 inhibited the binding of Sp1 transcription factor to its promoter sequence on the VEGF gene in U-87 cells. In the current molecular study, A1 diminished ERK 1/2, and JNK phosphorylation in U-87 cells.

Current study systematically demonstrated and revealed the molecular mechanism of action of A1 as a novel tumor metastatic inhibitor and an EMT inhibitor. This confirms its pharmacological value with multiple targets and contributes to drug development.

Acknowledgements

The authors thank Department of Biotechnology (DBT) New Delhi, India (No.BT/IN/DBT-CREST awards/25/BPS/2012-2013), University Grant Commission-

Special Assistance Programme-Department of Special Assistance (UGC-SPA-DSA) Government of India (No. f 4-1/2013(SAP-II) 14 October 2014) and the Indian Council of Medical Research (ICMR; No.3/2/2/101/2011-NCD-III), New Delhi for financial support.

References

1. Doss VA, Thangavel KP. Antioxidant and antimicrobial activity using different extracts of *Anacardium occidentale* L. International Journal of Applied Biology and Pharmaceutical Technology. 2011; 2:436-443.
2. Mathivadhani P, Shanthi P, Sachdanandam P. Hypoxia and its downstream targets in DMBA induced mammary carcinoma: Protective role of *Semecarpus anacardium* nut extract. Chem Biol Interact. 2007; 167:31-40.
3. Chakraborty S, Roy M, Taraphdar AK, Bhattacharya RK. Cytotoxic effect of root extract of *Tiliacora racemosa* and oil of *Semecarpus anacardium* nut in human tumor cells. Phytother Res. 2004; 18:595-600.
4. Sheela M, Kaveri K, Salimath BP. Inhibition of *in vivo* angiogenesis by *Anacardium occidentale* L. involves repression of the cytokine *VEGF* gene expression. Drug Discov Ther. 2008; 2:234-244.
5. Frixen UH, Behrens J, Sachs M, Eberle G, Voss B, Warda A, Löchner D, Birchmeier W. E-cadherin-mediated cell-cell adhesion prevents invasiveness of human carcinoma cells. J Cell Biol. 1991; 113:173-185.
6. Vleminckx K, Vakaet L Jr, Mareel M, Fiers W, Van Roy F. Genetic manipulation of E-cadherin expression by epithelial tumor cells reveals an invasion suppressor role. Cell. 1991; 66:107-119.
7. Frixen UH, Nagamine Y. Stimulation of urokinase-type plasminogen activator expression by blockage of E-cadherin-dependent cell-cell adhesion. Cancer Res. 1993; 53:3618-3623.
8. Perl AK, Wilgenbus P, Dahl U, Semb H, Christofori G. A causal role for E-cadherin in the transition from adenoma to carcinoma. Nature. 1998; 392:190-193.
9. Christofori G, Semb H. The role of the cell-adhesion molecule E-cadherin as a tumour-suppressor gene. Trends Biochem Sci. 1999; 24:73-76.
10. Hay ED. An overview of epithelio-mesenchymal transformation. Acta Anat (Basel). 1995; 154:8-20.
11. Kang Y, Massague J. Epithelial-mesenchymal transitions: Twist in development and metastasis. Cell. 2004; 118:277-279.
12. Elliott BE, Hung WL, Boag AH, Tuck, Alan B. The role of hepatocyte growth factor (scatter factor) in epithelial mesenchymal transition and breast cancer. Can J Physiol Pharmacol. 2002; 80:91-102.
13. Mercurio AM, Lipscomb EA, Bachelder RE. Non-angiogenic function of VEGF in breast cancer. J Mammary Gland Boil Neoplasia. 2005; 10:283-290.
14. Thiery J, Sleeman JP. Complex networks orchestrate epithelial-mesenchymal transitions. Nat Rev Mol Cell Biol. 2006; 7:131-142.
15. Hiroharshi S. Inactivation of the E-cadherin-mediated cell adhesion system in human cancers. Am J Pathol. 1998; 153:333-339.
16. Yang J, Mani SA, Donaher JL, Ramaswamy S, Itzykson RA, Come C, Savagner P, Gitelman I, Richardson A, Weinberg RA. Twist, a master regulator of morphogenesis, plays an essential role in tumor metastasis. Cell. 2004; 117:927-939.
17. Ashton AW, Yokata RR, John G. Inhibition of endothelial cell migration intercellular communication and vascular tube formation by thromboxane A. J Biol Chem. 1999; 274:35562-35570.
18. Zeng H, Sanyal S, Mukhopadhyay D. Tyrosine residues 951 and 1059 of vascular endothelial growth factor receptor-2 (KDR) are essential for vascular permeability factor/vascular endothelial growth factor-induced endothelium migration and proliferation, respectively. J Biol Chem. 2001; 276:32714-32719.
19. Pang X, Yi T, Yi Z, Cho SG, Qu W, Pinkaew D, Fujise K, Liu M. Morelloflavone, a biflavonoid, inhibits tumor angiogenesis by targeting rho GTPases and extracellular signal-regulated kinase signaling pathways. Cancer Res. 2009; 69:518-525.
20. Liang CC, Park AY, Guan JL. *In vitro* scratch assay: A convenient and inexpensive method for analysis of cell migration *in vitro*, Nat Protoc. 2007; 2:329-333.
21. Jayaraman L, Moorthy NC, Murthy KG, Manley JL, Bustin M, Prives C. High mobility group protein-1 (HMG-1) is a unique activator of p53. Genes Dev. 1998; 12:462-472.
22. Philip JY, Da Cruz Francisco J, Dey ES, Buchweishaija J, MKayula LL, Ye L. Isolation of anacardic acid from natural nut shell liquid (CNSL) using supercritical carbon dioxide. J Agric Food Chem. 2008; 56:9350-9354.
23. Barrallo-Gimeno A, Nieto M. The Snail genes as inducers of cell movement and survival: Implications in development and cancer. Development. 2005; 132:3151-3161.
24. Thiery J. Epithelial-mesenchymal transitions in development and pathologies. Curr Opin Cell Biol. 2003; 15:740-746.
25. Chu Q, Ling MT, Feng H, Cheung HW, Tsao SW, Wang X, Wong YC. A novel anticancer effect of garlic derivatives: Inhibition of cancer cell invasion through restoration of E-cadherin expression. Carcinogenesis. 2006; 11:2180-2189.
26. Zhang LL, Li L, Wu DP, Fan JH, Li X, Wu KJ, Wang XY, He DL. A novel anti-cancer effect of genistein: Reversal of epithelial mesenchymal transition in prostate cancer cells. Acta Pharmacol Sin. 2008; 29:1060-1068.
27. Su Y, Simmen RC. Soy isoflavone genistein upregulates epithelial adhesion molecule E-cadherin expression and attenuates beta-catenin signaling in mammary epithelial cells. Carcinogenesis. 2009; 30:331-339.
28. Belguise K, Guo S, Yang S, Rogers AE, Seldin DC, Sherr DH, Sonenshein GE. Green tea polyphenols reverse cooperation between c-Rel and CK2 that induces the aryl hydrocarbon receptor, slug, and an invasive phenotype. Cancer Res. 2007; 67:11742-11750.
29. Sehrawat A, Singh SV. Benzyl isothiocyanate inhibits epithelial-mesenchymal transition in cultured and xenografted human breast cancer cells. Cancer Prev Res. 2011; 4:1107-1117.
30. Yu XQ, Ao J, Ling E. A Toll receptor from Manduca sexta is in response to Escherichia coli infection. Mol Immunol. 2008; 45:543-552.
31. Yang AD, Camp ER, Fan F, Shen L, Gray MJ, Liu W, Somcio R, Bauer TW, Wu Y, Hicklin DJ, Ellis LM. Vascular endothelial growth factor receptor-1 activation mediates epithelial to mesenchymal transition in human pancreatic carcinoma cells. Cancer Res. 2006; 66:46-51.

32. Côme C, Magnino F, Bibeau F, De Santa Barbara P, Becker KF, Theillet C, Savagner P. Snail and Slug play distinct roles during breast carcinoma progression. Clin Cancer Res. 2006; 12:5395-5402.
33. Hajra KM, Chen DY, Fearon ER. The SLUG zinc-finger protein represses E-cadherin in breast cancer. Cancer Res. 2002; 62:1613-1618.
34. Cheng CW, Wu PE, Yu JC, Huang CS, Yue CT, Wu CW, Shen CY. Mechanisms of inactivation of E-cadherin in breast carcinoma: Modification of the two-hit hypothesis of tumor suppressor gene. Oncogene. 2001; 20:3814-3823.
35. Rayet B, Gelinas C. Aberrant rel/nfkb genes and activity in human cancer. Oncogene. 1999; 18:6938-6947.

(Received November 5, 2014; Revised December 21, 2014; Re-revised February 27, 2015; Accepted February 27, 2015)

Brief Report

DOI: 10.5582/ddt.2014.01048

Construction of recombinant adenoviral vector carrying *cyclinA2* gene

Yu Han[1], Liu Hong[2], Cuiping Zhong[1], Jianhua Qiu[1,*]

[1] *Department of Otolaryngology, Xijing Hospital, Fourth Military Medical University, Xi'an, Shaanxi, China;*
[2] *Xijing Hospital of Digestive Diseases, Fourth Military Medical University, Xi'an, Shaanxi, China.*

Summary **Cell cycle related molecules in mammalian cochleae could provide a new avenue to restore hearing loss caused by a variety of genetic and environmental insults. CyclinA2 is one of the most important regulators of cell cycle, but its role in the mammalian cochlea is still unknown. So, it is necessary to construct an adenovirus vector carrying *cyclinA2* gene for clarifying its function in the cochlea. In this study, the *cyclinA2* genes were cloned into the shuttle plasmid pDC316-mCMV-EGFP to construct pDC316-CyclinA2-mCMV-EGFP, which was co-transfected with the rescue plasmid pBHGloxΔE1,3Cre into 293 cells to obtain the recombinant adenovirus Ad.CyclinA2-EGFP. Then, the plasmid pDC316-CyclinA2-mCMV-EGFP and recombinant adenovirus Ad.CyclinA2-EGFP were identified by restriction enzymes and reverse transcription-polymerase chain reaction (RT-PCR). The recombinant adenovirus vector was purified by CsCl banding, and was titrated. Finally, the recombinant adenovirus vector carrying *cyclinA2* gene was constructed and confirmed by restriction enzyme analysis and RT-PCR. The titer of the recombinant adenovirus vectors reached 2.5×10^{-11} v.p/mL. Thus, we had successfully established the Ad.CyclinA2-EGFP vector, and it could express efficiently in various cells of cochlea. This study established the foundation for the further research of *cyclinA2* gene's function in the cochlea.**

Keywords: *cyclinA2*, adenovirus construction

1. Introduction

In the last decade, a series of gene therapy within the field of auditory neuroscience had undergone tremendous development. The inner ear offers several advantages for gene therapy: firstly, it is a well-compartmentalized receptacle isolated within the otic capsule, which is easily accessible through retroauricular injection and with lower risk of inoculating adjacent tissues. Secondly, it is composed of cochlear endolymph and perilymph that permit widespread diffusion of a locally introduced vector (*1,2*). Until now, varieties of viral vectors, including adenovirus, adeno-associated virus, retrovirus, and lentivirus, had been evaluated as delivery vehicles in gene therapy (*3-7*). Compared to the other viral vectors, adenovirus vectors hold a major advantage in that they were not dependent on cell replication and had their ability to transfect quiescent cells of the cochlea with high efficiency. Therefore, adenovirus had become among the most frequently used viral vectors in the inner ear, and it was very useful to construct adenovirus vectors for clarify functions of genes in the field of inner ear.

So far, several cell cycles related molecules had been determined to participate in the regulation of mammalian cochlea function, such as $p27^{Kip1}$ and Rb (*8-10*). These studies lead to the hypothesis that gentamicin-induced hair cells loss may be reversed by restarting cell cycle (*11*). CyclinA2 is one of the most important regulators of cell cycle, and it regulates two critical progression transitions: the G1/S transition into DNA synthesis and the G2/M entry into mitosis (*12*). Experimental data showed that cyclinA2 might promote the regeneration of cardiac muscle cells, which are considered as terminal cells, by cell cycle regulation (*13,14*). But it is not sure whether it provides insights into the regeneration of hair cells in

**Address correspondence to:*
Dr. Jianhua Qiu, Department of Otolaryngology, Xijing Hospital, Fourth Military Medical University, Xi'an, 710032, Shaanxi Province, China.
E-mail: jianhuaqi@126.com

mammalian. Therefore, it is very necessary to construct an adenovirus vector harboring *cyclinA2* gene for clarifying its function in the cochlea.

In the current study, the adenovirus vector carrying *cyclinA2* gene was constructed base on the AdMax vector systems. It would establish the foundation for further research of *cyclinA2* gene in the cochlea.

2. Materials and Methods

2.1. *Cells, enzymes, bacteria, plasmids and vectors*

Low-passage human embryonic kidney AD-293 cells and AdMax vector systems were obtained from Microbix Biosystems Corporation (Ontario, Canada). All cells were grown in Dulbecco's modified Eagle's medium (DMEM) containing 10% fetal calf serum at 37°C in saturated humidified air with 5% CO_2. The cells were sub-cultured once every three days. Restriction enzymes were purchased from New England Biolabs (MA, USA) and used according to the manufacturer's instructions. *E. coli* DH-5α was purchased from GIBCO (CA, USA). Human *cyclinA2* cDNA clonewas purchased from OriGene Technologies (MD, USA).

2.2. *Reverse Transcription-PCR Analysis*

PCR was employed to amplify human *cyclinA2* gene from cDNA clone. According to the sequence of GeneBank, specific *cyclinA2* gene primers were designed and synthesized as following: F: 5'-ATTGC GGCCGCATGCCGGGCACCTCGAGGCATT-3', R: 5'-GCCGATATC TCACACACTTAGTGTCTCTG-3'. NotI and EcoRV sites were introduced into the sense and antisense primers respectively. PCR was performed in a total volume of 20 μL consisting of 0.4 μL each primer, 1.6 μL each dNTP, 2 μL 10× polymerase reaction buffer, 0.3 μL Pyrbest DNA polymerase and 1 μL DNA template. The PCR proceeded for 25 cycles of 94°C for denaturing, 55°C for annealing, and 72°C for extension. The PCR products were electrophoretically separated on a 1% agarose gel and were visualized by ultraviolet light. PCR products were purified from the agarose gel using DNA purification kit.

2.3. *Construction and identification of homologous recombinant adenoviral plasmid*

The shuttle vector pDC316-mCMV-EGFP and antisense fragment of the *cyclinA2* gene were restriction digested with NotI and EcoRV respectively. The digested products were purified and ligated with T4 DNA ligase, and then co-transformed into *E.coli* DH-5α cells. Thus, the fragment of the *cyclinA2* gene was cloned into the shuttle plasmid pDC316-mCMV-EGFP, and the homologous recombinant adenoviral plasmid was generated. The pDC316-CyclinA2-mCMV-EGFP was restriction digested with NotI and EcoRV to validate the successful construction.

2.4. *Generation and identification of the recombinant adenovirus Ad.cyclinA2-EGFP*

The monolayer of 293 cells was co-transfected with pDC316-CyclinA2-mCMV-EGFP and adenovirus DNA plasmid pBHGloxΔE1,3Cre using Lipofectamine 2000 (Invitrogen, NY, America) and incubated for 7 days at 37°C as described in the manual. The 293 cells were scraped off flasks with a rubber policeman, and lysed for three consecutive freezing/thawing cycles. The crude recombinant virusAd.CyclinA2-EGFP was collected from the supernatant by centrifugation. Virus was amplified once in 293 cells and subjected to one round of plaque purification. Viral suspensions in 3% sucrose were stored at −80°C until thawed for subsequent experiments. After three cycles of freezing/thawing, 5 μL of viral lysate were used for detection of the cyclinA2 gene in adenoviral particles with RT-PCR and its titer was determined.

3. Results and Discussion

We assumed that manipulating cell cycle related molecules in mammalian cochleae could provide a new avenue to restore hearing loss caused by a variety of genetic mutations and environmental insults (*11*). Thus, it is very important to construct adenoviral vector carrying *cyclinA2* gene for a better understanding of the roles of this critical factor in the cochlea, which would provide insights into protection and therapy of hearing impairment.

In the present study, we had successfully established the Ad.CyclinA2-EGFP vector base on the AdMax vector systems. First, we performed PCR amplification, and the PCR product of the plasmid was a strip of about 1289bp in 1% agarose gel electrophoresis (Figure 1). The expression of the *cyclinA2* gene was verified by gene sequence examination. Then, the shuttle vector

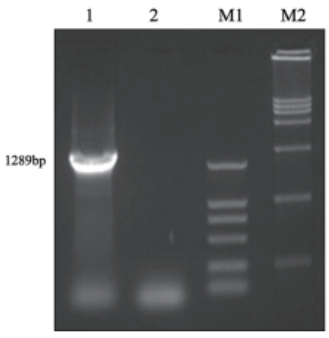

Figure 1. PCR identification of cyclinA2 gene. Lane 1: PCR products of *cyclinA2* gene. Lane 2: negative control. M1: DL200 Maker (2,000, 1,000, 750, 500, 250, 100 bp). M2: DL15000 Maker (15,000, 10,000, 7,500, 5,000, 2,500, 1,000 bp).

pDC316-CyclinA2-mCMV-EGFP was generated. As shown in Figure 2, the *cyclinA2* gene was released from the recombinant shuttle vector pDC316-CyclinA2-mCMV-EGFP by digesting with NotI and EcoRV. The 5.8 kb and 1.2 kb strips were detected by 1% agarose gel electrophoresis, representing the shuttle vector pDC316-mCMV-EGFP and reversal fragment of the cyclinA2 gene, respectively. Next, recombinants Ad.CyclinA2 -EGFP was generated in AD-293 cells. After recombinant adenoviral particles were transfected into AD-293 cells with Lipofectamine 2000 for seven days, the green fluorescence was monitored under fluorescence microscopy. As shown in Figure 3, compare with normal 293 cells, the appearance changes of 293 cells transfected with adenoviral particles were included losing their normal spindle, edema, grape-like, declining cell adhesion properties and plaque formation. And the recombinant adenovirus was prepared and purified by CsCl density gradient ultracentrifugation, and its titer was 2.5×10^{-11} v.p/mL.

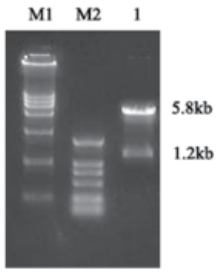

Figure 2. Digestion of pDC316-CyclinA2-CMV-EGFP with NotI and EcoRV. M1: DL15,000 (15,000, 10,000, 7,500, 5,000, 2,500, 1,000 bp). M2: DL2000 (2,000, 1,000, 750, 500, 250, 100 bp). Lane 1: pDC316- CyclinA2-CMV-EGFP.

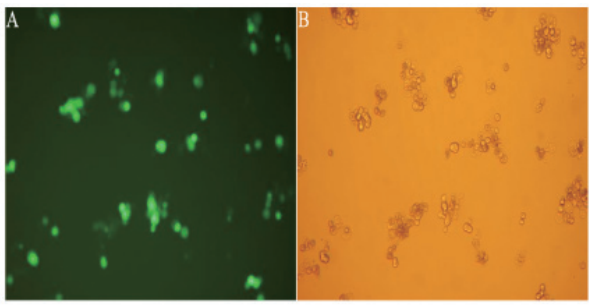

Figure 3. Cytopathic changes of the AD-293 cells transfected with adenoviral particles.

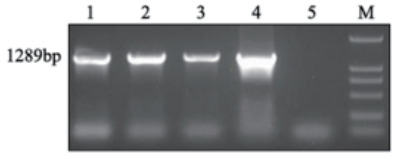

Figure 4. RT-PCR identification of the recombinant adenovirus. Lane 1: Ad.CyclinA2-EGFP stock solution. Lane 2: Ad.CyclinA2-EGFP stock solution diluted 10 times. Lane 3: Ad.CyclinA2-EGFP stock solution diluted 100 times. Lane 4: Positive control (pDC316-CyclinA2-mCMV-EGFP). Lane 5: Negative control. M: DL2000 Marker (2,000, 1,000, 750, 500, 250, 100 bp).

Finally, this vector was confirmed by restriction enzyme analysis and RT-PCR. Virus supernatant was collected by centrifugation of AD-293 cells after consecutive freezing/thawing cycles, and then was identified by RT-PCR amplification. As shown in Figure 4, a fragment of 1289 bp was obtained, indicating the correct generation of recombinant adenovirus.

With regard to gene therapy in the inner ear, adenovirus vector is one of the best viral vectors, which has ability to infect both dividing and non-dividing cells. In AdMax packaging system, the homologous recombination process was taken place in 293 cells, but not in bacteria. This system had lots of advantages, including easy operation, higher efficiency, and so on. Compared to AdEasy system, it only took 2 to 4 weeks to complete the recombination process with the greater than 98% success rate (*15*).

In conclusion, adenovirus vector harboring *cyclinA2* gene would be used to clarify its roles in the cochlea, including studies about hair cells regeneration. Our study established the foundation for the further research of *cyclinA2* gene's function in the cochlea.

Acknowledgements

This study was supported in part by grants from the National Natural Scientific Foundation of China (81100714).

References

1. Husseman J, Raphael Y. Gene therapy in the inner ear using adenovirus vectors. Adv Otorhinolaryngol. 2009; 66:37-51.
2. Ballana E, Wang J, Venail F, Estivill X, Puel JL, Arbonès ML, Bosch A. Efficient and specific transduction of cochlear supporting cells by adeno-associated virus serotype 5. Neurosci Lett. 2008; 442:134-139.
3. Staecker H, Li D, O'Malley BW Jr, Van De Water TR. Gene expression in the mammalian cochlea: A study of multiple vector systems. Acta Otolaryngol. 2001; 121:157-163.
4. Wenzel GI, Xia A, Funk E, Evans MB, Palmer DJ, Ng P, Pereira FA, Oghalai JS. Helper-dependent adenovirus-mediated gene transfer into the adult mouse cochlea. Otol Neurotol. 2007; 28:1100-1108.
5. Cooper LB, Chan DK, Roediger FC, Shaffer BR, Fraser JF, Musatov S, SelesnickSH, Kaplitt MG. AAV-mediated delivery of the caspase inhibitor XIAP protects against cisplatin ototoxicity. Otol Neurotol. 2006; 27:484-490.
6. Kiernan AE, Fekete DM. *In vivo* gene transfer into the embryonic inner ear using retroviral vectors. Audiol Neurootol. 1997; 2:12-24.
7. Pietola L, Aarnisalo AA, Joensuu J, Pellinen R, Wahlfors J, Jero J. HOX-GFP and WOX-GFP lentivirus vectors for inner ear gene transfer. Acta Otolaryngol. 2008; 128:613-620.
8. Liu Z, Zuo J. Cell cycle regulation in hair cell development and regeneration in the mouse cochlea. Cell Cycle. 2008; 7:2129-2133.

9. Löwenheim H, Furness DN, Kil J, Zinn C, Gültig K, Fero ML, Frost D, Gummer AW,Roberts JM, Rubel EW, Hackney CM, Zenner HP. Gene disruption of $p27^{Kip1}$ allows cell proliferation in the postnatal and adult organ of corti. Proc Natl Acad Sci U S A.1999; 96:4084-4088.
10. Sage C, Huang M, Karimi K, Gutierrez G, Vollrath MA, Zhang DS, García-AñoverosJ, Hinds PW, Corwin JT, Corey DP, Chen ZY. Proliferation of functional hair cells *in vivo* in the absence of the retinoblastoma protein. Science. 2005; 307:1114-1118.
11. Han Y, Qiu J, Qiao L, Zhong C. Gentamicin-induced deafness may be reversed by restarting cell cycle. Med Hypotheses. 2009; 72:368-369.
12. Pagano M, Pepperkok R, Verde F, Ansorge W, Draetta G. Cyclin A is required at two points in the human cell cycle. EMBO J. 1992; 11:961-971.
13. Gandia C, Armiñan A, García-Verdugo JM, Lledó E, Ruiz A, Miñana MD, Sanchez-Torrijos J, Payá R, Mirabet V, Carbonell-Uberos F, Llop M, Montero JA, Sepúlveda P. Human dental pulp stem cells improve left ventricular function, induce angiogenesis, and reduce infarct size in rats with acute myocardial infarction. Stem Cells. 2008; 26:638-645.
14. Woo YJ, Panlilio CM, Cheng RK, Liao GP, Suarez EE, Atluri P, Chaudhry HW. Myocardial regeneration therapy for ischemic cardiomyopathy with cyclin A2. J Thorac Cardiovasc Surg. 2007; 133:927-933.
15. Qi H. Construction of a recombinant adenovirus expression vector for human renal tumor- associated antigen G250 gene with AdMax system. Nan Fang Yi Ke Da Xue Xue Bao. 2008; 28:1617-1620, 1625.

(Received October 12, 2014; Revised February 5, 2015; Accepted February 6, 2015)

Brief Report

DOI: 10.5582/ddt.2015.01002

Circadian rhythm of serum 25 (OH) vitamin D, calcium and phosphorus levels in the treatment and management of type-2 diabetic patients

Tariq Masood[1], Rajeev S Kushwaha[1], Ranjana Singh[2], Shivani Sailwal[1], Himanshu Pandey[1], Amit Varma[3], Raj K Singh[1,*], Germaine Cornelissen[4]

[1] *Biochemistry Department, Shri Guru Ram Rai Institute of Medical & Health Sciences, Patel Nagar, Dehradun, India;*
[2] *Biochemistry Department, King George's Medical University, Lucknow, India;*
[3] *Medicine Department, Shri Guru Ram Rai Institute of Medical & Health Sciences, Patel Nagar, Dehradun, India;*
[4] *Halberg Chronobiology Center, University of Minnesota, MN, USA.*

Summary **The circadian time structure of serum 25 (OH) vitamin D (25-OHD), calcium (Ca) and phosphorus (P) may prove to be helpful in prevention, efficacy and management of diabetes mellitus. Ten newly diagnosed patients with type-2 diabetes mellitus (6 men and 4 women), 30-65 years of age, and 10 age-matched clinically healthy volunteers (7 men and 3 women) were synchronized for one week with diurnal activity from about 06:00 to about 22:00 and nocturnal rest. Breakfast was served around 08:00, lunch around 13:30 and dinner around 20:00. Drugs/nutraceuticals known to affect the vitamin D-calcium metabolism and status were not taken. Blood samples were collected at 6-h intervals for 24 h under standardized, 24-h synchronized conditions. Serum 25-OHD, Ca, P, Ca-P product and Ca-P ratio were determined. A marked circadian variation was demonstrated for 25-OHD in healthy volunteers (p = 0.030) and of borderline statistical significance in the diabetic patients (p = 0.083) by population-mean cosinor analysis. Similarly, healthy volunteers showed borderline significance for serum Ca, P and Ca-P ratio. The circadian acrophase of Ca occurred later in the patients as compared to healthy controls. Mapping the circadian rhythm (an important component of the broader time structure or chronome, which includes *a.o.*, trends with age and extra-circadian components) of vitamin D and calcium is needed for exploring their role as markers in the treatment and management of diabetic patients.**

Keywords: Circadian rhythm, diabetes mellitus, serum vitamin D, calcium, phosphorus, chronoprevention, marker rhythm

1. Introduction

Diabetes rates are increasing around the world, mainly driven by increasing levels of obesity (*1*). Over the past three decades, the number of people with diabetes mellitus (DM) has more than doubled globally, making it one of the most important public health challenges to all nations. Type-2 diabetes mellitus (T2DM) and prediabetes are increasingly observed among children, adolescents and younger adults. The causes of the epidemic of T2DM are embedded in a very complex group of genetic and epigenetic systems interacting within an equally complex societal framework that determines behavior and environmental influences. Prevention of T2DM is a 'whole-of-life' task and requires an integrated approach operating from the origin of the disease. It affects more than 300 million individuals in the world with significant morbidity and mortality worldwide (*2*). In parallel to the increase in the prevalence of DM, there has been a resurgence of vitamin D (vit D) deficiency worldwide (*3,4*). Though the most well-known role of vit D is the regulation of

**Address correspondence to:*
Dr. R K Singh, Biochemistry Department, Shri Guru Ram Rai Institute of Medical & Health Sciences, Patel Nagar, Dehradun, India.
E-mail: singhrk23a@hotmail.com

calcium (Ca) absorption and bone metabolism, it is becoming clear that this hormone has pleiotropic effects with possible role in human health including cancer, autoimmune, infectious, respiratory, and cardiovascular disease (*5-9*).

Hypovitaminosis D has recently emerged as one of the factors contributing to the development of both type-1 and type-2 DM (*10-13*). Serum 25 (OH) vitamin D (25-OHD) concentrations were reported to be lower in patients with type-2 DM as compared to non-diabetic controls (*14*). Since then, many cross-sectional and case-control studies have shown an association between 25-OHD concentrations and type-2 DM (*10-13*). Vit D is a steroid hormone that has a crucial role in the modulation of bone homeostasis. It has been described as a wonder vitamin because of its possible benefits related to diverse health outcomes including bone disease, coronary heart disease, and type-2 diabetes (*15,16*). 25-OHD is a circulating metabolite used as a clinical indicator of vit D status. Results from prospective epidemiological studies have shown that low circulating 25-OHD concentrations are associated with an increased risk of developing type-2 diabetes (*15,17*). Whether or not this association is causal is unknown, however (*16*), as it may be the result of residual confounding, which is plausible in observational studies of incident type-2 diabetes. Measurements of confounders (*e.g.*, physical activity) are susceptible to errors and are not adequately controlled for in epidemiological studies (*17*). Although results from clinical trials (*19,20*) have shown no effect of vit D supplementation on the incidence of type-2 diabetes, these findings require cautious interpretation because of issues with doses, combination treatment with calcium, compliance, and suitable conditions for generalization (*15*).

There is no mention in the available literature to our knowledge regarding the circadian variation (A daily cycle of biological activity based on a 24-h period and influenced by regular variations in the environment, such as the alternation of night and day) of serum 25-OHD concentrations in diabetic patients. The present study was planned to provide reference values for circadian changes of serum vit D, Ca and Phosphorus (P) in clinical health and to assess any deviation from such norms in diabetic patients in an attempt to understand the role of Ca and vit D in the management and treatment of type-2 DM.

2. Materials and Methods

2.1. *Study design*

This study was carried out in the Department of Biochemistry, Shri Guru Ram Rai Institute of Medical & Health Sciences, Patel Nagar, Dehradun in collaboration with the Department of Medicine, Shri Guru Ram Rai Institute of Medical & Health Sciences and Shri Mahant Indiresh Hospital, Patel Nagar, Dehradun, India. Two groups of subjects were investigated: a study group of 10 newly diagnosed patients (6 men; 4 women), 30 to 60 years of age, and a control group of 10 age matched clinically healthy volunteers (7 men and 3 women). This study was approved by Institutional Ethics Committee. The patients were thoroughly examined to ensure the absence of any other disease known to alter the status and rhythm of the variables examined herein. Prior to the collection of blood samples, participants refrained from taking any drug preparation that would affect or alter the Ca-vit D metabolism. All participants were kept (synchronized) for 1 week to a schedule of diurnal activity from about 06:00 to about 22:00 and nocturnal rest. All subjects took their usual (although not identical) meals three times daily: breakfast around 08:30, lunch around 13:30 and dinner around 20:30, without any change in their fluid intake. At 06:00, 12:00, 18:00 and 00:00, 6 mL of blood was collected from each subject in plain and sterile vials. The serum was separated and analyzed for Ca, P and 25-OHD, using VTROS 5.1 FS (Fusion) chemistry autoanalyzer and VITROS EciQ immunoassay analyzer and commercial kits supplied from Ortho Clinical Diagnostics, India - a division of Johnson & Johnson, USA.

2.2. *Statistical analysis*

Data were evaluated by conventional statistical analyses and by single and population-mean-cosinor procedures (*21-23*). Accordingly, the MESOR (Midline Estimating Statistic of Rhythm, a rhythm-adjusted mean), the circadian double amplitude (a measure of the extent of predictable change within a day) and the circadian acrophase (a measure of the timing of overall high values recurring each day) were determined. Furthermore, parameter tests were performed to compare each variable between healthy subjects and DM patients.

3. Results and Discussion

A circadian rhythm was demonstrated for serum vit D in healthy volunteers ($p = 0.030$) by population-mean cosinor analysis. Similarly, a circadian rhythm of borderline statistical significance was also demonstrated for vit D in patients ($p = 0.083$), and in healthy subjects for Ca ($p = 0.070$), P ($p = 0.102$), and the Ca-P ratio ($p = 0.091$) (Table 1). Serum 25-OHD concentration was maximum at 12:00 and minimum at 06:00 in diabetic patients as well as in healthy volunteers. Serum 25-OHD concentrations were numerically lower at all sampling times in patients in comparison to healthy subjects. Whereas the MESOR was not statistically

significantly different between the patients and the healthy controls, the circadian double amplitude was smaller in the patients (1.38 *vs*. 2.72). The circadian acrophase of serum calcium occurred later in the patients (19:12 *vs*. 11:15). The double circadian amplitude of serum phosphorus was smaller in the patients and the circadian acrophase occurred almost 14 h later in the diabetic patients in comparison to healthy counterparts. The circadian double amplitude of the Ca-P product was numerically larger in diabetic patients and the circadian acrophase occurred later (at 19:12 *vs*. 06:39) as compared to healthy controls. The MESOR of the Ca-P ratio was numerically higher in the patients, while the circadian double amplitude was numerically smaller. The circadian acrophase of Ca-P ratio occurred statistically significantly later in the diabetic patients.

Parameter tests were performed to compare each variable between healthy subjects and DM patients. The tests were carried out in 3 ways: first, by using the actual M, A, O estimates; second, by expressing the amplitude as a percentage of the MESOR; and third, by equating amplitudes to 1, thus restricting the test to be an acrophase test (Table 2). Using the original rhythm parameters, a difference in the (A, φ) pair is found for Ca (p = 0.029), the patients having a later phase and a smaller amplitude. A similar difference in (A, φ) pair is also of borderline statistical significance for P (p = 0.084). Similar results are obtained after expressing the amplitude as a percentage of the MESOR, with a (A, φ) pair difference found for Ca (p = 0.026) and for P (p = 0.083). In this case, a difference in (A, φ) pair is also of borderline statistical significance for the C-P product (p = 0.072). Phase tests do not show any statistically significant difference between the two groups, except for the Ca/P ratio (p = 0.041).

A marked circadian variation in serum vit D concentration in healthy volunteers (p = 0.030) with a borderline statistical significance in patients (p = 0.083) was found. The MESOR and the circadian double amplitude were lower in the patients who had a similar circadian acrophase as the healthy subjects. A lower MESOR and smaller circadian amplitude in diabetic patients has not been previously reported to our knowledge. However, hypovitaminosis D has been reported in both type-1 and type-2 diabetic patients (*10-13,14*). A borderline statistically significant circadian rhythm was also noticed for serum Ca, P and the Ca-P ratio in healthy volunteers. Altered vit D and calcium homeostasis may play a role in the development of type-2 diabetes. Vit D and calcium intakes were inversely associated with development of type-2 diabetes, and the benefits of the two nutrients appear to be additive. For both vit D and calcium, intakes from supplements rather than from diet were significantly associated with a lower risk of type-2 diabetes (*24*). The

Table 1. Circadian variation of plasma calcium (mg/dL), phosphorus (mg/dL) and vitamin D (ng/mL) in patients with type-2 diabetes mellitus and age-matched healthy controls

Variable	PR	p	Clinical health			PR	p	Diabetes mellitus		
			M ± CI	2A	Ø			M ± CI	2A	Ø
Ca	66	0.07	8.38 ± 0.93	0.96	-169°	68	0.29	8.42 ± 0.53	0.92	-288°
P	73	0.10	4.79 ± 0.51	0.64	-77°	65	0.50	4.42 ± 1.17	0.50	-289°
Vit D	72	0.03	11.49 ± 1.59	2.72	-200°	76	0.08	10.44 ± 2.47	1.38	-199°
CaxP	74	0.16	40.60 ± 7.26	6.14	-100°	66	0.41	38.30 ± 12.75	10.64	-288°
Ca: P	65	0.09	1.82 ± 0.21	0.44	-203°	84	0.74	2.05 ± 0.32	0.90	-332°

Ca: Calcium; P: Phosphorus; Vit D: Vitamin D; CaxP: Ca-P product; Ca/P: Ca-P ratio; PR: percent rhythm, average proportion of variance accounted for by fit of 24-h cosine curve to individual data series; p: p-value from zero amplitude (no-rhythm) test; M: MESOR, a rhythm adjusted mean value; 2A: double circadian amplitude, measure of extent of predictable change within a day; Ø: acrophase, measure of the timing of overall high recurring each day, expressed in (negative) degrees with 360° = 24 h and 0° = 00:00; CI: 95% Confidence Interval.

Table 2. Comparison of rhythm parameters between healthy volunteers and DM patients

Population No	k	M	A	Ø	p	Test of equality parameters			
						Parameters(S)	DF	F	p
1. Ca:H	10	8.38	0.48	-169°	0.070	A, Ø	2,34	3.95	0.028
Ca:DM	10	8.42	0.46	-288°	0.297				
2. Vit D:H	10	11.49	1.36	-200°	0.030	A, Ø	2,34	0.70	0.49
VitD:DM	10	10.44	0.69	-199°	0.083				
3. P:H	10	4.79	0.32	-77°	0.10	A, Ø	2,34	2.67	0.08
P:DM	10	4.42	0.25	-289°	0.50				
4. CaxP:H	10	40.60	3.07	-100°	0.16	A, Ø	2,34	2.10	0.13
CaxP:DM	10	38.30	5.32	-288°	0.40				
5. Ca%P:H	10	1.82	0.22	-203°	0.091	A, Ø	2,34	2.01	0.14
Ca%P:DM	10	2.05	0.04	-332°	0.74				

K = number of subjects; DF: Degree of freedom; period: 24 h; p: p-value from the zero-amplitude test (left) and p-value from the test of equality of (A, Ø) pairs between the two groups (right).

mechanisms by which vit D may affect the risk of type-2 diabetes are not clear. Both insulin resistance and impaired pancreatic β-cell function have been reported with vit D insufficiency (*11,25-28*). These observations together with the finding of vit D receptors in β-cells (*29*) and the finding of impaired insulin secretory capacity in mice lacking a functional vit D receptor (*30*) indicate an important role for vit D in regulating β-cell function. Short term intervention studies with vit D supplementation in patients with type-2 diabetes have shown conflicting results (*25,31*). The mechanisms by which calcium intake may alter diabetes risk are speculative. Abnormal regulation of intracellular calcium affecting both insulin sensitivity and insulin release has been suggested as a potential mechanism to account for the putative association between calcium insufficiency and risk of diabetes (*32*). The active form of vit D, 1α, 25-(OH)2D3, has been associated with metabolism control, cell growth, differentiation, antiproliferation, apoptosis, and adaptive/innate immune responses, besides its functions in the integrity of bone and calcium homeostasis. Therefore, insufficient calcium absorption may be the culprit mechanism for the observed associations in our study, either due to vit D insufficiency (from low intake) or low calcium intake. This hypothesis is further supported by data indicating that calcium is essential in normalizing glucose intolerance due to vit D deficiency *in vivo* (*33*). An important role of 1α, 25-(OH) 2D3 has recently been reported in the regulation of molecular clock (*34*). The delayed circadian acrophase of serum Ca and P and the lower MESOR and reduced circadian amplitude of vit D in type-2 diabetic patients, as observed in the present study, may play a role in the development of the disease and become a responsible risk factor deserving further investigation.

References

1. Garland CF, Garland FC, Gorham ED, Lipkin M, Newmark H, Mohr SB, Holick MF. The role of vitamin D in cancer prevention. Am J Public Health. 2006; 96:252-261.
2. Sherwin R, Jastreboff AM. Year in diabetes 2012: The diabetes tsunami. J Clin Endocrinol Metab. 2012; 97:4293-4301.
3. Lips P. Vitamin D status and nutrition in Europe and Asia. J Steroid Biochem Molecular Biol. 2007; 103:620-625.
4. Gannage-Yared MH, Chemali R, Yaacoub N, Halaby G. Hypovitaminosis D in a sunny country: Relation to lifestyle and bone markers. J Bone and Mineral Res. 2000; 15:1856-1862.
5. Mohr SB. A brief history of vitamin D and cancer prevention. Annals of Epidemiol. 2009; 19:79-83.
6. Janssens W, Lehouck A, Carremans C, Bouillon R, Mathien C, Decramer M. Vitamin D beyond bones in chronic obstructive pulmonary disease; time to act. Am J Respiratory Critical Care Med. 2009; 179:630-636.
7. Karatekin G, Kaya A, Salihoglu O, H. Balci, Nuhoglu A. Association of subclinical vitamin D deficiency in newborns with acute lower respiratory infection and their mothers. European J Clin Nut. 2007; 63:473-477.
8. Cantorna MT. Vitamin D and multiple sclerosis: An update. Nutrition Reviews. 2008; 66(Suppl 2):S135-S138.
9. Adorini L, Penna G. Control of autoimmune diseases by the vitamin D endocrine system. Nature Clin Pract Rheumatol. 2008; 4:404-412.
10. Isaia G, Giorginoand S, Adami S. High prevalence of hypovitaminosis D in female type 2 diabetic population. Diabetes Care. 2001; 24:1496.
11. Scragg R, Sowers M, Bell C. Serum 25-hydroxyvitamin D, diabetes, and ethnicity in the Third National Health and Nutrition Examination Survey. Diabetes Care. 2004; 27:2813-2818.
12. Scragg R. Vitamin D and type 2 diabetes: Are we ready for a prevention trial? Diabetes. 2008; 57:2565-2566.
13. Mattila C, Knekt P, Mannisto S, Rissanen H, Laaksonen MA, Montonen J, Reunanen A. Serum 25-hydroxyvitamin D concentration and subsequent risk of type 2 diabetes. Diabetes Care. 2007; 30:2569-2570.
14. Pietschmann P, Schernthaner G, Woloszczuk W. Serum osteocalcin levels in diabetes mellitus: Analysis of the type of diabetes and microvascular complications. Diabetologia. 1988; 31:892-895.
15. Pilz S, Kienreich K, Rutters F, de Jongh R, van Ballegooijen AJ, Grübler M, Tomaschitz A, Dekker JM. Role of vitamin D in the development of insulin resistance and type 2 diabetes. Curr Diab Rep. 2013; 13:261-270.
16. Rosen CJ, Adams JS, Bikle DD, Black DM, Demay MB, Manson JE, Murad MH, Kovacs CS. The non skeletal effects of vitamin D: An Endocrine Society scientific statement. Endocrine Rev. 2012; 33:456-492.
17. Forouhi NG, Ye Z, Rickard AP, Khaw KT, Luben R, Langenberg C, Wareham NJ. Circulating 25-hydroxyvitamin D concentration and the risk of type 2 diabetes: Results from the European Prospective Investigation into Cancer (EPIC)-Norfolk cohort and updated meta-analysis of prospective studies. Diabetologia. 2012; 55:2173-2182.
18. Wareham N, Rennie K. The assessment of physical activity in individuals and populations: Why try to be more precise about how physical activity is assessed? Int J Obes. 1998; 22:S30-S38.
19. De Boer IH, Tinker LF, Connelly S, Curb JD, Howard BV, Kestenbaum B, Larson JC, Manson JE, Margolis KL, Suskovick DS, Weiss NS. Calcium plus vitamin D supplementation and the risk of incident diabetes in the Women's Health Initiative. Diabetes Care. 2008; 31:701-707.
20. Avenell A, Cook JA, MacLennan GS, McPherson GC. For the RECORD trial group. Vitamin D supplementation and type 2 diabetes: A substudy of a randomised placebocontrolled trial in older people (RECORD trial, ISRCTN 51647438). Age Ageing. 2009; 38:606-609.
21. Halberg F, Johnson EA, Nelson W, Runge W, Sothern R. Autorhythmometry procedures for physiologic self-measurements and their analysis. Physiol Teacher. 1972; 1:1-11.
22. Bingham C, Arbogast B, Come1issen Guillaume G, Lee JK, Halberg F. Inferential statistical methods for estimating and comparing cosinor parameters. Chronobiologia. 1982; 9:397-439.

23. Cornelissen G, Halberg F. Chronomedicine. In: Encyclopedia of biostatistics (Armitage P, Colton T, eds.). John Wiley & Sons Ltd., Chichester, UK, 1998; 1:642-649.
24. Pittas AG, Dawson-Hughes B, Li T, Van Dam RM, Willett WC, Manson JE, Hu FB. Vitamin D and calcium intake in relation to type 2 diabetes in women. Diabetes Care. 2006; 29:650-656.
25. Borissova AM, Tankova T, Kirilov G, DakovskaL, Kovacheva R. The effect of vitamin D3 on insulin secretion andperipheral insulin sensitivity in type 2 diabetic patients. Int J Clin Pract. 2003; 57:258-261.
26. Baynes KC, Boucher BJ, Feskens EJ, Kromhout D. Vitamin D, glucose tolerance and insulinaemia in elderly men. Diabetologia. 1997; 40:344-347.
27. Chiu KC, Chu A, Go VL, Saad MF. Hypovitaminosis D is associated with insulin resistance and beta cell dysfunction. Am J Clin Nut. 2004; 79:820-825.
28. Norman AW, Frankel JB, Heldt AM, Grodsky GM. Vitamin D deficiency inhibits pancreatic secretion of insulin. Science. 1980; 209:823-825.
29. Johnson JA, Grande JP, Roche PC, Kumar R. Immunohistochemical localization of the 1, 25(OH)2D3 receptor and calbindin D28k in human and rat pancreas. Am J Physiol. 1994; 267:E356-E360.
30. Zeitz U, Weber K, Soegiarto DW, Wolf E, Balling R, Erben RG. Impaired insulin secretory capacity in mice lacking a functional vitamin D receptor. FASEB J. 2003; 17:509-511.
31. Orwoll E, Riddle M, Prince M. Effects of vitamin D on insulin and glucagon secretion in non-insulin-dependent diabetes mellitus. Am J Clin Nutr. 1994; 59:1083-1087.
32. Fujita T, Palmieri GM. Calcium paradox disease: Calcium deficiency prompting secondary hyperparathyroidism and cellular calcium overload. J Bone Miner Metab. 2000; 18:109-125.
33. Beaulieu C, Kestekian R, Havrankova J, Gascon-Barre M. Calcium is essential in normalizing intolerance to glucose that accompanies vitamin D depletion *in vivo*. Diabetes. 1993; 42:35-43.
34. Gutierrez-Monreal MA, Cuevas-Diaz Duran R, Moreno-Cuevas JE, Scott SP. A role for 1α, 25-dihydroxyvitamin D3 in the expression of circadian genes. J Biol Rhythms. 2014; 29:384-388.

(Received January 13, 2015; Revised January 19, 2015; Accepted February 10, 2015)

Case Report

DOI: 10.5582/ddt.2015.01005

Combination chemotherapy with S-1 and docetaxel for cutaneous angiosarcoma resistant to paclitaxel

Ikko Kajihara*, Hisashi Kanemaru, Taiga Miyake, Jun Aoi, Shinichi Masuguchi, Satoshi Fukushima, Masatoshi Jinnin, Hironobu Ihn

Department of Dermatology and Plastic Surgery, Faculty of Life Sciences, Kumamoto University, Kumamoto, Japan.

Summary **The prognosis of cutaneous angiosarcoma is very poor compared with that of other skin malignancies. The main reason for this is the limited regimens of chemotherapy available for angiosarcoma, because it is resistant to most common chemotherapeutic agents. Therefore, there is an urgent need to identify new treatment options. Recently, S-1 and docetaxel therapy was reported to be effective for advanced gastric cancer and metastatic extramammary Paget's disease. Therefore, we treated paclitaxel-resistant angiosarcoma patient with S-1/docetaxel chemotherapy. The progression-free survival was 5.0 months although grade 3 adverse events such as diarrhea and neutropenia developed. Our data need to be confirmed in a large number of patients, but S-1/docetaxel chemotherapy as an additional regimen seems to be an effective treatment option for paclitaxel-resistant angiosarcoma.**

Keywords: Angiosarcoma, chemotherapy, paclitaxel, S-1, docetaxel

1. Introduction

Angiosarcoma is a rare sarcoma derived from endothelial cells. The prognosis is poor because the five-year survival rate is generally 12-24% (*1*). The reported agents with efficacy against angiosarcoma are paclitaxel (PTX) (*2,3*), docetaxel (DOC) (*4,5*), gemcitabine (GEM) (*6*), bevacizumab (*7*) and sorafenib (*8*). However, it is difficult to inhibit the disease progressing to advanced angiosarcoma, which is resistant to standard chemotherapy. Therefore, it is necessary to identify new efficacious regimens. In recent years, combination chemotherapy using S-1 and DOC has demonstrated to have curative effects against gastric cancer (*9*) and metastatic extramammary Paget's disease (*10*). S-1 and DOC combination therapy for advanced gastric cancer is more effective than DOC monotherapy *in vitro* (*11*). We speculated that the efficacy of DOC monotherapy as second-line therapy may be inadequate in PTX-resistant cases because both DOC and PTX are tubulin inhibitors. Thus, we expected an enhanced therapeutic response resulting from the combined use DOC with S-1. We herein report PTX-refractory angiosarcoma patient who received S-1/DOC treatment.

2. Method

S-1/DOC chemotherapy was used as second-line therapy in patient with advanced angiosarcoma resistant to PTX. PTX-resistant was defined as the incidence of disease progression in angiosarcoma patients treated with PTX therapy. The protocol was basically oral S-1 (80 mg/m^2/day, day 1- day14) and intravenous DOC (40 mg/m^2, day 1) every four weeks in reference to a past report (*10*). The therapeutic efficacy was estimated every one month by examining the clinical symptoms, ultrasound (US) and/or computed tomography (CT) and/or positron-emission tomography (PET) findings. The progression-free survival (PFS) was evaluated from the day when S-1/DOC therapy was started until disease progress. Toxic effects were analyzed using the National Cancer Institute's Common Terminology Criteria version 4.0. When severe adverse events (more than grade 3) were observed, the dose of both S-1 and DOC was reduced by 20%. Institutional review board

**Address correspondence to:*
Dr. Ikko Kajihara, Department of Dermatology and Plastic Surgery, Faculty of Life Sciences, Kumamoto University, 1-1-1 Honjo, Kumamoto, Japan.
E-mail: kajiderma@gmail.com

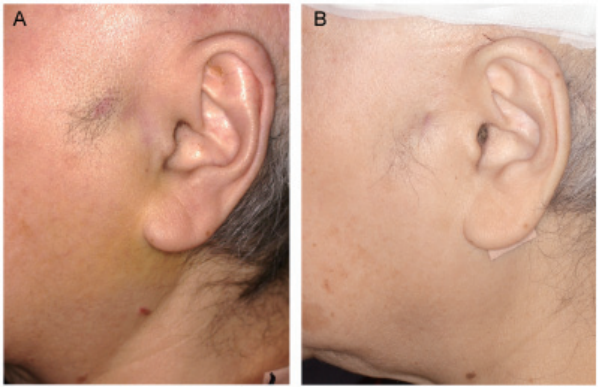

Figure 1. Purpura and purple nodules on the left cheek in case 1. (A) Before S-1 and docetaxel therapy. **(B)** Two months after the start of this regimen.

approval and written informed consent for this study were obtained according to the Declaration of Helsinki.

3. Case report

A 70-year-old female was diagnosed as having scalp angiosarcoma without lymph node or distant metastasis. The patient received four cycles of tri-weekly PTX therapy (175 mg/m^2), surgery (margin of 2 cm), radiation (total of 70 Gy) and eight cycles of tri-weekly PTX therapy as adjuvant chemotherapy. At the end of these treatments, the interval of the PTX regimen was six weeks, in compliance with her wishes, because US and PET indicated no recurrence. However, after four months of this regimen, she developed purpura and purple nodules on her left cheek (Figure 1A). A histopathological examination showed relapsed angiosarcoma. PET showed no metastasis in the lymph nodes or distant organs. We thought that her angiosarcoma cells developed tolerance to PTX. As a second-line treatment, monthly S-1 (120 mg, 80 mg/m^2) /DOC (60 mg, 40 mg/m^2) therapy was administered. After one cycle, she developed grade 3 diarrhea and neutropenia, so the dose of both agents was reduced by 20%. Two months later, her eruptions had gradually improved (Figure 1B). However, at five months after the initiation S-1/DOC therapy, PET revealed metastasis in the periauricular lymph nodes.

4. Discussion

To our knowledge, this study is the first report of the use of S-1/DOC therapy in patients with PTX-resistant angiosarcoma. We tried this regimen on the basis of the findings of *in vitro* experiments and previous clinical studies. First, both PTX and DOC essentially have the anti-tumor action through blocking tubulin. Second, S-1 has the antineoplastic efficacy through the inhibition of dihydropurimidine dehydrogenase activity (*12*). Thirdly, the combination chemotherapy with S-1 and DOC increased anti-cancer effects of treatment compared with DOC monotherapy in gastric cancer (*9,11*). Finally, S-1/DOC therapy was reported to be successful against metastatic extramammary Paget's disease (*10*). Taken together, we expected the synergy effect of S-1/DOC therapy for PTX-resistant angiosarcoma.

Our patient achieved a partial response for five months. Although that of GEM was 5.5 months in 19 taxane-exposed cutaneous angiosarcoma patients (*6*), that of sorafenib was 1.8 months in superficial angiosarcoma including chemotherapy-naïve patients (*8*). Our study may suggest that S-1/docetaxel therapy may at least stabilize the disease.

With regard to severe toxicity (more than grade3), there were severe adverse events observed in our case, including neutropenia and diarrhea. Other adverse events (all were only grade 1) included watering eyes and malaise. We speculated that the reason for severe toxicity may have been the functional decline of the bone marrow due to the previous PTX therapy. It will be necessary to adjust the initial dose for inextirpable angiosarcoma in the future.

Taken together, the present findings indicate that S-1/DOC therapy may be an alternative option for patients with PTX-resistant angiosarcoma because there were limited regimens for advanced angiosarcoma. However, further studies of this treatment in a large series of patients are needed to verify its efficacy and safety.

Acknowledgements

This study was supported in part by a grant for scientific research from the Japanese Ministry of Education, Science, Sports and Culture.

References

1. Vogt T, Brockmeyer N, Kutzner H, Schofer H. Brief s1 guidelines-cutaneous angiosarcoma and kaposi sarcoma. J Dtsch Dermatol Ges. 2013; 11:(Suppl 3):2-9, 2-10.
2. Fata F, O'Reilly E, Ilson D, Pfister D, Leffel D, Kelsen DP, Schwartz GK, Casper ES. Paclitaxel in the treatment of patients with angiosarcoma of the scalp or face. Cancer. 1999; 86:2034-2037.
3. Penel N, Bui BN, Bay JO, *et al*. Phase II trial of weekly paclitaxel for unresectable angiosarcoma: The angiotax study. J Clin Oncol. 2008; 26:5269-5274.
4. Nagano T, Yamada Y, Ikeda T, Kanki H, Kamo T, Nishigori C. Docetaxel: A therapeutic option in the treatment of cutaneous angiosarcoma: Report of 9 patients. Cancer. 2007; 110:648-651.
5. Fujisawa Y, Yoshino K, Kadono T, Miyagawa T, Nakamura Y, Fujimoto M. Chemoradiotherapy with taxane was superior to conventional surgery and radiotherapy in the management of cutaneous angiosarcoma: Multi-center, retrospective study. Br J Dermatol. 2014; 171:1493-1500.
6. Stacchiotti S, Palassini E, Sanfilippo R, Vincenzi B, Arena MG, Bochicchio AM, De Rosa P, Nuzzo A, Turano S, Morosi C, Dei Tos AP, Pilotti S, Casali PG. Gemcitabine in advanced angiosarcoma: A retrospective case series

analysis from the italian rare cancer network. Ann Oncol. 2012; 23:501-508.
7. Agulnik M, Yarber JL, Okuno SH, von Mehren M, Jovanovic BD, Brockstein BE, Evens AM, Benjamin RS. An open-label, multicenter, phase II study of bevacizumab for the treatment of angiosarcoma and epithelioid hemangioendotheliomas. Ann Oncol. 2013; 24:257-263.
8. Ray-Coquard I, Italiano A, Bompas E, *et al.* Sorafenib for patients with advanced angiosarcoma: A phase II trial from the french sarcoma group (GSF/GETO). Oncologist. 2012; 17:260-266.
9. Yoshida K, Ninomiya M, Takakura N, Hirabayashi N, Takiyama W, Sato Y, Todo S, Terashima M, Gotoh M, Sakamoto J, Nishiyama M. Phase II study of docetaxel and S-1 combination therapy for advanced or recurrent gastric cancer. Clin Cancer Res. 2006; 12:3402-3407.
10. Matsushita S, Yonekura K, Mera K, Kawai K, Kanekura T. Successful treatment of metastatic extramammary paget's disease with s-1 and docetaxel combination chemotherapy. J Dermatol. 2011; 38:996-998.
11. Wada Y, Yoshida K, Suzuki T, Mizuiri H, Konishi K, Ukon K, Tanabe K, Sakata Y, Fukushima M. Synergistic effects of docetaxel and s-1 by modulating the expression of metabolic enzymes of 5-fluorouracil in human gastric cancer cell lines. Int J Cancer. 2006; 119:783-791.
12. Tatsumi K, Fukushima M, Shirasaka T, Fujii S. Inhibitory effects of pyrimidine, barbituric acid and pyridine derivatives on 5-fluorouracil degradation in rat liver extracts. Jpn J Ccancer Res. 1987; 78:748-755.

(Received January 28, 2015; Revised February 10, 2015; Accepted February 11, 2015)

DD&T
Drug Discoveries & Therapeutics

Guide for Authors

1. Scope of Articles

Drug Discoveries & Therapeutics welcomes contributions in all fields of pharmaceutical and therapeutic research such as medicinal chemistry, pharmacology, pharmaceutical analysis, pharmaceutics, pharmaceutical administration, and experimental and clinical studies of effects, mechanisms, or uses of various treatments. Studies in drug-related fields such as biology, biochemistry, physiology, microbiology, and immunology are also within the scope of this journal.

2. Submission Types

Original Articles should be well-documented, novel, and significant to the field as a whole. An Original Article should be arranged into the following sections: Title page, Abstract, Introduction, Materials and Methods, Results, Discussion, Acknowledgments, and References. Original articles should not exceed 5,000 words in length (excluding references) and should be limited to a maximum of 50 references. Articles may contain a maximum of 10 figures and/or tables.

Brief Reports definitively documenting either experimental results or informative clinical observations will be considered for publication in this category. Brief Reports are not intended for publication of incomplete or preliminary findings. Brief Reports should not exceed 3,000 words in length (excluding references) and should be limited to a maximum of 4 figures and/or tables and 30 references. A Brief Report contains the same sections as an Original Article, but the Results and Discussion sections should be combined.

Reviews should present a full and up-to-date account of recent developments within an area of research. Normally, reviews should not exceed 8,000 words in length (excluding references) and should be limited to a maximum of 100 references. Mini reviews are also accepted.

Policy Forum articles discuss research and policy issues in areas related to life science such as public health, the medical care system, and social science and may address governmental issues at district, national, and international levels of discourse. Policy Forum articles should not exceed 2,000 words in length (excluding references).

Case Reports should be detailed reports of the symptoms, signs, diagnosis, treatment, and follow-up of an individual patient. Case reports may contain a demographic profile of the patient but usually describe an unusual or novel occurrence. Unreported or unusual side effects or adverse interactions involving medications will also be considered. Case Reports should not exceed 3,000 words in length (excluding references).

News articles should report the latest events in health sciences and medical research from around the world. News should not exceed 500 words in length.

Letters should present considered opinions in response to articles published in Drug Discoveries & Therapeutics in the last 6 months or issues of general interest. Letters should not exceed 800 words in length and may contain a maximum of 10 references.

3. Editorial Policies

Ethics: Drug Discoveries & Therapeutics requires that authors of reports of investigations in humans or animals indicate that those studies were formally approved by a relevant ethics committee or review board.

Conflict of Interest: All authors are required to disclose any actual or potential conflict of interest including financial interests or relationships with other people or organizations that might raise questions of bias in the work reported. If no conflict of interest exists for each author, please state "There is no conflict of interest to disclose".

Submission Declaration: When a manuscript is considered for submission to Drug Discoveries & Therapeutics, the authors should confirm that 1) no part of this manuscript is currently under consideration for publication elsewhere; 2) this manuscript does not contain the same information in whole or in part as manuscripts that have been published, accepted, or are under review elsewhere, except in the form of an abstract, a letter to the editor, or part of a published lecture or academic thesis; 3) authorization for publication has been obtained from the authors' employer or institution; and 4) all contributing authors have agreed to submit this manuscript.

Cover Letter: The manuscript must be accompanied by a cover letter signed by the corresponding author on behalf of all authors. The letter should indicate the basic findings of the work and their significance. The letter should also include a statement affirming that all authors concur with the submission and that the material submitted for publication has not been published previously or is not under consideration for publication elsewhere. The cover letter should be submitted in PDF format. For example of Cover Letter, please visit http://www.ddtjournal.com/downcentre.php (Download Centre).

Copyright: A signed JOURNAL PUBLISHING AGREEMENT (JPA) must be provided by post, fax, or as a scanned file before acceptance of the article. Only forms with a hand-written signature are accepted. This copyright will ensure the widest possible dissemination of information. A form facilitating transfer of copyright can be downloaded by clicking the appropriate link and can be returned to the e-mail address or fax number noted on the form (Please visit Download Centre). Please note that your manuscript will not proceed to the next step in publication until the JPA form is received. In addition, if excerpts from other copyrighted works are included, the author(s) must obtain written permission from the copyright owners and credit the source(s) in the article.

Suggested Reviewers: A list of up to 3 reviewers who are qualified to assess the scientific merit of the study is welcomed. Reviewer information including names, affiliations, addresses, and e-mail should be provided at the same time the manuscript is submitted online. Please do not suggest reviewers with known conflicts of interest, including participants or anyone with a stake in the proposed research; anyone from the same institution; former students, advisors, or research collaborators (within the last three years); or close personal contacts. Please note that the Editor-in-Chief may accept one or more of the proposed reviewers or may request a review by other qualified persons.

Language Editing: Manuscripts prepared by authors whose native language is not English should have their work proofread by a native English speaker before submission. If not, this might delay the publication of your manuscript in Drug Discoveries & Therapeutics.

The Editing Support Organization can provide English proofreading, Japanese-English translation, and Chinese-English translation services to authors who want to publish in Drug Discoveries & Therapeutics and need assistance before submitting a manuscript. Authors can visit this organization directly at http://www.iacmhr.com/iac-eso/support.php?lang=en. IAC-ESO was established to facilitate manuscript preparation by researchers whose native language is not English and to help edit works intended for international academic journals.

4. Manuscript Preparation

Manuscripts should be written in clear, grammatically correct English and submitted as a Microsoft Word file in a single-column format. Manuscripts must be paginated and typed in 12-point Times New Roman font with 24-point line spacing. Please do not embed figures in the text. Abbreviations should be used as little as possible and should be explained at first mention unless the term is a well-known abbreviation (*e.g.* DNA). Single words should not be abbreviated.

Title page: The title page must include 1) the title of the paper (Please note the title should be short, informative, and contain the major key words); 2) full name(s) and affiliation(s) of the author(s), 3) abbreviated names of the author(s), 4) full name, mailing address, telephone/fax numbers, and e-mail address of the corresponding author; and 5) conflicts of interest (if you have an actual or potential conflict of interest to disclose, it must be included as a footnote on the title page of the manuscript; if no conflict of interest exists for each author, please state "There is no conflict of interest to disclose"). Please visit Download Centre and refer to the title page of the manuscript sample.

Abstract: The abstract should briefly state the purpose of the study, methods, main findings, and conclusions. For article types including Original Article, Brief Report, Review, Policy Forum, and Case Report, a one-paragraph abstract consisting of no more than 250 words must be included in the manuscript. For News and Letters, a brief summary of main content in 150 words or fewer should be included in the manuscript. Abbreviations must be kept to a minimum and non-standard abbreviations explained in brackets at first mention. References should be avoided in the abstract. Key words or phrases that do not occur in the title should be included in the Abstract page.

Introduction: The introduction should be a concise statement of the basis for the study and its scientific context.

Materials and Methods: The description should be brief but with sufficient detail to enable others to reproduce the experiments. Procedures that have been published previously should not be described in detail but appropriate references should simply be cited. Only new and significant modifications of previously published procedures require complete description. Names of products and manufacturers with their locations (city and state/country) should be given and sources of animals and cell lines should always be indicated. All clinical investigations must have been conducted in accordance with Declaration of Helsinki principles. All human and animal studies must have been approved by the appropriate institutional review board(s) and a specific declaration of approval must be made within this section.

Results: The description of the experimental results should be succinct but in sufficient detail to allow the experiments to be analyzed and interpreted by an independent reader. If necessary, subheadings may be used for an orderly presentation. All figures and tables must be referred to in the text.

Discussion: The data should be interpreted concisely without repeating material already presented in the Results section. Speculation is permissible, but it must be well-founded, and discussion of the wider implications of the findings is encouraged. Conclusions derived from the study should be included in this section.

Acknowledgments: All funding sources should be credited in the Acknowledgments section. In addition, people who contributed to the work but who do not meet the criteria for authors should be listed along with their contributions.

References: References should be numbered in the order in which they appear in the text. Citing of unpublished results, personal communications, conference abstracts, and theses in the reference list is not recommended but these sources may be mentioned in the text. In the reference list, cite the names of all authors when there are fifteen or fewer authors; if there are sixteen or more authors, list the first three followed by *et al*. Names of journals should be abbreviated in the style used in PubMed. Authors are responsible for the accuracy of the references. Examples are given below:

Example 1 (Sample journal reference):
Nakata M, Tang W. Japan-China Joint Medical Workshop on Drug Discoveries and Therapeutics 2008: The need of Asian pharmaceutical researchers' cooperation. Drug Discov Ther. 2008; 2:262-263.

Example 2 (Sample journal reference with more than 15 authors):
Darby S, Hill D, Auvinen A, *et al*. Radon in homes and risk of lung cancer: Collaborative analysis of individual data from 13 European case-control studies. BMJ. 2005; 330:223.

Example 3 (Sample book reference):
Shalev AY. Post-traumatic stress disorder: Diagnosis, history and life course. In: Post-traumatic Stress Disorder, Diagnosis, Management and Treatment (Nutt DJ, Davidson JR, Zohar J, eds.). Martin Dunitz, London, UK, 2000; pp. 1-15.

Example 4 (Sample web page reference):
World Health Organization. The World Health Report 2008 – primary health care: Now more than ever. *http://www.who.int/whr/2008/whr08_en.pdf* (accessed September 23, 2010).

Tables: All tables should be prepared in Microsoft Word or Excel and should be arranged at the end of the manuscript after the References section. Please note that tables should not in image format. All tables should have a concise title and should be numbered consecutively with Arabic numerals. If necessary, additional information should be given below the table.

Figure Legend: The figure legend should be typed on a separate page of the main manuscript and should include a short title and explanation. The legend should be concise but comprehensive and should be understood without referring to the text. Symbols used in figures must be explained.

Figure Preparation: All figures should be clear and cited in numerical order in the text. Figures must fit a one- or two-column format on the journal page: 8.3 cm (3.3 in.) wide for a single column, 17.3 cm (6.8 in.) wide for a double column; maximum height: 24.0 cm (9.5 in.). Please make sure that artwork files are in an acceptable format (TIFF or JPEG) at minimum resolution (600 dpi for illustrations, graphs, and annotated artwork, and 300 dpi for micrographs and photographs). Please provide all figures as separate files. Please note that low-resolution images are one of the leading causes of article resubmission and schedule delays. All color figures will be reproduced in full color in the online edition of the journal at no cost to authors.

Units and Symbols: Units and symbols conforming to the International System of Units (SI) should be used for physicochemical quantities. Solidus notation (*e.g.* mg/kg, mg/mL, mol/mm^2/min) should be used. Please refer to the SI Guide www.bipm.org/en/si/ for standard units.

Supplemental data: Supplemental data might be useful for supporting and enhancing your scientific research and Drug Discoveries & Therapeutics accepts the submission of these materials which will be only published online alongside the electronic version of your article. Supplemental files (figures, tables, and other text materials) should be prepared according to the above guidelines, numbered in Arabic numerals (*e.g.*, Figure S1, Figure S2, and Table S1, Table S2) and referred to in the text. All figures and tables should have titles and legends. All figure legends, tables and supplemental text materials should be placed at the end of the paper. Please note all of these supplemental data should be provided at the time of initial submission and note that the editors reserve the right to limit the size and length of Supplemental Data.

5. Submission Checklist

The Submission Checklist will be useful during the final checking of a manuscript prior to sending it to Drug Discoveries & Therapeutics for review. Please visit Download Centre and download the Submission Checklist file.

6. Online submission

Manuscripts should be submitted to Drug Discoveries & Therapeutics online at http://www.ddtjournal.com. The manuscript file should be smaller than 5 MB in size. If for any reason you are unable to submit a file online, please contact the Editorial Office by e-mail at office@ddtjournal.com

7. Accepted manuscripts

Proofs: Galley proofs in PDF format will be sent to the corresponding author *via* e-mail. Corrections must be returned to the editor (proof-editing@ddtjournal.com) within 3 working days.

Offprints: Authors will be provided with electronic offprints of their article. Paper offprints can be ordered at prices quoted on the order form that accompanies the proofs.

Page Charge: A page charge of $140 will be assessed for each printed page of an accepted manuscript. The charge for printing color figures is $340 for each page. Under exceptional circumstances, the author(s) may apply to the editorial office for a waiver of the publication charges at the time of submission.

(Revised February 2013)

Editorial and Head Office:

Pearl City Koishikawa 603
2-4-5 Kasuga, Bunkyo-ku
Tokyo 112-0003
Japan
Tel: +81-3-5840-9697
Fax: +81-3-5840-9698
E-mail: office@ddtjournal.com

DD&T
Drug Discoveries & Therapeutics

JOURNAL PUBLISHING AGREEMENT (JPA)

Manuscript No.:

Title:

Corresponding author:

The International Advancement Center for Medicine & Health Research Co., Ltd. (IACMHR Co., Ltd.) is pleased to accept the above article for publication in Drug Discoveries & Therapeutics. The International Research and Cooperation Association for Bio & Socio-Sciences Advancement (IRCA-BSSA) reserves all rights to the published article. Your written acceptance of this JOURNAL PUBLISHING AGREEMENT is required before the article can be published. Please read this form carefully and sign it if you agree to its terms. The signed JOURNAL PUBLISHING AGREEMENT should be sent to the Drug Discoveries & Therapeutics office (Pearl City Koishikawa 603, 2-4-5 Kasuga, Bunkyo-ku, Tokyo 112-0003, Japan; E-mail: office@ddtjournal.com; Tel: +81-3-5840-9697; Fax: +81-3-5840-9698).

1. Authorship Criteria

As the corresponding author, I certify on behalf of all of the authors that:

1) The article is an original work and does not involve fraud, fabrication, or plagiarism.
2) The article has not been published previously and is not currently under consideration for publication elsewhere. If accepted by Drug Discoveries & Therapeutics, the article will not be submitted for publication to any other journal.
3) The article contains no libelous or other unlawful statements and does not contain any materials that infringes upon individual privacy or proprietary rights or any statutory copyright.
4) I have obtained written permission from copyright owners for any excerpts from copyrighted works that are included and have credited the sources in my article.
5) All authors have made significant contributions to the study including the conception and design of this work, the analysis of the data, and the writing of the manuscript.
6) All authors have reviewed this manuscript and take responsibility for its content and approve its publication.
7) I have informed all of the authors of the terms of this publishing agreement and I am signing on their behalf as their agent.

2. Copyright Transfer Agreement

I hereby assign and transfer to IACMHR Co., Ltd. all exclusive rights of copyright ownership to the above work in the journal Drug Discoveries & Therapeutics, including but not limited to the right 1) to publish, republish, derivate, distribute, transmit, sell, and otherwise use the work and other related material worldwide, in whole or in part, in all languages, in electronic, printed, or any other forms of media now known or hereafter developed and the right 2) to authorize or license third parties to do any of the above.

I understand that these exclusive rights will become the property of IACMHR Co., Ltd., from the date the article is accepted for publication in the journal Drug Discoveries & Therapeutics. I also understand that IACMHR Co., Ltd. as a copyright owner has sole authority to license and permit reproductions of the article.

I understand that except for copyright, other proprietary rights related to the Work (*e.g.* patent or other rights to any process or procedure) shall be retained by the authors. To reproduce any text, figures, tables, or illustrations from this Work in future works of their own, the authors must obtain written permission from IACMHR Co., Ltd.; such permission cannot be unreasonably withheld by IACMHR Co., Ltd.

3. Conflict of Interest Disclosure

I confirm that all funding sources supporting the work and all institutions or people who contributed to the work but who do not meet the criteria for authors are acknowledged. I also confirm that all commercial affiliations, stock ownership, equity interests, or patent-licensing arrangements that could be considered to pose a financial conflict of interest in connection with the article have been disclosed.

Corresponding Author's Name (Signature):

Date: